Free-flight Kinematics of Diptera

Inés Laura Dawson

St. John's College

University of Oxford

A thesis submitted for the degree of

Doctor of Philosophy

Trinity 2018

Supervisors: Dr. Simon M Walker and Prof. Graham K Taylor

To my parents:

Abstract

Insect flight is a complex behaviour that goes beyond pure mechanism. Integrating genetics, morphology, physiology, sensorimotor control, kinematics and aerodynamics, researching the multiform nature of insect flight is of great scientific interest and also a challenge. Consequently, exploring different strategies for reducing the dimensionality of large flight datasets to uncover meaningful relationships is critical to furthering our understanding of insect flight biomechanics. The aim of my DPhil is to explore different strategies for analysing large datasets of free-flight kinematics in three Dipteran species: *Drosophila melanogaster* (fruit fly), *Calliphora vicina* (blowfly) and *Eristalis tenax* (drone fly). In Chapter 2, I critically evaluate the *k*-means clustering algorithm as a means of partitioning dipteran body kinematics, and show that it is an unsuitable target for body kinematic data that shifts continuously. In Chapter 3, I show that sexual dimorphism in fruit flies affects their wing beat kinematics beyond size dimorphism. In Chapter 4, I used the *k*-nearest neighbour clustering algorithm to develop a way of predicting the gear stops that blowflies engage in based on their wing beat kinematics. In Chapter 5, I contrast the wing beat kinematics and aerodynamic profile of all three species. Overall, my thesis shows firstly, that fruit flies, blowflies and drone flies occupy distinct kinematic morphospaces, and secondly, that careful consideration should be given to the choice of technique used to reduce the dimensionality of the data.

Acknowledgements

This thesis represents the culmination of four years of hard work, brimming with highs and lows from countless memories and experiences: from learning how to set up lasers and high speed cameras and familiarising myself with my flying organisms, through the long days collecting data and the even longer evenings writing up, to presenting at conferences and meeting the welcoming community of academics in the animal flight world. This journey along the path of data collection, carrying out experiments and writing up that has led to this thesis has been an unforgettable one, and one that would not have been possible without the invaluable help and support of many people along the way.

Firstly, I would like to thank my supervisors Dr. Simon Walker and Professor Graham Taylor, without whom this thesis would not have been possible. Whilst the past four years have not been without their difficulties, I could not have wished for a better pair of supervisors to embark on this journey with. Thank you Simon, for being a thoughtful, kind and patient supervisor, as well as an inspiration for me to fulfil my academic potential, to enjoy MATLAB and to stretch myself academically. Thank you, too, Graham, for being a voice of reason and an astute mind in the face of adversity. I am also grateful to the BBSRC and the Oxford DTP program for funding my work and allowing my research to take place, and to all of my flies, who sacrificed themselves in the name of science.

I also want to thank my current and former fellow members of the Oxford Animal flight group: Jonathan Page, Indira Nagesh, Robin Mills, Tonya Muller, Anna Chabokdast, Marco Klein Heerenbrink, Leonidas-Romanos Davranoglou, Sofía Miñano, Lydia France, Natalia Pérez Campanero, Patrick Meyer Higgins, James Kempton, James Walker, Caroline Brighton, Kate Reynolds, Fergus McCorkell and Prof. Adrian Thomas, for their advice and support throughout my PhD.

I am also grateful to Lucy Taylor and Cedric Tan for their invaluable statistical advice on sexual selection. I am also indebted to Glen Harrison, Simon Ellis and Soohee Bradley for fixing my computer on countless occasions, to Heather Green, the staff at former Darwin's café, Tony and Jason from Works, the Zoology administrative staff and the porters, staff and cooks at St. John's College, for providing a stable support and for looking after me so well over the past few years in Oxford.

I am also grateful to those close to me in Oxford who have supported me in times of need and kept me sane on this journey. In no particular order, thank you Lucy Taylor, for our supper dates to unwind after work, Chico Camargo, for always being a grounding presence, Alex Greenhalgh, for keeping the ties between the silk and flight group strong, Ian Foo, for being an encouraging presence and keeping me sane and fed during the final weeks, Ellie Milnes-Smith, for being the best co-welfare officer, Suzie Ford, for our Pitts River lunch dates, Joe Mason, for your calming support and last but not least, Gareth Wilkes, for the peaceful and much needed tea breaks. I am also indebted to the love and support of my fellow DTP cohort group, Zoology graduates, St. John's College MCR and fellow Japanese van enthusiasts.

Likewise, I am grateful to my friends overseas, who have also been a cherished source of support and advice: Elisenda Ferrer, for being my best friend and even for getting *Els Catarres* to support the completion of my thesis, Iván Dequito, for always checking in at the right time, José Manuel Romero Ribas, for always fuelling my love and enthusiasm for Biology, Elena Bosch, for your lovely, positive letters of support, Ash Armanini, for inspiring me to pursue and persevere with my dreams and Jon Perry, for our endless conversations about Biology.

I am also grateful to Rhiannon and Lisa for their regular Zumba classes that have kept my stress levels at bay and limiting the thesis weight to just an emotional form, and to Toastmasters, Allstar Heroes, Oxford University Shorinji Kempo Club and WeCreateEDU for

helping me to develop as a more confident, expressive and competent human alongside my PhD.

Last, but certainly not least, I would like to thank my parents, Janet Dawson and Anthony Dawson, to whom this thesis is dedicated to and whose love and support I will never take for granted. They have believed in me ever since I was a young toddler who would stuff bugs in her pocket whilst proudly stating she wanted to become an entomologist when she was older, and have relentlessly supported me every step of the way. Thank you for your confidence in my abilities and for supporting me through each major life decision I have made: from pursuing my love of mathematics, to moving to Oxford at the age of 17 to pursue Biological Sciences, to embarking on the rollercoaster of a DPhil abroad. I am also grateful to my mum for proofreading my work and ensuring that as few as possible of my never-ending stream of Hispanicisms made it into the final version of this thesis that you are holding today.

Contents

Author Contributions

Regarding the thesis of Inés Laura Dawson, submitted for the degree of Doctor of Philosophy, Trinity Term 2018, entitled "Free-flight kinematics of dipterans", the author contributions towards the data chapters are as follows:

Chapter 2. Assessment of *k*-means clustering as a method for partitioning dipteran body kinematics

The *Drosophila melanogaster* dataset was collected by myself and the kinematic variables were processed using code developed by Dr. Simon Walker. The *Eristalis tenax* dataset was supplied by Dr. Simon Walker. The adaptation and improvement of Geurten's *k*-means clustering procedure was developed by myself. I was advised on the analysis and final manuscript by Dr. Simon Walker and Prof. Graham Taylor.

Chapter 3. The effect of sexual dimorphism on *Drosophila melanogaster* free-flight kinematics

The *Drosophila melanogaster* dataset is the same as used in Chapter 2. The line of analysis was developed by myself. The kinematic variables were processed using code developed by Dr. Simon Walker. Advice on statistics was provided by Prof. Graham Taylor and Dr. Cedric Tan. I was advised on the analysis and final manuscript by Dr. Simon Walker and Prof. Graham Taylor.

Chapter 4. Using wing beat kinematics as the basis for identifying the gear of free-flying *Calliphora vicina*

The free-flight *Calliphora vicina* dataset was collected by myself, whereas the tethered *Calliphora vicina* dataset was collected by Jonathan Page. The kinematic variables were processed using code developed by Dr. Simon Walker. I was advised on the analysis and final manuscript by Dr. Simon Walker and Prof. Graham Taylor.

Chapter 5. Kinematics of forward flight in three dipteran species

The *Drosophila melanogaster* free-flight dataset is the same as used in Chapter 2 and Chapter 3, the *Calliphora vicina* free-flight dataset is the same as used in Chapter 4, and the *Eristalis tenax* dataset was supplied by Dr. Simon Walker. The kinematic variables were processed using code developed by Dr. Simon Walker, and the quasi-steady blade element model was developed jointly by Dr. Simon Walker and Prof. Graham Taylor. I was advised on the analysis and final manuscript by Dr. Simon Walker and Prof. Graham Taylor.

Chapter 1

Introduction

A BRIEF HISTORY OF INSECT FLIGHT RESEARCH

From the mosquito's incredible 1000-beat-per-second flapping, to the bumblebee paradox, and the housefly's unmatched knack of eluding oncoming newspaper rolls, insect flight is undeniably a captivating field. While 80 years ago the explanation for these facts stumped scientists, our understanding of insect flight phenomena has substantially increased since then, due to the development of technology and advancement of novel techniques in insect flight research.

One of the principal challenges to overcome in insect flight research is the difficulty of empirically observing and describing an insect's swift motions during flight, and scientists have employed a variety of creative techniques to achieve this goal. For instance, Olavi Sotavalta was renowned for having perfect pitch and would identify the fundamental frequency of an insect's flight tone by pressing the test tube containing his study subject against his ear. He would then validate his measurements using double-beam cathode ray oscillographs[1–4]. Others have used stroboscopes, aligning their flicker frequency with the insect's wing beat frequency, or kymograph drums, although these were later found to apply a minimal amount of loading onto the wings, which decreased their natural wing beat frequency[5,6]. Of course, one of the fundamental techniques for determining wing beat frequency, as well as describing and analysing other kinematic and aerodynamic movements, is high speed photography and videography.

The use of high speed techniques used in animal locomotion research dates back to 1878, with Eadweard Muybridge's iconic "*Horse in Motion*" **(Image 1).** Muybridge had been instructed by Leland Stanford to investigate whether there was any moment during a horse's gallop when all four hooves were off the ground, as

Stanford was interested in testing Etienne Marey's controversial claim that suggested otherwise. Muybridge rigged a system with 12 cameras consecutively triggered by a set of tripwires as the horse galloped past them, refuting Marey's claim with the affirmation that horses are indeed airborne mid-gallop. In 1890, Marey himself would collect his own photographic sequences showing cantering and galloping horses passing through a transient airborne phase[7,8]. Two years later, von Lendenfeld would pioneer the *chambre chronophotographique* and would use it to document insect flight for the first time. Marey, Lendenfeld, Anschutz and Bull would improve upon various high speed photography and stroboscopic techniques, succeeding at capturing image sequences that surpassed 2000fps and reached exposures of 1/42,000, using ingenious methods to trigger the cameras and illuminate their subjects.

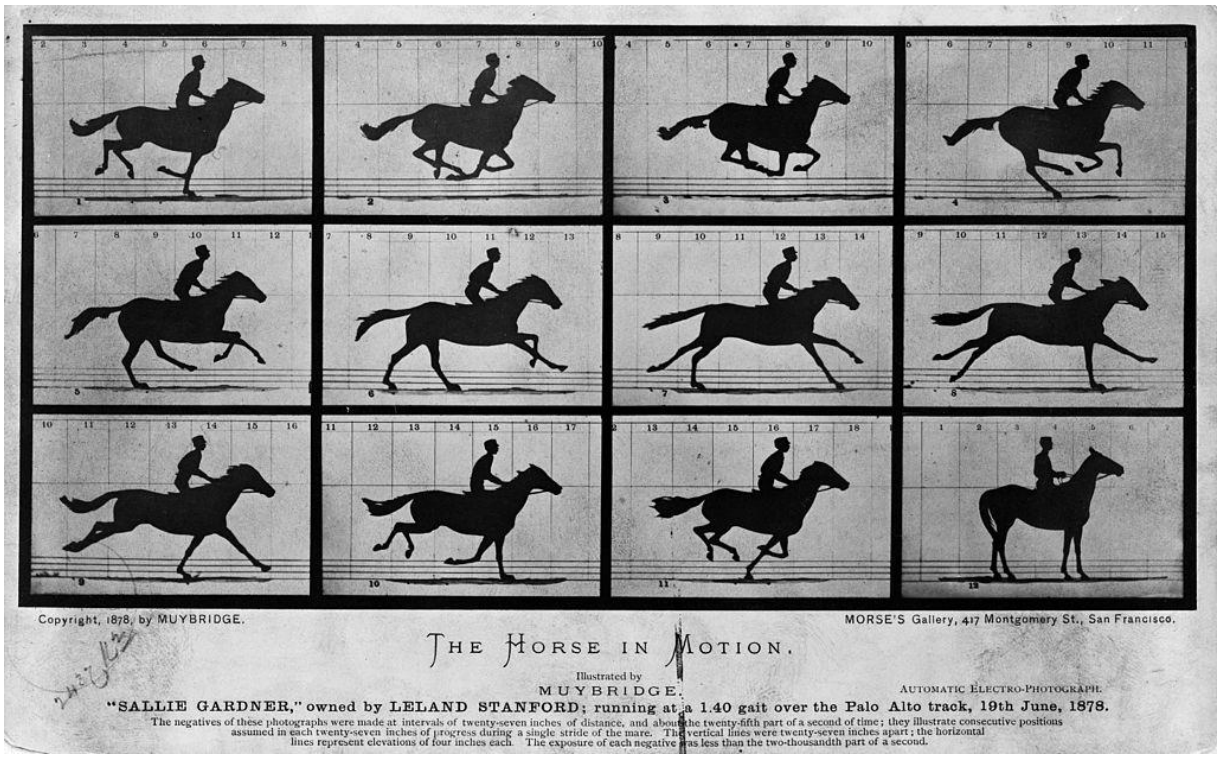

Image 1. Eadweard Muybridge's *Horse in Motion*, contradicting Marey's belief that horses always had at least one hoof on the ground, by showing that horses have an airborne phase during gallop as shown in plates 2 and 3.

These initial recordings served to document the motion of different insect wings in tethered flight and take off, as well as the movement of the halteres in flies. Bull also succeeded in documenting free-flying insects, in particular the motion of dragonfly wings in flight **(Image 2)**, noting that the downstroke generated lift and the upstroke thrust[9–12].

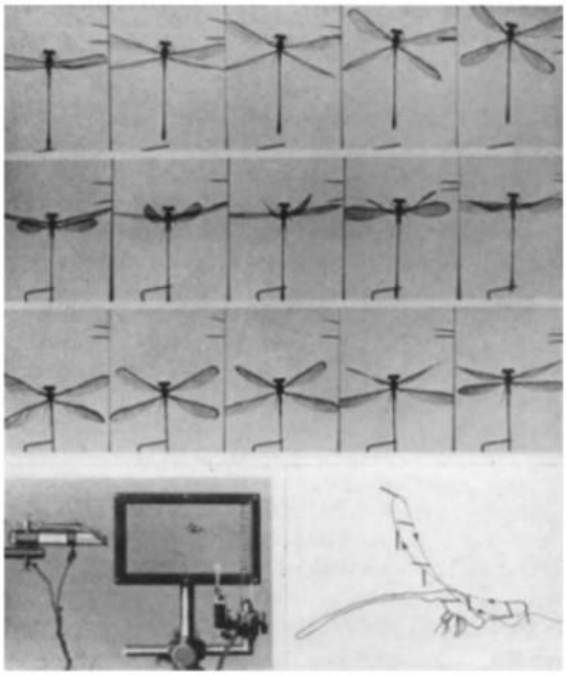

Image 2. Print from Bull's dragonfly high speed photography research, 1909. The dragonfly was released from electromagnetic tweezers, which synchronised the start of the high speed sequence with the moment the dragonfly initiated free-flight.

In parallel with the development of high speed photography techniques, early work in insect locomotion pushed the boundaries of electrophysiology to explore the relationship between sensory stimulation, nerve impulses and motor output. Heidermann described how the excitation spike in the direct flight muscles of the dragonfly *Aeshna corulea* led to a single muscle contraction[13]. Pringle followed in his footsteps and replicated his study on the movement of cockroach *Periplaneta*

americana L. legs, where he found similar results. In subsequent experiments, however, he found that nerve impulses were independent of muscle contractions in the flight muscles of the blowfly *Calliphora vicina* and the rhinoceros beetle *Oryctes nasicornis*, with their output wing beat frequencies far exceeding the rate of nerve impulses[14–17]. The frequency of muscle contraction was determined by the loading upon them, as well as temperature, which explained how the wings were able to beat so fast to match the thorax's oscillatory resonance. Most insect orders have muscles like the butterflies and the cockroaches, termed synchronous muscles, whereby one nerve impulse leads to one contraction. However, the Dipterans, Hymenopterans and Coleopterans have asynchronous flight muscles, which enable a single neural impulse to activate multiple flight muscle contractions, allowing for high wing beat frequencies to be achieved whilst maintaining a lower energy expenditure.

From its conception, the study of insect flight had always been an interdisciplinary field involving collaborations between photographers, inventors, physiologists and biologists, but in spite of this was mostly descriptive in its nature. As the 20th century began, engineers became interested in the study of insect flight and sought ways of applying their findings to technology and engineering. Building upon the foundations of high speed photography, Œhmichen, a helicopter designer who also used novel high speed techniques to record insects and birds, patented the electric stroboscope in 1917. Antoine Magnan, who was a French zoologist and aeronautical engineer, also used high speed technology to investigate insect flight in detail. Despite his passion for both fields, he is most renowned for authoring the infamous statement in "*Les vol des Insectes*": "*Tout d'abord poussé par ce qui se fait en aviation, j'ai appliqué aux insectes les lois de la résistance de l'air, et je suis arrivé avec M. Sainte-Laguë à cette conclusion que leur vol est impossible*"[18], which translates

to: "*First prompted by what is done in aviation, I applied the laws of air resistance to insects, and with M. Sainte-Laguë I arrived at the conclusion that their flight is impossible*".

Even today, Magnan's statement is widely and erroneously quoted and gave rise to the so-called bumblebee paradox, which stated that bumblebees should be incapable of flight due to the relatively small size of their wings. The misguided interpretation of his statement became the mantra of businesses such as Mary Kay®, who adopted the bumblebee as the symbol of excellence for her company, suggesting that workers could achieve grand accomplishments by exerting blind belief in their abilities, just as bumblebees were capable of flight due to their ignorance of the laws of aerodynamics[19,20].

Of course, we know that bumblebees and other insects are not violating the laws of physics when flying, but rather that traditional fixed wing aerodynamics are insufficient to explain the forces generated by insects in flight. Magnan had only applied the basic lift and drag equations using parameters from bumblebees:

$$L = \frac{1}{2}\rho U^2 A C_L$$

$$D = \frac{1}{2}\rho U^2 A C_D$$

where L is lift, D is drag, ρ is the fluid density of the fluid, U is the airspeed, A is the wing area, C_L is the lift coefficient and C_D is the drag coefficient.

These equations, however, are inadequate without further modifications when applied to insect flight. Insect flight does not uphold fixed wing assumptions, as insects engage in high frequency flapping flight and also twist and camber their

wings throughout the wing beat cycle. In fact, insects adopt much higher angles of attack in flight compared to fixed-wing aircrafts, meaning their values of C_L and C_D are substantially greater than those estimated for aeroplanes. Insects are also considerably smaller in scale, which affects the interaction of their wings and body with the air, compared to larger bodies such as aircrafts and larger birds.

Whilst Magnan's words were misrepresented, his findings fuelled the next challenge in insect flight research: to identify the role of unsteady effects and the extent of their contribution to aerodynamic forces throughout the wing beat cycle. Airflow behaviour in pure laminar and pure unsteady flow is well understood under fixed conditions, but many insects lie in the transition phase between uniformly laminar and unsteady flow, and their complex wing beat motion makes predicting the behaviour of the wake even more difficult.

Weis-Fogh and Jensen made good headway in tackling this challenge with desert locusts *Schistocerca gregaria*[21–24]. Instead of attempting to model insects like aeroplanes, they treated them like propellers and helicopter rotors, which more closely match their flapping nature. Rather than identifying and modelling unknown unsteady forces, they used ideas from Holst & Küchemann, Walker, and Osborne to make the case that adapting conventional aerodynamic theory into a quasi-steady system could be sufficient to explain the lift force generated by some insects[21,23,25–29]. Their quasi-steady model involved estimating aerodynamic forces with a steady-state framework for consecutive snapshots in time, assuming independence from previous instants whilst accounting for adjustments in wing movement throughout the wing beat cycle. Their model also involved numerous simplifications, such as a horizontal stroke plane, stroke and deviation angles that were symmetrical and

perfectly sinusoidal, vertical lift, and negligible induced wind. When these were applied to desert locusts, they concluded that a simplified quasi-steady system was sufficient in explaining the minimum lift required to keep them aloft in fast forward flight without speculating whether there were any unsteady effects at play as well[23,30].

Weis-Fogh was determined to extend his theory and describe the aerodynamic principles of insect flight spanning a broader range of flight speeds and Reynolds numbers under a primarily steady-state framework. He validated his observations in a wide range of animals, spanning hummingbirds, Vogel's hovering *Drosophila virilis*, beetles, lepidopterans and bats, although he was careful to point out that the sufficiency of a quasi-steady system to explain the produced lift forces did not preclude the involvement of unsteady effects at certain points in the wing beat[30–32]. This was an encouraging finding, as it meant that Weis-Fogh's aerodynamic principles could be applied to predict most insects' aerodynamic forces using easily obtainable estimates and with no prior knowledge of any of the unsteady effects they employed, such as clap-and-fling, delayed stall and rotational forces.

Nonetheless, his conclusion did not apply to all organisms. For instance, he noted that *Encarsia formosa*, a minute chalcidoid wasp operating at a Reynolds number between 10 and 20, and the hoverfly *Episyrphus balteatus*, which adopt unique body postures and inclined stroke planes in flight, both had minimum lift coefficients that were too large to be explained through steady state mechanisms alone[30]. This prompted him to speculate on the various unsteady mechanisms which could be involved in generating the unexplained lift forces.

The earliest unsteady mechanism identified was the Wagner effect, which describes the gradual rise of airflow circulation to a steady state value after initiating flight[33,34]. However, unlike most unsteady mechanisms which aim to account for the outstanding lift in insect flight, the Wagner effect lowers the effect of quasi-steady forces shortly after initiating flight[35–37]. Weis-Fogh observed that *Encarsia* flew in a two-step characteristic motion which he dubbed the clap-and-fling, which he believed could mitigate the Wagner effect. The 'clap' is the upstroke motion until pronation, where the wing tips come into contact or close proximity dorsally. The close contact ensures that the circulation of both wings converge and cancel each other out, eliminating the vorticity generated over the trailing edge and providing additional thrust by decreasing the potential for the Wagner effect[30,38–40]. The 'fling' is initiated after pronation as the leading edges separate. This motion causes circulation to attach quicker as the low-pressure area that originates when the wings are flung apart causes fluid to occupy the region. However, not all insects perform the clap-and-fling motion, and the lift enhancement from it is not estimated to be very high beyond take off, suggesting that it is unlikely to be the only unsteady mechanism exploited by insects, or the unsteady mechanisms sustaining insects with inclined stroke planes in flight[41,42].

Ellington continued Weis-Fogh's work in his ground-breaking seminal papers from 1984, which represented a major overhaul in insect flight research[40,42–46]. He rigorously tested Weis-Fogh's steady-state paradigm through a proof-by-contradiction, as he was aware of the limitations of Weis-Fogh's approach and felt the margin between the maximum predicted lift production and minimum lift requirements were too small in several insects. He elaborated on Weis-Fogh's quasi-steady model to account for non-horizontal stroke planes, adapted Rankine-Froude

momentum theory for insect flight and used more detailed kinematics, and argued that if the maximum lift predicted from the quasi-steady blade element model was lower than the mean lift required in hovering flight, then quasi-steady assumptions were insufficient to explain insect flight[40,43–45,47]. On the other hand, if it was greater, the model would remain unfalsified as it did not negate the presence of other unsteady effects[42,43]. When accounting for non-horizontal stroke planes and induced wind, Ellington arrived at the opposite conclusion to Weis-Fogh, finding that most hovering insects did not hold up to a quasi-steady analysis as accounting for inclined stroke planes raised the induced power requirement by 15-60%[42].

Ellington's work also redefined how insect flight measurements were collected, and he provided a framework for making parameters non-dimensional, enabling comparisons between organisms that spanned a wide range of sizes, Reynolds numbers and flight speeds[40,44,45]. For instance, he proposed the usage of the advance ratio, J, which is the inverse of reduced frequency, k. Reduced frequency was first introduced by Walker in 1925, and was non-dimensionalised by Küssner to describe the ratio between forward speed and vibration velocity of aeroplane wings with a small amplitude[25,26,28]. They found that when $k < 0.2$, unsteady effects did not need to be accounted for. Ellington noted that quasi-steady models applied best to fast-forward flight in insects, such as that of cruising locusts, and the boundary point in advance ratio between unsteady effects contributing a substantial amount to lift generation has been found to lie at $J = 1$[48].

Ellington's findings served to uncover the need to explore unsteady effects. Ennos studied wing flexion in Dipteran flies in great detail and proposed that their timing and speed of rotation could be linked to the modulation of lift generation[49–

[51]. A decade later, using high-speed photography to visualise airflow around the wings of the hawkmoth *Manduca sexta*, Ellington, van den Berg, Willmott and Thomas found photographic evidence for a leading-edge vortex **(Image 3)**, although the exact aerodynamic principles underlying it remained unclear[52]. Some postulate that the force developed by leading-edge vortices (LEVs) is perpendicular to the plane of the wing and thus generates additional lift and drag[53,54]. Others think it more likely that it is the result of dynamic or delayed stall, which occurs when the leading-edge vortex (LEV) forms during the translational phase of the downstroke and enables the wings to travel at much higher angles of attack than aircraft, generating additional lift before stalling[55,56], although these perspectives are not mutually exclusive.

Unsteady effects are not confined to the translational phase of the wing beat. In many insects, rotational mechanisms also play a role in enhancing lift. LEVs can be formed as the wing flips over during pronation or supination, where it recaptures the vorticity upon translation and can enhance its circulation[57].

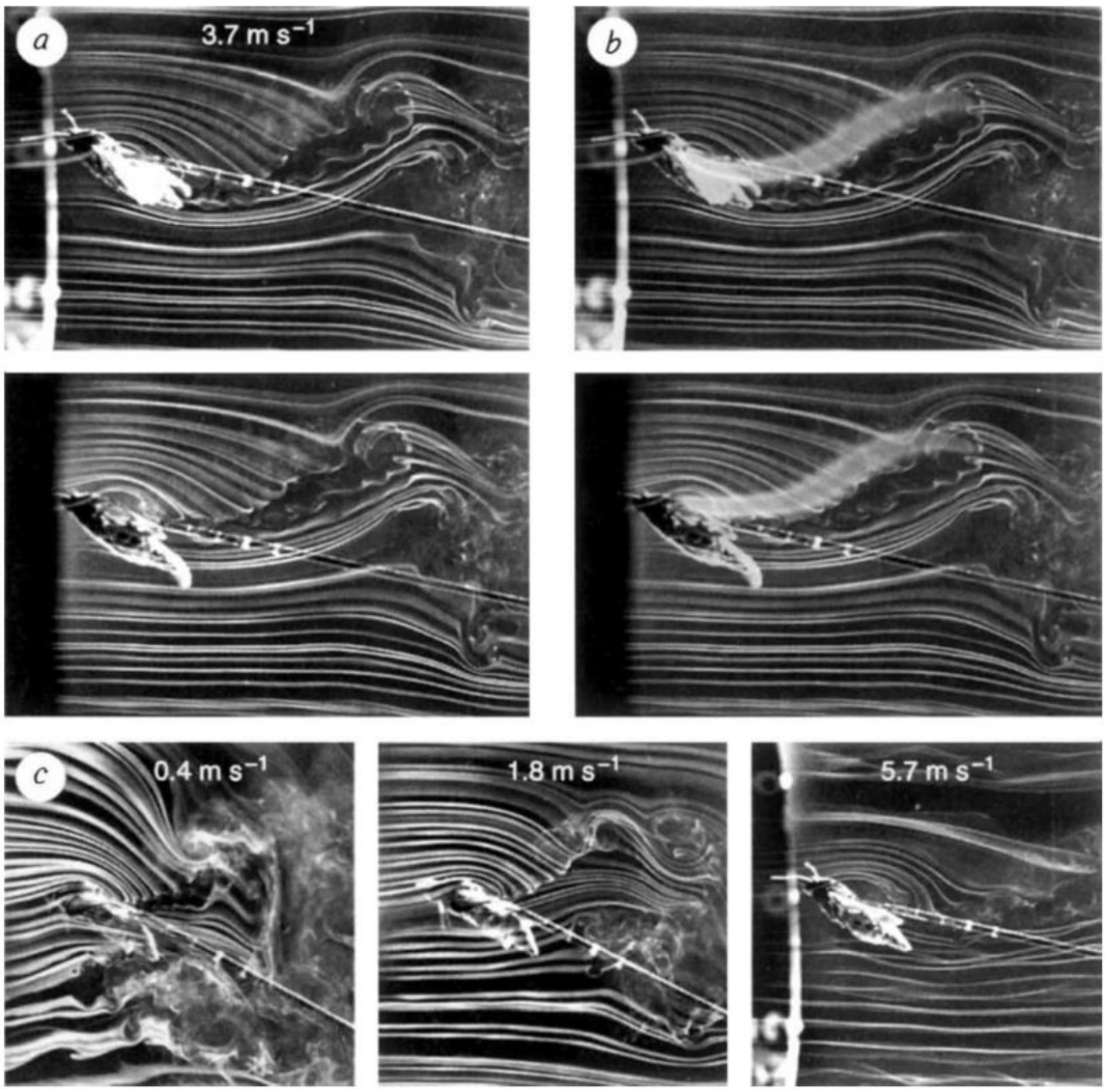

Image 3. Courtesy of Ellington et al. 1996, *Leading-edge vortices in insect flight*[52]. Airflow visualisation showing the formation and evolution of a leading-edge vortex during the downstroke in *Manduca sexta* (a), with a superimposed drawing highlighting features of the flow (b) and the formation of leading-edge vortices at different forward speeds.

Following the advent of modern digital high-speed cameras, the limiting factor in obtaining data for flight analysis was no longer the development of high-speed technology, but rather the power to subsequently process and analyse the large volumes of data collected. Many of the ground-breaking papers in insect flight

research were based on a small number of sequences with a low volume of wing beats. This was due less to the difficulty involved in collecting recordings—although the experimental technique required is not to be underestimated—than to the fact that the relevant measurements needed to derive the wing beat kinematics had to be tracked and calculated manually. This made manual tracking one of the most time-consuming aspects of insect flight analysis and greatly limited the quantity of data that could be feasibly analysed.

In recent years, however, the steady increase in computational power along with the development of automated processes and simulation software tools have meant that the volume of analysable data has risen inexorably, making the main challenge of researching insect flight one of data reduction, and not just data collection[58]. As such, one of the primary challenges this thesis must deal with is tackling large volumes of high resolution kinematic data and identifying effective ways of segmenting it for analysis.

INSECT FLIGHT KINEMATICS

As has been mentioned previously, the study of insect flight involves a wide range of disciplines: from physiology and anatomy to aerodynamics, kinematics and genomics; each discipline supplies one small piece of the puzzle towards obtaining a broader picture of insect flight. This thesis focuses primarily on dipteran flight dynamics, and principally on kinematics, although some aspects of aerodynamics are briefly touched upon in the final chapter.

Flight kinematics refers to the motion of the body and wings of the insect during flight, without necessarily considering the forces that produce such motion. This makes it possible to draw conclusions about how insects generate different aerial manoeuvres by making adjustments to their wing and body positions without requiring a complete understanding of the aerodynamic principles behind their flight.

Obtaining flight kinematic information has always represented a technical challenge for scientists. Most insects are small in size and flap at high wing beat frequencies. Most dipterans beat their wings in excess of 100Hz, which requires specialised equipment such as macro lenses and sophisticated high-speed cameras before they can be properly visualised[1,59].

One of the more rewarding challenges of working with living organisms is the trade-off between collecting data that is as close to their natural free-flight behaviour as possible, whilst also collecting a sufficient volume of high-quality data with which to perform an analysis. A tethered set-up can simplify data collection by fixing the insect in a stationary position in front of a high-speed multi-camera set-up. Large volumes of data can be obtained once the flight response has been triggered, although this comes at the expense of accuracy of representation of their natural flight behaviour—insects under tethered conditions have fewer degrees of freedom available to them, and are also known to behave differently[60–62]. Under true free-flight conditions, gathering data may appear to be more arbitrary, in the sense of being dependent on the individual whim of the insect, which can choose where it goes and whether it flies where we would like it to fly. When designing a free-flight enclosure for data collection, therefore, it is essential to consider if the insect's

environment is visually rich, in order to avoid biased sensorimotor responses to the surroundings. The enclosure must also be sufficiently large to give it the freedom to engage in as wide an envelope of free-flight behaviour as possible, yet at the same time sufficiently confined that it will frequently cross the same recording volume in order to enable successful data collection. Multi-camera set-ups are essential to enable a time-series of 3D coordinates from the body and wings to be tracked and processed into parameters of interest, although they have the drawback of further restricting the recording volume through which the insect must fly. Digitization of 3D coordinates is carried out through geometric analysis such as photogrammetry, which relies on knowing exactly where the cameras are positioned in order to accurately project points in different camera views into 3D space[63–65]. One of the aims of this thesis is to successfully tackle the difficulty of collecting and analysing a large volume of high-resolution kinematic data of natural dipteran free-flight.

Overcoming the biological behavioural challenge is only the first step in collecting data for kinematic flight analysis. There is also the technical challenge of extracting appropriate standardised kinematic parameters for analysis. Whilst insect flight kinematics have been studied for well over 100 years, as stated above, it was Ellington's seminal work that enabled insect flight kinematic research to make the transition towards a more standardised and quantitative field by adapting aeronautical concepts from engineering and applying them to insects[40,42–46].

One of Ellington's chief contributions was to set out a standard coordinate system that enabled the body kinematic parameters to be defined with respect to the insect's body, together with a coordinate system fixed in the stroke plane. This plane is defined by the arc containing the wing base through which the wings flap

back and forth in each wing beat, and in this plane the wing tip positions can be defined as spherical coordinates[45]. The wing beat is typically split into the upstroke and the downstroke, with the wing beat cycle conventionally commencing at the start of the downstroke. The majority of aerodynamic lift force is considered to be generated during the downstroke motion of the wings, although many species are also capable of generating lift force on the upstroke[36,66]. Ellington provided a standardised way of calculating different kinematic flight parameters of interest, such as wing beat frequency, stroke plane, stroke amplitude and the timing of wing rotation amongst others, and also introduced non-dimensional parameters such as advance ratio and non-dimensional velocity to describe insect motion whilst allowing cross-species comparisons to be made[45]. As described earlier, Ellington also integrated different kinematic parameters into the estimation of aerodynamic forces by means of a quasi-steady blade element model, and carried out a proof-by-contradiction to see if adapting steady-state equations to quasi-steady assumptions was sufficient in estimating lift and drag forces generated during flight[40,42,45]. Ellington's framework has been adapted in our methodology, as the majority of our wing beat kinematics are defined with respect to the body rather than to the stroke plane, and will feature extensively throughout this thesis.

As well as flapping dorsoventrally, insect wings also undergo deformation during the wing beat cycle in the form of camber and wing twist[30,45,49,51,67,68]. There is substantial evidence that both cambering and the timing of wing rotation during flight play an important role in aerodynamic lift generation; as for instance, varying the timing of supination in the wing beat influences the forces produced during the wing beat cycle[36,65,69–73]. In spite of this, many studies that have historically considered insect flight kinematics have foregone measuring wing twist due to the

difficulty of accurately measuring the degree of deformation in the wings from flight recordings, and the simplicity of modelling wings as flat plates in models and simulations[74–76]. One of the key improvements to Ellington's kinematic framework offered in this thesis is to provide an accurate measurement of wing twist for the kinematic analysis, and considering the wings as non-rigid plates that undergo span-wise torsion in our estimations of aerodynamic forces.

DIPTERAN SPECIES

Insect flight research has uncovered the many diverse ways in which insects use their wings in flight. Beetles (Coleoptera) and earwigs (Dermaptera) for example, have sophisticated origami-like folds on their wings allowing them to rapidly deploy and fold them away under their modified forewings for protection, and which have served as inspiration for foldable bio-inspired technology[77–83]. Dragonflies (Odonata), unlike the majority of insect orders, have direct muscles that attach directly onto the base of the wings enabling them to adjust their wings independently so they can engage in agile manoeuvres when targeting prey[84,85]. Many butterflies and moths (Lepidoptera) combine cryptic and aposematic colouring to protect them from potential predators both whilst flying and when perching[86]. Locusts (Orthoptera) excel at sustained, cruising flight, such that they can fly for hours on end[87]. Bumblebees (Hymenoptera) are capable of carrying loads amounting up to half of their body weight whilst navigating between food sources and their hives[88–90]. This thesis focuses on flies (Diptera), which are easily amongst the most adept and acrobatic of fliers.

The dipterans are the fourth most diverse and speciose insect order with over 125,000 species described and over 1,000,000 projected to exist[91]. There are multiple hypotheses that aim to explain why dipterans are so speciose and successful. It is known that the Brachycera suborder within the Diptera have been able to radiate quickly due to having a lower extinction rate, and it is likely that their wings and capacity for agile flight is intrinsically linked to this, due to their involvement in predator aversion, dispersal, niche occupation, foraging, seeking out mates and courtship[91–93].

Dipteran flight is unique in many ways. Unlike the majority of insect orders, Dipterans only have a single pair of wings with an aerodynamic role: the forewings. The hindwings have been modified through evolution into halteres, a unique sensory organ shaped like a drumstick. The halteres are subject to Coriolis forces, providing sensory feedback on the angular velocity of the body to the fly, and are necessary for stable dipteran flight[94–97]. The dipteran sensory system is fast and highly integrated, as they perceive information from their surroundings through their compound eyes, ocelli, campaniform sensillae, Johnston's organs and neck sensors, among others.

To the detriment of those who swat flies, dipterans also boast high flicker fusion frequencies, of up to 100Hz higher than any vertebrate. In some blowfly species, the flicker fusion rate exceeds 220 stimuli per second, allowing them to detect and react to stimuli far quicker than us[98,99]. Along with coleopterans and hymenopterans, flies have asynchronous flight muscles, which enable them to attain much higher flapping speeds than the 50-60Hz ceiling set by insects with synchronous muscles, in the range of 100Hz up to >1000Hz in some mosquito species[100]. Asynchronous muscles also result in a higher reliance on resonance to

attain the wing beat frequency, leading to a greater degree of autocorrelation across consecutive wing beats[100].

The dipterans' prowess in flight, the relative ease of obtaining and rearing them for experimental purposes, and the fact they only have a single pair of wings are factors that make flies an attractive study organism in the field of insect flight. This thesis primarily focuses on three species of fly: *Drosophila melanogaster*, *Calliphora vicina* and *Eristalis tenax*.

Drosophila melanogaster, also known as the fruit flies, are small flies in the range of 1 – 2mm that are often attracted to fermenting substances, affording them the name of vinegar flies in Spain. Due to their small size, fast generation time and predictable rearing, *D. melanogaster* is a model organism in many fields of biology. This means it is easy to obtain genetically uniform lines and to perform genetic experiments to uncover links between genes, phenotype, morphology and function. Experiments manipulating genes as well as mapping natural genetic differences that affect wing shape and flight performance have been carried out in the literature, and their flight has been extensively studied[32,101–105].

Drosophila melanogaster is also a sexually dimorphic species, where the females are substantially larger than the males, and the males use their wings not only for powered flight but for generating courtship song. *Drosophila* courtship song is composed of two stereotyped patterns: pulse song, which is characterised by distinct consecutive bursts of pulses; and sine song, a pure sinusoidal waveform with a carrier frequency of 150 – 200Hz and a power amplitude a quarter of that of the pulse song[106,107]. In this thesis, we aim to explore the effect of sexual dimorphism on *Drosophila* flight kinematics.

Calliphora vicina, also known as blowflies, are remarkable insects renowned for their forensic importance, their wide geographical distribution and their agile flight. Capable of tracking decaying flesh by its smell alone, blowflies are reliably amongst the first colonisers of cadavers, even in the dark, where females mate and lay their eggs[108–112]. Males generally feed off nectar from flowers, but are also drawn to rotting flesh, where they can find and mate with females[109–112]. Unlike most insects, they are capable of successful flight at sub 10˚C air temperatures and are one of the few sub-Antarctic insect species to boast functional flapping flight[113–116].

Compared to other insect species, and unlike *Drosophila melanogaster*, there is relatively low sexual size dimorphism in *Calliphora vicina*. The compound eyes of the male blowfly are generally larger than the female's, and are conjoined on the dorsofrontal area of the male's head, which is specialised to detect females[117]. *Calliphora* species established in the Kerguelen islands display a stable degree of sexual dimorphism relating to wing size and shape, with lower wing loading on females[114]. Otherwise, sexual dimorphism in *Calliphora* is primarily behavioural. Females carry out more dispersal flights compared to males, seeking out multiple locations to lay their eggs[118,119].

Blowfly steering muscles have also been extensively studied in tethered flight with techniques such as electrophysiology and microtomography, as they use them to carry out fine-tuned adjustments to their flight manoeuvres[120–125]. The blowfly also shares a sophisticated gear change mechanism with other dipteran species of the suborder Brachycera. The blowfly's gear change mechanism is a physical structure in its wing hinge with three possible stops, which enable it to adjust its

flight kinematics. In this thesis, we aim to explore whether it is possible to predict what gear they are engaging in on the basis of their kinematic parameters alone.

Finally, *Eristalis tenax*, also known as drone flies, due to their resemblance to honeybee drones, are territorial flies that often engage in hovering to attract females[111]. Although they display a lower degree of sexual dimorphism compared to *Drosophila*, they do display sexually dimorphic behaviour, as the males perform hovering saccades around their flowers to mark their territory and attract females.

THESIS STRUCTURE

In this thesis I aim to explore different strategies for analysing large datasets of detailed free-flight kinematics in *Drosophila melanogaster*, *Calliphora vicina* and *Eristalis tenax*. While three species is insufficient to carry out a true comparative study, the large, detailed and standardised volume of data collected allows for an in-depth insight into the flight kinematics of these three species, whilst also exploring novel approaches to reduce and partition the data.

Chapter 2, "**Assessment of *k*-means clustering as a method for partitioning dipteran body kinematics**", tests a data reduction approach originally developed by Geurten[126,127], with the objective of replicating his findings with a higher resolution free-flight dataset of the same species of hoverfly (*Eristalis tenax*) and to test it with a *Drosophila melanogaster* dataset, with the objective of determining if it is a valid way of partitioning the body kinematics in dipteran flight as a means to find the associated coupled wing beat kinematics.

Chapter 3, "**The effect of sexual dimorphism on *Drosophila melanogaster* free-flight kinematics**", aims to see whether sexual dimorphism generates and explains differences in flight kinematics between male and female flies, answering an important but overlooked question in *Drosophila melanogaster* flight.

Chapter 4, **"Using wing beat kinematics as the basis for identifying the gear of free-flying *Calliphora vicina*"**, explores free-flight wing beat kinematics of *Calliphora vicina* and uses a *k*-nearest neighbour (*k*-NN) clustering algorithm to predict the gear stop position that free-flying blowflies are engaging in, on the basis of a classified tethered dataset of *Calliphora vicina*.

Chapter 5, **"Kinematics of forward flight in three dipteran species"**, examines the similarities and differences in wing beat kinematics between *Drosophila melanogaster*, *Calliphora vicina* and a dataset of *Eristalis tenax*, as well as applying a detailed quasi-steady blade element model that accounts for wing torsion to estimate the aerodynamic forces generated in free-flight.

Finally, in Chapter 6, **"General discussion"**, I amalgamate the findings of my thesis, discuss the limitations of the analysis and present its future directions.

Overall, my thesis aims to provide insights into the free-flight kinematics of *Drosophila melanogaster* and *Calliphora vicina*, and it critically explores the validity of various techniques for partitioning and reducing flight kinematic data.

BIBLIOGRAPHY

1. Sotavalta, O. The flight-tone (wing stroke frequency) of insects. *Acta Entomol. Fenn.* **4,** 1–117 (1947).

2. Sotavalta, O. Flight-tone and Wing-stroke Frequency of Insects and the Dynamics of Insect Flight. *Nature* **170,** 1057–1058 (1952).

3. Sotavalta, O. Recordings of High Wing-Stroke and Thoracic Vibration Frequency in Some Midges. *Biol. Bull.* **104,** 439–444 (1953).

4. Sotavalta, O. The effect of wing inertia on the wing-stroke frequency of moths, dragonflies and cockroach. *Ann Ent Fenn.* 93–101 (1954).

5. Vanderplank, F. L. Air-speed/Wing-tip speed ratios of insect flight. *Nature* **165,** 806–807 (1950).

6. Hargrove, J. W. The flight performance of tsetse flies. *J. Insect Physiol.* **21,** 1385–1395 (1975).

7. Marey, E.-J. & Demeny, G. *Cheval (bixio). Petit galop. Jambes seules.* (Station Physiologique, 1890).

8. Marey, E.-J. & Demeny, G. *Cheval (cob). Pied seuls. Trot.* (Station Physiologique, 1891).

9. Bull, L. Application of the electric spark to the chronophotography of rapid motions. *Comptes Rendus l'Academie des Sci.* **138,** 155–157 (1904).

10. Bull, L. Researches on the flight of the insect. *Comptes Rendus l'Academie des Sci.* **149,** 942–944 (1904).

11. Bull, L. Motional mechanism of the insect wing. *Comptes Rendus l'Academie*

des Sci. **138,** 590–592 (1904).

12. Bull, L. Inclinations of the wing surface of the insect during flight. *Comptes Rendus l'Academie des Sci.* **150,** 129–131 (1910).

13. Heidermann, C. Reizphysiologische Untersuchungen an Libellenflugmuskulatur von Aeschna coerulea. *Zool. Jb.* **50,** 1–30 (1931).

14. Pringle, J. W. S. The motor mechanism of the insect leg. *J. Exp. Biol.* **16,** 220–231 (1939).

15. Pringle, J. W. S. The excitation and contraction of the flight muscles of insects. *J. Physiol.* **108,** 226–232 (1949).

16. Darwin, F. W. & Pringle, J. W. S. The Physiology of Insect Fibrillar Muscle. I. Anatomy and Innervation of the Basalar Muscle of Lamellicorn Beetles. *Proc. R. Soc. B Biol. Sci.* **151,** 194–203 (1959).

17. Machin, K. E., Pringle, J. W. S., F.R.S. & Tamasige, M. The Physiology of Insect Fibrillar Muscle. IV. The Effect of Temperature on a Beetle Flight Muscle. *Proc. R. Soc. London B* **155,** 493–499 (1962).

18. Magnan, A. *Le vol des insectes*. (Hermann, 1934).

19. Kay Ash, M. *Mary Kay*. (Harper & Row, 1981).

20. Kay Ash, M. *Miracles Happen*. (William Morrow Publishing, 2003).

21. Weis-Fogh, T. & Jensen, M. Biology and Physics of Locust Flight. 1. Basic Principles in Insect Flight - A Critical Review. *Philos. Trans. R. Soc. London Ser. B-Biological Sci.* **239,** 415–458 (1956).

22. Weis-Fogh, T. Biology and Physics of Locust Flight II. Flight Performance of

the Desert Locust (Schistocerca gregaria). *Philos. Trans. R. Soc. London* **Series B,** 459–510 (1956).

23. Jensen, M. Biology and Physics of Locust Flight. III. The Aerodynamics of Locust Flight. *Philos. Trans. R. Soc. London Ser. B-Biological Sci.* **239,** 511–552 (1956).

24. Weis-Fogh, T. Biology and Physics of Locust Flight. IV. Notes on Sensory Mechanisms in Locust Flight. *Philos. Trans. R. Soc. London Ser. B-Biological Sci.* **239,** 553–584 (1956).

25. Küssner, H. G. Zusammenfassender Bericht über den instationären Auftrieb von Flügeln. *Luftfahrtforschung* **13,** 410–424 (1936).

26. Küssner, H. . & Schwarz, L. Der schwingende Flügel mit aerodynamisch ausgeglichenem Ruder. *Luftfahrtforschung* **17,** 337–354 (1940).

27. Holst, V. E. V & Küchemann, D. Biologische und aerodynamische Probleme des Tierfluges. *Naturwissenschaften* **29,** 348–362 (1941).

28. Walker, G. T. The Flapping Flight of Birds. *J. R. Aeronaut. Soc.* **29,** 590–594 (1925).

29. Osborne, M. F. M. Aerodynamics of Flapping Flight with Application to Insects. *J. Exp. Biol.* **28,** 221–245 (1951).

30. Weis-Fogh, T. Quick Estimates of Flight Fitness in Hovering Animals, Including Novel Mechanisms for Lift Production. *J. Exp. Biol.* **59,** 169–230 (1973).

31. Weis-Fogh, T. Energetics of Hovering Flight in Hummingbirds and in

Drosophila. *J. Exp. Biol.* **56,** 79–104 (1972).

32. Vogel, S. Flight in Drosophila I. Flight performance of tethered flies. *J. Exp. Biol.* **44,** 567–578 (1966).

33. Wagner, H. Uber die Entstehung des dynamischen Auftriebes von Traflgugeln. *Zeitschrift fur Angew. Math. und Mech.* **35,** 17 (1925).

34. Walker, P. B. *Experiments on the growth of circulation about a wing with a description of an apparatus for measuring fluid motion*. (1931).

35. Dickinson, M. H. & Götz, K. Unsteady aerodynamic performance of model wings at low reynolds numbers. *J. exp. Biol.* **174,** 45–64 (1993).

36. Dickinson, M. H., Lehmann, F. O. & Sane, S. P. Wing rotation and the aerodynamic basis of insect flight. *Science* **284,** 1954–1960 (1999).

37. Sane, S. P. The aerodynamics of insect flight. *J. Exp. Biol.* **206,** 4191–4208 (2003).

38. Lighthill, M. J. On the Weis-Fogh mechanism of lift generation. *J. Fluid Mech.* **60,** 1–17 (1973).

39. Maxworthy, T. Experiments on the Weis-Fogh mechanism of lift generation by insects in hovering flight. Part 1. Dynamics of the 'fling'. *J. Fluid Mech.* **93,** 47–63 (1979).

40. Ellington, C. P. The Aerodynamics of Hovering Insect Flight. IV. Aerodynamic Mechanisms. *Philos. Trans. R. Soc. London* **B,** 79–113 (1984).

41. Marden, J. H. Maximum lift production during takeoff in flying animals. *J. Exp. Biol.* **130,** 235–238 (1987).

42. Ellington, C. P. The Aerodynamics of Hovering Insect Flight. VI. Lift and Power Requirements. *Philos. Trans. R. Soc. London* **B,** 145–181 (1984).

43. Ellington, C. P. The Aerodynamics of Hovering Insect Flight. I. The Quasi-Steady Analysis. *Philos. Trans. R. Soc. London* **B,** 1–15 (1984).

44. Ellington, C. P. The Aerodynamics of Hovering Insect Flight. II. Morphological Parameters. *Philos. Trans. R. Soc. London* **B,** 17–40 (1984).

45. Ellington, C. P. The Aerodynamics of Hovering Insect Flight. III. Kinematics. *Philos. Trans. R. Soc. London* **B,** 41–78 (1984).

46. Ellington, C. P. The Aerodynamics of Hovering Insect Flight V. A Vortex Theory. *Philos. Trans. R. Soc. London* **B,** 115–144 (1984).

47. Stepniewski, W. Z. & Keys, C. N. *Rotary-Wing Aerodynamics*. (1984).

48. Ho, S., Nassef, H., Pornsinsirirak, N., Tai, Y. C. & Ho, C. M. Unsteady aerodynamics and flow control for flapping wing flyers. *Prog. Aerosp. Sci.* **39,** 635–681 (2003).

49. Ennos, R. A. The Importance of Torsion in the Design of Insect Wings. *J. Exp. Biol.* **140,** 137–160 (1988).

50. Ennos, A. R. The inertial cause of wing rotation in Diptera. *J. Exp. Biol.* **140,** 161–169 (1988).

51. Ennos, R. A. The kinematics and aerodynamics of the Free Flight of some Diptera. *J. Exp. Biol.* **142,** 49–85 (1989).

52. Ellington, C. P., vandenBerg, C., Willmott, A. P. & Thomas, A. L. R. Leading-edge vortices in insect flight. *Nature* **384,** 626–630 (1996).

53. Polhamus, E. C. Predictions of vortex-lift characteristics by a leading-edge suction analogy. *J. Aircr.* **8,** 193–199 (1971).

54. Kuethe, A. M. & Chow, C. *Foundations of aerodynamics : bases of aerodynamic design*. (J. Wiley, 1998).

55. Nabawy, M. R. A. & Crowther, W. J. The role of the leading edge vortex in lift augmentation of steadily revolving wings : a change in perspective. *J. R. Soc. Interface* **14,** 20170159 (2017).

56. Venkata, S. K. & Jones, A. R. Leading-Edge Vortex Structure over Multiple Revolutions of a Rotating Wing. *J. Aircr.* **50,** 1312–1316 (2013).

57. Ellington, C. P., van den Berg, C., Willmott, A. P. & Thomas, A. L. R. Leading-edge vortices in insect flight. *Nature* **384,** 626–630 (1996).

58. Moore, G. E. Cramming more components onto integrated circuits. *Electronics* **38,** 114–117 (1965).

59. Corben, H. C. Wing-beat frequencies, wing-areas and masses of flying insects and hummingbirds. *J. Theor. Biol.* **102,** 611–623 (1983).

60. Kutsch, W., Van Der Wall, M. & Fischer, H. Analysis of free forward flight of Schistocerca gregaria employing telemetric transmission of muscle potentials. *J. Exp. Zool.* **284,** 119–129 (1999).

61. Schilstra, C. & Hateren, J. H. Blowfly flight and optic flow. I. Thorax kinematics and flight dynamics. *J. Exp. Biol.* **202,** 1481–1490 (1999).

62. Dudley, R. & Ellington, C. P. Mechanics of forward flight in bumblebees. II. Quasi-steady lift and power requirements. *J. Exp. Biol.* **148,** 53–88 (1990).

63. Richard Hartley, A. Z. *Multiple View Geometry*. *Journal of Chemical Information and Modeling* **53,** (2003).

64. Ristroph, L., Berman, G. J., Bergou, A. J., Wang, Z. J. & Cohen, I. Automated hull reconstruction motion tracking (HRMT) applied to sideways maneuvers of free-flying insects. *J. Exp. Biol.* **212,** 1324–1335 (2009).

65. Walker, S. M., Thomas, A. L. R. & Taylor, G. K. Photogrammetric reconstruction of high-resolution surface topographies and deformable wing kinematics of tethered locusts and free-flying hoverflies. *J. R. Soc. Interface* **6,** 351–366 (2009).

66. Bomphrey, R. J., Nakata, T., Phillips, N., Walker, S. M. & Video, S. Smart wing rotation and trailing-edge vortices enable high frequency mosquito flight. doi:10.1038/nature21727

67. Willmott, A. P. & Ellington, C. P. The mechanics of flight in the hawkmoth Manduca sexta. I. Kinematics of hovering and forward flight. *J. Exp. Biol.* **200,** 2705–2722 (1997).

68. Walker, S. M., Thomas, A. L. R. & Taylor, G. K. Deformable wing kinematics in the desert locust: how and why do camber, twist and topography vary through the stroke? *J. R. Soc. Interface* **6,** 735–747 (2009).

69. Young, J., Walker, S. M., Bomphrey, R. J., Taylor, G. K. & Thomas, A. L. R. Details of insect wing design and deformation enhance aerodynamic function and flight efficiency. *Science* **325,** 1549–1552 (2009).

70. Vanella, M., Fitzgerald, T., Preidikman, S., Balaras, E. & Balachandran, B. Influence of flexibility on the aerodynamic performance of a hovering wing. *J.*

Exp. Biol. **212,** 95–105 (2009).

71. Du, G. & Sun, M. Aerodynamic effects of corrugation and deformation in flapping wings of hovering hoverflies. *J. Theor. Biol.* **300,** 19–28 (2012).

72. Du, G. & Sun, M. Effects of unsteady deformation of flapping wing on its aerodynamic forces. *Appl. Math. Mech. (English Ed.* **29,** 731–743 (2008).

73. Du, G. & Sun, M. Effects of wing deformation on aerodynamic forces in hovering hoverflies. *J. Exp. Biol.* **213,** 2273–2283 (2010).

74. Sun, M. & Tang, J. Unsteady aerodynamic force generation by a model fruit fly wing in flapping motion. *J. Exp. Biol.* **205,** 55–70 (2002).

75. Bos, F. M., Lentink, D., Van oudheusden, B. W. & Bijl, H. Influence of wing kinematics on aerodynamic performance in hovering insect flight. *J. Fluid Mech.* **594,** 341–368 (2008).

76. Lu, H., Lua, K. B., Lim, T. T. & Yeo, K. S. Aerodynamics of a two-dimensional hovering wing in ground effect. 7–10 (2014).

77. Brackenbury, J. H. Wing Folding in Beetles. in *BT - IUTAM-IASS Symposium on Deployable Structures: Theory and Applications* (eds. Pellegrino, S. & Guest, S. D.) 37–44 (Springer Netherlands, 2000).

78. Haas, F. & Beutel, R. G. Wing folding and the functional morphology of the wing base in Coleoptera. *Zoology* **104,** 123–141 (2001).

79. Saito, K., Nomura, S., Yamamoto, S., Niyama, R. & Okabe, Y. Investigation of hindwing folding in ladybird beetles by artificial elytron transplantation and microcomputed tomography. *Proc. Natl. Acad. Sci.* **114,** 5624–5628 (2017).

80. Saito, K., Yamamoto, S., Maruyama, M. & Okabe, Y. Asymmetric hindwing foldings in rove beetles. *Proc. Natl. Acad. Sci.* **111,** 16349–16352 (2014).

81. Haas, F. & Wootton, R. J. Two basic mechanisms in insect wing folding. *Proc. R. Soc. B-Biological Sci.* **263,** 1651–1658 (1996).

82. Deiters, J., Kowalczyk, W. & Seidl, T. Simultaneous optimisation of earwig hindwings for flight and folding. *Biol. Open* **5,** 638–644 (2016).

83. Faber, J. A., Arrieta, A. F. & Studart, A. R. Bioinspired spring origami. *Science (80-.).* **359,** 1386–1391 (2018).

84. Smith, D. S. The organization of the flight muscle in a dragonfly, Aeshna Sp. (Odonata). *J. Biophys. Biochem. Cytol.* **11,** 119–145 (1961).

85. McGavin, G. & Lewington, R. *Essential Entomology: An Order-by-order Introduction*. (Oxford University Press, 2001).

86. Ruxton, G. D., Sherratt, T. N. & Speed, M. P. *Avoiding Attack: The Evolutionary Ecology of Crypsis, Warning Signals and Mimicry*. (Oxford University Press, 2004). doi:10.1093/acprof:oso/9780198528609.001.0001

87. Baker, P. S., Gewecke, M. & Cooter, R. J. The natural flight of the migratory locust, Locusta migratoria L. - III. Wing-beat frequency, flight speed and attitude. *J. Comp. Physiol. □ A* **141,** 233–237 (1981).

88. Beil, M., Horn, H. & Schwabe, A. Analysis of pollen loads in a wild bee community (Hymenoptera : Apidae) – a method for elucidating habitat use and foraging distances. *Apidologie* **39,** 456–467 (2008).

89. Crall, J. D., Ravi, S., Mountcastle, A. M. & Combes, S. A. Bumblebee flight

performance in cluttered environments: effects of obstacle orientation, body size and acceleration. *J. Exp. Biol.* **218,** 2728–2737 (2015).

90. Unwin, D. M. & Corbet, S. A. Wingbeat frequency, temperature and body size in bees and flies. *Physiol. Entomol.* **9,** 115–121 (1984).

91. Mayhew, P. J. Why are there so many insect species? Perspectives from fossils and phylogenies. *Biol. Rev.* **82,** 425–454 (2007).

92. Ding, S., Li, X., Wang, N., Cameron, S. L. & Mao, M. The Phylogeny and Evolutionary Timescale of Muscoidea (Diptera : Brachycera : Calyptratae) Inferred from Mitochondrial Genomes. 1–17 (2015). doi:10.1371/journal.pone.0134170

93. Yeates, D. K., Wiegmann, B. M., Courtney, G. W. & Meier, R. Phylogeny and systematics of Diptera : Two decades of progress and prospects *. **590,** 565–590 (2007).

94. Pringle, J. W. S. The Gyroscopic Mechanism of the Halteres of Diptera. *Philos. Trans. R. Soc. B Biol. Sci.* **233,** 347–384 (1948).

95. Nalbach, G. The halteres of the blowfly Calliphora - I. Kinematics and dynamics. *J. Comp. Physiol. A* **173,** 293–300 (1993).

96. Nalbach, G. & Hengstenberg, R. The halteres of the blowfly Calliphora - II. Three-dimensional organization of compensatory reactions to real and simulated rotations. *J. Comp. Physiol. A* **175,** 695–708 (1994).

97. Dickinson, M. H. Haltere-mediated equilibrium reflexes of the fruitfly , Drosophila melanogaster. 903–916 (1999). doi:10.1098/rstb.1999.0442

98. Boström, J. E. *et al.* Ultra-Rapid vision in birds. *PLoS One* **11,** 3–9 (2016).

99. Autrum, H. Über das zeitliche Auflösungsvermögen des Insektenauges. *Nachr. Ges. Wiss. Göttingen, Math.-physik. Kl.* **2,** 13–18 (1948).

100. Dudley, R. *The Biomechanics of Insect Flight: Form, Function, Evolution*. (Princeton University Press, 2002).

101. Vogel, S. Flight in Drosophila II. Variation in stroke parameters and wing contour. *J. Exp. Biol.* **46,** 383–392 (1967).

102. Vogel, S. Flight in Drosophila: III. Aerodynamic Characteristics of Fly Wing Sand Wing Models. *J. Exp. Biol.* **46,** 431–443 (1967).

103. Fry, S. N., Sayaman, R. & Dickinson, M. H. The aerodynamics of hovering flight in Drosophila. *J. Exp. Biol.* **208,** 2303–2318 (2005).

104. Gidaszewski, N. A., Baylac, M. & Klingenberg, C. P. Evolution of sexual dimorphism of wing shape in the Drosophila melanogaster subgroup. *BMC Evol. Biol.* **9,** (2009).

105. Ray, R. P., Nakata, T., Henningsson, P. & Bomphrey, R. J. Enhanced flight performance by genetic manipulation of wing shape in Drosophila. *Nat. Commun.* **7,** 10851 (2016).

106. Menezes, B. F., Vigoder, F. M., Peixoto, A. A., Varaldi, J. & Bitner-Mathe, B. C. The influence of male wing shape on mating success in Drosophila melanogaster. *Anim. Behav.* **85,** 1217–1223 (2013).

107. Von Schilcher, F. The function of pulse song and sine song in the courtship of Drosophila melanogaster. *Anim. Behav.* **24,** 622–625 (1976).

108. Aak, A. & Knudsen, G. K. Sex differences in olfaction-mediated visual acuity in blowflies and its consequences for gender-specific trapping. *Entomol. Exp. Appl.* **139,** 25–34 (2011).

109. Aak, A., Knudsen, G. K. & Soleng, A. Wind tunnel behavioural response and field trapping of the blowfly Calliphora vicina. *Med. Vet. Entomol.* **24,** 250–257 (2010).

110. Marshall, S. A. *Flies: The Natural History & Diversity of Diptera*. (Firefly Books, 2012).

111. Colyer, C. N. & Hammond, C. O. *Flies of the British Isles*. (Frederick Warne & Co. Ltd., 1968).

112. Bharti, M. Studies on life cycles of forensically important flies , Calliphora vicina and Musca domestica nebulo at different temperatures. *J. Entomol. Res.* **33,** 273–275 (2009).

113. Faucherre, J., Cherix, D. & Wyss, C. Behavior of Calliphora vicina (Diptera, Calliphoridae) under extreme conditions. *J. Insect Behav.* **12,** 687–690 (1999).

114. Laparie, M. *et al.* Wing morphology of the active flyer Calliphora vicina (Diptera: Calliphoridae) during its invasion of a sub-Antarctic archipelago where insect flightlessness is the rule. *Biol. J. Linn. Soc.* **119,** 179–193 (2016).

115. Deonier, C. C. Carcass Temperatures and Their Relation to the Winter Blowfl Populations and Activity in the Southwest. *J. Econ. Entomol.* **33,** 166–170 (1940).

116. Nuorteva, P. Studies on the significance of flies in the transmission of

poliomyelitis. IV. The composition of the blowfly fauna in different parts of Finland during the year 1958. *Ann. Entomol. Fenn.* **25,** 137–162 (1959).

117. Wicklein, M. *et al.* Sexual Dimorphism in Calliphora vicina. in *Animal Vision Conference* (2012).

118. MacLeod, J. & Donnelly, J. Dispersal and Interspersal of Blowfly Populations. *J. Anim. Ecol.* **32,** 1–32 (1963).

119. Davies, L. Lifetime reproductive output of Calliphora vicina and Lucilia sericata in outdoor caged and field populations; flight vs. egg production? *Med. Vet. Entomol.* **20,** 453–458 (2006).

120. Balint, C. N. & Dickinson, M. H. Neuromuscular control of aerodynamic forces and moments in the blowfly, Calliphora vicina. *J. Exp. Biol.* **207,** 3813–3838 (2004).

121. Balint, C. N. & Dickinson, M. H. The correlation between wing kinematics and steering muscle activity in the blowfly Calliphora vicina. *J. Exp. Biol.* **204,** 4213–4226 (2001).

122. Walker, S. M. *et al.* In Vivo Time-Resolved Microtomography Reveals the Mechanics of the Blowfly Flight Motor. *PLoS Biol.* **12,** e1001823 (2014).

123. Tu, M. & Dickinson, M. Modulation of Negative Work Output From a Steering Muscle of the Blowfly Calliphora Vicina. *J. Exp. Biol.* **192,** 207–24 (1994).

124. Tu, M. S. & Dickinson, M. H. The control of wing kinematics by two steering muscles of the blowfly (Calliphora vicina). *J. Comp. Physiol. A.* **178,** 813–830 (1996).

125. Dickinson, M. H. & Tu, M. S. The function of dipteran flight muscle. *Comp. Biochem. Physiol. - A Physiol.* **116,** 223–238 (1997).

126. Geurten, B. R. H., Kern, R., Braun, E. & Egelhaaf, M. A syntax of hoverfly flight prototypes. *J. Exp. Biol.* **213,** 2461–2475 (2010).

127. Braun, E., Geurten, B. & Egelhaaf, M. Identifying prototypical components in behaviour using clustering algorithms. *PLoS One* **5,** (2010).

Chapter 2

Assessment of *k*-means clustering as a method for partitioning dipteran body kinematics

Assessment of *k*-means clustering as a method for partitioning dipteran body kinematics

Inés L. Dawson*, Graham K. Taylor*, Simon M. Walker†

* Oxford Flight Group, University of Oxford, The John Krebs Field Station, Department of Zoology, Wytham, Oxford, OX2 8QJ, UK

† Faculty of Biological Sciences, University of Leeds, Leeds, LS2 9JT, UK

Insect flight is a complex behaviour, and the interaction between the wing and body kinematic parameters of free-flying insects has not yet been fully explored. Recent studies have suggested that clustering may be a useful tool for categorising distinct but coupled flight behaviours to create a syntax of insect flight. We applied an adapted version of the *k*-means clustering algorithm to the body kinematic parameters of free-flying *Drosophila melanogaster* (fruit fly) and *Eristalis tenax* (hoverfly) to detect distinct flight modes and associate them with their characteristic wing beat kinematics. We found that neither fruit flies nor hoverflies exhibit distinct flight modes, but rather shift continuously between different body kinematics. This rejects the claim of a 'syntax' of insect flight, and suggests that clustering algorithms are not an appropriate method for characterising dipteran flight, and claims of an insect flight syntax founded upon such methods should therefore be treated with scepticism.

INTRODUCTION

The mechanisms underpinning the generation of lift and manoeuvre performance under the conditions in which insects fly have captivated scientists for decades. Significant technological developments, such as increased computational power, the use of high-speed videography, particle image velocimetry (PIV), computational fluid dynamics (CFD) and electrophysiology have broadened our general understanding of how insects interact with the air around them in general terms[1,2,11–15,3–10]. Nevertheless, there is still plenty to be learnt about how different insects carry out different aerial manoeuvres.

In terms of process, insect flight goes beyond pure mechanism. It is the result of the integration of genetics, wing and muscle structure, intricate neural circuitry, sensory input, motor output and aerodynamics. Deciphering the extent to which different kinematics vary in order to generate different aerial manoeuvres will contribute to our understanding of how these different components interact. Nonetheless, an endeavour of this kind requires both a large volume of wing beats and a suitable strategy to reduce the kinematic data to subsets that are more meaningful for analysis.

One way of reducing the tiers of complexity involved in insect flight is to group similar or frequently co-occurring behaviours together. With the aid of clustering algorithms, it is possible to break down flight behaviour from a set of continuous parameters into a set of categories that describe similar parametric measures, such as hovering flight, forward flight and saccades. There is evidence that certain translational and rotational body kinematics are coupled during some stages of insect flight. In order to remain airborne and generate aerial manoeuvres, an insect

needs to make sequential adjustments to its body and wing beat kinematics. Examples of such sequential motions include the characteristic saccadic motions or body adjustments associated with forward flight[16,17,26–34,18–25]. Body pitch and forward speed, for example, are inversely correlated in flying insects, since to a first approximation, the flapping wings act as a simple actuator disk, whose output depends on the body angle relative to the horizontal plane when the stroke plane angle is kept fixed to the body pitch[25–27,35]. The angle of attack and the resulting output forces produced during forward flight also depend on the stroke plane angle[25]. It has been noted that, at higher speeds, the stroke plane angle is adjusted to become more inclined with respect to the horizontal plane, although the degree to which they are associated has not so far been fully explored[27]. Increase in forward speed has been associated with a slight decrease in stroke amplitude in some insects, such as *Locusta migratoria* and *Manduca sexta*, but not in others, such as *Drosophila melanogaster*[27,32,36,37]. Furthermore, many dipteran species such as *Drosophila* and *Eristalis* also engage in the sudden turns interspersed between segments of forward flight, known as saccades[16–18,21,22,24,38,39]. Dipteran species of the suborder Brachycera have also been noted to have steering muscles that operate like switches, enabling the individual to adjust its wing beat kinematics in flight[7,34,40–43].

Some attention has been devoted to the partitioning insect flight activity into prototypical movements that can be characterised in terms of measures of relevant body kinematics[44–46]. Geurten *et al.* 2010 employed clustering techniques to compartmentalise the flight manoeuvres of free-flying hoverflies into prototypical movements (PMs) and determined the probabilities of transitioning between different PMs. Their objective was to arrive at a 'syntax' of hoverfly flight[44,45].

Identifying individual clusters in flight could prove useful for determining whether specific changes in flight patterns occur in *Drosophila*, since if this were the case, it might be the result of gear changes like those found in other Dipteran species[34,40,47]. However, it remains to be shown whether gear changes map onto discrete clusters of body kinematics. In addition, clustering algorithms provide a way of simplifying and reducing the dimensionality of the data. From the perspective of a control model of insect flight, determining which parameters play a major role in particular manoeuvres would offer valuable insights into which neuromotor pathways are involved in triggering specific flight motions[6–8,46]. Finally, clustering the data and establishing the relationship between body kinematics and their respective wing kinematics would be useful for researching wing kinematics associated with certain characteristic body motions. By exploring body kinematics that relate exclusively to forwards flight, the link between body position, velocity and different wing kinematics can be properly determined.

The objectives of this study are firstly, to explore an adapted *k*-means clustering algorithm as a method for assessing the potential for clustering the body kinematic parameters of free-flying *Drosophila melanogaster*, and secondly, to test the replicability and reliability of Geurten's results[44,45] using a larger dataset of free-flying *Eristalis tenax*[40].

METHODS

Two datasets were employed in this analysis. The *Eristalis tenax* dataset, that was used to contrast the results found by Geurten was supplied by Walker et al. 2012 and comprised the body kinematic parameters for 26451 wing beats from 879 recordings of 36 individual hoverflies[40]. The *Drosophila melanogaster* dataset was collected using similar techniques to the *Eristalis tenax* dataset.

Drosophila dataset

Rearing

Drosophila melanogaster (Oregon R) fruit flies were reared at 20°C under a 12:12 light/dark cycle and under two different experimental conditions: high-density and low-density. Under high-density rearing conditions, there were 8 laying females per vial, and under low-density rearing conditions, there were 5 females per vial. The laying adults were placed on new food every morning. Adult flies emerged in early October 2014. Adult flies that had emerged on the same day and at the same rearing density were placed in the same vial and were segregated by sex. Although individual flies were not recorded, their eclosion date, sex and rearing-density conditions were known.

Free-flight recording

Flight experiments took place in a transparent polyester cylinder of 30cm length x 20cm diameter in which the fruit flies were able to fly freely. Flies selected for flight were at least 5 days old to ensure their wings had fully developed. Between 5 and 20 fruit flies were present in the recording chamber, all of the same sex, age and rearing density and recordings were made over a period of up to 5 hours. Once

a recording block was terminated, the flies were not reused for collecting recordings. Recordings were captured by four Photron FASTCAM SA3 high-speed cameras (Photron Ltd, Bucks, UK) with 180mm macro lenses running at 4800fps and resolution of 640x576px. Backlight illumination was provided by two 805nm 200W infrared pulsed lasers (HIS-5000, Oxford Lasers Ltd, Oxford, UK), both routed through two split liquid light guides. Each light guide delivered short pulses of 20μs through a collimating Fresnel lens synchronised with the camera frame rate. The Fresnel lens collimates the light and provides sufficient illumination to eliminate motion blur at such a high exposure time but without interfering with the flight path of the insects. Since the infrared wavelength lies outside the perceptible light spectrum of fruit flies, it does not constitute a visual disturbance to them[48].

Flight was prompted by mechanically vibrating the cylinder, using cotton balls dipped in vinegar and ethanol as attractors. Recordings were initiated both manually and by IR triggers connected to the Photron recording programme. Temperature in the recording arena varied between 23 and 28˚C. Each fly recording was accompanied by data regarding age, date and time of recording, air temperature, sex and rearing-density.

Flight processing

The cameras were calibrated using custom-written photogrammetric software running in MATLAB (MATLAB R2013b, 8.2.0.701, The MathWorks Inc. Natick MA, 2013). Flight recordings were processed using custom-written *Drosophila* tracker software adapted and optimised from the *Eristalis* tracking software written by Walker[40,49]. The tracker uses an automatic shape-carving algorithm that uses each camera perspective to calculate the voxels corresponding to the body and wings. The

body kinematic measurements of position and orientation were smoothed using a quantic smoothing spline, with a tolerance factor calculated from the residuals of fitting a third-order Butterworth filter and a cut-off frequency of 150Hz for the body parameters of *Drosophila* and 80Hz for Eristalis, so as to minimise the contamination of body kinematic parameters by the wing beat motion.

Two axis systems were employed to describe the kinematic parameters and body positions:

Lab-fixed coordinate system

The lab-fixed coordinate system is a right-handed inertial axis system $\{x_W, y_W, z_W\}$, where the z_W axis points in the direction of gravity, and the x_W and y_W axes are directed arbitrarily in the horizontal plane. The origin of this coordinate system is arbitrary.

Primary body-fixed coordinate system

The body-fixed axis system is a rotating right-handed axis system $\{x_B, y_B, z_B\}$, with its origin located at the centre of mass of the insect. The x_B axis is defined as the anterior-posterior body axis, and the y_B axis points towards the right, passing through the wing bases. It follows from these definitions that the z_B axis points ventrally.

The translational parameters measure the position, velocity and acceleration of the body with respect to the lab-fixed axis system $\{x_W, y_W, z_W\}$, where the velocity and acceleration components may be resolved in either the lab-fixed axis system $\{x_W, y_W, z_W\}$, the primary body-fixed axis system $\{x_B, y_B, z_B\}$, or the horizontal body-fixed axis system $\{x_H, y_H, z_H\}$. For notational simplicity, we assume the components

are resolved in the primary body-fixed axis system unless specified otherwise by an L or H subscript. The rotational parameters describe the orientation and angular velocity of the primary body-fixed axis system $\{x_B, y_B, z_B\}$, with respect to the lab-fixed axis system $\{x_W, y_W, z_W\}$, where the angular velocity components are resolved exclusively in the primary body-fixed axis system $\{x_B, y_B, z_B\}$.

Nomenclature:

$[x, y, z]$ Position of the centre of mass of the insect, i.e. position of $\{x_B, y_B, z_B\}$ with respect to $\{x_W, y_W, z_W\}$. Units: m.

$[u, v, w]$ Velocity of the centre of mass of the insect, i.e. velocity of $\{x_B, y_B, z_B\}$ with respect to $\{x_W, y_W, z_W\}$. For convenience we refer to u_B as forwards velocity, and u_H as heading velocity, where by definition u_H is simply the projection of u_B onto the horizontal. Similarly, we refer to w_H as the upwards velocity. Units: ms^{-1}.

$[\dot{u}, \dot{v}, \dot{w}]$ Acceleration of the centre of mass of the insect, i.e. acceleration of $\{x_B, y_B, z_B\}$ with respect to $\{x_W, y_W, z_W\}$. We refer to $\dot{w}_H$ as the upwards acceleration. Units: ms^{-2}.

$[\varphi,\theta,\psi]$ Orientation of $\{x_B, y_B, z_B\}$ with respect to $\{x_W, y_W, z_W\}$, expressed as a sequence of Euler angles in the order φ,θ,ψ, where φ is bank angle, θ is pitch angle, ψ is yaw angle. Units: deg.

$[p, q, r]$ Angular velocity of the insect, where p is roll rate, q is pitch rate, and r is yaw rate. Units: deg s^{-1}.

K-means clustering algorithm

K-means clustering is an algorithmically simple form of cluster analysis. For a predetermined number of *k* clusters, *k*-means clustering assigns each data point from the data set to one of *k* centroids. The aim is to minimise the total distance between the data points and their centroids. These calculations are performed iteratively. The initial placement of the centroids is assigned randomly, and all data points are assigned to the centroid coordinates closest to them, thus forming a cluster. In successive iterations, centroid coordinates are recalculated so as to minimise the distance between all points assigned to each cluster. Since the cluster centres have moved, the data points assigned to each centroid are recalculated. This process is iterated until either the centroid positions and data points assigned to each one fulfil some specific predetermined criterion, such as a maximum number of algorithm iterations or until the centroid positions vary below a preselected tolerance threshold.

K-means clustering has several disadvantages associated with the assumptions it makes:

a) The iterative nature of the algorithm allows for the possibility of centroid positions converging on a local minimum as a consequence of the initial placement of the centroid coordinates. This can be overcome by running multiple replicates of the programme, thus creating a trade-off between computational time and robust results.

b) *K*-means clustering is best suited to detecting clusters that are spherical and elliptical in shape, but is not the best clustering option for detecting clusters forming different topological shapes. Hence, data that clusters in concentric circles or

elongated clusters, where the intra-cluster point distance is less than the inter-cluster distance, are poor candidates for this clustering algorithm. In multidimensional systems, the structure of the clusters is difficult to visualise and predict *a priori*. This requires a way of determining the quality of the clusters located.

c) *K*-means clustering requires the number of clusters for detection to be specified beforehand. Since, in certain situations, this is unknown, a way is needed to determine in advance the number of clusters to be found.

In order to find clusters in our dataset that would be indicative of the presence of prototypical flight behaviour or predetermined flight modes, we followed a method similar to the one presented by Geurten[44,45] for *Eristalis tenax* kinematic data.

1. *K*-means parameters

In order to associate body kinematics with specific prototypical movements, Geurten et al. used just five parameters: $[u, v, w]$ and $[\sim, q, r]$. Geurten's dataset had only accounted for roll velocity for a portion of their dataset, and the parameter was excluded from their model. Our dataset employed eight parameters: the translational body velocities $[u, v, w]$, the angular body velocities $[p, q, r]$, bank angle φ and the body tilt angle θ. We elected to include bank angle and the body tilt angle, as they are known to be associated with different manoeuvres, such as turns and forward flight respectively. Yaw angle was not included as a parameter in the clustering analysis, because its value depends on which direction the fly is facing at the beginning of each recording, which is arbitrary in the recording volume. The yaw

angle therefore provides no specific kinematic information other than to serve as a reference point for changes from the initial position.

The parameters were all z-scored. Z-scoring enables comparisons of variables from separate distributions by converting each element into a variable in the context of a standard normal distribution with a mean of 0 and standard deviation of 1. Because certain movements can be performed in the same manner in both the clockwise and anticlockwise directions, these were adjusted for in the following manner: r was treated as an absolute value, and the remaining parameters of v, q and φ were signed conditionally, depending on whether their pre-z-scored signs were the same as the yaw velocity sign.

2. Determination of *k*

The number of clusters present in the data was not known *a priori*. Geurten[44,45] employed a combination of two methods to evaluate the quality and stability of the clusters generated and to determine the optimal number of clusters into which to partition their data. The Geurten quality measure assesses whether the clusters represent distinct clouds of data points. The stability measure assesses the repeatability of the clusters when the starting conditions and the dataset are altered. Optimising both measures indicates the best number of clusters for further analysis of the dataset.

2.1 Stability variation

In order to verify whether the same clusters were found in separate algorithm runs, we bootstrapped the data, omitting half of the flight sequences in each run for

Drosophila melanogaster. Based on estimates from 100,000 test runs, this bootstrapping method eliminates 50±2.3 % (mean ± one standard deviation) of the data, due to the unequal length of the flight sequences. To account for its larger dataset size, 90% of sequences were omitted for *Eristalis tenax*. The initial coordinates of the centroids were generated randomly when running the algorithm. Each bootstrapped value was run 128 times, with 100 replicates and 100 iterations, for a number of clusters *k* increasing from 2 to 30 inclusive in integer steps.

In order to measure cluster stability, we tested to see whether successive iterations of the algorithm produced similar centroid positions. To evaluate whether the centroid coordinates found in two separate runs A and B of the *k*-means algorithm were sufficiently similar, we computed the Euclidean distance between a list of all centroid coordinates from run A and all those from run B. The two centroids of A and B that were closest together were paired together as being the same centroid, the distance between the two was recorded and they were removed from the list. The process was repeated successively until all centroids were paired with their closest equivalent in the other run. The total normalised distance was calculated to represent the difference in centroid positions across both runs. Running the programme 128 times with a high number of replicates and iterations increased the chances of distinguishing between overall low distance values that occurred only once and consistently low distance values. The latter would be a sign of stable clusters and evidence of potential good standing in the Geurten quality measure.

2.2 Quality assessment

The Geurten quality measure involved calculating the ratio of inter-cluster to intra-cluster variation. This is measured by calculating the shortest squared Euclidean distance between the centroid coordinates and neighbouring cluster centres divided by the mean squared Euclidean distance between all data points in the cluster. A larger outer distance relative to a small inner distance indicates a distinct cluster and yields a higher Geurten quality measure value. Geurten selected a number of k clusters with a Geurten quality measure score of 1.5, which represented the maximum score obtained in their dataset. Values under 1 indicate that the average distance between clusters is no different from the average distance between points. Based on Geurten's assessment, values above 1.3 show a more promising structure from the point of view of clear cluster definition is concerned, albeit not necessarily a strong one.

We replicated the Geurten quality measure, and complemented it with the previously described distance value and the silhouette value. The silhouette value, or silhouette score, is a standard score used to interpret and evaluate the results of a cluster analysis both graphically and quantitatively. Silhouette values depend only on the partition of the elements, which means that they are a good way of comparing differences when using the same algorithm for different numbers of clusters[50]. The silhouette values display a measure, ranging from -1 to +1, of how close a point in one cluster is to points in neighbouring clusters. High silhouette values show that the data point is far away from neighbouring clusters, whereas negative values suggest that the point may have been assigned to the wrong cluster. Values close to 0 suggest that the point is on or near the boundary between two neighbouring

clusters. Because the *k*-means algorithm automatically assigns each point to its closest cluster centre, all silhouette values should be non-negative. The mean silhouette score provides an overall evaluation of how good the clusters found by the clustering algorithm is.

As per the literature, mean silhouette values of 0.51 and above suggest that a reasonable to strong structure has been found for the clusters, and a score of >0.71 is highly suggestive of a strong underlying structure. Low silhouette values indicate that the structure found is weak and possibly artificial, and silhouette values <0.25 indicate that there is no substantial structure at all, meaning that many points assigned to one cluster could easily be assigned to a different one[51].

RESULTS

A total of 4054 wingbeats from 265 individual recordings of fruit fly flight and a total of 26451 wingbeats from 879 recordings of 36 free-flying hoverflies were processed and analysed.

A variety of body and wing kinematics were obtained from the processed measurements.

1. Body Kinematics

The univariate distribution of the body kinematic parameters for both *Drosophila melanogaster* and *Eristalis tenax* were unimodal for both species, and presented no unusual features, such as bi- or multimodality, that might suggest different flight modes.

2. Clustering analysis

K-means clustering analysis was performed for 128 paired runs (256 runs for the Geurten quality measures, 128 for the paired distance values) with 100 replicates of a maximum of 100 iterations per replicate for values of k from 2 to 30 clusters.

2.1 Repeatability

Distance values were calculated for the complete dataset, for the bootstrapped data, and for the comparison of the centroid positions between the bootstrapped data and the full dataset. These values are shown for *Drosophila melanogaster* **(Figure 1a)** and *Eristalis tenax* **(Figure 1b)** respectively.

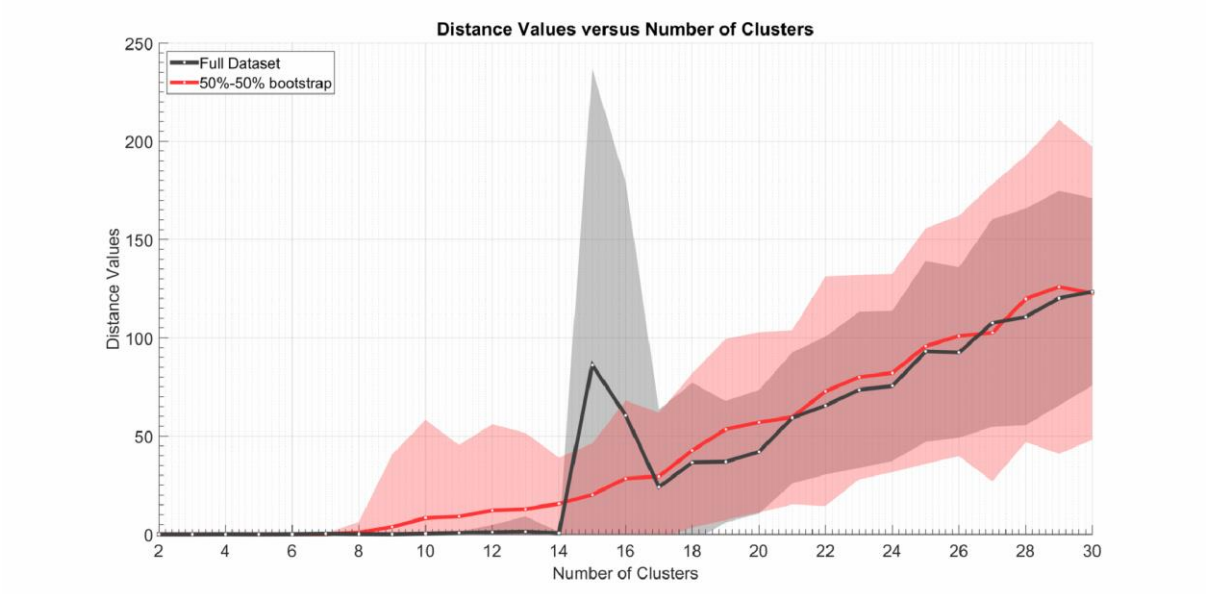

Figure 1a. Plot showing distance values plotted against the number of clusters for the *Drosophila melanogaster* dataset. The figure shows the mean (solid lines) ± one standard deviation (shaded area) distance values between paired runs for the full dataset (black line) and the 50% bootstrapped data (red line). A number of clusters that is repeatable and stable should have low distance values.

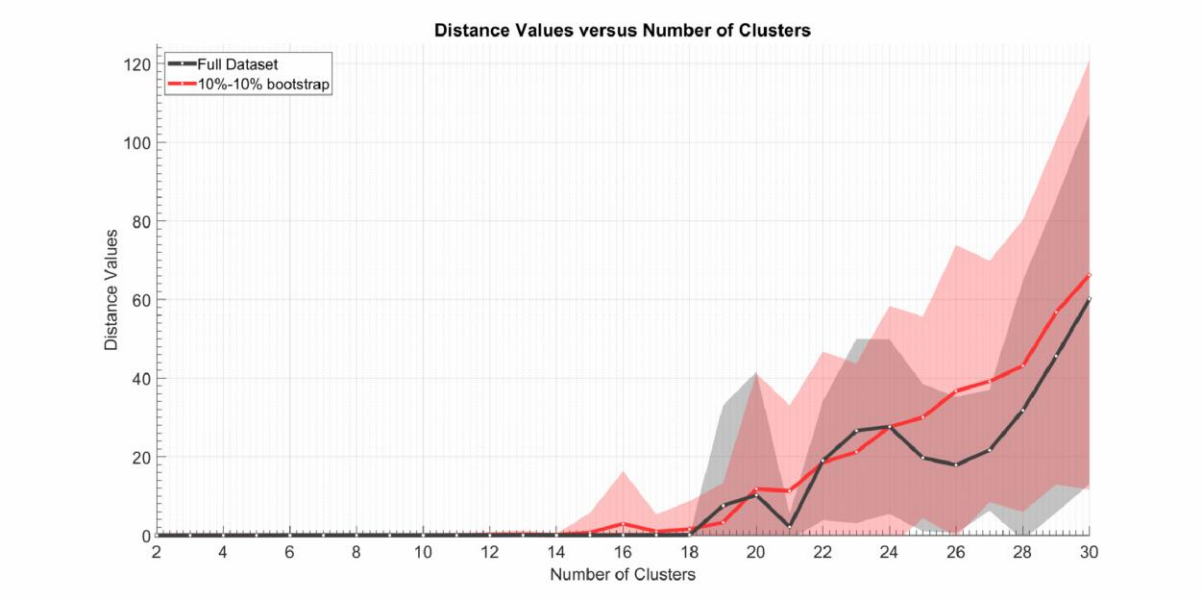

Figure 1b. Distance values plotted against the number of clusters for *Eristalis tenax* dataset. The figure shows the mean (solid lines) ± one standard deviation (shaded area) of the distance values between paired runs for the full dataset (black) and 10% of the bootstrapped data (red). A number of clusters that is repeatable and stable should have low distance values.

In *Drosophila melanogaster*, centroid positions repeat for up to 14 clusters, at which point there is a noticeable spike in distance values at 15 and 16 clusters, followed by a steady linear increase for increasing numbers of clusters. In *Eristalis tenax*, the centroid positions are repeatable for up to 18 clusters. The low distance values indicate that for the same number of iterations, the *k*-means algorithm is most likely to stably converge on the same centroid position coordinates for each *k* number of clusters. Above 16 clusters, the distance values and their variance increase. Distance values decrease non-linearly with an increased number of iterations, which means that many more iterations would be necessary to obtain repeatable and robust centroid positions for more than 14 and 18 clusters for *Drosophila melanogaster* and *Eristalis tenax* respectively.

The distance values for bootstrapped values show that the centroid positions are robust up to around 8 and 15 clusters respectively for *Drosophila* and *Eristalis*

datasets, after which there is a gradual increase in both distance values and variance. The confidence intervals of the bootstrapped values overlap with the non-bootstrapped values, indicating that the clustering algorithm remains similarly robust for up to 30 clusters when applied to 50% and 10% of the *Drosophila melanogaster* and *Eristalis tenax* data compared to the full datasets.

2.2. Geurten quality measure

The ratio of intercluster variation to intracluster variation for *Drosophila melanogaster* **(Figure 1c)** and for *Eristalis tenax* **(Figure 1d)** is expressed below.

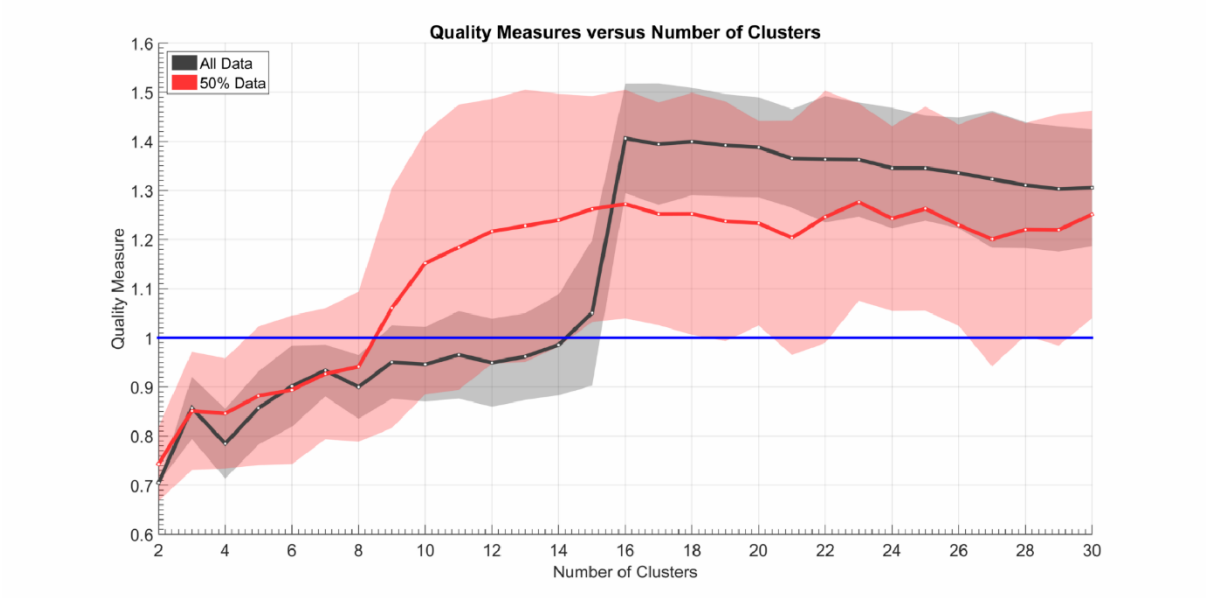

Figure 1c. Geurten quality measure values for *Drosophila melanogaster* for each number of clusters between 2 and 30. The black line represents the Geurten quality measure mean±s.d. for the full dataset; the red line represents the Geurten quality measure mean±s.d. for the 50% bootstrapped data. The blue line at y=1 indicates the point at which inter- and intracluster variation is identical. Values below 1 have more intracluster variation than intercluster variation, whereas values above one have more intercluster variation than intracluster variation. The Geurten Quality Measure is poor until *k* becomes high.

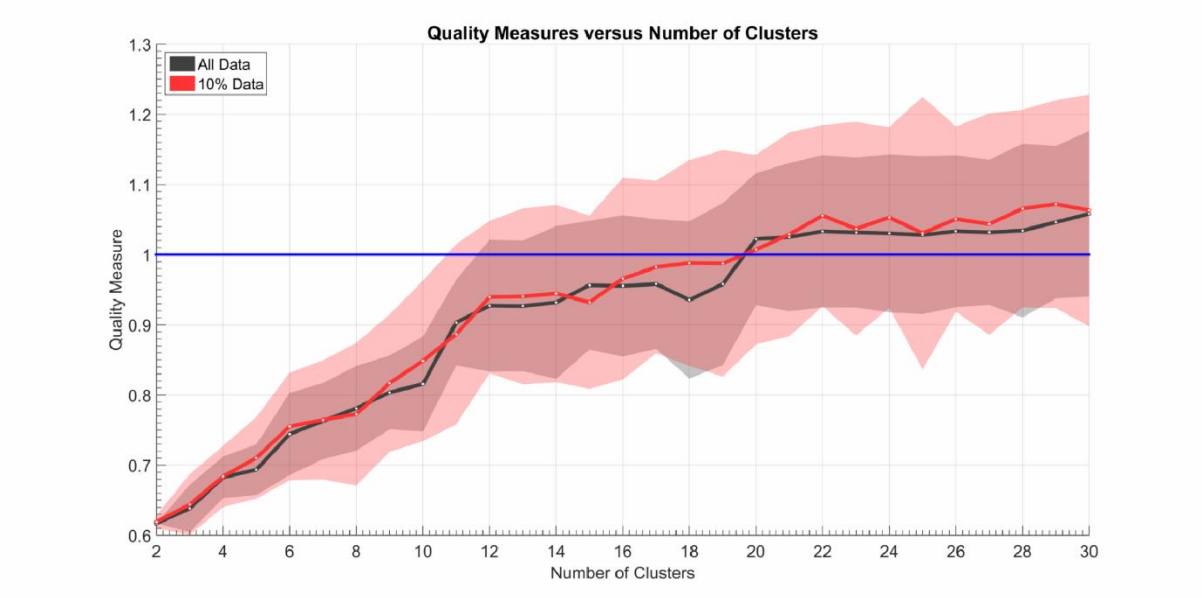

Figure 1d. Geurten quality measure values for *Eristalis tenax* for each number of clusters between 2 and 30. The black line represents the Geurten quality measure mean±s.d. for the full dataset; the line red represents the Geurten quality measure mean±s.d. for the 10% bootstrapped data. The blue line at y=1 indicates the point at which inter- and intracluster variation is identical. Values below 1 have more intracluster variation than intercluster variation, whereas values above one have more intercluster variation than intracluster variation. The Geurten Quality Measure is poor until *k* becomes high.

The Geurten quality measure for the full *Drosophila melanogaster* dataset gradually increases from 0.7 to 0.95 up to 14 clusters. At 16 clusters there is a noticeable spike to a Geurten quality measure of approximately 1.4. Between 16 and 30 clusters, the Geurten quality measure gradually decreases to a mean value of 1.3. These values are still lower than the 1.5 Geurten quality measure observed in Geurten's dataset, and occur at high values of *k* for which the distance values for those cluster values are too great for the centroid positions to be robust and reliable. The Geurten quality measure for the bootstrapped data is much more variable, but is also consistently below the 1.5 value defined by Geurten. The standard deviations are higher for the bootstrapped values, which may be due to the lower density of the data. The Geurten quality measure for *Eristalis tenax* is substantially lower than the

Drosophila dataset and all values are consistently below 1 for the first 20 clusters, but also remain well below the 1.5 Geurten quality measure reported from Geurten's dataset.

The Geurten quality measure is expected to increase as the number of clusters increases as a result of the dataset being partitioned into a higher number of clusters. This is consistent with the trend observed in *Eristalis*. The sharp increase observed in *Drosophila* is surprising, but in spite of this, the Geurten quality measure decreases rather than increases with an increasing number of clusters. Geurten quality measures above 1 correspond to k clusters that are unstable according to distance values. For the stable number of clusters of 14 and below in *Drosophila*, and 18 in *Eristalis*, the Geurten quality measure is consistently below 1. The data therefore shows that, for stable clusters, the intra-cluster variation is greater than intercluster variation, meaning that the clusters found through the k-means clustering algorithm are not well defined.

To test the level of bias in the Geurten quality measure, and whether the use of different numbers of parameters affected the overall value of the Geurten quality measure, we generated a mock dataset including 8 parameters and 5,000 randomly generated values from a Z-distribution per parameter and calculated the mean Geurten quality measure over 25 iterations for 2 to 8 parameters across 2 to 30 clusters in single integer steps **(Figure 2)**. As the number of clusters increased, so did the Geurten quality measure for all numbers of parameters. An increased number of input parameters also increased the offset of the Geurten quality measure; the simulation with 8 input parameters reached a mean Geurten quality measure of over 1.4 for higher cluster values, despite there being no clusters in the

mock dataset. This is a concern, as it could lead to a false structure being identified when there is none. In the case of our dataset, we would expect our results to have a larger Geurten quality measure because we used 8 input parameters rather than 5; as such, the lower Geurten quality measure values obtained from our data are a further indication that there is no structure within the data.

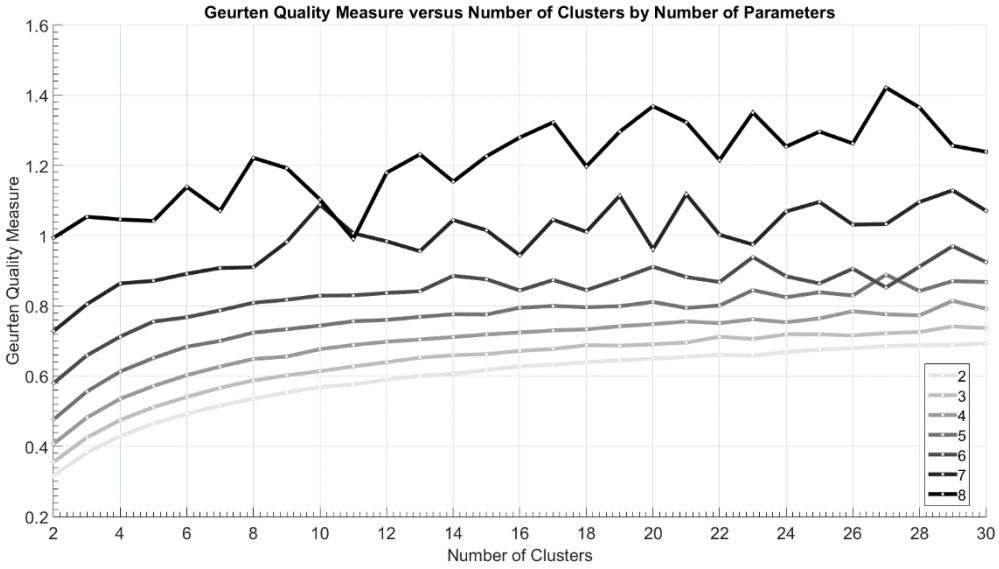

Figure 2. Plot of Geurten Quality Measure from 5,000 randomly generated values from a Z-distribution over 25 iterations for 2 to 8 input parameters across 2 to 30 clusters in single integer increments. Since the dataset is randomly generated, no clusters should be found in the dataset, and an unbiased measurement should therefore produce a constant score for an increasing number of clusters and input parameters.

2.3. Silhouette scores

The silhouette scores were very low, under 0.5, across *Drosophila melanogaster* **(Figure 1e)** and *Eristalis tenax* **(Figure 1f)**, with the exception of 2 clusters. The higher mean silhouette values for the bootstrapped data can also be explained as due to the lower data density. The high silhouette score for two clusters is due a small portion of data being segregated from the rest. In this case, the high

silhouette score at 2 clusters showed a division between the majority of wingbeats exhibiting low rotational body velocity and a minority of wing beats with very high rotational body velocity. This phenomenon is a common artefact in low cluster numbers for large datasets, and does not therefore represent the presence of two solid structures, nor does it encompass the variety of flight manoeuvres performed by *Drosophila melanogaster* and *Eristalis tenax*[50].

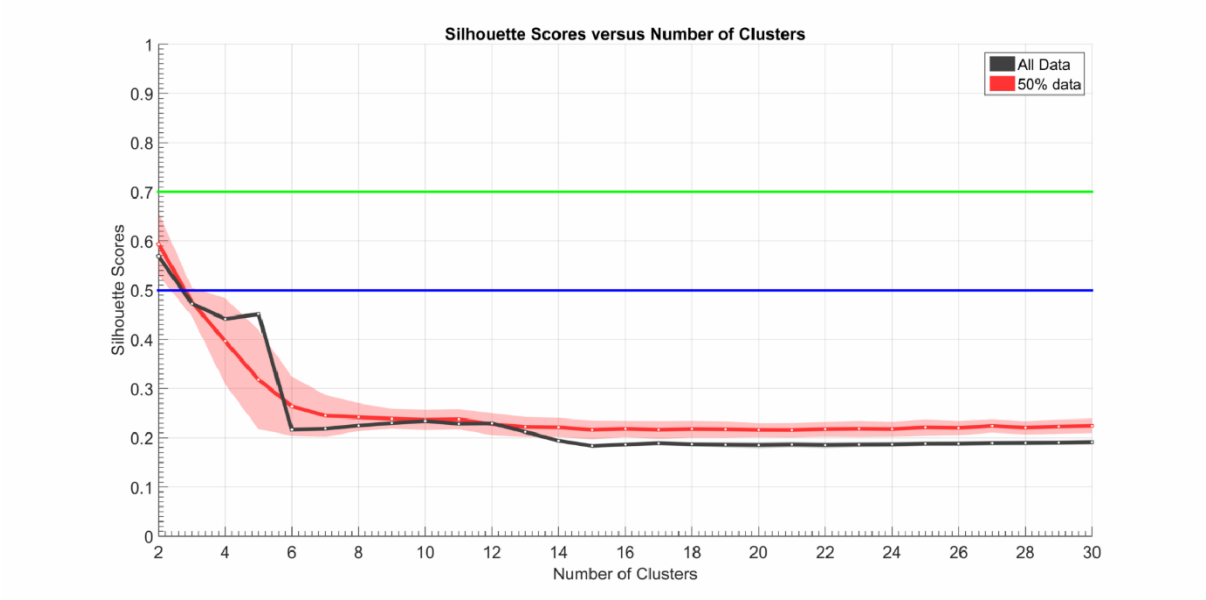

Figure 1e. *Drosophila melanogaster* silhouette score values for each number of clusters between 2 and 30. The black line represents the mean±s.d. silhouette scores for the full dataset; the red line represents the mean±s.d. silhouette scores for the 50% bootstrapped dataset. The blue line represents the threshold for a 'reasonable structure', and the green line represents the threshold for a 'strong structure'[51].

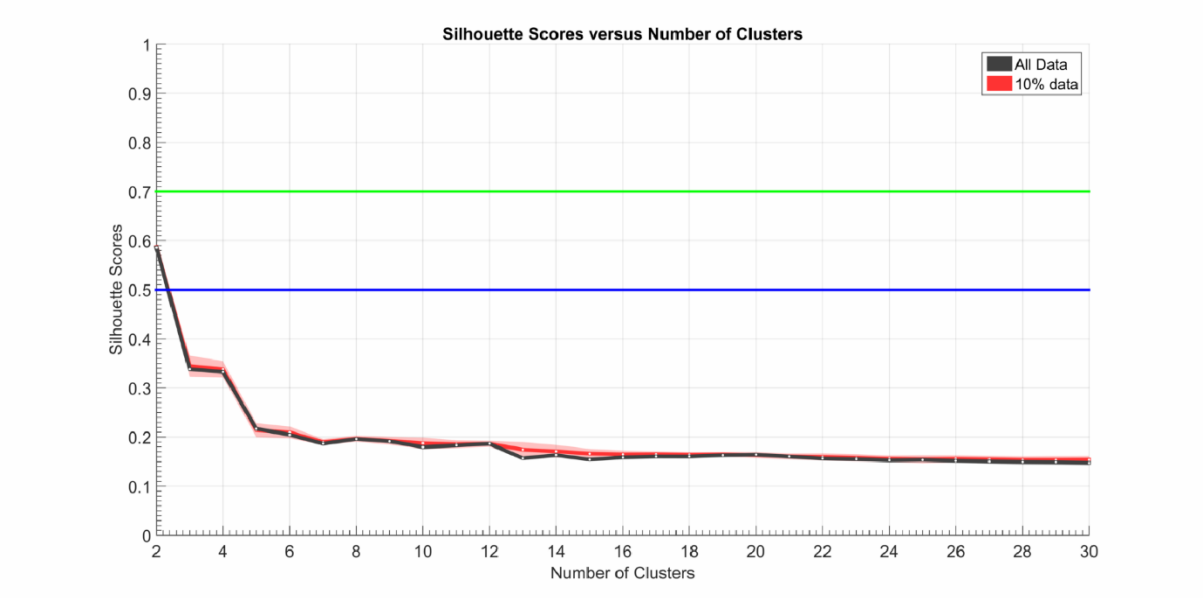

Figure 1f. *Eristalis tenax* silhouette score values for each number of clusters between 2 and 30. The black line represents the mean±s.d. silhouette scores for the full dataset; the red line represents the mean±s.d. silhouette scores for the 10% bootstrapped dataset. The blue line represents the threshold for a 'reasonable structure', and the green line represents the threshold for a 'strong structure'[51].

DISCUSSION

When the observations from the two quality evaluation methods and the repeatability measures were combined, neither the *Drosophila melanogaster* nor the *Eristalis tenax* dataset appeared to partition into an optimal number of clusters, suggesting that there is no evidence for the existence of genuine clusters in the data. It follows that Geurten's methodology is inappropriate for trying to identify a 'syntax of flight' as outlined by Geurten. We replicated Geurten's methodology with a higher resolution dataset based on free-flight data, and used the same species of hoverfly as Geurten. We also took into account additional parameters like bank angle and rolling velocity, which are involved in asymmetrical manoeuvres such as saccades

and evasive manoeuvres, and we extended the evaluation method using standardised silhouette scores.

There are various possible reasons to account for why Geurten et al. arrived at different conclusions. Firstly, Geurten et al. collected their data at a lower frame rate, which would have provided an estimated 2–5 frames per wing beat. This is substantially lower than the resolution used in our dataset. Secondly, the Geurten quality measure increases as the number of clusters increases as a result of the way it is calculated. This introduces an element of bias, as a higher number of clusters is expected to have a higher baseline Geurten quality measure than a lower number of clusters. Thirdly, we used more body kinematic parameters. Lower dimensionality of the data may alter the values of the Geurten quality measure and also introduce systematic bias into the system. We found that a larger number of input parameters increased the offset of the quality measure, and it is surprising therefore that our values were so low in comparison. Finally, Geurten et al. did not accompany their own measure with other quality evaluation measures, such as silhouette scores, which are traditionally used to assess *k*-means clusters. The overall bias in the evaluation method may have led Geurten et al. to attribute more significance than was warranted to an arbitrary conclusion. In view of our results and the methodological bias found, the clustering method employed by Geurten is flawed and the attempt to cluster dipteran flight behaviour on the basis of body kinematics alone may itself be an oversimplification.

Different clustering techniques, such as the mean shift clustering algorithm, or those that do not make strong assumptions about the geometry of the clusters may yield better results. Body kinematics are generally coupled to the wing kinematics,

which are initiated mechanically, which means that the body movements observed are likely to be substantially dampened. Hence, dipteran flight behaviour may be better characterised as continuous transitions across various combinations of body kinematics. The results obtained do not suggest that the flight behaviour of *Eristalis tenax* and *Drosophila melanogaster* can be reliably clustered on the basis of body kinematic parameters alone[40,44,45].

An alternative approach would be to apply a MILCA (Mutual Information based Least-dependent Component Analysis) algorithm, such as the one employed by Chakraborty et al[46]. Rather than classify the entire dataset into discrete categories, the MILCA algorithm is designed to detect specific quasi-periodic patterns in the dataset that can be attributed to time-specific adjustments in body and wing-kinematics[46,52]. Unfortunately, the method employed relies on a specific volume of at least 2,000 consecutive wing beats in order to reliably extract independent components from the data. The mean number of wing beats per free-flight recording was 15±13 wing beats for *Drosophila melanogaster* and 30±22 wing beats for *Eristalis tenax*. Obtaining such a large volume of consecutive wing beats would be viable for tethered flight, but not for free flapping flight at the present time. For this reason, the MILCA algorithm is currently not a good candidate for free-flight datasets.

Whilst the *k*-means clustering algorithm may not be suited to tackling the complex problem of detecting and characterising discrete changes in body kinematics, it is not without its place in insect flight research. It remains a valid technique for partitioning data into a predefined number of categories, which is helpful for reducing the volume of data or exploring well defined areas of available

kinematic spaces, provided that any reduction or partition found by the *k*-means clustering algorithm is not interpreted as representing a discrete set of manoeuvres employed by insects, since the partition is arbitrary. In order to explore discrete changes in flight behaviour, other models with fewer restrictions on cluster geometry and focussing on wing kinematic parameters of interest would be more suitable for exploring the way they are involved in observable adjustments in body kinematics and aerodynamic force generation, and for elucidating how insects generate different flight manoeuvres. Nonetheless, the *k*-means clustering algorithm provides no evidence or support for a 'syntax' of insect flight. Future studies therefore should be more careful when applying data reduction techniques to avoid imposing a structure on data where there is none to be found.

BIBLIOGRAPHY

1. Weis-Fogh, T. Biology and Physics of Locust Flight II. Flight Performance of the Desert Locust (Schistocerca gregaria). *Philos. Trans. R. Soc. London* **Series B,** 459–510 (1956).
2. Sane, S. P. The aerodynamics of insect flight. *J. Exp. Biol.* **206,** 4191–4208 (2003).
3. Fry, S. N., Sayaman, R. & Dickinson, M. H. The aerodynamics of free-flight maneuvers in Drosophila. *Science* **300,** 495–498 (2003).
4. Young, J., Walker, S. M., Bomphrey, R. J., Taylor, G. K. & Thomas, A. L. R. Details of insect wing design and deformation enhance aerodynamic function and flight efficiency. *Science* **325,** 1549–1552 (2009).
5. Dickson, W. B., Straw, A. D. & Dickinson, M. H. Integrative Model of

Drosophila Flight. *AIAA J.* **46,** 2150–2164 (2008).

6. Heide, G. & Götz, K. G. Optomotor control of course and altitude in Drosophila melanogaster is correlated with distinct activities of at least three pairs of flight steering muscles. *J. Exp. Biol.* **199,** 1711–1726 (1996).
7. Balint, C. N. & Dickinson, M. H. The correlation between wing kinematics and steering muscle activity in the blowfly Calliphora vicina. *J. Exp. Biol.* **204,** 4213–4226 (2001).
8. Balint, C. N. & Dickinson, M. H. Neuromuscular control of aerodynamic forces and moments in the blowfly, Calliphora vicina. *J. Exp. Biol.* **207,** 3813–3838 (2004).
9. Ellington, C. P. The Aerodynamics of Hovering Insect Flight. I. The Quasi-Steady Analysis. *Philos. Trans. R. Soc. London* **B,** 1–15 (1984).
10. Ellington, C. P. The Aerodynamics of Hovering Insect Flight. II. Morphological Parameters. *Philos. Trans. R. Soc. London* **B,** 17–40 (1984).
11. Ellington, C. P. The Aerodynamics of Hovering Insect Flight. III. Kinematics. *Philos. Trans. R. Soc. London* **B,** 41–78 (1984).
12. Ellington, C. P. The Aerodynamics of Hovering Insect Flight. IV. Aerodynamic Mechanisms. *Philos. Trans. R. Soc. London* **B,** 79–113 (1984).
13. Ellington, C. P. The Aerodynamics of Hovering Insect Flight V. A Vortex Theory. *Philos. Trans. R. Soc. London* **B,** 115–144 (1984).
14. Ellington, C. P. The Aerodynamics of Hovering Insect Flight. VI. Lift and Power Requirements. *Philos. Trans. R. Soc. London* **B,** 145–181 (1984).
15. Birch, J. M. The influence of wing-wake interactions on the production of aerodynamic forces in flapping flight. *J. Exp. Biol.* **206,** 2257–2272 (2003).
16. Bender, J. & Dickinson, M. Visual stimulation of saccades in magnetically

tethered Drosophila. *J. Exp. Biol.* **209,** 3170–3182 (2006).

17. Bender, J. A. & Dickinson, M. H. A comparison of visual and haltere-mediated feedback in the control of body saccades in Drosophila melanogaster. *J. Exp. Biol.* **209,** 4597–4606 (2006).
18. Collett, T. S. & Land, M. F. Visual control of flight behaviour in the hoverfly *Syritta pipiens l. J. Comp. Physiol.* **99,** 1–66 (1975).
19. Boeddeker, N. & Hemmi, J. M. Visual gaze control during peering flight manoeuvres in honeybees. *Proc. R. Soc. B Biol. Sci.* **277,** 1209–1217 (2010).
20. Eckmeier, D. *et al.* Gaze strategy in the free flying zebra finch (Taeniopygia guttata). *PLoS One* **3,** (2008).
21. van Hateren, J. H. & Schilstra, C. Blowfly flight and optic flow. II. Head movements during flight. *J. Exp. Biol.* **202,** 1481–1490 (1999).
22. Schilstra, C. & van Hateren, J. H. Stabilizing gaze in flying blowflies. *Nature* **395,** 654 (1998).
23. Mronz, M. & Lehmann, F.-O. The free-flight response of Drosophila to motion of the visual environment. *J. Exp. Biol.* **211,** 2026–2045 (2008).
24. Wagner, H. Flight Performance and Visual Control of Flight of the Free-Flying Houseflu (Musca Domestica L.) I. Organization of the Flight Motor. *Philos. Trans. R. Soc. London* **B,** 527–551 (1986).
25. Dickson, W. B. The effect of advance ratio on the aerodynamics of revolving wings. *J. Exp. Biol.* **207,** 4269–4281 (2004).
26. David, C. T. The relationship between body angle and flight speed in free-flying Drosophila. *Physiol. Entomol.* **3,** 191–195 (1978).
27. Willmott, A. P. & Ellington, C. P. The mechanics of flight in the hawkmoth Manduca sexta. I. Kinematics of hovering and forward flight. *J. Exp. Biol.* **200,**

2705–2722 (1997).

28. Taylor, G. K. Mechanics and aerodynamics of insect flight control. *Biol. Rev. Camb. Philos. Soc.* **76,** 449–471 (2001).

29. Götz, K. G., Hengstenberg, B. & Biesinger, R. Optomotor Control of Wing Beat and Body Posture in Drosophila. *Biol. Cybern.* **35,** 101–112 (1979).

30. Zanker, J., Egelhaaf, M. & Warzecha, A.-K. On the coordination of motor output during visual flight control of flies. *J. Comp. Physiol. A* **169,** 127–134 (1991).

31. Zanker, J. M. On the mechanism of speed and altitude control in Drosophila melanogaster. *Physiol. Entomol.* **13,** 351–361 (1988).

32. Hollick, F. The Flight of the Dipterous Fly Muscina stabulans fallén. *Philos. Trans. R. Soc. London* **230,** 357–390 (1940).

33. Nachtigall, W. & Roth, W. Correlations Between Stationary Measurable Parameters of Wing Movement and Aerodynamic Force Production in the Blowfly (Calliphora vicina R . -D .). *J. Comp. Physiol. A* **150,** 251–260 (1983).

34. Nalbach, G. The gear change mechanism of the blowfly (Calliphora erythrocephala) in tethered flight. *J. Comp. Physiol. A* **165,** 321–331 (1989).

35. Vogel, S. Flight in Drosophila I. Flight performance of tethered flies. *J. Exp. Biol.* **44,** 567–578 (1966).

36. Vogel, S. Flight in Drosophila: III. Aerodynamic Characteristics of Fly Wing Sand Wing Models. *J. Exp. Biol.* **46,** 431–443 (1967).

37. Gewecke, M. Antennae: another wind-sensitive receptor in locusts. *Nature* **225,** 1263–1264 (1970).

38. Land, M. F. Head Movement of Flies during Visually Guided Flight. *Nature* **243,** 299–300 (1973).

39. Dickinson, M. H. The initiation and control of rapid flight maneuvers in fruit flies. *Integr. Comp. Biol.* **45,** 274–281 (2005).

40. Walker, S. M., Thomas, A. L. R. & Taylor, G. K. Operation of the alula as an indicator of gear change in hoverflies. *J. R. Soc. Interface* **9,** 1194–1207 (2012).

41. Tu, M. S. & Dickinson, M. H. The control of wing kinematics by two steering muscles of the blowfly (Calliphora vicina). *J. Comp. Physiol. A.* **178,** 813–830 (1996).

42. Tu, M. & Dickinson, M. Modulation of Negative Work Output From a Steering Muscle of the Blowfly Calliphora Vicina. *J. Exp. Biol.* **192,** 207–24 (1994).

43. Pfau, H. K. Fliegt unsere Schmeissfliegt mit Gangshaltung? *Naturwissenschaften* **60,** 160 (1973).

44. Geurten, B. R. H., Kern, R., Braun, E. & Egelhaaf, M. A syntax of hoverfly flight prototypes. *J. Exp. Biol.* **213,** 2461–2475 (2010).

45. Braun, E., Geurten, B. & Egelhaaf, M. Identifying prototypical components in behaviour using clustering algorithms. *PLoS One* **5,** (2010).

46. Chakraborty, S., Bartussek, J., Fry, S. N. & Zapotocky, M. Independently Controlled Wing Stroke Patterns in the Fruit Fly Drosophila melanogaster. *PLoS One* **10,** e0116813 (2015).

47. Walker, S. M. *et al.* In Vivo Time-Resolved Microtomography Reveals the Mechanics of the Blowfly Flight Motor. *PLoS Biol.* **12,** e1001823 (2014).

48. Bertholf, L. M. The extent of the spectrum for Drosophila and the distribution of stimulative efficiency in it. *Z. Vgl. Physiol.* **18,** 32–64 (1932).

49. Walker, S. M., Thomas, A. L. R. & Taylor, G. K. Photogrammetric reconstruction of high-resolution surface topographies and deformable wing

kinematics of tethered locusts and free-flying hoverflies. *J. R. Soc. Interface* **6,** 351–366 (2009).

50. Rousseeuw, P. J. Silhouettes: A graphical aid to the interpretation and validation of cluster analysis. *J. Comput. Appl. Math.* **20,** 53–65 (1987).

51. Kaufman, L. & Rousseeuw, P. J. in *Finding Groups in Data: An Introduction to Cluster Analysis* p.88 (2009).

52. Hyvärinen, A., Karhunen, J. & Oja, E. *Independent Component Analysis*. (2001).

Chapter 3

The effect of sexual dimorphism on *Drosophila melanogaster* free-flight kinematics

The effect of sexual dimorphism on *Drosophila melanogaster* free-flight kinematics

Inés L. Dawson*, Graham K. Taylor*, Simon M. Walker†

* Oxford Flight Group, University of Oxford, The John Krebs Field Station, Department of Zoology, Wytham, Oxford, OX2 8QJ, UK

† Faculty of Biological Sciences, University of Leeds, Leeds, LS2 9JT, UK

Drosophila melanogaster (fruit flies) are sexually dimorphic insects, in which the male is significantly smaller than the female. The males use their wings to generate sexual courtship song, as well as for flight, which has implications for their wing beat kinematics and flight behaviour at large due to sexual selection. We examined the effect of wing size and sex on different kinematic parameters. Although we found heading velocity between males and females to be explained by the size dimorphism in wing length alone, sex was a factor that explained variation alongside or instead of wing length in many individual wing beat kinematic parameters, such as wing beat frequency, stroke amplitude, stroke plane and the timing of wing beat rotation. Finally, we provide some potential explanations for the sexually dimorphic differences in flight kinematics between male and female flies.

INTRODUCTION

Wings are one of the defining anatomical features in insects and are found in all insects, except for the two extant wingless basal insect orders, Zygentoma and Archaeognatha, and insect species that have lost flight secondarily, such as the Braulidae[1]. Wings are most commonly used for powered flapping flight and are one of the probable reasons for the radiations that occurred in the insect orders. The capacity for flight has given insects the ability to colonise previously inaccessible niches, new ways of escaping from predators, of searching for food and pursuing potential mates, all of which has aided in specialization and lowered extinction rates[2]. Nevertheless, flight is also an energy-intensive activity and consequently wing morphology and behaviours associated with flight are under intense natural selection to ensure that energy expenditure and flight efficiency are optimised to the needs of the insect.

In many species, wings are used not only for flight, but have other functions too. The forewings of Coleopterans, for instance, have evolved into elytra, which provide the beetle with a hardened carapace that protects it from predators and other external threats[3]. Many insects also have visual patterns on their wings. Some patterns aid in camouflage, as in cryptic butterflies, while others are aposematic and send a clear message to potential predators that their target insect prey may be unpalatable[4]. Both types of patterning have a protective function, which is syntonic with flight in raising the individual's fitness. Some insects, however, also use their wings for signalling purposes in courtship rituals. Orthopterans, for example, stridulate their wings in order to attract potential mates. Insects that use their wings to generate sound draw attention to themselves, which potentially puts them at risk

of predation and parasitisation[5,6]. In insects, courtship songs and calls are often attuned to highly specific frequencies, which aids in species recognition and signals high fitness[7–13]. The wing morphology required to produce such songs may not be optimal for high performance flight. When wings are decoupled from flight during courtship, wing morphology and behaviour may be subject to intrasexual selection[14]. In intrasexual selection, the wings are subject to both natural and sexual selection in males, but only to natural selection in females, thus leading to sexual dimorphism, which may lead to differences in size, colour, shape or structure between males and females of the same species.

Sexual dimorphism is observed in many animals. The most common phenotypic difference is sexual size dimorphism. It is estimated that females are larger than males in over 70% of insect orders. Odonata, where females are typically smaller than the males, are an exception[15]. Sexual size dimorphism in insects is significantly influenced by growth rate, developmental time and critical size for pupation[16,17].

Drosophila melanogaster (fruit fly) is one of many insect species to exhibit sexual dimorphism, with male and female individuals having different phenotypes. *Drosophila melanogaster* males are generally smaller than females. The male's posterior abdominal segment is rounder in shape and is uniformly pigmented, whereas the females exhibits a narrow band on each abdominal segment. Males have sex combs, a row of densely-packed bristles on the fourth segment of their front leg pair, which are absent on females. Males also use their wings during courtship to attract females. When the male finds a female to court, he first orients himself in her direction and taps her abdomen with the tarsi of his forelegs. If the female moves away, the male follows her, and if she remains stationary, the male remains behind

her and proceeds to produce the courtship song. The male extends the wing closest to her and vibrates it. During these vibrations, he produces a species-specific courtship song, which increases female receptivity and enables the courtship ritual to proceed[18–22].

The signal characteristics and duration of wing vibration have been shown to be important for successful courtship, with increased duration of wing vibrations correlating positively with successful copulation. Although the male fruit fly is smaller on average than his female counterpart, males that are larger in size are more successful in mating under competitive conditions and throughout their lifetime. It has been shown that the smaller males are under strong selective pressure to generate an attractive courtship song, which may be disruptive of selection for increased flight capacity[23–26].

Previous studies have explored the effect of wing morphology on the fitness of *Drosophila melanogaster* with variable conclusions. There is notable wing shape dimorphism between males and females. One study showed that sexual dimorphism in the variation of wing morphology in *Drosophila* species has a low phylogenetic signal and can evolve rapidly, which is congruent with the notion that sexual selection and success in courtship are strong drivers of evolution[27]. The wings of female fruit flies have a greater aspect ratio and are less rounded than those of male fruit flies, which are also distally wider with a greater separation between their second to fifth longitudinal veins, a pattern also observed in smaller flies reared at high densities[28,29]. These differences in wing shape could be due to antagonistic selection, that is, the female shape may perform better in flight, while the male shape performs better in generating courtship song. Menezes et al 2013[30] took a natural

population of *Drosophila melanogaster* and artificially selected for individuals with more rounded and more elongated wing shapes in order to measure the effect of wing shape on reproductive success. Males with elongated wings had increased mating success, and also displayed variations in courtship song, although not enough to explain the effect of increased mating success. They also found that smaller males were more successful, which was also contrary to previous research[30]. A later study by Dawson, Perry, Vigoder & Ritchie (unpublished) using RNAi manipulated wings suggested that males with more rounded wings generated longer bouts of sine song that increased female receptivity, whereas wings with a higher aspect ratio generated longer bouts of pulse song.

There has, however, been little research exploring the effects of sexual dimorphism on flight. Previous research has explored the role of external factors on wing morphology, and the effect of wing morphology on flight performance. Many studies have shown that wing development is highly plastic in response to temperature, so that flies reared in the cold during the pupal stage develop longer wings with a greater wing area and higher take-off rates under cold conditions[31,32]. The lower wing loading enables the fly to offset the energetic limitations imposed by lower temperatures and to increase the energetic efficiency of the cold-reared flies[33,34]. The effect of the interaction between sex and developmental temperature on body mass, a key sexual dimorphic feature, is significant. If developmental conditions have a different effect on phenotypic traits in each sex, this could apply to other characteristics of wings and flight. The observed variation in wing morphology under experimental conditions is also consistent with natural observations of wing length across latitudinal clines in various *Drosophila* species[33,35,36].

Ray et al. used RNAi to genetically manipulate the development of *Drosophila melanogaster* wings by generating phenotypes with a larger aspect ratio than the wild type, and then assessed their flight performance under different conditions. They found that fruit flies with higher aspect ratio wings had a significantly higher turning rate than those with more rounded wings[37]. Fruit flies depend on agile manoeuvres to avoid predation, as most predators have the advantage of speed by virtue of their larger body size. Evasive manoeuvres have been found to be more unsuccessful in preventing predation, whilst erratic and random turning behaviour are more successful in hindering predation attempts[38]. The study on novel wing shapes, however, was only carried out on female flies, because their larger size made them easier to visualise in flight. Whether the same effects are found in male flies has not yet been explored.

Whereas sexual dimorphism and plasticity have been documented in wing traits between male and female *Drosophila*, and experimental studies have shown that certain wing shapes are more successful for generating courtship song and are antagonistic to those that perform better in flight, the effects of naturally occurring sexual dimorphism on flight performance remain unexplored. This study aims to test for the effect of sexual dimorphism on the free-flight kinematics of *Drosophila melanogaster*, and to establish whether observable differences can be explained by sexual size dimorphism, or whether flight ability and behaviour are mediated differently due to other or additional factors, such as wing shape.

METHODS

The *Drosophila melanogaster* dataset used in this study is the same as the one collected and processed in Chapter 2.

Three axis systems were employed to describe the kinematic parameters and body positions:

Lab-fixed coordinate system

The lab-fixed coordinate system is a right-handed inertial axis system $\{x_W, y_W, z_W\}$, where the z_W axis points in the direction of gravity, and the x_W and y_W axes are directed arbitrarily in the horizontal plane. The origin of this coordinate system is arbitrary.

Primary body-fixed coordinate system

The body-fixed axis system is a rotating right-handed axis system $\{x_B, y_B, z_B\}$, with its origin located at the centre of mass of the insect. The x_B axis is defined as the anterior-posterior body axis, and the y_B axis points towards the right, passing through the wing bases. It follows from these definitions that the z_B axis points ventrally.

Horizontal body-fixed coordinate system

The horizontal body-fixed axis system is a rotating right-handed axis system $\{x_H, y_H, z_H\}$, with its origin located at the centre of mass of the insect. The z_H axis points vertically upwards, so is always parallel to (though oppositely signed) to the z_L axis, but moves with the insect. The x_H axis is defined as the projection of the x_B

axis onto the horizontal plane. The y_H axis therefore points to the left, but is not used to define any of the parameters in this thesis.

Morphometric measurements

R Wing length Wing length is estimated by taking the mean measurement of the estimated position of the wing base and the wing tip for each individual sequence. Systematic variation in length estimation is present depending on the part of the stroke that is measured, variation in wing base and wing hinge positioning during the wing beat and the inability of the tracking software to accurately detect the wing tip location during certain phases of the wing beat. Units: mm.

c Wing chord Wing chord is the chord length of each blade, measured by taking the absolute difference in length between the leading and trailing edge of the wing plane across the centre of each blade. Chord length is perpendicular to the wing tip to wing base axis throughout the sequence.

L Body Length Body length is estimated from the mean measurement of the length of the major axis of the body voxels.

The mean value of the morphometric measurements are taken per sequence for *Drosophila melanogaster*, as there were multiple individuals present in the flight arena.

The translational parameters measure the position, velocity and acceleration of the body with respect to the lab-fixed axis system $\{x_W, y_W, z_W\}$, where the velocity and acceleration components may be resolved in either the lab-fixed axis system $\{x_W, y_W, z_W\}$, the primary body-fixed axis system $\{x_B, y_B, z_B\}$, or the horizontal body-

fixed axis system $\{x_H, y_H, z_H\}$. For notational simplicity, we assume the components are resolved in the primary body-fixed axis system unless specified otherwise by an L or H subscript. The rotational parameters describe the orientation and angular velocity of the primary body-fixed axis system $\{x_B, y_B, z_B\}$, with respect to the lab-fixed axis system $\{x_W, y_W, z_W\}$, where the angular velocity components are resolved exclusively in the primary body-fixed axis system $\{x_B, y_B, z_B\}$.

Nomenclature:

$[x, y, z]$ Position of the centre of mass of the insect, i.e. position of $\{x_B, y_B, z_B\}$ with respect to $\{x_W, y_W, z_W\}$. Units: m.

$[u, v, w]$ Velocity of the centre of mass of the insect, i.e. velocity of $\{x_B, y_B, z_B\}$ with respect to $\{x_W, y_W, z_W\}$. For convenience we refer to u_B as forwards velocity, and u_H as heading velocity, where by definition u_H is simply the projection of u_B onto the horizontal. Similarly, we refer to w_H as the upwards velocity. Units: ms^{-1}.

$[\dot{u}, \dot{v}, \dot{w}]$ Acceleration of the centre of mass of the insect, i.e. acceleration of $\{x_B, y_B, z_B\}$ with respect to $\{x_W, y_W, z_W\}$. We refer to $\dot{w}_H$ as the upwards acceleration. Units: ms^{-2}.

$[\varphi,\theta,\psi]$ Orientation of $\{x_B, y_B, z_B\}$ with respect to $\{x_W, y_W, z_W\}$, expressed as a sequence of Euler angles in the order φ,θ,psi, where φ is bank angle, θ is pitch angle, psi is yaw angle. Units: deg.

$[p, q, r]$ Angular velocity of the insect, where p is roll rate, q is pitch rate, and r is yaw rate. Units: deg s^{-1}.

4.3 Wing kinematics

All right wing kinematics within the body-axis system have their origin in the wing base and are defined with respect to the stroke plane and with respect to a right-handed axis system $\{x_R, y_R, z_R\}$. Left wing kinematics are defined similarly, but with respect to a left-handed axis system $\{x_L, y_L, z_L\}$.

~	Period	The time between two consecutive stroke reversals, when the angular velocity of the wing tip passes through zero at the end of the upstroke. Units: ms.
n	Wing beat frequency	The reciprocal of the wing beat period, which is the duration of the wing beat in ms. All measurements are normalised by the wing beat period to a resolution of 100 equidistant time points per wing beat. Units: Hz.
β	Stroke plane angle	The inclination of the stroke plane, which is the plane including the wing base and wing tip position at each stroke reversal, calculated for each half stroke, with respect to the body length axis, indicated as the angle formed by the line joining the wing tip at the beginning and end of the downstroke with the $y_B z_B$-plane. Units: deg.
β'	Stroke plane angle world	Inclination of the stroke plane with respect to the $x_W y_W$-plane. Units: deg.
σ	Stroke angle	The angle between the wing tip and its projection on the $y_R z_R$-plane. The beginning of the downstroke is

positive as clockwise rotation is positive, and negative at its ending. The stroke angle is 0° when it passes through the y-axis. Units: deg.

θ Deviation angle The angle taken between the wing tip and its projection on the $x_R z_R$ plane. It increases during the downstroke and decreases during the upstroke. The deviation angle is 0° when it passes through the y-axis. Units: deg.

Φ Stroke amplitude The angle between the lines joining the wingtip position at the beginning and end of each downstroke per wing beat. Units: deg.

ω Angle of incidence The angle of incidence, or wing pitch angle, is calculated from the local pitch of the wing. The wing outline is rotated about the z-axis by the minus deviation angle and about the x-axis by the minus stroke angle. The local pitch angle is the angle measured from the xy-plane to the ventral side of the wing chord. Spanwise variation in local twist angle is then estimated by regressing the local pitch angle against the radius from the wing base, against six evenly spaced angles from 30% to 80% of the wing length. The extreme values are excluded due to obscuration from the body near the wing base and due to the shortening of the wing chord towards both extremes, both of which impede an accurate measure of the angle. Units: deg.

d/w Timing of stroke reversal The moment at the end of the downstroke when the wing reverts to initiate the upstroke in a wing beat cycle of length 1, measured as the ratio of downstroke to wing beat duration within the wing beat. Units: non-dimensional.

~ Timing of pronation. Pronation is the transition from the upstroke to the downstroke at the point when the wing reaches 90° and is perpendicular to the stroke plane. The timing indicates the moment with respect to the start of the downstroke when pronation occurs. Units: non-dimensional.

~ Timing of supination. Supination is the transition from the downstroke to the upstroke at the point when the wing reaches 90° and is perpendicular to the stroke plane. The timing indicates the moment with respect to the start of the downstroke when pronation occurs. Units: non-dimensional.

~ Relative timing of supination. Supination is the transition from the downstroke to the upstroke at the point when the wing reaches 90° and is perpendicular to the stroke plane. The timing indicates the moment with respect to end of the downstroke when pronation occurs. Units: non-dimensional.

Statistical analysis

Most statistical analyses such as the student t-test, Levene test, Spearman rank-correlation and Cohen's d effect size were performed using MATLAB functions.

Cohen's *d* effect size indicates the standardised difference between two means divided by the pooled standard deviation:

$$d = \frac{\mu_2 - \mu_1}{\sqrt{\frac{s_1^2 + s_2^2}{2}}}$$

Where μ is the mean from each group, and s is the standard deviation from each group.

Linear mixed effect models were run with the lme4 package in the R environment[39].

To account for multiple comparisons, a False Discovery Rate test (FDR) was conducted on statistical tests at the 5% level, and the significance of all p-values in this study remained unchanged after the correction (**Supplementary Material 1**)[40].

RESULTS

In total, 4054 wing beats of *Drosophila melanogaster* from 265 sequences were analysed: 2077 wingbeats from 100 sequences corresponded to male flies, and 1977 wingbeats from 165 sequences corresponded to female flies.

Morphometrics

Wing length in males was significantly shorter than in females (t_{263} = 25.69, d = 3.19, p < .0001), whilst wing chord was not (t_{263} = -1.73, p = 0.084,). Body length (t_{263} = 12.32, d = 1.58, p < .0001) and body volume (t_{263} = 14.18, d = 1.84, p < .0001) were also significantly larger in females. The ratio between wing length and body length was not significantly different between males and females (t_{263} = -0.522, p = 0.60) **(Figure 3)**.

Body length showed greater variance than wing length within each sex (females: $\chi^2(1)$ = 64.02, p < .0001, males: $\chi^2(1)$ = 13.60, p = 0.0002), although the standard variance was not significantly different between males and females for wing length ($\chi^2(1)$ = 2.37, p = 0.12) and body length ($\chi^2(1)$ = 2.124, p = 0.15). Body length and wing length were significantly negatively correlated for female fruit flies ($r_s(265)$ = -0.197, p = 0.011), but not for male fruit flies ($r_s(265)$ = 0.106, p = 0.30).

Rearing density conditions did not affect wing nor body length in either males or females (body length males: t_{84} = 0.1203, d = 0.026, p = 0.90; body length females: t_{102} = -0.572, d = 0.115, p =0.57; wing length males: t_{84} = -1.16, d = 0.241, p = 0.25; wing length females: t_{102} = 0.865, d = 0.167, p = 0.39).

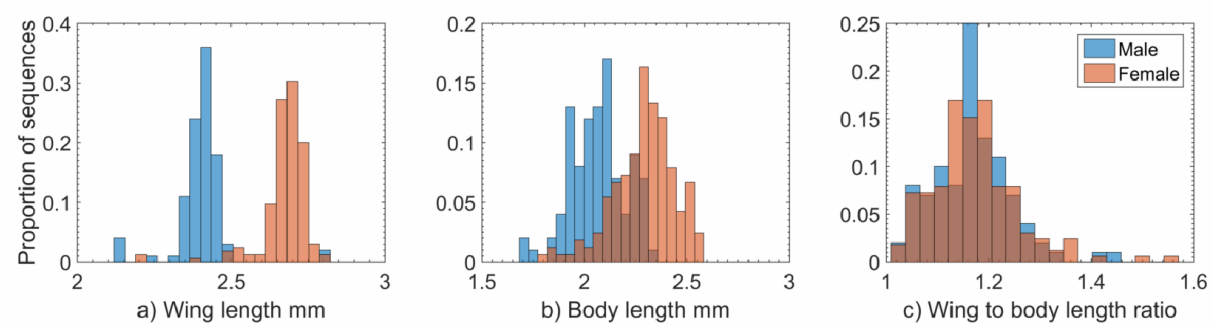

Figure 3. a) Wing length (mm) distribution to proportion of male (blue) and female (red) sequences b) Body length (mm) distribution to proportion of male (blue) and female (red) sequences c) Wing to body length ratio to proportion of male (blue) and female (red) sequences.

Flight speed

Despite there being 60% more individual recordings corresponding to female flies than male flies, the number of wing beats analysed are comparable across both sexes. Our hypothesis was that the number of wing beats captured per sequence was related to the time that the fly spent in the central volume of the recording, which was likely determined by the fly's flight speed. We therefore examined whether sequence length depended on fly heading velocity.

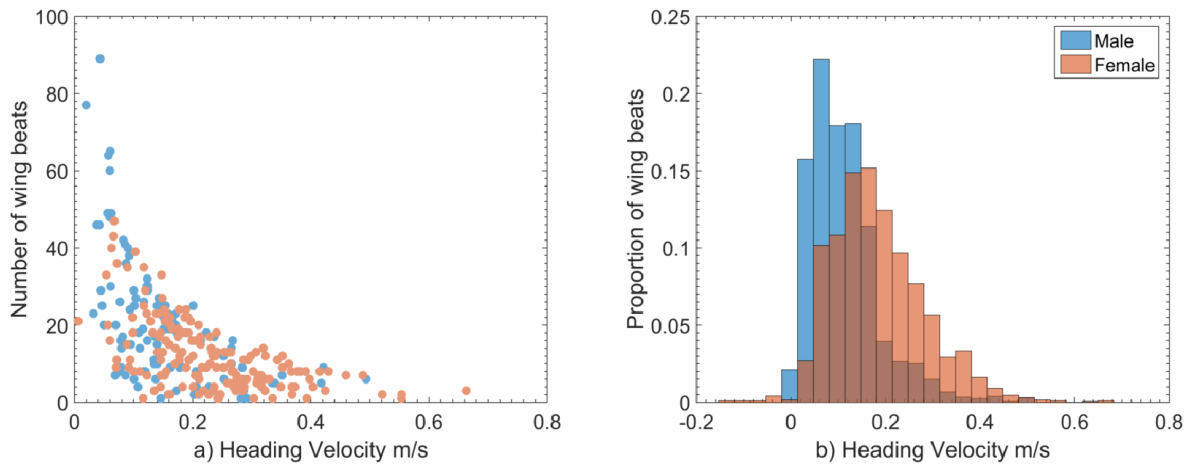

Figure 4. a) Mean sequence heading velocity (ms^{-1}) by number of wing beats per sequence for male (blue) and female (red) fruit flies. b) Normalised heading velocity distribution for males (blue) and females (red). On average, females fly at a higher heading velocity than males.

The number of wing beats captured between male and female sequences was significantly higher in males than females (t_{263} = -5.55, d = 0.65, p < .0001); from a Spearman's rank correlation analysis, the number of wing beats from a sequence was significantly inversely correlated with the mean heading velocity measured in the sequence ($r_s(265)$ = -0.645, p < .0001) **(Figure 4a)**. Mean heading velocity was significantly higher in female fruit flies than male fruit flies, at 0.18±0.098m/s versus 0.11±0.074m/s respectively (t_{4052} = 26.76, d = 0.838, p < .0001) **(Figure 4b)**. In small dipteran species, flight speed is also known to be correlated with air temperature, and this was the case for male fruit flies ($r_s(100)$ = 0.401, p < .0001), but not for female fruit flies ($r_s(165)$ = 0.118, p = 0.13), although there was a lower variation in the air temperatures the female flies flew in.

To test whether sex had a significant effect over and above body size, we fitted a linear mixed effects model with ANCOVA controlling for wing length as a covariate of sex. We specified heading velocity as the response variable, wing length, sex and temperature as fixed effects and sequence as random effects. From a type II Wald chi-square test, sex did not explain any additional variation (χ^2 = 1.38, p = 0.24) after wing length (χ^2 = 5.04, p = 0.025) and temperature (χ^2 = 8.04, p = 0.004567), with wing length and temperature increasing heading velocity by 0.167±0.074ms^{-1} and 0.0212±0.0075ms^{-1} respectively.

However, as sexual dimorphism in *Drosophila melanogaster* goes beyond size, there may be other wing beat parameters that differ between male and female fruit flies on the basis of sex above and beyond size.

Summary wing beat kinematics

Wing beat frequency is higher in males than in females

Wing beat frequency in females was significantly lower than in male fruit flies (t_{4052} = -29.91, d = 0.938, p < .0001) **(Figure 5a)** (See **Table 1** for summary values of all kinematic parameters tested). Wing beat frequency was related to wing length, and also to temperature **(Figure 6)**. Studies have shown that experimentally shortening a fly's wings increases its oscillatory frequency due to decreased inertia[41], and increased temperature is also correlated with faster wing beat frequency in many insects, particularly those of a lower body size[42–48].

Although temperature is known to be correlated with wing beat frequency in *Drosophila* flight and courtship song[49,50], the range of air temperatures the flies flew in was not very broad, with no significant correlation found between temperature and mean sequence wing beat frequency in male ($r_s(100) = 0.0354$, p = 0.73) nor female fruit flies ($r_s(165) = 0.0402$, p = 0.61).

In order to explore whether sex and wing length were significant factors, we built a linear mixed effects model with wing beat frequency as a response variable, sex and wing length as fixed effects and sequence as random effects. Wing length did not explain any additional variation ($\chi^2 = 0.311$, p = 0.58) after sex ($\chi^2 = 8.46$, p = 0.0036) in wingbeat frequency.

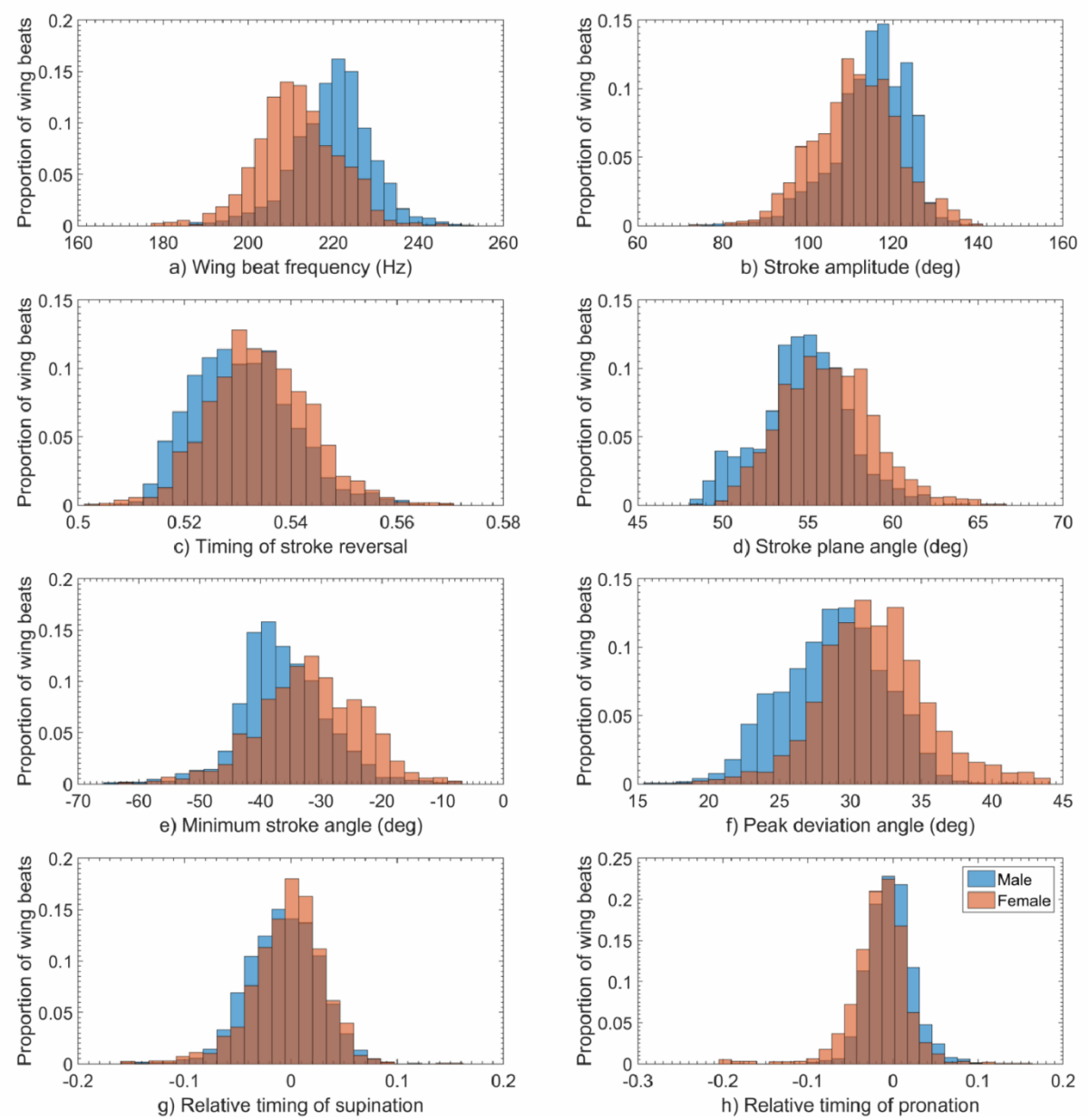

Figure 5. Normalised distribution of wing beat parameters for males (blue) and females (red). a) Wing beat frequency. b) Stroke amplitude. c) Timing of stroke reversal d) Stroke plane angle. e) Minimum stroke angle. f) Peak deviation angle.

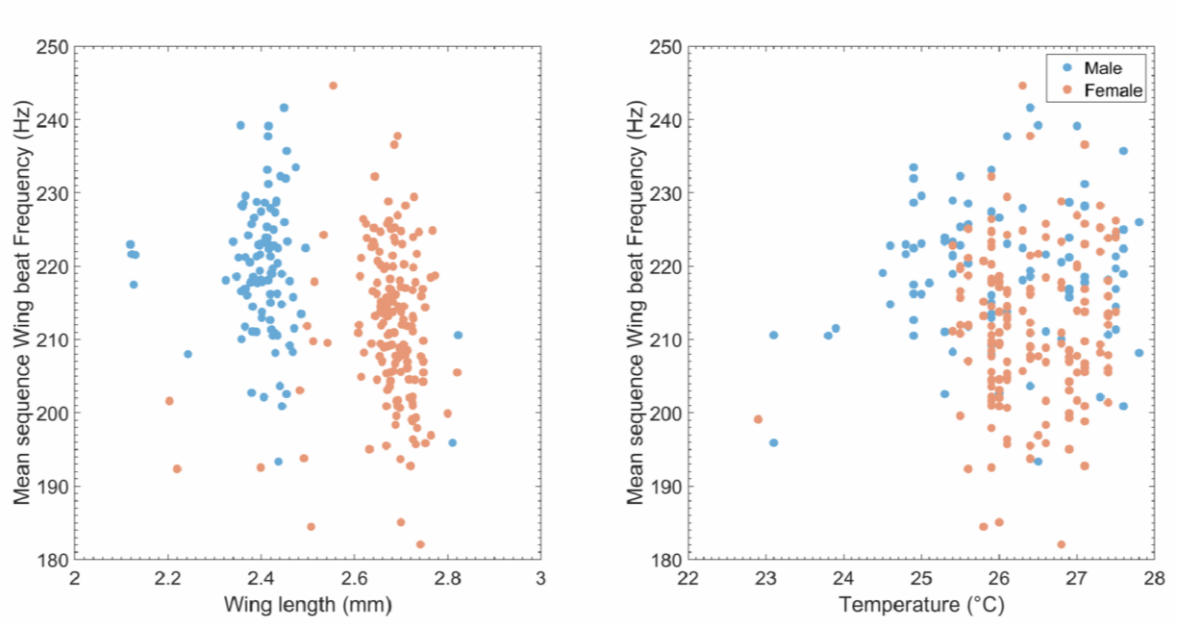

Figure 6. a) Sequence wing length (mm) by mean sequence wing beat frequency (Hz) for male (blue) and female (red) fruit flies. b) Sequence temperature (°C) by mean sequence wing beat frequency (Hz) for male (blue) and female (red) fruit flies.

Stroke amplitude is higher in males than in females

The stroke amplitude was higher on average in males than in females (t_{4052} = -11.99, d = 0.376, p<.0001) **(Figure 5b)**. The stroke amplitude between upstroke and downstroke was not significantly different in male (t_{4052} = -0.825, p = 0.41) and female (t_{4052} = -1.12, p = 0.26) fruit flies.

There was a negative correlation between wing length and their mean sequence stroke amplitude in male fruit flies ($r_s(100)$ = -0.213, p =0.034), and in female fruit flies ($r_s(165)$ = -0.361, p<.0001). Temperature was also inversely correlated with stroke amplitude in male fruit flies ($r_s(100)$ = -0.449, p<.0001) but not in female fruit flies ($r_s(165)$ = -0.102, p=0.19).

To test the role of sex as a significant factor above and beyond wing length and temperature, stroke amplitude was specified as a response variable in a linear mixed effects model, with sex, wing length and temperature as fixed effects and sequence as random effects. Wing length (χ^2 = 61.46, p<.0001), sex (χ^2=31.004, p<0.0001) and temperature (χ^2=13.37, p=0.00026) were all significant factors that explained the variation in stroke amplitude.

Upwards acceleration increased linearly with stroke amplitude (R^2 = 0.238, $F_{1,265}$ = 82.16, p<.0001). For every degree of increased stroke amplitude, upwards acceleration decreased by -0.065 ± 7.255 m/s^2. No significant relationship was found between stroke amplitude and heading acceleration (R^2 = 0.0088, $F_{1,265}$ = 2.34, p=0.13).

Timing of stroke reversal happens later in females than males

The timing of stroke reversal happened significantly later in females than males (t_{4052} = 11.38, d = 0.357, p = <.0001), although there was substantial overlap with the same range of values recorded for both males and females **(Figure 5c)**. When examining the role of sex and wing length as a factor affecting the timing of stroke reversal, sex was found to be a significant factor (χ^2=4.52, p=0.033), and wing length did not explain any additional effect than what was already given by sex (χ^2=0.264, p=0.26).

Stroke plane angle is higher in females than in males

The mean stroke plane angle was higher in females than in males (t_{4052} = 17.18, d = 0.54, p<.0001) **(Figure 5d)**. The stroke plane angle of the upstroke and the downstroke was not significantly different in males (t = -0.546, p=0.59), but was in females (t=-2.15, d=0.0142, p=0.032), although the effect size was very low.

When examining the role of sex and wing length as a factor affecting stroke plane angle, sex was found to be a significant factor (χ^2=14.02, p=0.00018), whilst wing length did not explain any significant additional than what was already given by sex (χ^2=2.41, p=0.12).

Wing beat characterisation

Mean stroke angle, deviation angle and angle of incidence followed similar trajectories in males and females, although there were significant differences between males and females in the distribution of minimum stroke angle (t_{4052} = 18.50, d = 0.580, p <.0001) **(Figure 5e)** and peak deviation angle (t_{4052} = 24.94, d = 0.783, p<.0001) **(Figure 5f)**. Mean minimum stroke angles for males and females were -36.3±7.2˚ and -31.8±8.4˚, respectively. Mean peak deviation angle for males and females were 28.8± 3.6˚ and 31.7± 3.8˚, respectively **(Figure 7)**.

When examining the role of sex, wing length and temperature as factors affecting the minimum stroke angle and controlling for sequence, all three were found to be significant factors although wing length accounted for substantially more variation (χ^2=30.3, p<.0001) than sex (χ^2=6.37, p=0.012) and temperature (χ^2=4.004, p=0.045). All three factors were also significant in affecting peak

deviation angle, with sex explaining the most variation (χ^2=61.7, p<.0001) compared to wing length (χ^2=23.2, p<.0001) and temperature (χ^2=7.25, p=0.0071).

Not surprisingly, since stroke and deviation angle were measured relative to the body, peak stroke and deviation angle were both tightly correlated with stroke amplitude (stroke angle: r = -0.754, p<.0001, deviation angle: r = 0.564, p<.0001), although the correlation between minimum stroke angle and stroke amplitude was significantly tighter (t = -95.5, p<.0001).

Minimum stroke angle was also found to be correlated with increasing heading and upwards velocity in both males (Heading velocity: r(100) = 0.401, p <.0001; Upwards velocity: r(100) = 0.437, p <.0001) and females (Heading velocity: r(165) = 0.349, p <.0001; Upwards velocity: r(165) = 0.38, p <.0001).

Supination

The timing of supination between male and female flies was significantly different although the effect size is low (t_{4039} = -3.31, d = 0.104, p =0.0009) **(Figure 5g)**. When examining the role of sex and wing length as a factor affecting the timing of supination, sex (χ^2=10.4, p=0.0013) and wing length (χ^2=16.79, p<.0001) were found to be a significant factors.

Supination is also correlated with stroke amplitude and timing of stroke reversal, with higher stroke amplitude angles being associated with earlier timing of supination in both males (r(100) = -0.45, p <.0001) and females (r_s(165) = -0.515, p <.0001), and timing of stroke reversal and supination varying positively for males (r(100) = 0.30 , p <.0001) and females (r(165) = 0.34, p <.0001). Using the Steiger and Williams test, we determined that absolute timing of supination correlated more

tightly than relative timing of supination with timing of stroke reversal (t = -15.4, p<.0001).

Pronation

Timing of pronation between male and female flies differed significantly (t_{3835} = 13.51, d = 0.434, p <.0001) **(Figure 5h)**. When examining the role of sex and wing length as a factor affecting the timing of pronation, sex (χ^2=31.4, p<.0001) and wing length (χ^2=11.5, p=0.00069) were found to be a significant factors. The timing of pronation is positively correlated with the timing of supination in males (r(100) = 0.254 , p <.0001) and females (r(165) = 0.315 , p <.0001). Unlike timing of supination, the timing of pronation was not correlated with the timing of stroke reversal (r(4054) = 0.0182, p =0.26).

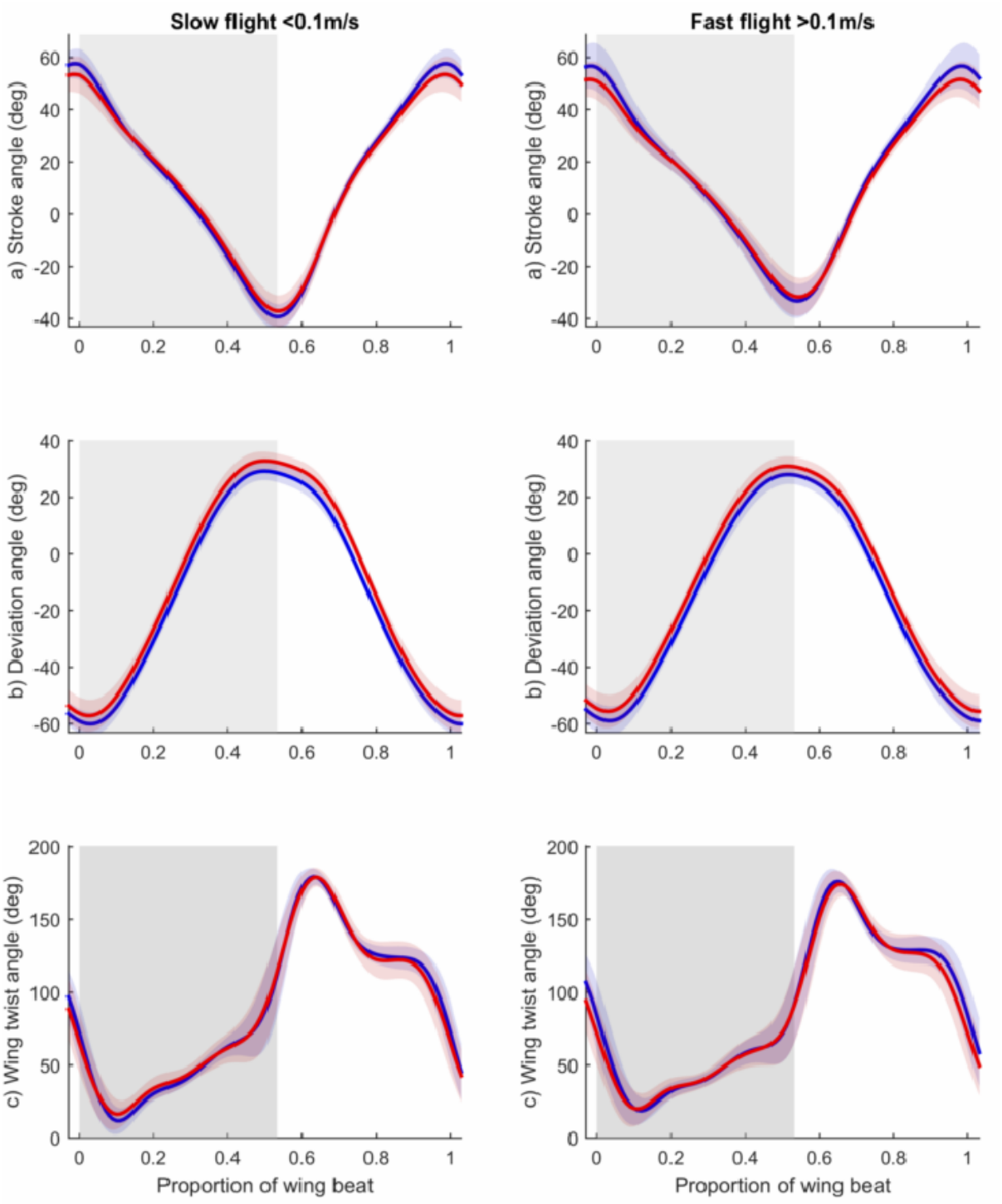

Figure 7. Depicting average (a) stroke angle, (b) deviation angle and (c) angle of incidence throughout the wing beat for slow forward flight (<0.1m/s) (left) and fast forward flight (>0.1m/s) (right) in males (blue) and females (red). Even when distinguishing differences in flight speed, the differences and similarities between male and female wing beat characterisation remain constant.

Parameter	t-value	d.f.	Cohen's *d*	p-value	Sex higher
Wing length	25.69	263	3.19	< .0001	Female
Wing chord	-1.73	263	-	0.084	No difference
Body length	12.32	263	1.58	<.0001	Female
Body volume	14.18	263	1.84	<.0001	Female
Wing length/Body length ratio	-0.522	263	-	0.60	No difference
Wing beats per sequence	-5.55	263	0.65	<.0001	Male
Heading velocity	26.76	4052	0.838	<.0001	Female
Wing beat frequency	-29.91	4052	0.938	<.0001	Male
Stroke amplitude	-11.99	4052	0.376	<.0001	Male
Timing of stroke reversal	11.38	4052	0.357	<.0001	Female
Stroke plane angle	17.18	4052	0.54	<.0001	Female
Minimum stroke angle	18.50	4052	0.58	<.0001	Female
Peak deviation angle	24.94	4052	0.78	<.0001	Female
Supination	-3.31	4039	0.10	0.0009	Male
Pronation	13.51	3835	0.43	<.0001	Female

Table 1. Summary comparison table of featured morphometric, body and wing kinematic parameters in the text between males and females, indicating the two-tailed t-value difference, the degrees of freedom, Cohen's *d*, the significance level and the sex where the mean is higher if significantly different.

DISCUSSION

Wing length

Wing length and body length are generally positively correlated in insects[51–56], so that it was surprising to find an inverse correlation between wing length and body length in female fruit flies, and a lack of correlation in males, which means, in effect, that larger males tend on average to have relatively shorter wings. There may be several reasons for this. It may be more advantageous for larger body sizes to have relatively shorter wings, or for smaller body sizes to have relatively longer wings. Insects with larger bodies are more likely to have longer, larger wings, which would be heavier in flight[57]. There may therefore be pressure to develop smaller wings that would be less energetically expensive to oscillate in flight, although this does not explain why flies with smaller body lengths should have relatively longer wing lengths.

Previous studies have shown that there is substantial developmental plasticity with respect to adult wing shape and size in *Drosophila melanogaster*, so that certain environmental, genetic and molecular factors at the larval and pupal stage may affect the final wing proportions[28,29,31,58–66]. For instance, fruit flies pupating at elevated air temperatures (25˚C) develop smaller wings with smaller cells than their counterparts reared at lower air temperatures (<18˚C). Whilst wing area in *Drosophila melanogaster* is hyperallometric to body size in response to temperature, it is also hypoallometric under conditions of variable nutrition[58]. In view of this, our two rearing backgrounds were unlikely to generate any variability in wing length, as the higher density treatment was still well below the threshold for larval overcrowding and starvation, and our morphometric analysis supported this

assumption[58,59]. The flies were reared in a temperature-controlled environment of 20˚C, so temperature-dependent plasticity was unlikely. Nonetheless, it is possible that larvae with smaller body sizes may have pupated at a relatively lower air temperature than their larger counterparts due to their increased surface-to-body-volume ratio, which could have led to the development of relatively larger wings. Another possible explanation is a trade-off in larval resource allocation, whereby smaller larvae may invest more resources in wing development during the pupal stage, and vice versa. Females are under selective pressure to maximise resources for egg laying, which may occur at the expense of wing length, particularly as larger body size in females is correlated with increased fecundity[67–70]. Larger body size may therefore give females an additional size advantage for rejecting unwanted copulation attempts from male flies without needing to resort to evasion by flight.

The fact that the same correlation is not observed in males could simply be a factor of sample size, or it may be due to the action of different selective pressures operating on male and female fruit flies, which could be related to their body size, the involvement of the wings in male courting behaviour and the need to allocate resources for egg laying in females. Further research would be necessary to discern whether such cues determining sex-dependent wing length exist and what their precise mechanism of action is.

Wing beat frequency

The allometry of wing beat frequency has been extensively explored across flying insects[42,44,50,71,72]. Wing beat frequency is known to vary inversely with wing inertia, as is the case in mechanically resonant systems, such as the rhythmic

deformation of an insect's thorax by their indirect flight muscles and pleurosternal muscles[57]. Whilst larger insects generally have larger and heavier wings, wing amputation experiments and studies on atmospheric density have shown that it is the wing inertial load that directly alters wing beat frequency[41,43,73–76]. Temperature is also known to influence wing beat frequency, probably due to the increased muscle activation[45,46,77–79], and *Drosophila* species in warmer habitats have been found to adopt greater wing beat frequencies[80]. Although we used a thermostat was used to control and keep the temperature constant, air temperature varied between 22.9˚C and 27.8˚C during the experiments, and 80% of the sequences were found to be between 25˚C and 27.5˚C. In spite of this, wing beat frequency was not correlated with air temperature, even though air temperature was found to mildly influence several other kinematic parameters. This is a relatively low range of temperature variation which may be insufficient to generate observable temperature-dependent differences in free-flight wing beat frequency. Both wing length and sex affected wing beat frequency, although when accounting for sex as a covariate, sex significantly explained variation in wing beat frequency in *Drosophila melanogaster*, whereas wing length provided no additional explanation for the variation that was not already accounted for by sex. Females have longer wings and a higher wing inertial load compared to males, which reduces their wing beat frequency. The difference in wing length and wing beat frequency appears to be directly linked to sex.

Wing beat frequency in flies is likely to also have some involvement with sexual selection, particularly in males. Whilst *Drosophila melanogaster* do not employ flight displays to court females, they do generate frequency-specific sine song and pulsed song to increase the female's receptivity to mating. Males may also be expected to

have less variation in their wing beat frequency compared to females, as the frequency of the vibrations are used for species recognition and to signal fitness. A study of *Drosophila pseudoobscura* comparing wing beat frequencies in different populations found significantly different mean numbers of sex combs on the forelimbs of males and wing beat frequencies in different races of flies[80], suggesting that sexual selection may have been a driver of directional evolution on sexual traits in these populations.

Stroke amplitude

Stroke amplitude decreases with increasing wing length, which is correlated with increasing heading velocity and upwards velocity. This is consistent with correlations found between extreme values of peak stroke and deviation angle and upwards and heading velocity. Unlike *Calliphora* and *Eristalis* flies, *Drosophila* are less able to decouple lift and thrust production between the upstroke and downstroke of the wing beat, and display less independent control between the upstroke and the downstroke[78,81,82]. There was no significant difference between the stroke amplitude of the upstroke and downstroke, and increased amplitude was associated with lower body velocity in both upwards and forwards components.

Stroke amplitude was negatively correlated with air temperature in males, but displayed no significant relationship in females. This difference may be due to the fact that the breadth of temperatures recorded on male sequences was greater than female sequences, or the result of chance. It is known that peak muscle performance in *Drosophila* is achieved at body temperatures of around 30˚C[83]. Whilst larger bodied insects such as blowflies and bees can endogenously raise their body

temperature over air temperature[50,84,85], it is less likely in *Drosophila* due to their small body size and increased surface-to-volume ratio. Heading velocity also increased with temperature, suggesting that sequences taken at higher ambient temperatures may have facilitated enhanced flight muscle performance.

In general terms, stroke amplitude was greater in males than in females, with shorter stroke amplitude being reserved for higher heading velocities in *Drosophila*. This difference was due to both wing length and sex and could indicate that male and female fruit flies display different flight behaviours, with female flight being faster and more directional compared to males. This could be to minimise the time spent flying in order to reserve energy for egg-laying, or to escape from looming predators to protect themselves and their future young. On the other hand, it may be that the smaller size of the male is less optimal for fast forward flight, as the increasing relative viscosity associated with a smaller body size tends to make attaining higher heading velocities less energetically efficient due to increased drag.

Stroke reversal and wing rotation

Earlier timing of stroke reversal was linked to higher wing beat frequencies, suggesting that the duration of the downstroke in flight determines the wing beat period. Early timing of stroke reversal was also linked to higher stroke amplitude, which is consistent with higher wing beat frequencies being associated with slower heading velocities.

Timing of stroke reversal is positively correlated with supination, but not with pronation. This suggests that the timing of supination is primarily dictated by the

timing of stroke reversal: the earlier the timing of stroke reversal, the earlier the timing of supination, and vice versa. These findings are surprising since they appear to contradict the literature. In our study, early timing of rotation is associated with lower heading and upwards body velocities[86]. Studies on wing rotation suggest that early timing of wing rotation during pronation and supination would generate rotational force peaks in the wing stroke, whereas our study found the opposite. A delay in timing of supination would be expected to generate negative lift. However, it is possible that there is a temporal delay between the generation of the force peak and a measurable difference in body kinematics.

The timing of supination is inversely, albeit non-linearly, correlated with stroke amplitude. Low stroke amplitude correlates with delayed supination, and early supination is correlates exclusively with larger stroke amplitudes.

Stroke plane angle, stroke angle and deviation angle

The stroke plane angle differed significantly between male and female fruit flies, and was explained by sex, not by wing length. There was also a striking difference between the distribution of peak stroke and deviation angles in male and female fruit flies. Sex, wing length and temperature were all explanatory factors in each one. Whilst the deviation angle trajectory resembled a harmonic wave, the trajectory of the stroke angle more closely resembled a triangular or saw-tooth wave. Not surprisingly, the two measures were correlated with stroke amplitude, since the more extreme the values of the stroke and deviation angles adopted by the wings, the greater the stroke amplitude. Stroke amplitude was more tightly correlated with minimum stroke angle than with peak deviation angle. This suggests that variation

in wing position across the anterior-posterior axis with respect to the body leads to a greater range of motion than above and below the stroke plane. The deviation angle was positively correlated with stroke plane angle, which is also unsurprising as higher stroke plane angles would lead to the wing adopting more extreme deviation angle positions with respect to the wing base.

There was no strong relationship between stroke plane angle and stroke amplitude or heading or upwards velocity and accelerations, which also replicates previous findings on tethered flies[78,87].

Heading velocity

The range of heading velocities observed in our flies were congruent with those recorded in the literature[88–90]. Our peak heading velocity of 0.7m/s was slightly lower than the measured peak velocities in the literature[90], although we recognise that our recording system makes allowance for the overrepresentation of slower forward flight, and a corresponding underrepresentation of faster forwards flight. This is because a minimum number of full wing beats are necessary for a recorded sequence to be selected for analysis, and in a small recording volume, slower heading velocities are more likely to be overrepresented. There was a non-linear relationship between mean heading velocity and sequence length, with sequence length for lower heading velocities being much more variable. This variability is due to several factors:

a) Recordings occasionally contained the presence of individuals in the background which interfered with the tracking software, requiring the duration of the analysed sequence had to be artificially shortened.
b) Individual fruit flies flying close to the edge of the arena minimises their time in the flight arena to a minimum, leading to a shorter than average sequence duration.
c) Individuals flapping at lower heading velocities did not always follow linear trajectories. Some manoeuvres, such as turns, greatly increased the average duration of the fly within the recorded flight arena.

Whilst sex was a significant factor explaining variation in most wing kinematic parameters alongside, and occasionally above and beyond, wing length, it did not explain any additional variation in heading velocity when accounting for wing length, suggesting that individuals with longer wings are more likely to engage is faster flight. The size factor is not unexpected, as larger animals are known to fly faster than their smaller counterparts, as well as animals with higher wing aspect ratios[91].

Heading velocity was also found to vary positively with temperature in males, but not females, which was probably due to the difference in temperature variation the flies were exposed to. However, the effect of a temperature was lower by one order of magnitude than the effect of wing length.

Although males and females were recorded for a similar number of days, and a similar number of wing beats were collected for each sex, two thirds more sequences of females than males were recorded, with female sequences tending to be much shorter and with higher mean heading velocities. The greater heading velocity in

females was ultimately explained by their longer wing length, suggesting that individuals with longer wings require a faster base speed. However, the difference in wing length does not necessarily explain the overrepresentation of female sequences, particularly as faster flight sequences were harder to obtain for analysis. The increased number of flight sequences may indicate an increased motivation for females to initiate flight than males, which may be due to differences in behaviour between male and female fruit flies.

Females may engage in flight exclusively for escape and directional behaviours that increase their survival. A slow flying female might be an easier target for any looming predator, and females that are predated upon will be unable to lay eggs. The mostly short and fast flight trajectories recorded from the females could represent brief escape behaviours, by means of which the females try to reduce their flight time to a minimum. The females in this study were virgins and had not been exposed to or courted by males beyond the day of emergence. Males on the other hand may adopt different flight strategies involved in sexual competition. In our flight recordings, the flies were segregated by sex. It is unlikely therefore that the male flight behaviour recorded would represent courtship behaviour. It is possible however that by flying more slowly they would be better able to explore their surroundings, either searching for potential mates or monitoring other male fruit flies, both of which would be aided by a slower heading velocity. Different studies have reviewed the differences in behaviour between male and female fruit flies, with most agreeing that male flies display higher levels of activity and disperse more than females[92–96]. On the other hand, it may be that a male's smaller size prevents him from reaching faster heading velocities, as, with decreasing body size, mean angular velocity of the wing must increase to support its mass in flight[97]. Indeed, male fruit

flies displayed a significantly higher average angular wing velocity than female fruit flies.

Limitations

The nature of the data collection, which involved the presence of multiple individual flies of the same sex and age in the flight arena, meant that we did not know whether each sequence in a recording day corresponded to the same fly or a different one. This presents some potential pseudoreplication problems in analysis, although the statistical tests selected should be robust to this uncertainty.

During the collection period we also observed that not all flies flew or responded to a looming stimulus. This suggests that the flies from the OreR line that we used, whilst genetically uniform, may not be selected for optimised flight performance. The rearing conditions in which this line of flies has been bred and maintained for thousands of fly generations do not expose the flies to the same type of threats as wild type flies, such as parasites, predators or fluctuating climate conditions, which may have led to relaxed selection of some traits. In the absence of true natural selection threats, therefore, it may be expected that sexual selection will be the primary driver of trait evolution, since mating success will continue to determine which genes are passed on to subsequent generations in these artificially selected lines. The greater population density and the small enclosures in which OreR fruit flies are reared do not allow for certain types of flight to occur; at most they are only able to fly for several centimetres across a small vial, either to approach or evade other flies and the substrate. Studies have shown that increased flight performance can be selected for in *Drosophila*, indicating genetic variation in flight performance[98–100]. This could be an indication that laboratory lines may not select

for flight performance because of their rearing conditions, and the findings of this study with regards to flight may differ from the performance by wild type *Drosophila melanogaster* flies, which experience a different balance of natural and sexual selection.

BIBLIOGRAPHY

1. Gullan, P. J. & Cranston, P. S. *The Insects: An Outline of Entomology*. (Wiley-Blackwell, 2010).

2. Mayhew, P. J. Why are there so many insect species? Perspectives from fossils and phylogenies. *Biol. Rev.* **82,** 425–454 (2007).

3. Fédrigo, O. & Wray, G. A. Developmental Evolution: How Beetles Evolved Their Shields. *Curr. Biol.* **20,** 64–66 (2010).

4. Ruxton, G. D., Sherratt, T. N. & Speed, M. P. *Avoiding Attack: The Evolutionary Ecology of Crypsis, Warning Signals and Mimicry*. (Oxford University Press, 2004). doi:10.1093/acprof:oso/9780198528609.001.0001

5. Zuk, M. & Kolluru, G. R. Exploitation of sexual signals by predators and parasitoids. *Q. Rev. Biol.* **73,** 3–22 (1998).

6. Vincent, C. M. & Bertram, S. M. The Parasitoid Fly Ormia ochracea (Diptera: Tachinidae) can use juvenile crickets as hosts. *Florida Entomol.* **92,** 598–600 (2009).

7. Saarikettu, M., Liimatainen, J. O. & Hoikkala, A. The role of male courtship song in species recognition in Drosophila montana. *Behav. Genet.* **35,** 257–

263 (2005).

8. West-Eberhard, M. J. in *Insect Communication* 283–324 (1984).

9. Searcy, W. A. & Anderssen, M. Sexual selection and the evolution of song. *Annu. Rev. Ecol. Syst.* **17,** 507–533 (1986).

10. Talyn, B. C. & Dowse, H. B. The role of courtship song in sexual selection and species recognition by female Drosophila melanogaster. *Anim. Behav.* **68,** 1165–1180 (2004).

11. Ewing, A. W. Functional Aspects of Drosophila Courtship. *Biol. Rev.* **58,** 275–292 (1983).

12. Balakrishnan, R. & Pollack, G. S. Recognition of courtship song in the field cricket, Teleogryllus oceanicus. *Anim. Behav.* **51,** 353–366 (1996).

13. Simmons, L. W. The calling song of the field cricket, Gryllus bimaculatus (de geer): constraints on transmission and its role in intermale competition and female choice. *Anim. Behav.* **36,** 380–394 (1988).

14. Grodnitsky, D. L. Evolution and classification of insect flight kinematics. *Evolution (N. Y).* **49,** 1158–1162 (1995).

15. Stillwell, R. C. *et al.* Sex Differences in Phenotypic Plasticity Affect Variation in Sexual Size Dimorphism in Insects: From Physiology to Evolution. *Annu. Rev. Entomol.* **55,** 227–245 (2010).

16. Blanckenhorn, W. U. *et al.* Proximate Causes of Rensch's Rule: Does Sexual Size Dimorphism in Arthropods Result from Sex Differences in Development Time? *Am. Nat.* **169,** 245–257 (2007).

17. Testa, N. D., Ghosh, S. M. & Shingleton, A. W. Sex-Specific Weight Loss Mediates Sexual Size Dimorphism in Drosophila melanogaster. *PLoS One* **8,** (2013).

18. Bastock, M. & Manning, A. The Courtship of Drosophila Melanogaster. *Behaviour* **8,** 85–110 (1955).

19. Ewing, A. W. & Bennet-Clark, H. C. The Courtship Songs of Drosophila. *Behaviour* **31,** 288–301 (1968).

20. Bennet-Clark, H. C. & Ewing, A. W. Pulse Interval as a Critical Parameter in Courtship Song of Drosophila melanogaster. *Anim. Behav.* **17,** 755- (1969).

21. Von Schilcher, F. The function of pulse song and sine song in the courtship of Drosophila melanogaster. *Anim. Behav.* **24,** 622–625 (1976).

22. Shirangi, T. R., Stern, D. L. & Truman, J. W. Motor Control of Drosophila Courtship Song. *Cell Rep.* **5,** 678–686 (2013).

23. Partridge, L. & Farquhar, M. Lifetime Mating Success of Male Fruitflies. *Anim. Behav.* **31,** 871–877 (1983).

24. Zamudio, K. R., Huey, R. B. & Crill, W. D. Bigger isn't always better: body size, developmental and parental temperature and male territorial success in Drosophila melanogaster. *Anim. Behav.* **49,** 671–677 (1995).

25. Prasad, B. R. G., Hegde, S. N. & Krishna, M. S. Positive relation between male size and remating success in some populations of Drosophila bipectinata. *Zool. Stud.* **47,** 75–83 (2008).

26. Ewing, A. W. Body size and courtship behaviour in Drosophila melanogaster.

Anim. Behav. **9,** 93–99 (1960).

27. Gidaszewski, N. A., Baylac, M. & Klingenberg, C. Evolution of sexual dimorphism of wing shape in the Drosophila melanogaster subgroup. *BMC Evol. Biol.* **9,** 110 (2009).

28. Bitner-Mathé, B. C. & Klaczko, L. B. Plasticity of Drosophila melanogaster wing morphology: Effects of sex, temperature and density. *Genetica* **105,** 203–210 (1999).

29. Siomava, N., Wimmer, E. A. & Posnien, N. Extensive sexual wing shape dimorphism in Drosophila melanogaster, Ceratitis capitata. 1–32 (2017). doi:10.1101/135749

30. Menezes, B. F., Vigoder, F. M., Peixoto, A. A., Varaldi, J. & Bitner-Mathé, B. C. The influence of male wing shape on mating success in Drosophila melanogaster. *Anim. Behav.* **85,** 1217–1223 (2013).

31. Azevedo, R. B. R., James, A. C., McCabe, J. & Partridge, L. Latitudinal Variation of Wing: Thorax Size Ratio and Wing-Aspect Ratio in Drosophila melanogaster. *Evolution (N. Y).* **52,** 1353 (1998).

32. Frazier, M. R., Harrison, J. F., Kirkton, S. D. & Roberts, S. P. Cold rearing improves cold-flight performance in Drosophila via changes in wing morphology. *J. Exp. Biol.* **211,** 2116–2122 (2008).

33. Huey, R. B., Gilchrist, G. W., Balanya, J., Pascual, M. & Serra, L. Rapid evolution redux: a size cline in South American Populations of an introduced fly. *Science (80-.).* **287,** 308–309 (2000).

34. Starmer, W. T. & Wolf, L. L. Causes of variation in wing loading among

Drososphila species. *Biol. J. Linn. Soc.* **37,** 247–261 (1989).

35. Imasheva, A. G., Bubli, O. A. & Lazebny, O. E. Variation in wing length in eurasian natural populations of drosophila melanogaster. *Heredity (Edinb).* **72,** 508–514 (1994).

36. Gilchrist, G. W., Huey, R. B., Balanyà, J., Pascual, M. & Serra, L. A time series of evolution in action: A latitudinal cline in wing size in South American Drosophila subobscura. *Evolution (N. Y).* **58,** 768–780 (2004).

37. Ray, R. P., Nakata, T., Henningsson, P. & Bomphrey, R. J. Enhanced flight performance by genetic manipulation of wing shape in Drosophila. *Nat. Commun.* **7,** 10851 (2016).

38. Combes, S. A., Rundle, D. E., Iwasaki, J. M. & Crall, J. D. Linking biomechanics and ecology through predator-prey interactions: flight performance of dragonflies and their prey. *J. Exp. Biol.* **215,** 903–913 (2012).

39. Bates, D., Mächler, M., Bolker, B. & Walker, S. Fitting Linear Mixed-Effects Models using lme4. *J. Stat. Softw.* **67,** (2014).

40. Benjamini, Y. & Hochberg, Y. Controlling the false discovery rate - a practical and powerful approach to multiple testing. *J. R. Stat. Soc. Ser. B-Methodological* **57,** 289–300 (1995).

41. Sotavalta, O. Recordings of High Wing-Stroke and Thoracic Vibration Frequency in Some Midges. *Biol. Bull.* **104,** 439–444 (1953).

42. Ha, N. S., Truong, Q. T., Goo, N. S. & Park, H. C. Relationship between wingbeat frequency and resonant frequency of the wing in insects. *Bioinspiration and Biomimetics* **8,** (2013).

43. Sotavalta, O. The flight-tone (wing stroke frequency) of insects. *Acta Entomol. Fenn.* **4,** 1–117 (1947).

44. May, M. L. Wingstroke frequency of dragonflies (Odonata: Anisoptera) in relation of temperature and body size. *J. Comp. Physiol.* **144,** 229–240 (1981).

45. Foster, B. Y. J. A. & Robertson, R. M. Temperature Dependency of Wing-beat Frequency in Intact and Deafferented Locusts. *J. exp. Biol.* **162,** 295–312 (1992).

46. Noach, E. J. K., Van der Klis, H., De Jong, G. & Scharloo, W. Wing beat frequencies in Drosophila melanogaster selected for different wing lengths. *Netherlands J. Zool.* **47,** 241–253 (1997).

47. Villarreal, S. M., Winokur, O. & Harrington, L. The impact of temperature and body size on fundamental flight tone variation in the mosquito vector Aedes aegypti (Diptera: Culicidae): Implications for acoustic lures. *J. Med. Entomol.* **54,** 1116–1121 (2017).

48. Machin, K. E., Pringle, J. W. S., F.R.S. & Tamasige, M. The Physiology of Insect Fibrillar Muscle. IV. The Effect of Temperature on a Beetle Flight Muscle. *Proc. R. Soc. London B* **155,** 493–499 (1962).

49. Ritchie, M. G., Saarikettu, M., Livingstone, S. & Hoikkala, a. Characterization of female preference functions for Drosophila montana courtship song and a test of the temperature coupling hypothesis. *Evolution* **55,** 721–727 (2001).

50. Unwin, D. M. & Corbet, S. A. Wingbeat frequency, temperature and body size in bees and flies. *Physiol. Entomol.* **9,** 115–121 (1984).

51. Bullock, S. H. Relationships among Body Size , Wing Size and Mass in Bees

from a Tropical Dry Forest in México. *J. Kansas Entomol. Sociwty* **72,** 426–439 (1999).

52. Shingleton, A. W., Frankino, W. A., Flatt, T., Nijhout, H. F. & Emlen, D. J. Size and shape: The developmental regulation of static allometry in insects. *BioEssays* **29,** 536–548 (2007).

53. Emlen, D. J. & Allen, C. E. Genotype to Phenotype: Physiological Control of Trait Size and Scaling in Insects. *Integr. Comp. Biol.* **43,** 617–634 (2004).

54. Danforth, B. N. The evolution of hymenopteran wings: the importance of size. *J. Zool.* **218,** 247–276 (1989).

55. Dudley, R. *The Biomechanics of Insect Flight: Form, Function, Evolution*. (Princeton University Press, 2002).

56. Corben, H. C. Wing-beat frequencies, wing-areas and masses of flying insects and hummingbirds. *J. Theor. Biol.* **102,** 611–623 (1983).

57. Dudley, R. The biomechanics of insect flight: Form, function, evolution. *Biomech. insect flight Form, Funct. Evol.* i–xii, 1-476 (2000).

58. Shingleton, A. W., Estep, C. M., Driscoll, M. V. & Dworkin, I. Many ways to be small: Different environmental regulators of size generate distinct scaling relationships in Drosophila melanogaster. *Proc. R. Soc. B Biol. Sci.* **276,** 2625–2633 (2009).

59. Lefranc, A. & Bundgaard, J. Controlled variation of body size by larval crowding in Drosophila melanogaster. *Dros. Inf. Serv.* **83,** 171–174 (2000).

60. David, J. R. *et al.* Genetic variability of sexual size dimorphism in a natural

population of Drosophila melanogaster: an isofemale-line approach. *J. Genet.* **82,** 79–88 (2003).

61. Gidaszewski, N. A., Baylac, M. & Klingenberg, C. P. Evolution of sexual dimorphism of wing shape in the Drosophila melanogaster subgroup. *BMC Evol. Biol.* **9,** (2009).

62. Robertson, F. W. The ecological genetics of growth in Drosophila 6. The genetic correlation between the duration of the larval period and body size in relation to larval diet. *Genet. Res.* **1,** 74–92 (1963).

63. Nijhout, H. F. The control of body size in insects. *Dev. Biol.* **261,** 1–9 (2003).

64. Partridge, L., Barrie, B., Fowler, K. & French, V. Thermal evolution of pre-adult life history traits in Drosophila melanogaster. *J. Evol. Biol.* **7,** 645–663 (1994).

65. Stern, D. L. & Emlen, D. J. The developmental basis for allometry in insects. *Development* **126,** 1091–1101 (1999).

66. Milan, M., Campuzano, S. & Garcia-Bellido, A. Cell cycling and patterned cell proliferation in the Drosophila wing during metamorphosis. *Dev. Biol.* **93,** 11687–11692 (1996).

67. Robertson, F. W. Studies in quantitative inheritance XI. Genetic and environmental correlation between body size and egg production inDrosophila Melanogaster . *J. Genet.* **55,** 428 (1957).

68. Tantawy, A. . O. . & Vetukhiv, M. . O. . Effects of Size on Fecundity, Longevity and Viability in Populations of Drosophila pseudoobscura. *Am. Soc. Nat.* **94,** 395–403 (1960).

69. Gromko, M. H., Briot, A., Jensen, S. C. & Fukui, H. H. Selection on Copulation Duration in Drosophila. **45,** 69–81 (2015).

70. Lefranc, a & Bundgaard, J. The influence of male and female body size on copulation duration and fecundity in Drosophila melanogaster. *Hereditas* **132,** 243–247 (2000).

71. Deakin, M. a B. Formulae for insect wingbeat frequency. *J. Insect Sci.* **10,** 96 (2010).

72. Byrne, D. N., Buchmann, S. L. & Spangler, H. G. Relationship Between Wing Loading, Wingbeat Frequency and Body Mass in Homopterous Insects. *J. exp. Biol* **135,** 9–23 (1988).

73. Sotavalta, O. Flight-tone and Wing-stroke Frequency of Insects and the Dynamics of Insect Flight. *Nature* **170,** 1057–1058 (1952).

74. Sotavalta, O. The effect of wing inertia on the wing-stroke frequency of moths, dragonflies and cockroach. *Ann Ent Fenn.* 93–101 (1954).

75. Chadwick, L. E. & Williams, C. M. The effects of atmospheric pressure and composition on the flight of Drosophila. *Biol. Bull.* **97,** 115–137 (1949).

76. Chadwick, L. E. Stroke Amplitude as a Function of Air Density in the Flight of Drosophila. *Univ. Chicago Press Assoc. with Mar. Biol. Lab.* **100,** 15–27 (1951).

77. Schneider, P. Contributions to the flight biology of beetles. 4. Body temperature, flight behaviour and wing-beat frequency. *Zool. Anz.* **205,** 1–19 (1980).

78. Karl Georg Götz. Flight control in Drosophila by visual perception of motion.

Kybernetik **4,** 199–208 (1968).

79. Taylor, L. R. Analysis of the Effect of Temperature on Insects in Flight. *J. Anim. Ecol.* **32,** 99–117 (1963).

80. Reed, S. C., Williams, C. M. & Chadwick, L. E. Frequency of wing-beat as a character for separating species races and geographic varieties of Drosophila. *Genetics* **27,** 349–361 (1942).

81. Nachtigall, W. & Roth, W. Correlations Between Stationary Measurable Parameters of Wing Movement and Aerodynamic Force Production in the Blowfly (Calliphora vicina R . -D .). *J. Comp. Physiol. A* **150,** 251–260 (1983).

82. Vogel, S. Flight in Drosophila II. Variation in stroke parameters and wing contour. *J. Exp. Biol.* **46,** 383–392 (1967).

83. Lehmann, F.-O. Ambient temperature affects free-fight performance in the fruit fly Drosophila melanogaster. *J. Comp. Physiol. B.* **169,** 165–171 (1999).

84. Stavenga, D. G., Schwering, P. B. W. & Tinbergen, J. A three-compartment model describing temperature changes in tethered flying blowflies. *J. Exp. Biol.* **185,** 325–333 (1993).

85. Stone, G. N. & Willmer, P. G. Warm-up rates and body temperatures in bees: The importance of body size, thermal regime and phylogeny. *J. Exp. Biol.* **147,** 303–328 (1989).

86. Dickinson, M. H., Lehmann, F. O. & Sane, S. P. Wing rotation and the aerodynamic basis of insect flight. *Science (80-.).* **284,** 1954–1960 (1999).

87. Zanker, J. M. On the mechanism of speed and altitude control in Drosophila

melanogaster. *Physiol. Entomol.* **13,** 351–361 (1988).

88. Ennos, R. A. The kinematics and aerodynamics of the Free Flight of some Diptera. *J. Exp. Biol.* **142,** 49–85 (1989).

89. Ellington, C. P. The Aerodynamics of Hovering Insect Flight. III. Kinematics. *Philos. Trans. R. Soc. London* **B,** 41–78 (1984).

90. David, C. T. The relationship between body angle and flight speed in free-flying Drosophila. *Physiol. Entomol.* **3,** 191–195 (1978).

91. Tennekes, H. *The Simple Science of Flight: From Insects to Jumbo Jets*. (MIT Press, 2009).

92. Simon, J. C., Dickson, W. B. & Dickinson, M. H. Prior mating experience modulates the dispersal of drosophila in males more than in females. *Behav. Genet.* **41,** 754–767 (2011).

93. Martin, J. R. A portrait of locomotor behaviour in Drosophila determined by a video-tracking paradigm. *Behav. Processes* **67,** 207–219 (2004).

94. Burnet, B., Burnet, L., Connollyt, K. & Wihiamson, N. A genetic analysis of locomotor activity in Drosophila melanogaster. *Genetics* **61,** 111–119 (1988).

95. Belgacem, Y. H. & Martin, J. R. Hmgcr in the corpus allatum controls sexual dimorphism of locomotor activity and body size via the insulin pathway in Drosophila. *PLoS One* **2,** (2007).

96. Dankert, H. *et al.* High-throughput Ethomics in Large Groups of Drosophila. *Nat. Methods* **6,** 451–457 (2009).

97. Lehmann, F. O. & Dickinson, M. H. The control of wing kinematics and flight

forces in fruit flies (Drosophila spp.). *J. Exp. Biol.* **201,** 385–401 (1998).

98. Weber, K. E. Selection on wing allometry in Drosophila melanogaster. *Genetics* **126,** 975–989 (1990).

99. Weber, K. E. Large genetic change at small fitness cost in large populations of Drosophila melanogaster selected for wind tunnel flight: Rethinking fitness surfaces. *Genetics* **144,** 205–213 (1996).

100. Marden, J. H., Wolf, M. R. & Weber, K. E. Aerial performance of Drosophila melanogaster from populations selected for upwind flight ability. *J. Exp. Biol.* **200,** 2747–2755 (1997).

Chapter 4

Using wing beat kinematics as the basis for identifying the gear of free-flying *Calliphora vicina*

Using wing beat kinematics as the basis for identifying the gear of free-flying *Calliphora vicina*

Inés Dawson*, Jonathan Page*, Graham Taylor*, Simon Walker†

* Oxford Flight Group, University of Oxford, The John Krebs Field Station, Department of Zoology, Wytham, Oxford, OX2 8QJ, UK

† Faculty of Biological Sciences, University of Leeds, Leeds, LS2 9JT, UK

The gear change mechanism in the wing hinge of the blowfly is known to modulate wing beat kinematics in *Calliphora vicina*, but has only been studied under tethered conditions due to experimental limitations. We used a detailed tethered dataset and a *k*-nearest neighbour (*k*-NN) clustering algorithm to infer the gear stop positions in free-flying *Calliphora vicina*. Using two validation metrics, our algorithm reached an estimated 81% accuracy in identifying gear stop position in free-flying individuals. We found three independently varying groups of parameters. The gear change mechanism primarily affected peak stroke and deviation angles, which directly influenced stroke amplitude, timing of stroke reversal and timing of wing rotation at stroke reversal, which enable blowflies to modulate their forward speed. Gear stop position was also found to influence wing beat frequency, although there were patterns of variation unexplained by gear stop position and alula state in the tethered dataset, suggesting muscular involvement. The gear change mechanism did not directly influence stroke plane angle, which was most closely correlated with body kinematics.

INTRODUCTION

Calliphora vicina (blowflies) are remarkable flyers and perform their manoeuvres through their ability to make fine adjustments to their wing beat kinematics, which are controlled by their sophisticated wing hinge[1–3]. Although there is as yet no consensus about the components of the Brachyceran wing hinge mechanism and its exact function, it is thought to be associated with a gear change mechanism, whereby the steering muscles are able to control the interaction between different sclerites in the wing hinge and alter wing beat kinematics during flight, and in some species, even disengage the wings from the flight motor[4–12].

In *Calliphora*, the gear change mechanism involves the interaction between two anatomical components: the pleural wing process (PWP), a grooved sclerotised thoracic projection that extends dorsally from the pleural plate, and the radial stop (RS), which is a sclerotised ventral projection from the radial vein of the wing **(Image 4)**. The number of grooves on the PWP varies according to species, but there are generally two in the more derived Brachyceran species, including *Calliphora*, one in the more basal Brachyceran species, and non-Brachyceran species merely have a smooth groove that the RS can interact with[8]. How this mechanism works exactly has generated controversy in the literature[5,7–10,13,14], although studies have shown that some wing beat kinematics in *Calliphora*, such as stroke amplitude and stroke angle at the end of the downstroke, are multimodally distributed, and that gear changes in *Calliphora* allow them to perceptibly alter their flight kinematics for different purposes[5,15,16].

The gear change mechanism in *Calliphora* allows them to position the radial stop (RS) in one of two notches on the dorsal surface of the pleural wing process

(PWP) during the lower half of the stroke, which limits the anterior motion of the wing, or they can also completely disengage the RS on either side of the PWP. Generally, blowflies are considered to be capable of adopting one of three gears in flight. Gear 1 is the interaction between the RS and the distal PWP groove; Gear 2 is the interaction between the RS and the proximal PWP groove; and Gear 3 is the RS disengaged on the proximal area of the PWP **(Image 4)**. Studies with tethered *Calliphora* show that they usually adopt Gear 3, with the RS rarely making contact with the PWP during the wingstroke. Gear 0, where the RS is disengaged beside the distal area of the PWP has also been observed, although it is considered to be an erroneous manoeuvre by the blowfly and is associated with anomalous wing beat kinematics[15,16].

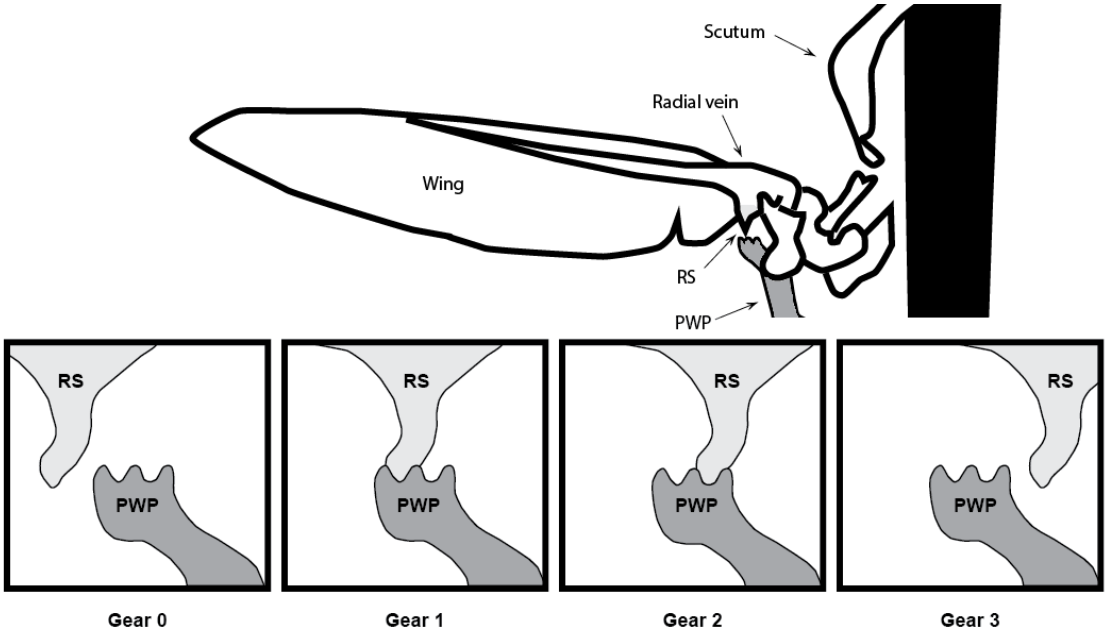

Image 4. Top: Diagram of the wing hinge displaying the radial vein, wing, radial stop (RS), pleural wing process (PWP) and scutum. Bottom: Gear stop positions based on the interaction between the radial stop (RS) and the pleural wing process (PWP). The body is on the right and the wing extends to the left of the diagram. Gear 0 is an anomalous and rare position, whereas blowflies regularly switch between Gears 1, 2 and 3 to modulate their flight kinematics.

All flight studies to date that have examined the performance of the gear change mechanism have involved tethered flies, due to the impossibility of observing the gear stop position in free-flying flies. Likewise, the majority of flight studies to date detailing blowfly wing kinematics also involve tethered individuals, which are known to behave differently from free-flying flies. Studies of free-flying and 'almost' free-flying blowflies (with coils mounted on their heads and thorax) are few and far between and focus mostly on behaviour, saccades, body kinematics and flight trajectories in *Calliphora* and *Lucilia* (Calliphoridae), and relating these to their flight performance and flight control in response to optic flow[17–23]. The ability to make recordings of free-flight trajectories, however, comes at the expense of not being able to monitor the gear stop position.

Our objective in this study, therefore, is to quantitatively describe the wing beat kinematics of unmanipulated, free-flying *Calliphora vicina* using high speed videography, and to propose an algorithmic method to predict which gear they are operating in on the basis of their instantaneous wing beat kinematics. This algorithm is trained using a dataset of tethered *Calliphora vicina*, containing measurements of the same flight kinematic parameters alongside the observed gear stop position for each wing beat. Whilst it may not be possible to associate the absolute value of a single kinematic variable to a specific gear stop due to overlap, it may be possible to achieve a higher degree of confidence using a multitude of kinematic variables.

METHODS

Animals

Late instar larvae of *Calliphora vicina* were obtained from a local pet store and reared on red meat. They were stored in a cool, dry room at 20°C. Adult flies emerged from late April to early July 2016, and were stored in different enclosures based on their emergence date. Adults were fed on a combination of milk powder formula and mashed banana. Individual adult flies of at least 2-3 days post-eclosion with a hardened cuticle and well developed wings were selected for recording in free-flight experiments. A subset of individuals were weighed post-flight to provide a basis for a scaling factor to estimate the weight of the individual in each recording.

Tethered flight dataset

The training input used for the *k*-nearest neighbour (*k*-NN) algorithm to identify the gear position of our free-flight dataset was a dataset of tethered *Calliphora vicina* containing wing beat kinematic and gear stop position measurements, collected by Jonathan Page (in prep.)[15,16]. The background and rearing conditions for the tethered blowflies were the same as our free-flight dataset. Prior to tethering, the flies were cold anaesthetised so as to attach to a metal rod with a mixture of beeswax and colophonium onto their scutum. A fan was used to both trigger flight in the tethered flies as well as to maintain an appropriate flight temperature during the experiments. The tethered flies were positioned in such a way that the PWP and RS interaction could be recorded using high-speed macrophotography and classified for each wing beat during the flight experiments. The overall wing beat kinematics were recorded too, so that the wing beat

kinematics could be correlated with the gears. The position of the alula (hinged flap at the proximal end of the wing, which is also involved in modulating wing beat kinematics), which could be flipped or flat, was recorded too, although for the purposes of our training algorithm we elected to only predict the gear stop position. In total, the tethered flight dataset contained 11,512 wing beats of 26 individuals from 75 sequences.

Free-flight recording

The free-flight recordings form the core dataset of this study. Free flight experiments took place in a spherical white dome 1m in diameter. The interior of the dome was decorated with pieces of card to provide a visual environment for the fly. A UV light was placed at the top of the flight arena to serve as an attractant, as *Calliphora vicina* are capable of detecting it[24]. A pedestal with a slice of mashed banana was also provided for the fly to feed on between flights to maintain constant weight and energy levels. Only one fly was placed in the dome at a time, and flight experiments were made over a period of 4-8 hours.

Flight was often unprompted, but was occasionally stimulated mechanically by waving a stick in the flight area to trigger the fly's looming response. Recordings were captured by four Photron FASTCAM SA3 high-speed cameras, model 120K-M2 (Photron Ltd, Bucks, UK) with 180mm Sigma macro lenses running at 4800fps and resolution of 768x640px. A shutter speed of 1/60000th of a second was chosen to freeze the frame in motion. Backlight illumination was provided by four pulsed custom built IR LED lights. Recordings were automatically triggered by two IR Arduino triggers when the fly crossed the centre of the recording volume.

Flight processing

The cameras were calibrated using custom-written photogrammetric software running in MATLAB (MATLAB R2015a, 8.2.0.701, The MathWorks Inc. Natick MA, 2015). Flight recordings were processed using custom-written *Calliphora* tracker software adapted and optimised from the *Eristalis* tracking software from Walker et al.[6,25]. The tracker automatically detects the position of the fly and extracts its body and wing kinematic parameters for each stroke cycle. Further details on the operation of this tracking software are available in Walker et al. and Chapter 1 of this thesis[6,25]. Three axis systems were employed to describe the kinematic parameters and body positions:

Lab-fixed coordinate system

The lab-fixed coordinate system is a right-handed inertial axis system $\{x_W, y_W, z_W\}$, where the z_W axis points in the direction of gravity, and the x_W and y_W axes are directed arbitrarily in the horizontal plane. The origin of this coordinate system is arbitrary.

Primary body-fixed coordinate system

The body-fixed axis system is a rotating right-handed axis system $\{x_B, y_B, z_B\}$, with its origin located at the centre of mass of the insect. The x_B axis is defined as the anterior-posterior body axis, and the y_B axis points towards the right, passing through the wing bases. It follows from these definitions that the z_B axis points ventrally.

Horizontal body-fixed coordinate system

The horizontal body-fixed axis system is a rotating right-handed axis system $\{x_H, y_H, z_H\}$, with its origin located at the centre of mass of the insect. The z_H axis points vertically upwards, so is always parallel to (though oppositely signed) to the z_W axis, but moves with the insect. The x_H axis is defined as the projection of the x_B axis onto the horizontal plane. The y_H axis therefore points to the left, but is not used to define any of the parameters in this thesis.

The morphometric, body and wing beat kinematic parameters used are as described in further detail in **Chapter 2** and **Chapter 3** of this thesis.

_k_-nearest neighbour algorithm

The *k*-nearest neighbour (*k*-NN) algorithm was used to predict the gear stop position of each wing beat of *Calliphora vicina* based on its free-flying wing beat kinematics by training it on a classified tethered dataset where the gear stop positions were known alongside the wing beat kinematics. The *k*-NN algorithm is a non-parametric method for regression and classification. Classification algorithms take training inputs to build models that will predict the class membership of unclassified data. The training input for *k*-NN are parametric vectors in a multidimensional feature space and a class label vector. When presented with unclassified parametric vectors as input for prediction, the algorithm examines the *k* training data points nearest to the unlabelled sample, and assigns the most frequent class to them.

To train the model to identify blowfly gears on the basis of wing beat kinematics, a dataset of summary kinematics from tethered blowflies[15,16] were

inputted as parametric vectors, and the gear position for each wing beat was inputted as the class label vector. The summary kinematic parameters selected were wing beat frequency, stroke plane amplitude, timing of stroke reversal and peak stroke angle, as they were found to be significantly associated with the gear change mechanism[15,16]. The parameters from both the free-flying and tethered datasets were combined and z-scored under a grand mean and standard deviation, so that the normalised kinematic parameters were measured on the same scale in both the tethered and free-flight datasets. Although the datasets being z-scored are skewed and multimodal, it is still appropriate to z-score them for use as input parameters. A non-normal distribution will remain non-normal after being z-scored, although the values are expressed around a mean of 0 and standard deviation of 1, rather than relative to an absolute standard. The gear stop vector had four possible values: Gear 1, Gear 2 and Gear 3 for the standard positions within the pleural wing process groove, and Gear 0, for when the gear change mechanism was disengaged on the distal side of the PWP. Occurrences of Gear 0 are rare, and are considered to be anomalous during flight.

The *k*-NN algorithm is deterministic, which means that under identical conditions, the same input training data and the same input data for prediction will always yield the same classification vector for the unclassified model parameters. *k*-NN is also sensitive to local feature structure, so using a higher value of *k* neighbours can help reduce the effect of noise in the training dataset in classification, but can also have a smoothing effect which can bias the output classification towards the more abundant class in the training dataset, even if the data point would be better classified otherwise. To counteract the bias effect of higher values of *k*, inverse weighted distances were applied to the *k* nearest samples, whereby the class of

closer data samples were weighted higher than the class of data samples that lay further away. For continuous input parameters, such as the blowfly kinematic parameters, standardised Euclidean distance is the recommended distance measure.

The best combination of z-scored kinematic parameters for prediction and the ideal number of *k* neighbours was unknown a priori, so that the performance of the classifier was performed for all 15 possible combinations of kinematic parameters, with *k* being 1 up to 100 nearest neighbours.

We used two measures to examine the best combination of wing beat kinematic parameters and the number *k* of neighbours for the *k*-NN:

Cross-validation

As the correct classification of the test data is unknown, the training data can be tested using a cross-validation test, in which the training data is split into an input and test data. The process is repeated *M* times, with the dataset being split into $\frac{M-1}{M}$ for training, and the remainder for testing. The success rates of the predicted gear classifications were then compared to the real gear classification for each iteration, and the success rate was averaged for each set of parameters and *k* neighbours used. Values of 1 through 10 in integer increments were used for *M*.

Test-validation

As the training dataset had the potential to differ from our test dataset due to the different conditions of the tethered and free-flying blowflies, we also used the predictions generated on our free-flying dataset as a training model for the original training dataset, and compared the success rate. This method has the advantage of detecting parameters that differ significantly between both datasets for exclusion.

However, the success rate only reflects the accuracy at predicting the training dataset's class membership, and not that of the test dataset.

To determine the optimal combination of input kinematic parameters, as well as the optimal *k* number of neighbours, the weighted mean of the success rates of the two measures was taken, with cross-validation and test-validation being weighted at 50% each. The combination of parameters with the highest weighted success rate was selected with the optimum number of neighbours to obtain the predictions of gear stops which were subsequently used in analysis.

Statistical analysis

Linear mixed effect models were run with the lme4 package (Bates & Sarkar, 2006) in the R environment (R Development Core Team, 2017). All other statistical analyses were conducted using MATLAB.

RESULTS

In total, 2708 wing beats of free-flying *Calliphora vicina* from 274 sequences from 28 individuals were analysed.

Morphometrics

Body length and wing length were positively related ($R^2 = 0.60$, $F_{1,28} = 39.68$, $p < .0001$) **(Figure 8a)**, although wing length and wing chord are not related ($R^2 = 0.0049$, $F_{1,28} = 0.13$, $p = 0.72$) **(Figure 8b).**

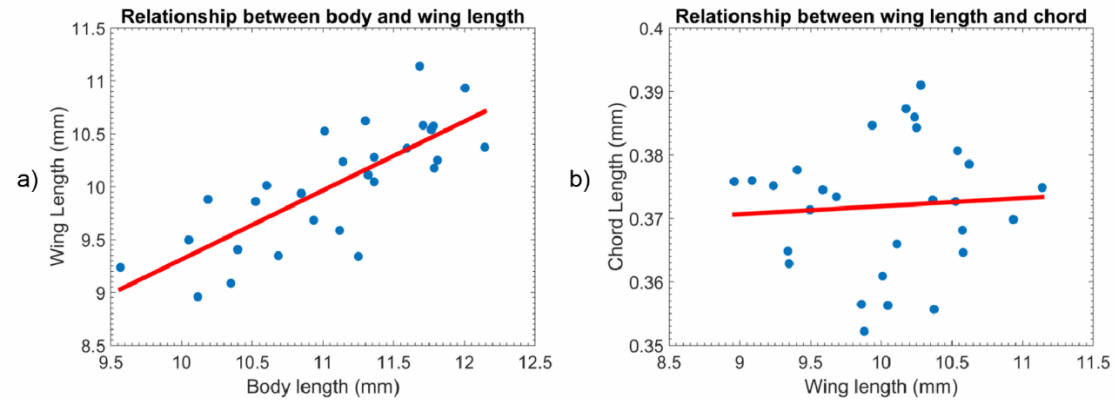

Figure 8. a) Relationship between body length (mm) and wing length (mm). b) Relationship between wing length (mm) and chord length (mm).

Some of the summary wing beat kinematics are multimodal, which is consistent with the existence of multiple gear stops in blowfly kinematics. This will be explored in further detail in the following section.

Predicting gear stops in free-flight

Comparison of free-flight and tethered flight

The summary free-flight kinematics revealed a multimodal distribution across some of the parameters. This is consistent with the existence of multiple gear stops, which blowflies are able to switch between during flight. In order to predict which gear each wing beat from the free-flying dataset belongs to, the tethered dataset was used as a training dataset[15,16]. The distributions of the kinematic parameters of the tethered flies were significantly different to those of the free-flying flies **(Table 2, Figure 9)**.

A Mann Whitney U test showed that the wing beat frequency was 15Hz slower in tethered flies than free-flying flies ($U_{0.05(2),274,75}$ = 48197, d = 0.80, p < .0001), although the distribution shape and spread closely mirrored each other. Mean stroke amplitude was not significantly different between tethered and free-

flying flies ($U_{0.05(2),274,75}$ = 45027, p = 0.94), although the variance of the stroke plane amplitude was significantly higher in tethered flies (Bartlett's statistic = 34.29, p<.0001). The multimodal nature is more noticeable in tethered flies than in the free-flying *Calliphora*. In the tethered dataset, the long tail of low amplitude typically belongs to Gear 0, the two lowest maxima to Gear 1 and Gear 2, and the final highest peaks correspond to Gear 3 with the alula out and retracted respectively. The mean timing of stroke reversal occurred later in tethered flies ($U_{0.05(2),274,75}$ = 40877, d = 1.18, p < .0001) and had a significantly greater variance (Bartlett's statistic = 116.6, p<.0001). The mean peak stroke angle was not significantly different between tethered and free-flying flies ($U_{0.05(2),274,75}$ = 45404, p = 0.60), but the tethered flies do have a significantly greater variance (Bartlett's statistic = 82.7, p<.0001).

Wing beat parameter	Tethered flight	Free-flight
Wing beat frequency (Hz)	150.9±19.9	166.2±19.7
Stroke amplitude (degrees)	106.4±27.6	105.5±16.4
Timing of stroke reversal	0.547±0.043	0.511±0.017
Peak stroke angle (˚)	27.3±27.0	25.0±12.8

Table 2. Mean and standard deviation of key wing beat parameters for tethered and free-flying blowflies.

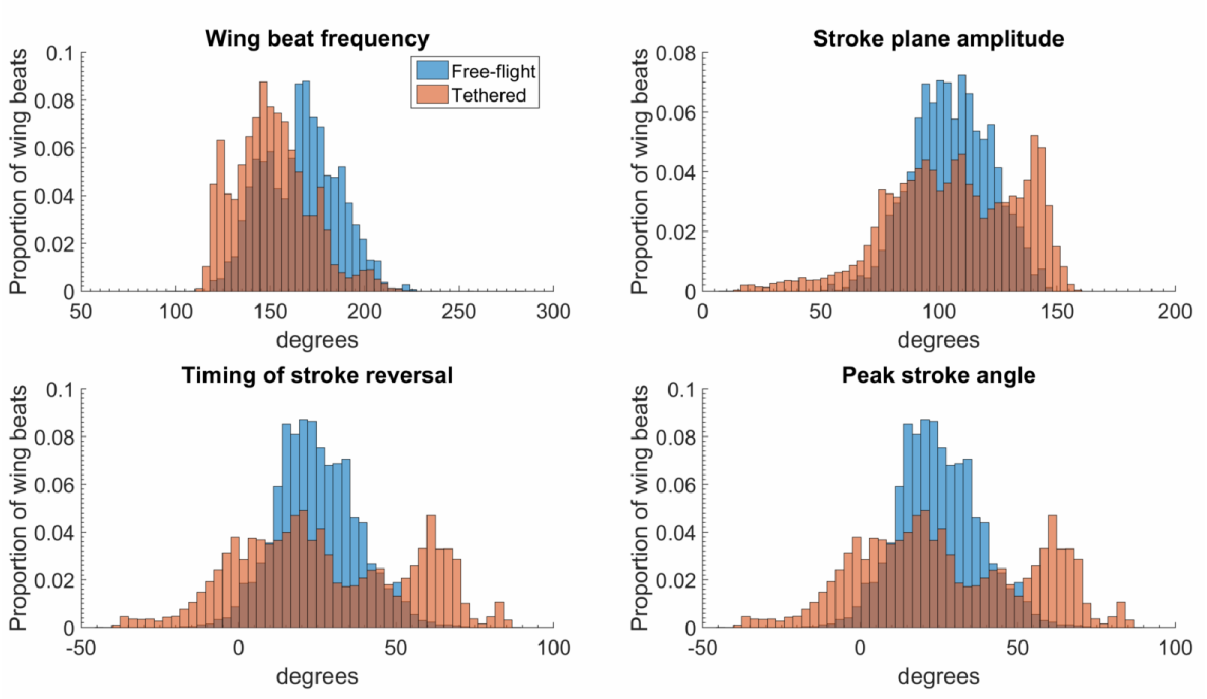

Figure 9. Comparison of normalised distribution of free-flying (blue) and tethered (orange) blowfly kinematics. a) Wing beat frequency (Hz) b) Stroke amplitude (degrees) c) Timing of stroke reversal (downstroke to wingbeat duration ratio) d) Peak stroke angle (degrees)

Optimising the k-NN algorithm

Before inputting the tethered dataset into the *k*-NN algorithm, and training it on the free-flight dataset, both were z-scored together so that the normalised kinematic parameters were measured on the same scale in both the tethered and free-flight datasets.

To find the optimal combination of kinematic parameters for predicting the gear classification, we tested all possible combinations of the four z-scored parameters with *k* neighbours from 1 to 100, and used them to calculate the two validation measurements from them. The combination of cross validation and test validation measurements were contrasted, and the weighted averages of their

success rate were calculated **(See Table 3 and Supplementary Material 2 in appendices)**.

Based on this, the optimal combination of parameters was wing beat frequency, stroke plane amplitude and peak stroke angle with 26 neighbours was accurate in correctly predicting 81.25% of the gears of the training dataset (test-validation was accurate in predicting 86.6% of wing beats in Gear 1, 51.3% in Gear 2 and 93.3% in Gear 3, whereas the cross-validation was accurate in predicting 84.8% of wing beats in Gear 1, 55.6% in Gear 2 and 94.4% in Gear 3). Although understandably the combination of all four parameters yielded a better prediction overall for cross-validation, the test-validation was considerably lower compared to other combinations, and the combined score was lower than the best three-parameter model.

Parameters	Weighted average result (% correct)
WBF	74.19
SPA	74.91
TSR	67.49
PSA	69.20
WBF, SPA	80.98
WBF, TSR	73.31
WBF, PSA	77.07
SPA, TSR	73.53
SPA, PSA	75.48
TSR, PSA	71.51
WBF, SPA, TSR	76.91
WBF, SPA, PSA	81.25
WBF, TSR, PSA	76.22
SPA, TSR, PSA	76.01
WBF, SPA, TSR, PSA	79.39

Table 3. Weighted average success rate (test-validation = 50%, cross-validation = 50%) from predictions on the training data for each combination of parameters (WBF = wing beat frequency, SPA = stroke plane amplitude, TSR = timing of stroke reversal, PSA = peak stroke angle, % = percentage of correct predictions from training dataset).

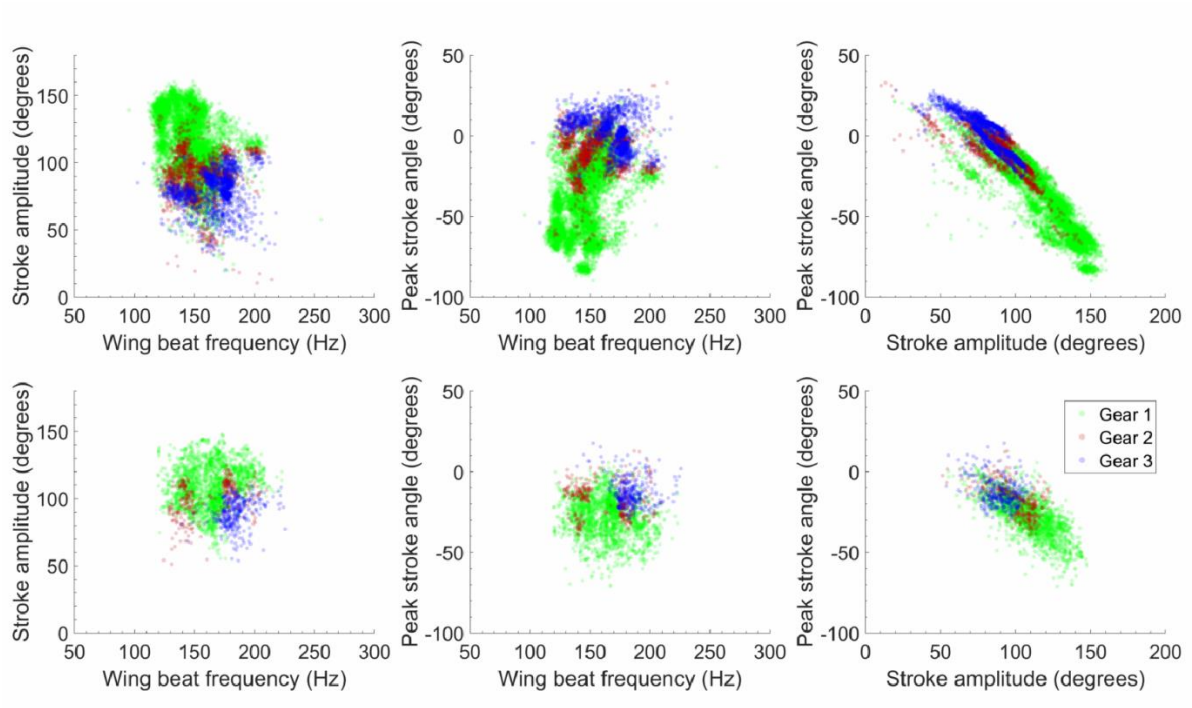

Figure 10. 1) Gear stops of tethered *Calliphora vicina* of the selected wing beat parameters (wing beat frequency, stroke plane amplitude and peak stroke angle), colour coded by gear (Gear 1: blue; Gear 2: red; Gear 3: green) for a) Wing beat frequency vs. stroke amplitude (degrees) b) Wing beat frequency (Hz) vs. peak stroke angle (degrees) c) Stroke amplitude (degrees) vs. peak stroke angle (degrees) 2) Predicted gear stops of free-flying *Calliphora vicina* from the *k*-NN model with 26 nearest neighbours and wing beat frequency, stroke amplitude and peak stroke angle as training parameters, colour coded by gear (Gear 1: blue; Gear 2: red; Gear 3: green) for a) Wing beat frequency vs. stroke amplitude (degrees) b) Wing beat frequency (Hz) vs. peak stroke angle (degrees) c) Stroke amplitude (degrees) vs. peak stroke angle (degrees)

Comparisons

Gear stops

Gear 1	Gear 2	Gear 3	Gear 0
350	331	2027	0

Table 4. Number of wing beats classified according to gear category. n=2708

Tethered vs. free-flight

	Gear 1	Gear 2	Gear 3	Gear 0
Tethered	14.98%	13.78%	69.27%	1.97%
Free-flight	12.92%	12.22%	74.85%	0%

Table 5. Percentage of wing beats according to gear category, and gear category and alula state in tethered blowflies (n = 11,512) and free-flying blowflies (n = 2708).

Summary free-flight wing beat kinematics by predicted gear stop

Parameter	Gear 1	Gear 2	Gear 3
Wing beat frequency (Hz)	184.0±11.9	163.0±21.7	163.6±18.7
Stroke amplitude (˚)	89.4±10.1	100.5±12.8	109.0±16.0
Timing of stroke reversal	0.502±0.013	0.507±0.017	0.513±0.017
Peak stroke angle (˚)	13.1±8.1	18.0±10.0	28.2±12.2
Advance ratio	0.122±0.055	0.132±0.053	0.114±0.055

Table 6. Summary wing beat kinematics and advance ratio (mean ± standard deviation) of wing beats according to gear stop category.

Despite the tethered dataset displaying a broader range of kinematics, the proportion of gears predicted in the free-flying dataset is comparable in quantity to those of the tethered dataset **(Table 4 and 5)**. There are significant differences in mean kinematics across all three gears in all four parameters (wing beat frequency: $F_{2,2705} = 187.63$, $p<0.0001$; stroke amplitude: $F_{2,2705} = 279.46$, $p<0.0001$; timing of stroke reversal: $F_{2,2705} = 75.16$, $p<0.0001$; peak stroke angle: $F_{2,2705} = 332.77$, $p<0.0001$) **(Table 6)**, with the exception of wing beat frequency in gears 2 and 3.

Wing beat kinematics

Wing beat frequency

Wing beat frequency varies inversely with wing length **(Figure 11)**. Mean wing beat frequency and wing length of each individual was used to account for pseudoreplication. The predicted wing beat frequency of an individual blowfly is -14.595(wing length in mm) + 315.35 when wing beat frequency is measured in Hz ($R^2 = 0.1927$; $F_{1,28} = 6.207$; $p = 0.0194$).

Figure 11. Inverse relationship between wing length (mm) and wing beat frequency (Hz).

We built a linear mixed effects model to explore the relationship between advance ratio and wing beat frequency, with advance ratio specified as the response variable, wing beat frequency and predicted gear stop as fixed effects, and sequence nested within individual as random effects. There was insufficient data for the model

to converge on a random slopes and intercepts model, so that only random intercepts were considered in the model. Predicted gear stop and wing beat frequency both affected advance ratio (Gear: $\chi^2(1)=153.06$, $p<.0001$; Wing beat frequency: $\chi^2(1)=187.30$, $p<.0001$), with wing beat frequency reducing advance ratio by -0.00129±0.00009Hz **(Figure 12a)**.

When the wing beat frequency distributions for each gear were examined, they all stood out for being multimodal. The state of the alula in the tethered dataset did not explain the multimodality, as the wing beat frequency distributions for both the flipped and flat distributions were bimodal too.

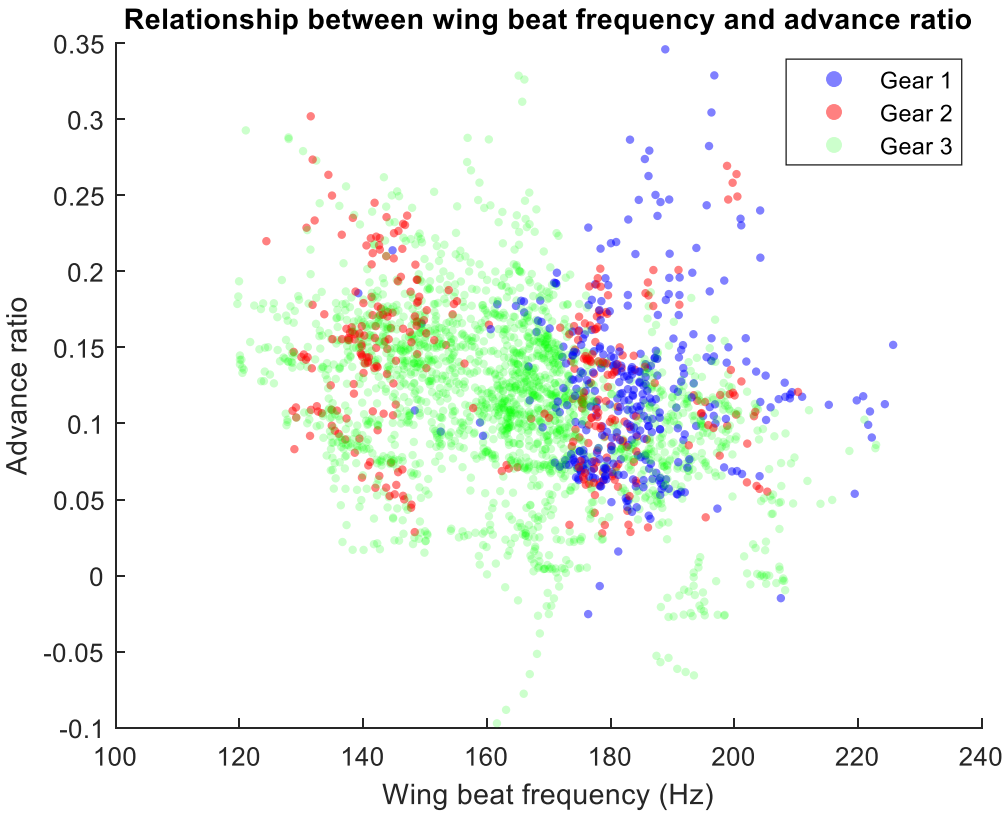

Figure 12a. Inverse relationship between wing beat frequency (Hz) and advance ratio colour coded by gear (Gear 1: blue; Gear 2: red; Gear 3: green)

Stroke amplitude

Stroke amplitude also has a multimodal distribution, although the peaks are less well defined, suggesting substantial overlap between different gear changes or insufficient data to distinguish them. *Calliphora* are also known to have greater control between the wing beat of the upstroke and the downstroke, and from a paired t-test, the difference between upstroke and downstroke amplitude is significantly different (t_{2707} = -3.00, p = 0.0027).

Stroke amplitude is known to influence forward speed. A linear mixed effects model was performed to explore the relationship between advance ratio and stroke amplitude, specifying advance ratio as the response variable, stroke amplitude and predicted gear stop as fixed effects and sequence nested within individual as random effects. There was insufficient data for the model to converge on a random slopes and intercepts model, so only random intercepts were considered in the model. Stroke amplitude and predicted gear all influenced advance ratio (Stroke amplitude: $\chi^2(1)=1453.0$, p<.0001; Gear: $\chi^2(1)=13.56$, p=0.0011). Amplitude affected advance ratio, reducing it by -0.001429±0.00004 **(Figure 12b)**.

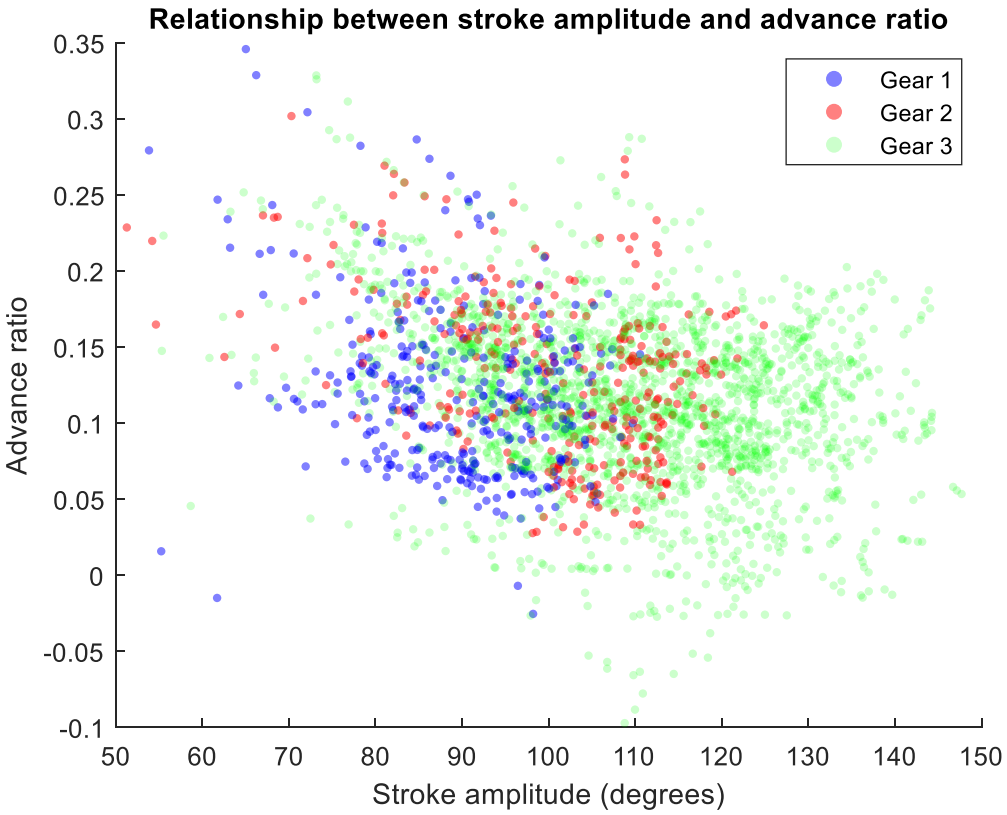

Figure 12b. Inverse relationship between stroke amplitude (degrees) and advance ratio colour coded by gear (Gear 1: blue; Gear 2: red; Gear 3: green).

Stroke amplitude is associated with upwards acceleration, as well as heading velocity. We constructed a similar linear mixed effects model, this time using upward acceleration as a response variable. Stroke amplitude and predicted gear stop affected upward acceleration (stroke amplitude: $\chi^2(1)=461.0$, $p<.0001$; Gear: $\chi^2(1)=8.07$, $p=0.018$), with stroke amplitude decreasing upward acceleration by -0.124±0.006ms^{-2} **(Figure 13)**.

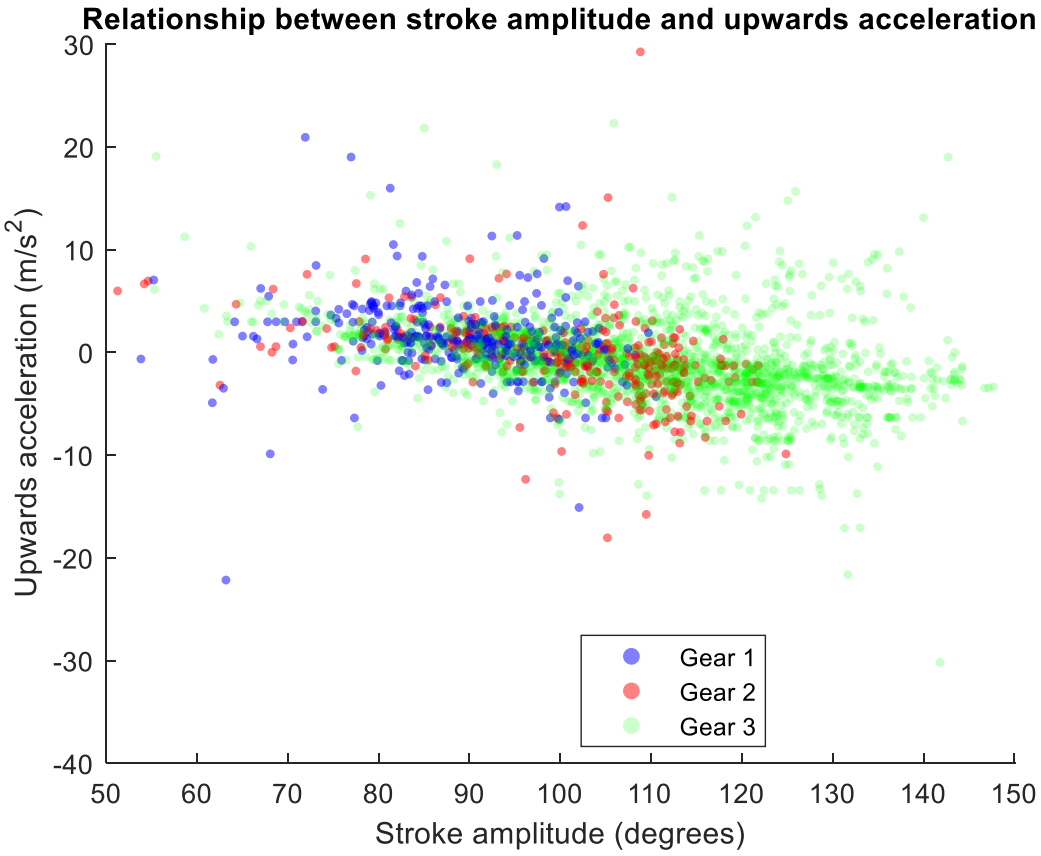

Figure 13. Relationship between stroke amplitude (degrees) and upwards acceleration colour coded by gear (Gear 1: blue; Gear 2: red; Gear 3: green)

Stroke plane

Stroke plane is unimodal in distribution, suggesting that gear change may have little effect on stroke plane, and that it is strongly linked to the blowfly's body kinematics. Roll angle is affected by stroke plane ($\chi^2(1)=999.5$, p=<.0001) but not by predicted gear ($\chi^2(1)=0.98$, p=0.61), with stroke plane decreasing it by -2.02±0.064 degrees **(Figure 14a)**.

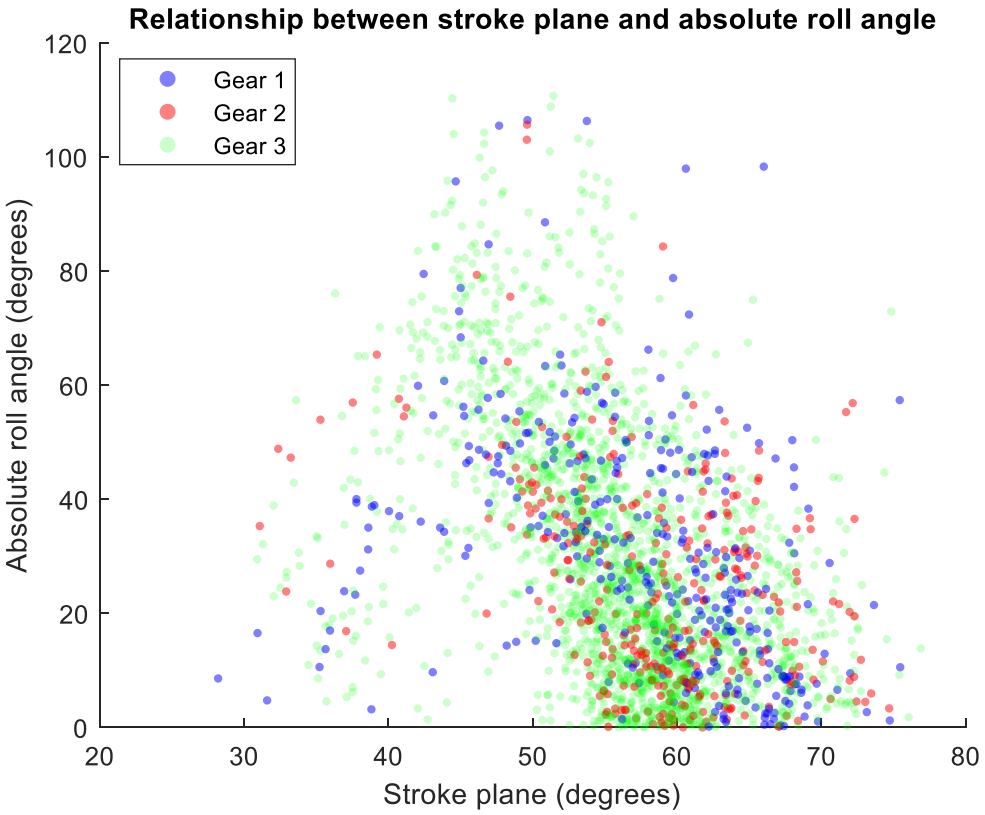

Figure 14a. Relationship between stroke plane and absolute roll angle colour coded by gear (Gear 1: blue; Gear 2: red; Gear 3: green)

Stroke plane also affects pitch angle **(Figure 14b)**. In a linear mixed effects model, stroke plane angle and predicted gear stop both affected pitch angle (stroke plane: $\chi^2(1)=711.5$, p=<.0001; Gear: $\chi^2(1)=15.0$, p = 0.00055). Stroke plane increased it by 1.07±0.04 degrees.

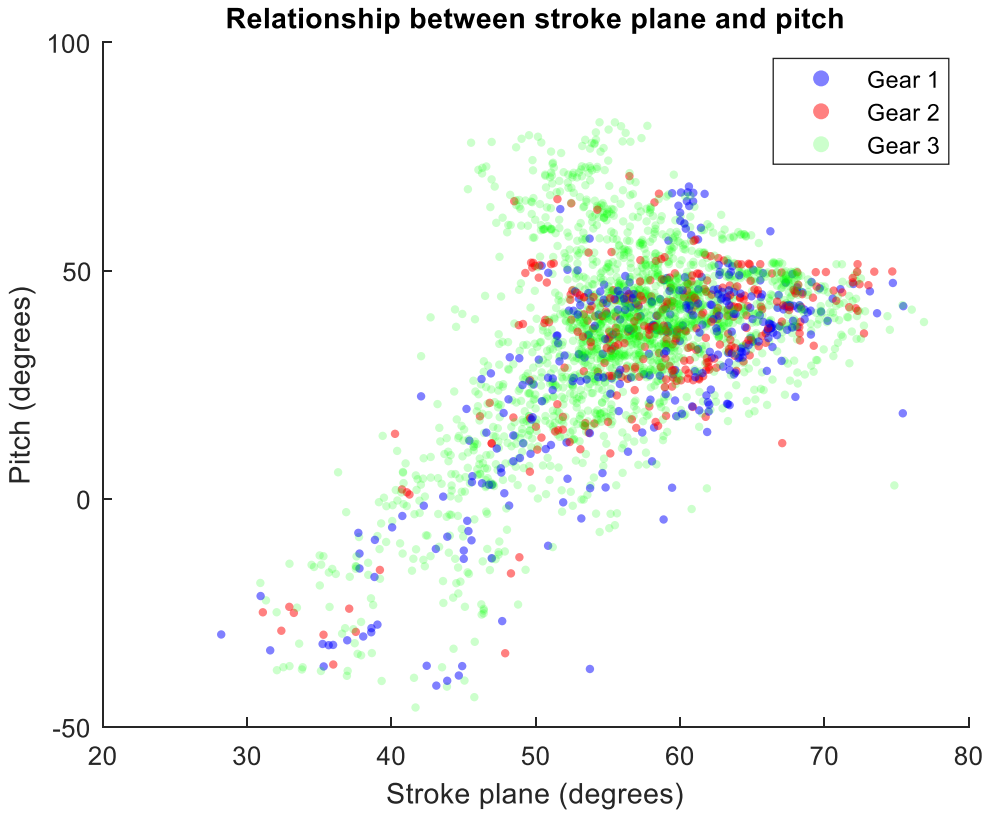

Figure 14b. Relationship between stroke plane (degrees) and pitch angle (degrees), colour coded by gear stop (Gear 1: blue; Gear 2: red; Gear 3: green).

The effect between stroke plane and pitch is non-linear, stroke plane increases to a pitch angle of ~50˚ and then decreases for greater pitch angles. This decrease is associated with advance ratio, with lower advance ratios combining elevated pitch angles and decreasing stroke plane **(Figure 14c)**.

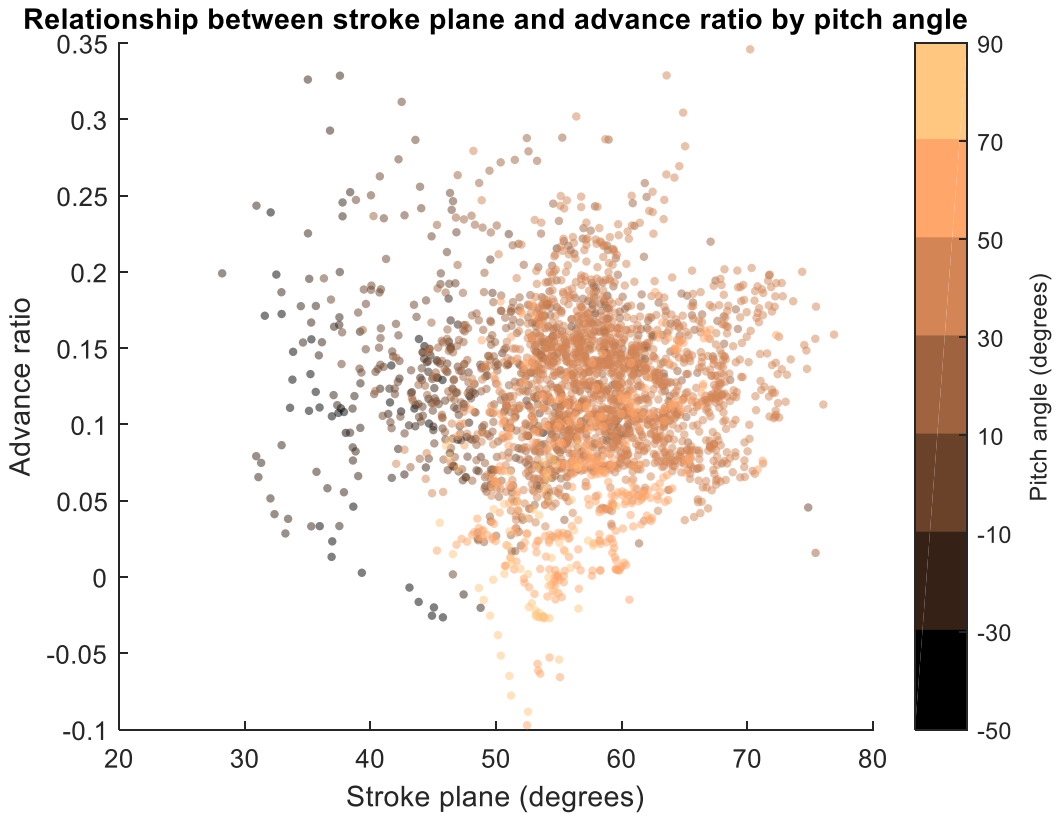

Figure 14c. Relationship between stroke plane angle (degrees) and advance ratio, colour coded by pitch angle.

Timing of stroke reversal

There is an inverse relationship between wing length and timing of stroke reversal. Unlike the tethered flight dataset, the bimodal features in the free-flying sequences are less obvious. Later relative timing of stroke reversal within the wing beat cycle is rare and is observed only in individuals with shorter wings **(Figure 15a)**.

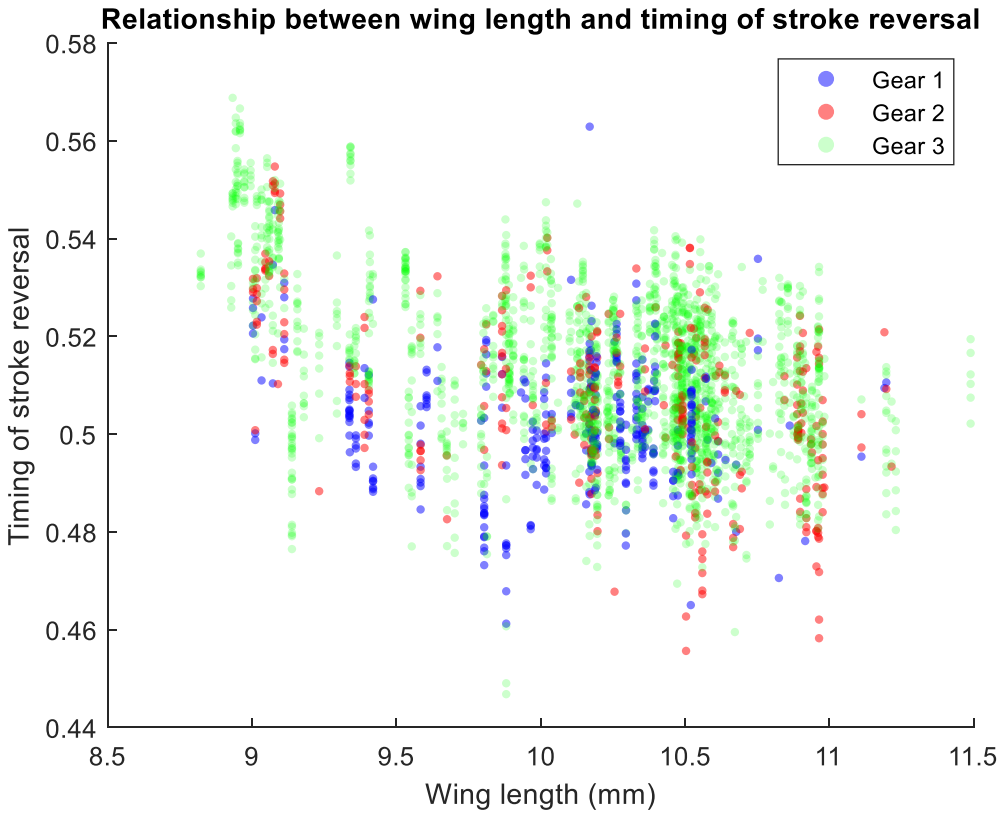

Figure 15a. Relationship between wing length (mm) and timing of stroke reversal, colour coded by gear stop (Gear 1: blue; Gear 2: red; Gear 3: green).

Timing of stroke reversal is correlated with stroke amplitude (R=0.70, p<.00001) **(Figure 15b)**. Constructing a linear mixed effects model with timing of stroke reversal as a response variable, sequence nested within individual as random effects and wing length and predicted gear stop as fixed effects, all fixed effects affected stroke reversal (Wing length: $\chi^2(1)=37.47$, p<.0001; Gear: $\chi^2(1)=142.97$, p<.0001), with wing length decreasing it by -0.016±0.003.

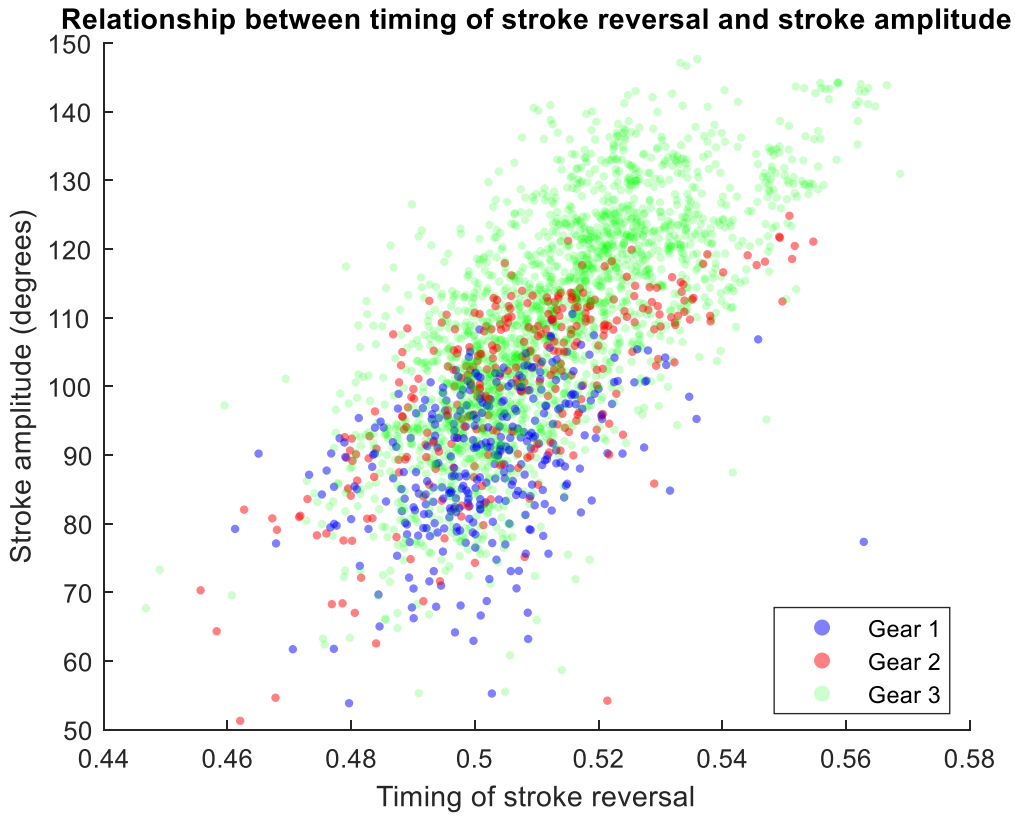

Figure 15b. Relationship between stroke amplitude (degrees) and timing of stroke reversal, colour coded by gear stop (Gear 1: blue; Gear 2: red; Gear 3: green).

Characteristic wing beat

The pattern of wing motion in *Calliphora vicina* is harmonic. The stroke angle is less sinusoidal and more triangular in pattern, showing a linear decrease during the downstroke, and a linear increase during the upstroke. The deviation angle displays a harmonic back and forth motion. There is little variability mid-stroke for the deviation angle, but more so for the stroke angle during the entire motion **(Figure 16)**.

As to be expected, peak stroke angle is correlated with wing amplitude, with lower values of peak stroke angle yielding higher amplitude values (r = -0.7332, p =<.0001). The same pattern is observed for deviation angle and stroke amplitude (r

= 0.6939, p=<.0001), although interestingly the correlation between minimum stroke angle and stroke plane amplitude is significantly tighter (t = 3.42, p=0.00063).

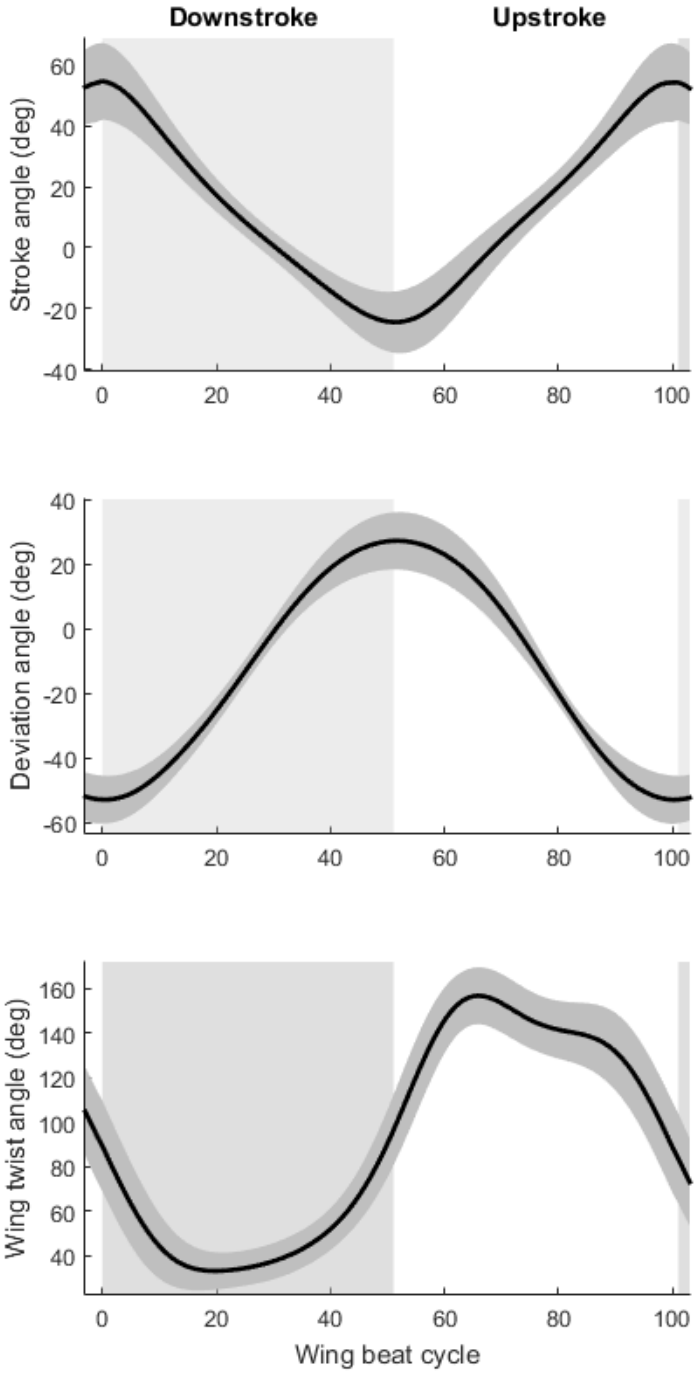

Figure 16. Mean wing beat characterisation with standard deviation. The grey block background marks the downstroke period, the white block the upstroke period. a) stroke angle b) deviation angle c) angle of incidence

Wing length and deviation angle are also tightly related. Longer wing lengths generally result in lower peak deviation angles, although increasing the gear stop enables all individuals to achieve larger peak deviation angles. To assess the effect of wing length on peak deviation angle, we performed a linear mixed effects model using peak deviation angle as the response variable, wing length and predicted gear stop as fixed effects, and sequence nested within individual as random effects. Both fixed effects affected peak deviation angle (Wing length: $\chi^2(1)=83.94$, p=<.0001; Gear: $\chi^2(1)=431.93$, p<.0001), with wing length reducing peak deviation angle by -12.5±1.4. On average, each increase in gear stop increased mean peak deviation angle by ~4˚ **(Figure 17a*)***.

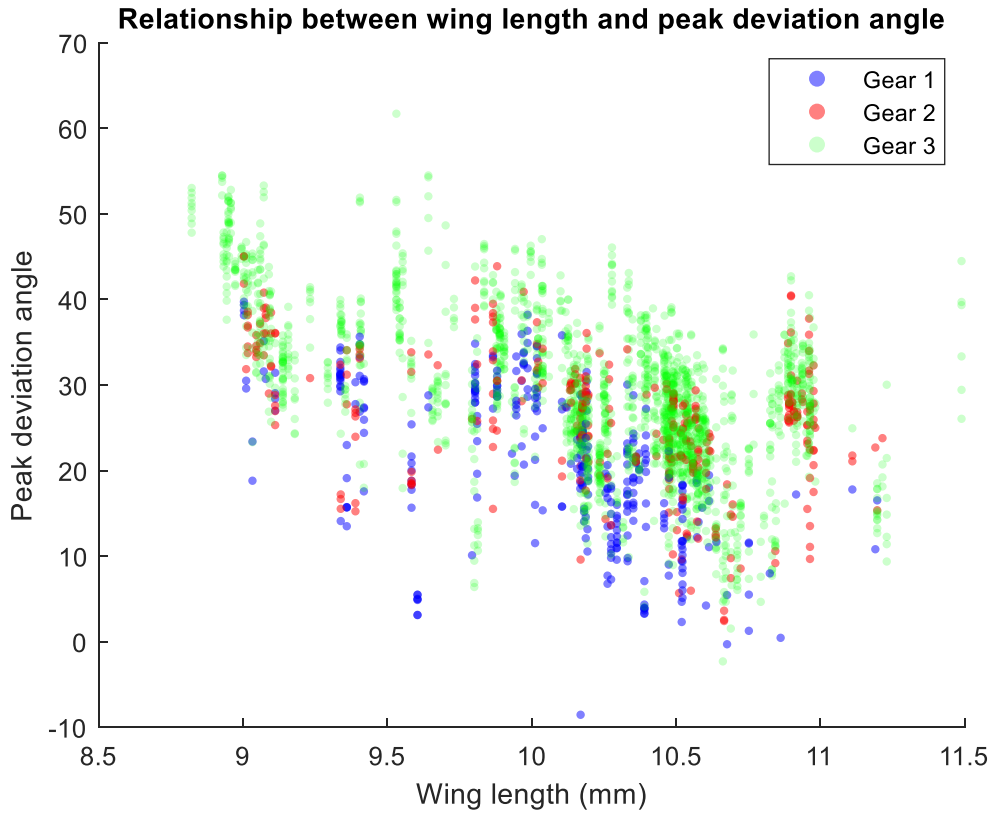

Figure 17a. Relationship between wing length (mm) and peak deviation angle (degrees), colour coded by gear stop (Gear 1: blue; Gear 2: red; Gear 3: green).

Peak stroke angle is not influenced by wing length ($\chi^2(1)=2.38$, $p=0.12$), although predicted gear stops is a significant factor (Gear: $\chi^2(1)=466.1$, $p<.0001$), with increasing gear stops decreasing minimum stroke angle by approximately 5˚ **(Figure 17b)**.

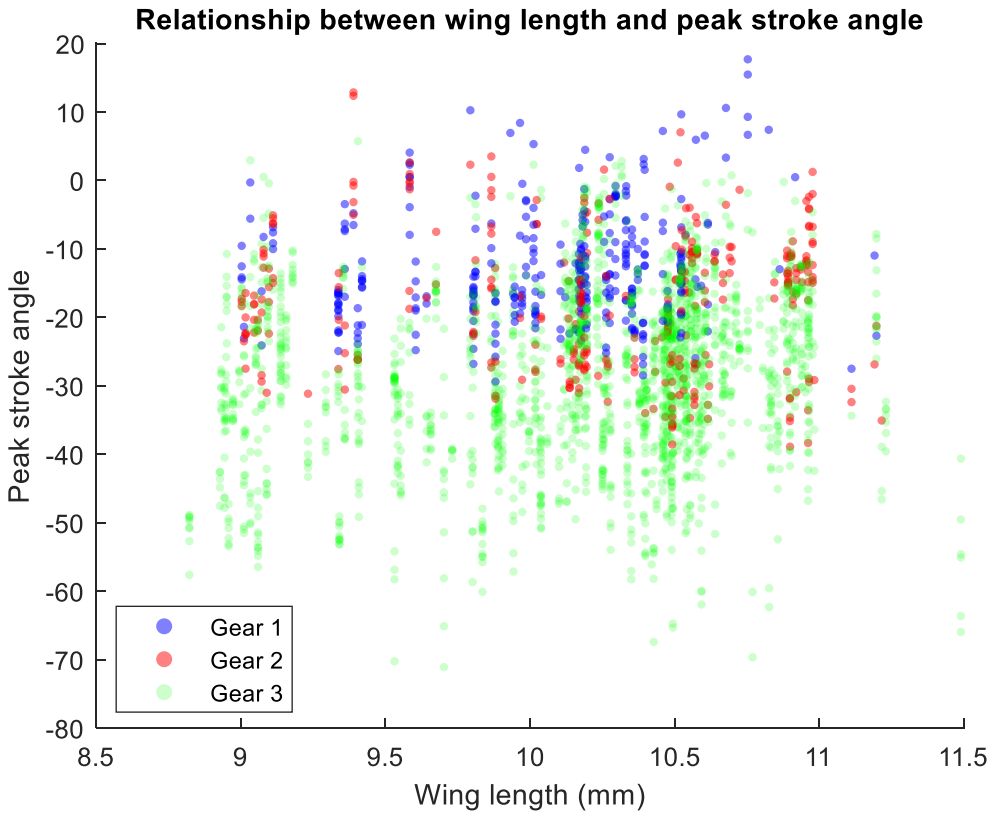

Figure 17b. Relationship between wing length (mm) and peak stroke angle (degrees), colour coded by gear stop (Gear 1: blue; Gear 2: red; Gear 3: green).

The angle of incidence, or wing twist, displays a more complex pattern of change. We will focus on the timing of supination and pronation, the point in the wing beat when the wing rotates through 90˚ at the beginning of the upstroke and downstroke respectively.

Supination

Unlike other kinematic parameters, where the sample size was n=2708, there are only n=2568 wing beats in which supination was successfully measured. Timing of supination is influenced by stroke amplitude. Only stroke amplitude was found to be significant after building a linear mixed effects model with timing of supination as the response variable, stroke amplitude and predicted gear stops as fixed effects and individual nested within sequence as random effects (Stroke amplitude: $\chi^2(1)=171.3$, p=<.0001; Gear: $\chi^2(1)=1.52$, p=0.47), with stroke amplitude reducing timing of supination by -0.00062±0.00005 **(Figure 18a)**.

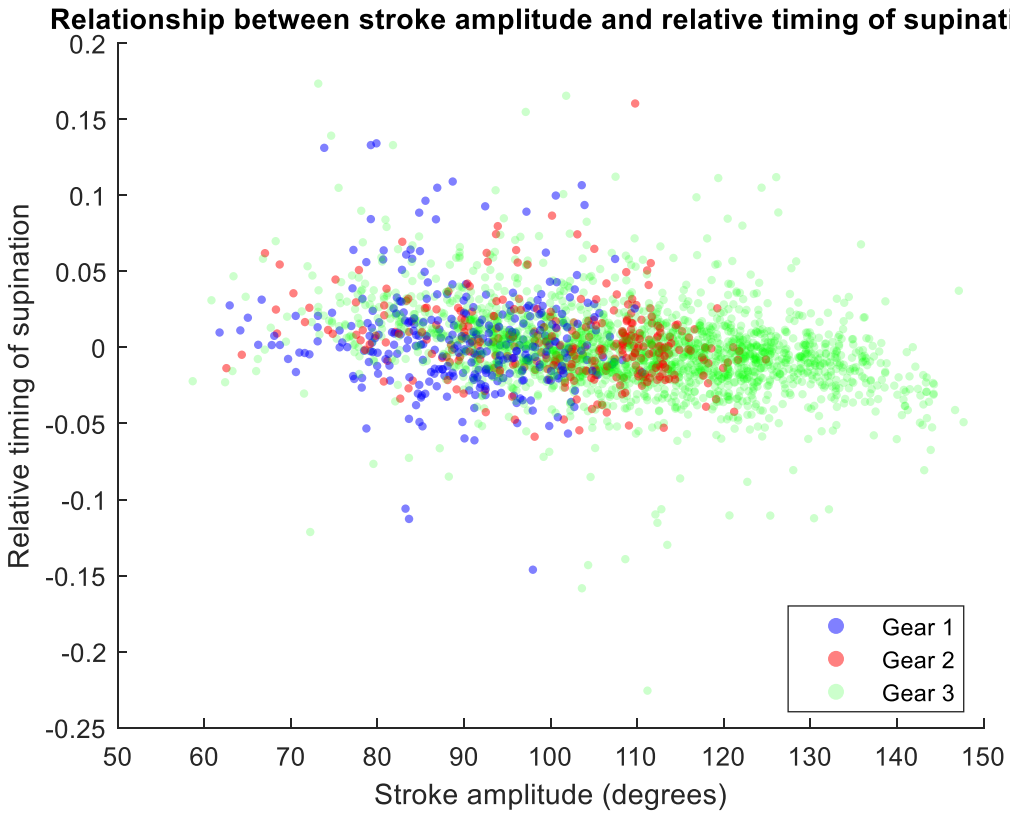

Figure 18a. Relationship between wing length (mm) and peak stroke angle (degrees), colour coded by gear stop (Gear 1: blue; Gear 2: red; Gear 3: green).

Timing of supination and predicted gear stop also significantly affect advance ratio (Timing of supination: $\chi^2(1)=38.62$, p=<.0001; Gear: $\chi^2(1)=93.62$, p<.0001), increasing it by 0.110±0.008 **(Figure 12c)**.

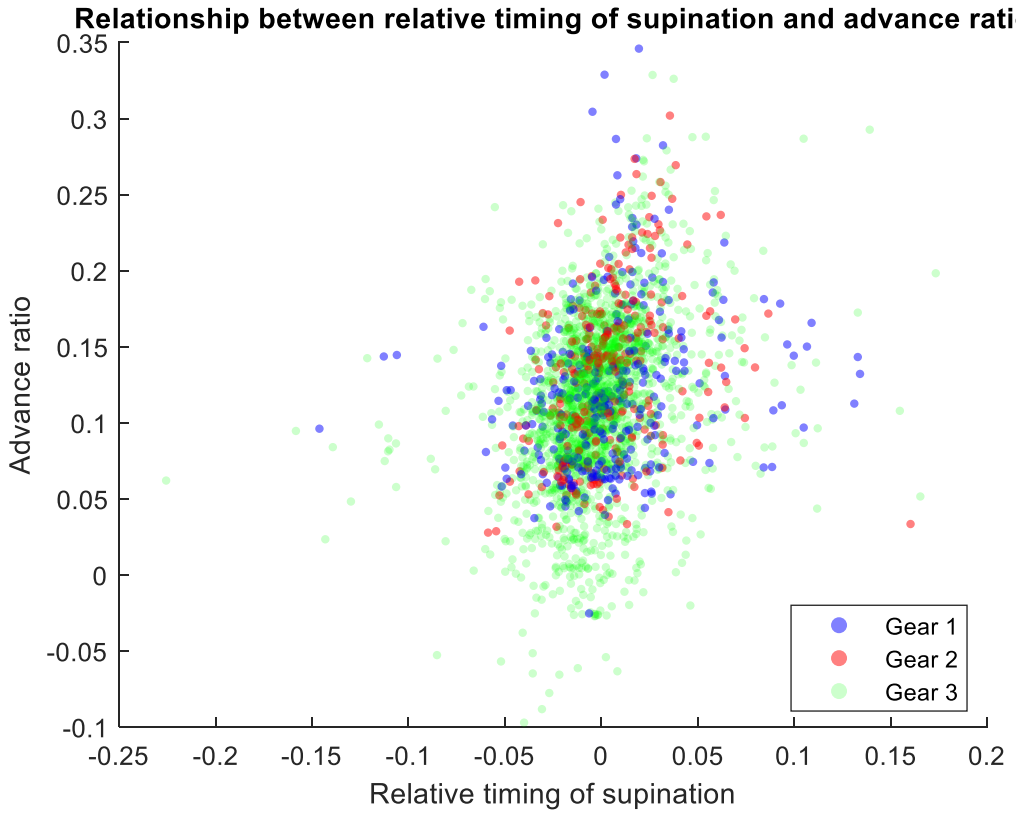

Figure 12c. Inverse relationship between relative timing of supination and advance ratio colour coded by gear (Gear 1: blue; Gear 2: red; Gear 3: green).

Pronation

Only 2433 pronation measurements were made, since early and late pronation were easily excluded if they occurred on the edges of the recording. Timing of pronation is influenced by stroke amplitude. After building a linear mixed effects model with pronation as the response variable, stroke amplitude, and predicted gear stops as fixed effects, and individual nested within sequence as random effects, only stroke amplitude was found to be significant (Stroke amplitude:

$\chi^2(1)=79.65$, p=<.0001; Gear: $\chi^2(1)=5.51$, p=0.063), which reduced timing of pronation by -0.00064±0.00007 **(Figure 18b)**.

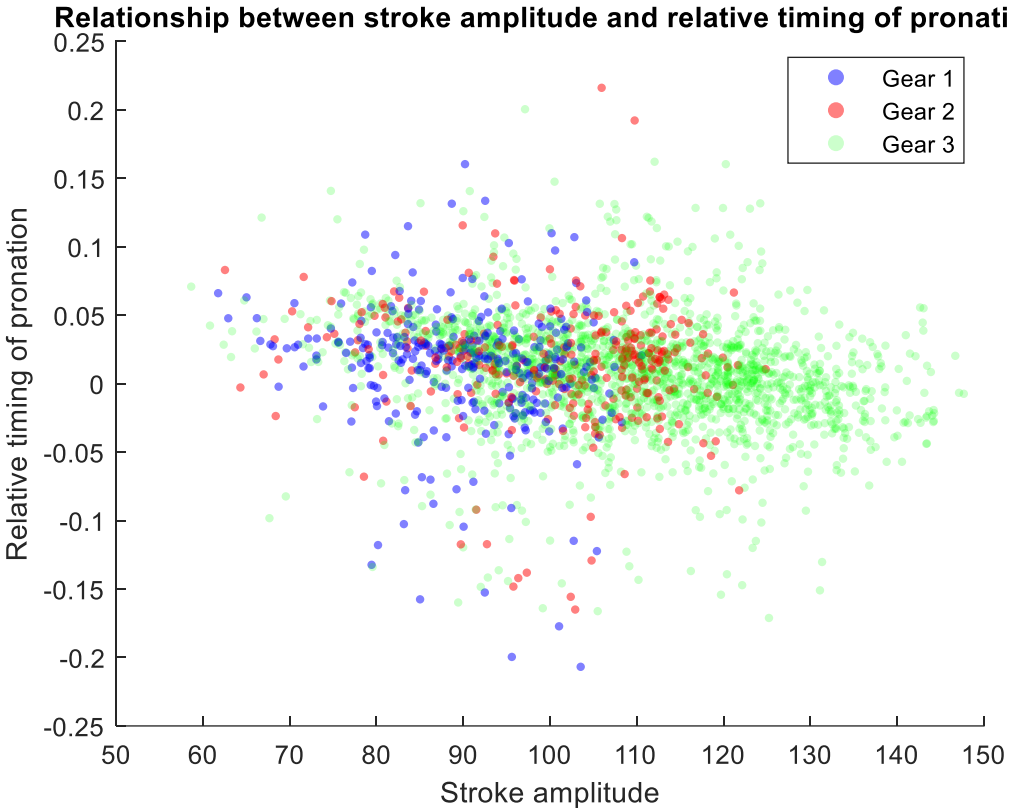

Figure 18b. Relationship between stroke amplitude (degrees) and relative timing of pronation, colour coded by gear stop (Gear 1: blue; Gear 2: red; Gear 3: green).

Timing of pronation and predicted gear stop all significantly affect advance ratio (Timing of pronation: $\chi^2(1)=66.04$, p=<.0001; Gear: $\chi^2(1)=99.12$, p<.0001), increasing it by 0.096±0.012 **(Figure 12d)**.

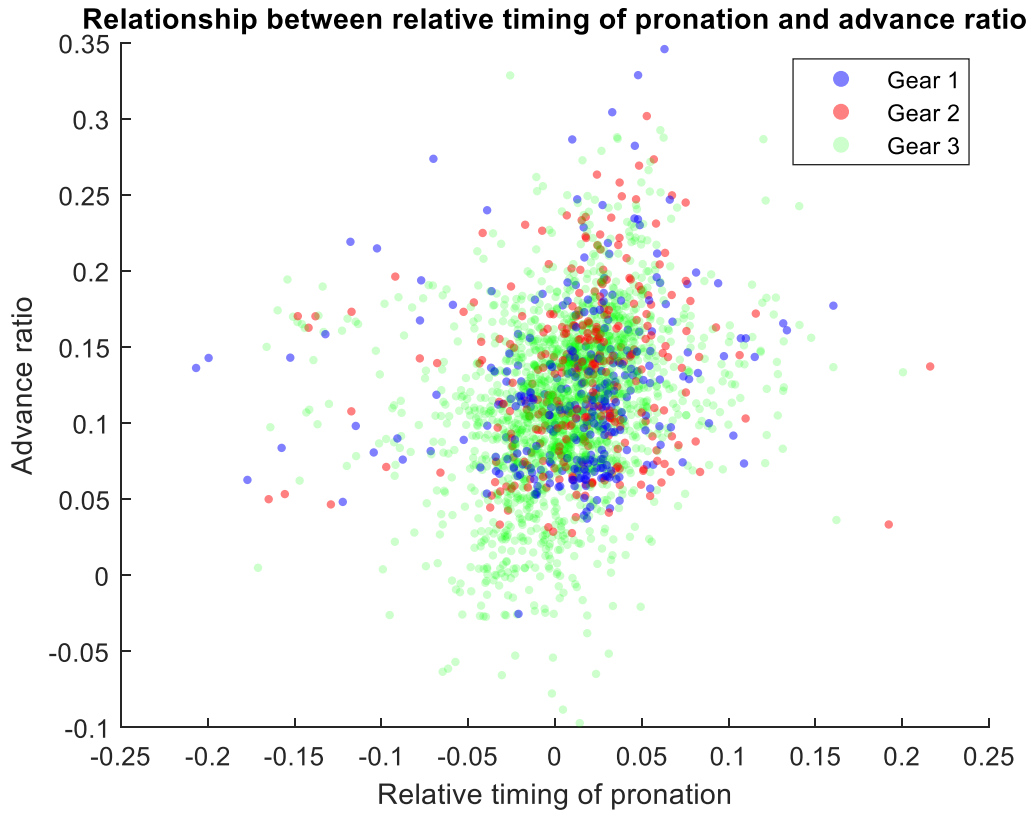

Figure 12d. Relationship between relative timing of pronation and advance ratio, colour coded by gear stop (Gear 1: blue; Gear 2: red; Gear 3: green; Gear 4: black).

Role of gears in kinematic changes

Finally, we examined the effect of gear stop on wing beat kinematics as a whole. We performed a one-way ANOVA analysis to determine whether different gear stops had significantly different wing beat kinematics. For those with significant values, a post-hoc Tukey HSD test with Bonferroni correction was run to distinguish which means were significantly different.

For all wing beat parameters, there were significant differences between the different gear stop changes (Stroke amplitude: $F_{2,2694}$ = 437.2624, p<.0001; Wing beat frequency: $F_{2,2694}$ = 39.94, p<.0001; Peak stroke angle: $F_{2,2694}$ = 708.08, p<.0001; Timing of stroke reversal: $F_{2,2694}$ = 118.49, p<.0001; Advance ratio: $F_{2,2694}$ = 103.88,

p<.0001), with most presenting significant differences in all groups **(Table 7)**. It is clear that different gear stops modulate blowfly kinematics in different ways.

Parameter	Groups		Lower 95% CI	Mean diff	Upper 95% CI	p
Stroke amplitude	1	2	17.58	20.96	24.34	p<.0001
	1	3	17.79	20.35	-22.90	p<.0001
	2	3	-3.23	-0.61	2.00	p = 1
Wing beat frequency	1	2	-13.80	-11.05	-8.30	p<.0001
	1	3	-21.76	-19.68	-17.61	p<.0001
	2	3	-10.76	-8.64	-6.51	p<.0001
Peak stroke angle	1	2	2.80	4.91	7.01	p<.0001
	1	3	13.58	15.17	16.76	p<.0001
	2	3	8.63	10.26	11.89	p<.0001
Timing of stroke reversal	1	2	-0.0085	-0.0054	-0.0024	p<.0001
	1	3	-0.0133	-0.0110	-0.0088	p<.0001
	2	3	-0.0079	-0.0056	-0.0032	p<.0001
Advance ratio	1	2	-0.0206	-0.0105	0.0005	p = 0.036
	1	3	0.000011	0.0076	0.0152	p = 0.050
	2	3	0.0104	0.0181	0.0259	p<.0001

Table 7. Results from post-hoc Tukey HSD test showing Gear stop means compared, lower 95% confidence interval for the difference in means, difference in means, upper 95% confidence interval for the difference in means and p-value for each wing beat parameter.

DISCUSSION

Comparison between free-flight and tethered flight

The differences between *Calliphora* free-flight and tethered flight kinematics are incontrovertible. The two main probable reasons for these differences are as follows: Firstly, tethered insects generally behave differently to freely-flying insects, as previous studies have shown. The act of tethering an insect disrupts its sensory feedback loops, which lead to atypical wing beat kinematics and lower force

production[26,27]. A tethered *Manduca sexta* for example, displays lower stroke amplitude and 46% less oxygen consumption than free-flying moths[28]. Honeybees, which require elevated thoracic temperatures to successfully take off, display lower thoracic temperatures and aerodynamic output compared to free-flying bees[29–31]. Tethered locusts have 16% lower wing beat frequencies than their free-flying counterparts, which translates into a 39% slower preferred forward speed and generates approximately 60% of the lift required to stay aloft[27,32–36]. Tethered *Drosophila melanogaster* also exhibit 20% lower wing beat frequencies and 10% lower stroke amplitude values than hovering free-flying fruit flies[37]. Tethered flies also tend to have lower power output, leading to underestimates of their peak performance[38]. The second likely reason for the differences between free-flight and tethered flight kinematics, apart from the disruptions to sensory feedback loops, is that tethered *Calliphora vicina* flew under different conditions from those of free-flying *Calliphora*, which may have led to them attempting to initiate a different envelope of manoeuvres. The tethered blowflies were subject to an airstream from a fan, which may have led to more varied or different kinematics, such as avoidant manoeuvres to escape from their current position, or fast forward flight in response to the airstream. Finally, the tethered dataset contained over four times as many wing beats, which allows for a potentially broader envelope of flight behaviours to be captured. Overall, tethered and free-flying flies occupy a mostly overlapping range of kinematic parameters, suggesting their differences come down to tethered and free-flying flies sampling a different range of those kinematics.

Our results in these aspects resemble previous findings in the literature. Tethered *Calliphora vicina* display wing beat frequencies that are 10% lower on average than their free-flying counterparts, as is evidenced by the positioning of the

multimodal peaks. Other kinematic parameters, such as stroke amplitude, stroke reversal and peak stroke angle, occupied a far larger range than those measured in free-flying *Calliphora*, and despite sharing a large degree of overlap, the profile of the distribution was significantly different. It is difficult to know whether the wider spread is a product of abnormal kinematics as a result of tethering, or whether the tethered experiment was more successful in collecting a wider range of kinematic behaviours than the free-flying dataset.

Whilst we cannot test whether the tethered kinematics represent a wider range than those that occur naturally, we expect the kinematics from our free-flight dataset to represent a narrower range from all possible free-flight behaviours. Our fastest recorded heading velocity was 1.5m/s **(Supplementary Material 3)**, which is higher than the 1.2m/s peak velocities recorded by Schilstra and van Hateren, but lower than the peak values of 1.65m/s and 2.5m/s observed by Nachtigall and Roth, and Bomphrey et al. respectively[18,21,39]. The 1.2m/s and 1.65m/s figures both came from almost free-flying blowflies and so may be artificially lower due to experimental limitations. The blowflies in the former study had coils mounted on their head and thorax, whilst the blowflies in the latter study were tethered to a fine wire and placed within a wind tunnel[18,39]. Schilstra's blowflies also flew in an enclosure almost ten times smaller than the one in which our flies were placed, which may also have limited their peak velocity[18]. Having a smaller volume available for flight affects peak and mean flight speed, as collisions in small enclosures are more likely to occur at higher speeds[40]. On the other hand, Bomphrey's blowflies flew in an enclosure that was 8 times larger than ours, which may have appeared visually larger to the blowflies because of the mirrored walls in the experimental set-up and the fact collisions against the mirrors were recorded, thus stimulating them

to attain higher flight speeds. Indeed, he observed that blowflies reached two preferred velocity modes, at 1.2 and 2.3m/s[21]. Notably, Ennos did not provide velocity data in his study, but based on his peak advance ratio, we estimated the peak velocities of his blowflies to be 2.25 – 2.50m/s, which is unusually high for the small enclosure he used[17]. The faster reported speed may be explained by his experimental set-up, since he prompted flight by disturbing a large number of individuals in his flight arena, and forward speed is known to correlate with looming retinal responses[17,19]. Alongside a smaller flight enclosure, our experimental set-up is also biased towards capturing wing beats belonging to slower heading velocities. By filming a small air volume to track the wing beat kinematics in detail, the longest sequences with the most wing beats are likely to display slower heading velocities, whereas higher heading velocities almost exclusively yield short recordings with fewer consecutive wing beats. On the other hand, our peak ascent rate exceeded the measurements observed by Bomphrey et al. by 0.09m/s, although peak descent rates were lower than those registered in other studies. Both of these factors likely explain the narrower range of wing beat kinematics collected in our free-flight experiments.

Limitations of the *k*-NN model

At present, there is no way to empirically identify in which gear stop free-flying blowflies are flying in. Whilst the success rates calculated from the cross-validation and test-validation techniques give an indication of the effectiveness of different model parameters in correctly identifying classifications of the original tethered dataset from subsets of the tethered dataset and predictions made from the free-flight dataset, they provide little information about the accuracy of the

prediction of the free-flight dataset itself and rely on the training and test dataset being similar enough to make those inferences. Whilst the flies used in both tethered and free-flight experiments shared a similar rearing background, and similar wing beat kinematics likely originate from similar physical configurations of the PWP/RS, it is likely that the inherent differences between tethered and free-flight described earlier have contributed to inaccuracies in the prediction of gear stops in the free-flight dataset, and probably account for the discrepancies between success rates in validation and cross-validation tests, which rely on the training dataset alone, and the test-validation, which measures the accuracy of the test dataset in predicting the classification of the training one.

Given that the *k*-NN algorithm relies on local features in the data for classification and prediction, it is possible that differences between tethered and free-flight distributions could affect the prediction of points lying near the boundaries of separate classifications. A strategy that may increase the success rate of the classification algorithm is to reduce the number of categories, such as combining Gear 1 and Gear 2, which both involve a physical interaction between the PWP and the RS, as a single category. Although all three operate differently, Gear 1 and Gear 2 are more similar and display a greater overlap in kinematics within the tethered dataset than Gear 3. Another option to increase the accuracy of the model would be to identify further key input parameters.

Gear function

All three gears were shown to have different effects on the wing beat kinematics of free-flying *Calliphora vicina*. The fourth gear, Gear 0, is considered an anomalous wing beat, in which the radial stop has overshot and missed the groove

in the pleural wing process to engage in Gear 1. It was not predicted to occur in our free-flying dataset, and was excluded from analysis.

Predicted gear stops had the strongest effect on peak stroke angle, peak deviation angle and stroke amplitude. Unsurprisingly, both stroke angle and deviation angle are strongly correlated with stroke amplitude, as higher peak deviation angles and lower minimum stroke angles will lead to an increased arc throughout the half stroke, yielding a greater stroke amplitude. Deviation angle is linked to wing length and blowflies with shorter wings reach higher mean peak deviation angles than individuals with longer wings. Nevertheless, all individuals were able to increase their peak stroke and deviation angles and thus their amplitude, by increasing gear stops from Gear 1 through to Gear 3. A decreased stroke amplitude is correlated with an increased advance ratio in all individuals, which suggests that Gear 1 and Gear 2 are used to increase forward speed. Gear 3, on the other hand, was associated with a broader range of kinematics with a lower advance ratio closer to slow forwards flight. *Calliphora vicina* rarely engage in true hovering flight, but rather adopt a unique body position and increase their stroke amplitude to increase their vertical lift production[17,41]. Wing beats with larger stroke amplitudes also initiate *pronation* and supination earlier, suggesting that the downstroke continues even after the wing has started to rotate. Increased amplitude and early supination are generally associated with hovering flight and vertical lift production[17,42]. Blowflies travelling at faster speeds, however, have delayed supination, which is consistent with Ennos' observations of free-flying blowflies[17]. Ennos suggested that delayed supination in *Calliphora vicina* is the result of greater ventral wing flexion during the wing beat, which leads to a faster recoil and rapid, but delayed supination, which can generate increased lift during the upstroke, as

well as serve as a mechanism to reduce the stress on the wing hinge[17,43]. On the other hand, Dickinson's research on wing rotation suggests that delayed supination could lead to decreased lift and increased drag[42].

Timing of stroke reversal was also related to stroke amplitude, with delayed timing being associated with increased stroke plane amplitude. This relationship is substantially different to the timing of stroke reversal in tethered blowflies. Timing of stroke reversal did not exceed 0.6 in any free-flying blowfly, but did so in 10% of tethered flies. The delayed rotation was associated with low amplitude values, unlike the free-flying blowflies. It is unclear whether this an artefact of tethering, or due to the narrower subset of kinematics represented in free-flying blowflies.

Stroke plane angle is independent to most kinematic parameters, with the exception of peak deviation angle, due to the way it is measured. This is explained by the fact that the most extreme values for deviation angle measured in our frame of reference would be caused by a larger stroke plane angle. Otherwise, stroke plane angle is most tightly linked to body kinematics, which is not surprising given that it dictates the angle between the stroke plane of the wings and the body and allows the insect to adjust the direction of its forces accordingly, which leads to changes in rotation and acceleration. The non-linear relationship between pitch and stroke plane is particularly interesting. For pitch angles under 50˚, stroke plane increases linearly. Lower pitch values are associated with faster forwards flight, as the thrust vector is angled forwards. Once the pitch angle is over 50˚, the stroke plane angle begins to decrease again, and is associated with slow forwards flight. This, therefore, enables the blowfly to adopt a unique body position for hovering and engaging in vertical flight. Lower stroke plane angles are also associated with higher absolute

roll angles, suggesting that roll manoeuvres are initiated by the wings. There is no clear relationship between gear stop positions and the stroke plane angle, suggesting that one does not mediate the other. This is unsurprising, as the gear stops directly affect the wing beat kinematics rather than the body kinematics, and as shown in Chapter 1, changes in body kinematics are generally continuous.

Finally, wing beat frequency exhibited a more complex relationship with each gear and was also independent of other flight parameters. Mean wing beat frequency varied inversely with advance ratio in our free-flying flies, although other studies have suggested that an increase in *Calliphora vicina* wing beat frequency yields faster flight speeds[17,44]. Mean wing beat frequency is highest in Gear 1, and is lower in Gear 2 and 3, which is congruent with the idea that lower gears help to generate faster forwards flight if increased wing beat frequency is used to fly faster. The wing beat frequency distribution with Gear 3 was bimodal, which was not explained by alula state in the tethered dataset, and points to the involvement of the axillary or thoracic muscles.

In our dataset, Gear 3 was by far the most common gear stop adopted in our dataset. This is hardly surprising given that Gear 3 appears to be associated with kinematics that generate slower forward flight and that our dataset over-represents slower flight. Nevertheless, the tethered dataset also suggests that most wing beats are also in Gear 3. These observations would be consistent with those of researchers who noted that the pleural wing process and radial stops of blowflies showed very little signs of wear and tear, even when they were old, as Gear 3 does not involve the RS engaging with the PWP, which may contribute to their lack of erosion[10].

Overall, the use of *k*-NN to infer the gear stop position in *Calliphora vicina* will enable more in-depth understanding of free-flying blowfly manoeuvres. Which validation methods are most accurate remain unclear due to the differences between flight behaviour in tethered and free-flying datasets, but preliminary results with an estimated ~81% accuracy are very promising. In free-flying blowflies, the gear stop mechanism appears to enable the fly to adjust its flight speed. It does so primarily by affecting peak stroke and deviation angles. This leads to adjustments in stroke amplitude and related parameters such as the timing of stroke reversal and supination. It also affects wing beat frequency, although the full relationship is at present unclear, and is independent of stroke plane, which is correlated with the adjustment of body kinematics. Above all, the *k*-NN algorithm appears to be a promising tool for measuring complex behaviours that cannot be directly measured, provided that appropriate input parameters are used.

BIBLIOGRAPHY

1. Snodgrass, R. E. The thorax of insects and the articulation of the wings. *Proc. U.S. Natl. Museum* **36,** (1909).

2. Tu, M. S. & Dickinson, M. H. The control of wing kinematics by two steering muscles of the blowfly (Calliphora vicina). *J. Comp. Physiol. A.* **178,** 813–830 (1996).

3. Hedenstrom, A. How Insect Flight Steering Muscles Work. *Plos Biol.* **12,** 4 (2014).

4. Pfau, H. K. Fliegt unsere Schmeissfliegt mit Gangshaltung?

Naturwissenschaften **60,** 160 (1973).

5. Nalbach, G. The gear change mechanism of the blowfly (Calliphora erythrocephala) in tethered flight. *J. Comp. Physiol. A* **165,** 321–331 (1989).

6. Walker, S. M., Thomas, A. L. R. & Taylor, G. K. Operation of the alula as an indicator of gear change in hoverflies. *J. R. Soc. Interface* **9,** 1194–1207 (2012).

7. Miyan, J. A. & Ewing, A. W. Is the 'click' mechanism of dipteran flight an artefact of CCl4 anaesthesia? *J. Exp. Biol.* **116,** 313–322 (1985).

8. Miyan, J. A. & Ewing, A. W. How Diptera move their wings: a re-examination of the wing base articulation and muscle systems concerned with flight. *Philos. Trans. R. Soc. London B* **311,** 271–302 (1985).

9. Pfau, H. K. Short Communication. Critical Comments on a 'Novel Mechanical Model of Dipteran Flight' (Miyan & Ewing, 1985). *J. Exp. Biol.* **128,** 463–468 (1987).

10. Wisser, A. Wing beat of Calliphora erythrocephala: Turning axis and gearbox of the wing base (Insecta, Diptera). *Zoomorphology* **107,** 359–369 (1988).

11. Balint, C. N. & Dickinson, M. H. The correlation between wing kinematics and steering muscle activity in the blowfly Calliphora vicina. *J. Exp. Biol.* **204,** 4213–4226 (2001).

12. Chowdhury Salford University, Salford M5 4WT (UK)), V. (Department of B. & Parr, M. J. The 'switch mechanism' and sound production in tsetse flies (Diptera: Glossinidae). *Journal of Natural History (UK)* **v. 15,** (1981).

13. Boettiger, E. G. & Furshpan, E. The Mechanics of Flight Movements in Diptera. *Biol. Bull.* **102,** 200–211 (1952).

14. Dickinson, M. H. & Tu, M. S. The function of dipteran flight muscle. *Comp. Biochem. Physiol. - A Physiol.* **116,** 223–238 (1997).

15. Page, J. W. The Gear Change Mechanism of Dipteran Flight. in *Society of Experimental Biology: Mechanics and Biological Function of the Arthropod Exoskeleton* (2015).

16. Page, J. W. The biomechanics of dipteran flight muscles. in *Society of Experimental Biology: Open Biomechanics* (2017).

17. Ennos, R. A. The kinematics and aerodynamics of the Free Flight of some Diptera. *J. Exp. Biol.* **142,** 49–85 (1989).

18. Schilstra, C. & Hateren, J. H. Blowfly flight and optic flow. I. Thorax kinematics and flight dynamics. *J. Exp. Biol.* **202,** 1481–1490 (1999).

19. Boeddeker, N., Kern, R. & Egelhaaf, M. Chasing a dummy target: smooth pursuit and velocity control in male blowflies. *Proc. R. Soc. B Biol. Sci.* **270,** 393–399 (2003).

20. Boeddeker, N. & Egelhaaf, M. A single control system for smooth and saccade-like pursuit in blowflies. *J. Exp. Biol.* **208,** 1563–1572 (2005).

21. Bomphrey, R. J., Walker, S. M. & Taylor, G. K. The typical flight performance of blowflies: Measuring the normal performance envelope of Calliphora vicina using a novel corner-cube arena. *PLoS One* **4,** (2009).

22. Aak, A. & Knudsen, G. K. Sex differences in olfaction-mediated visual acuity in

blowflies and its consequences for gender-specific trapping. *Entomol. Exp. Appl.* **139,** 25–34 (2011).

23. Kern, R., Boeddeker, N., Dittmar, L. & Egelhaaf, M. Blowfly flight characteristics are shaped by environmental features and controlled by optic flow information. *J. Exp. Biol.* **215,** 2501–2514 (2012).

24. Hunt, T. & Turner, I. Enhancement of ultra violet light as a insect attractant by the addition of a secondary attractant wavelength of light. *Proc. 1st Int. Conf. Insect Pests Urban Environ.* 487 (1993).

25. Walker, S. M., Thomas, A. L. R. & Taylor, G. K. Photogrammetric reconstruction of high-resolution surface topographies and deformable wing kinematics of tethered locusts and free-flying hoverflies. *J. R. Soc. Interface* **6,** 351–366 (2009).

26. Dudley, R. & Ellington, C. P. Mechanics of forward flight in bumblebees. II. Quasi-steady lift and power requirements. *J. Exp. Biol.* **148,** 53–88 (1990).

27. Kutsch, W., Van Der Wall, M. & Fischer, H. Analysis of free forward flight of Schistocerca gregaria employing telemetric transmission of muscle potentials. *J. Exp. Zool.* **284,** 119–129 (1999).

28. Heinrich, B. Temperature regulation of the sphinx moth, Manduca sexta. II. Regulation of heat loss by control of blood circulation. *J. Exp. Biol.* **54,** 153–66 (1971).

29. Sotavalta, O. *On the thoracic temperature of insects in flight*. (Suomalaisen Kirjallisuuden Seuran Kirjapainon Oy, 1954).

30. Esch, H. Body temperature and flight performance of honey bees in a servo-

mechanically controlled wind tunnel. *J. Comp. Physiol. ??? A* **109,** 265–277 (1976).

31. Harrison, J. F. & Fewell, J. H. Environmental and genetic influences on flight metabolic rate in the honey bee, Apis mellifera. *Comp. Biochem. Physiol. Part A Mol. Integr. Physiol.* **133,** 323–333 (2002).

32. Gewecke, M. The influence of air-current sense organs on flight behavior of Locusta migratoria. *J. Comp. Physiol.* **103,** 79–95 (1975).

33. Gewecke, M. & Kutsch, W. Development of flight behaviour in maturing adults of Locusta migratoria: I. Flight performance and wing-stroke parameters. *J. Insect Physiol.* **25,** 249–253 (1979).

34. Baker, P. S., Gewecke, M. & Cooter, R. J. The natural flight of the migratory locust, Locusta migratoria L. - III. Wing-beat frequency, flight speed and attitude. *J. Comp. Physiol. □ A* **141,** 233–237 (1981).

35. Kutsch, W. & Stevenson, P. Time-correlated flights of juvenile and mature locusts - a comparison between free and tethered animals. *J. Insect Physiol.* **27,** 455–459 (1981).

36. Gee, C. E. & Robertson, R. M. Free-flight ability in locusts recovering from partial deafferentation. *Naturwissenschaften* **85,** 167–170 (1998).

37. Fry, S. N., Sayaman, R. & Dickinson, M. H. The aerodynamics of hovering flight in Drosophila. *J. Exp. Biol.* **208,** 2303–2318 (2005).

38. Lehmann, F. O. & Dickinson, M. H. The changes in power requirements and muscle efficiency during elevated force production in the fruit fly Drosophila melanogaster. *J. Exp. Biol.* **200,** 1133–1143 (1997).

39. Nachtigall, W. & Roth, W. Correlations Between Stationary Measurable Parameters of Wing Movement and Aerodynamic Force Production in the Blowfly (Calliphora vicina R . -D .). *J. Comp. Physiol. A* **150,** 251–260 (1983).

40. Stevenson, R., Corbo, K., Baca, L. & Le, Q. Cage size and flight speed of the tobacco hawkmoth Manduca sexta. *J. Exp. Biol.* **198,** 1665–72 (1995).

41. Ellington, C. P. The Aerodynamics of Hovering Insect Flight. III. Kinematics. *Philos. Trans. R. Soc. London* **B,** 41–78 (1984).

42. Dickinson, M. H., Lehmann, F. O. & Sane, S. P. Wing rotation and the aerodynamic basis of insect flight. *Science* **284,** 1954–1960 (1999).

43. Wootton, R. J. Support and deformability in insect wings. *J. Zool.* **193,** 447–468 (1981).

44. Ennos, R. A. A Comparative Study of the Flight Mechanism of Diptera. *Wild* **372,** 355–372 (1987).

Chapter 5

Kinematics of forward flight in three dipteran species

Kinematics of forward flight in three dipteran species

Inés L. Dawson*, Graham K. Taylor*, Simon M. Walker†

* Oxford Flight Group, University of Oxford, The John Krebs Field Station, Department of Zoology, Wytham, Oxford, OX2 8QJ, UK

† Faculty of Biological Sciences, University of Leeds, Leeds, LS2 9JT, UK

Dipterans are among the most adept fliers of all insects due to their ability to quickly adjust their flight patterns in response to a changing environment. They occupy a wide range of ecological niches, which is reflected in their varying morphologies and behaviours. We explored how the flight of three species of fly, *Drosophila melanogaster* (fruit flies), *Calliphora vicina* (blowflies) and *Eristalis tenax* (drone flies), varied across a range of similar aerial manoeuvres, by comparing their wing beat kinematics as well as their lift and drag forces, using a quasi-steady blade element model. Each of the three species occupies a distinct kinematic morphospace with increasing forward flight. *Drosophila* and *Calliphora* displayed more similar variation in their wing beat kinematics with increasing forward flight, which may be due to their sharing similar ecological niches. Conversely, *Drosophila* displayed a different aerodynamic force production profile compared to *Eristalis* and *Calliphora*, which is likely due to the difference in Reynolds number as a result of their physical size.

INTRODUCTION

Dipteran flies are amongst nature's most adept fliers and their morphologies, kinematics and aerodynamics have been studied in both tethered and free-flight contexts. However, most studies that focus on how wing motion varies during the wing beat cycle are either free-flight studies based on a very limited number of wing beats, or tethered flight studies, which make it possible to collect larger volumes of flight data, but have the disadvantage that the tethering affects the insect's sensorimotor feedback loop and so alters its kinematics and flight output forces[1–9]. Free-flight studies with ample data usually examine trajectories and body kinematics in response to optic flow, but do not gather in-depth information about their wing beat kinematics[10–12].

Measuring the aerodynamic forces generated during flight also presents a challenge in insect flight research. Tethered insects can be placed on a force balance to measure their force directly, but this is subject to the same caveats described previously[13]. Other methods, such as particle image velocimetry (PIV), allow the wake around the insect to be tracked, but often yield better results under tethered conditions[14–16]. An alternative to directly or indirectly measuring the forces is to estimate them using models with appropriate measurements as inputs. Modelling tends to present the trade-off of achieving greater realism by accounting for more parameters, which is also more computationally expensive versus simplifying certain aspects of the process, but allowing for a much faster processing time.

One approach that can take advantage of empirically collected data without being too computationally demanding is to apply a quasi-steady blade element model (QSBEM) to estimate the aerodynamic forces generated during flight. The

quasi-steady assumption of a QSBEM is that the forces generated during the wing beat are time-independent, which means that the forces can be calculated at any instant in time during the wing beat cycle using the angle of attack and instantaneous velocity, therefore treating the wing as if it were a fixed airfoil. The blade element model divides the wing into parallel chord-wise blades and assumes that the total force generated by the wing at that instant is equal to the total force generated by each of the blades.

The objective of this study is to compare and contrast the kinematics and aerodynamic forces produced by *Drosophila melanogaster*, *Calliphora vicina* and *Eristalis tenax* in free flight. We used the free-flight kinematics, including wing twist, as inputs to a QSBEM developed by Taylor & Walker (in prep.) to estimate the wing beat-averaged forces in flight, lift and drag coefficients and aerodynamic force contribution profile for *Drosophila* and *Calliphora* and contrast them with those of *Eristalis* (Taylor & Walker, in prep.).

Whereas *Drosophila* (fruit fly), *Calliphora* (blowfly) and *Eristalis* (drone fly) are all dipterans found in the Muscomorpha infraorder, they occupy very distinct ecological niches[17,18]. *Eristalis* is from the Syrphidae family, which probably emerged during the Early Cretaceous[19]. *Eristalis* is a territorial bee mimic that hovers and performs saccades to guard its territory. Some species of hoverfly, including *Eristalis*, also use hovering flight behaviour as a courtship display to attract females. They are relatively large flies, and operate at a Reynolds number (ratio of inertial and viscous forces, which describes the nature of the fluid that flows past a body) of approximately 1600. *Calliphora* and *Drosophila* are both schizophorans, which originated in the most recent and successful Dipteran radiation in the early

Paleocene[17,19,20]. The Muscomorpha and particularly the Schizophora encompass over a third of the extant diversity of dipterans today and display a huge degree of ecological diversity[18,19]. *Drosophila melanogaster* are model organisms, and their flight, genetics and behaviour have been extensively researched. They display sexual size dimorphism, with males being substantially smaller than the females[21]. They operate at a Reynolds number of approximately 130. *Calliphora vicina* males generally feed off nectar, but are also adept at tracing cadavers to seek out females to reproduce with them[18,22–24]. In terms of body size, *Calliphora* is an order of magnitude larger than the fruit fly, but smaller than the drone fly, and operates at a Reynolds number of approximately 1200.

We hypothesise that it is likely that similarities in flight kinematics and aerodynamics could be dictated by shared morphology and phylogeny, whereas specific differences may be linked to their particular ecologies and physical size constraints.

METHODS

Three datasets were used in this study. The *Drosophila melanogaster* dataset was collected and processed as outlined in **Chapters 2** and **3**, the *Calliphora vicina* dataset was collected and processed as outlined in **Chapter 4**, and the *Eristalis tenax* dataset was collected as outlined in Walker et al.[25]. The wing beat kinematic parameters used are the same as those defined in **Chapters 2** and **3**.

Body weight

The weight of 42 *Drosophila melanogaster* individuals of different rearing backgrounds from the same batch were weighed after death, and most of the *Calliphora vicina* individuals were weighed after the experiment using a UMX2 microbalance (Mettler Toledo Ltd., UK) with a readability of 0.1μg, and provided the basis for a scaling factor to estimate the weight of individuals in each recording. The subset of *Calliphora vicina* individuals that were not weighed included those that accidentally escaped or died prematurely.

The rearing conditions, age, and in the case of *Drosophila melanogaster*, the sex, of the weighed flies were known, as was the estimated body volume V of their recordings. The exact weight of the individual in each sequence was unknown due to the impracticality of weighing individuals before and after each flight experiment, and in the case of *Drosophila* due to the presence of multiple flies in the flight arena during recordings. We therefore estimated the mass of each individual in the fight experiments by scaling their measured volume by the mean density of weighed flies of the same background. The scaling factor was calculated by taking the mean interquartile weight and mean interquartile body volume of the flies of equal sex and rearing conditions. The product of the body volume and the scaling factor is the estimate of the fruit fly's weight.

Advance ratio

Advance ratio was used to accurately compare the change in wing beat kinematics at different heading velocities across different species. The advance ratio is a non-dimensional term adapted from helicopter and rotor-theory describing the ratio of the relative speed of the fluid to the rotor-speed. In the case of insects, this

would be the ratio of their heading velocity x_H to the flapping wing velocity. Ellington defined advance ratio for insect flight as follows:

$$J = \frac{x_H}{2\Phi nR}$$

Where x_H is forwards heading velocity, Φ is stroke amplitude, n is wing beat frequency and R is wing length.

Advance ratios close to 0 denote hovering flight, as the insect advances very little with respect to its wing motion. Larger advance ratios denote fast forward flight, as the downstroke force progressively dominates due to the increased heading velocity.

The following advance ratio categories were selected to describe forward flight in all three species, and were used for convenience of presentation, but are not used in any of the statistical analyses:

Range	Category
< -0.01	Backwards flight
-0.01 – 0.01	Hovering flight
0.01 – 0.05	Slow forward flight
0.05 – 0.13	Medium forward flight
> 0.13	Fast forward flight

Table 8. Advance ratio categories to describe forward flight.

Ellington originally defined hovering flight in insects as an advance ratio of J<|±0.1|[6], though we have chosen a more conservative categorisation. Ellington's broader definition was made to qualify more of his sequences for analysis within the hovering category because he had a lower volume of data at his disposal and for all practical purposes, the aerodynamics are unaffected by the body's motion in slow forward flight[6]. When the advance ratio distributions of all three species are considered, it becomes apparent that J<|±0.1| is not representative of true hovering flight from the perspective of net body displacement. The reason we chose more conservative categories is to do with the fly's net body displacement. Even when the advance ratio is small, the fly still beats its wings very quickly. The average *Calliphora vicina* flying at an advance ratio of 0.05, which is half of what Ellington considered to be within the envelope of hovering flight, and flapping with an average wing beat frequency of 166Hz is travelling at 0.38m/s, which is not a negligible distance to travel in a second for an insect with a body length of less than 15mm **(Image 5)**. For *Drosophila melanogaster*, this equates to a forward speed of 0.09m/s, which is a similarly large net displacement for a body length of 2mm. In both species, J = 0.05 equates to a net displacement of ~20% of their body length per wing beat.

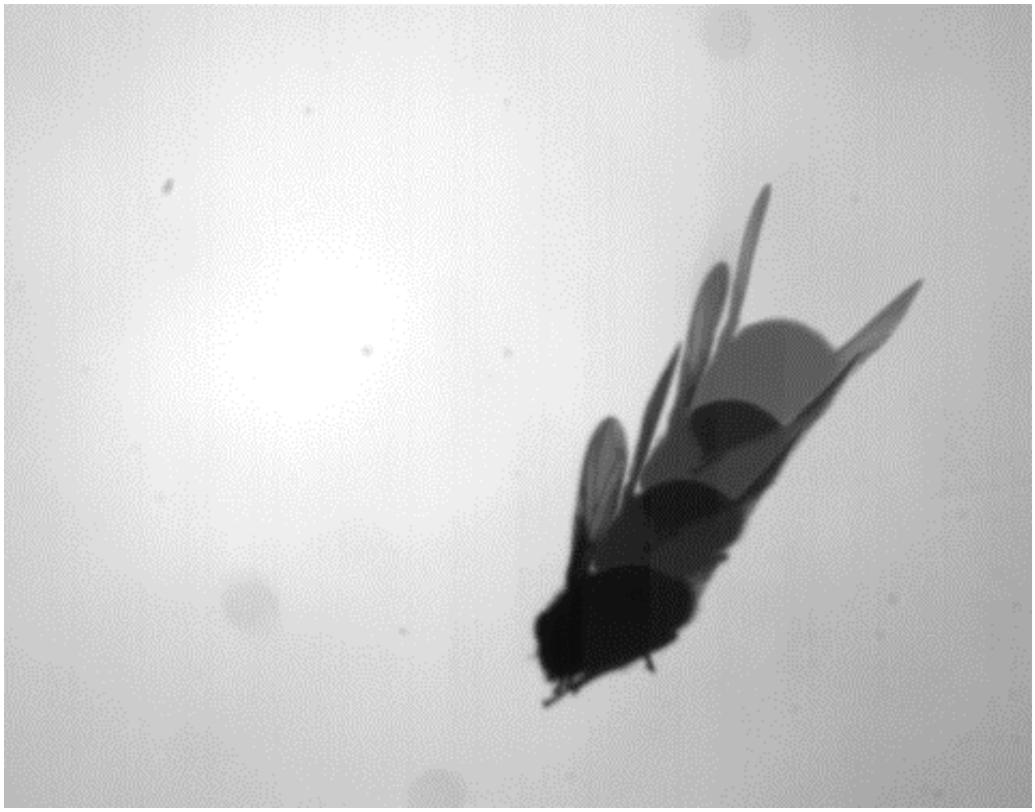

Image 5. Four consecutive wing beats of *Calliphora vicina* at J=0.05.

Kinematic correlation-standard deviation matrix

To make it easier to compare relationships between different kinematic variables within and between species, a special correlation-standard deviation table was built for each species. All values for each kinematic variable for each species were collated and z-scored. The correlation coefficient for each pair of variables was then calculated, and the degree of correlation between each pair of kinematic variables expressed relative to the same pair of kinematic variables in other species. The numbers on the diagonal represent the standard deviation of the z-scored variable. To account for multiple comparisons, a False Discovery Rate test (FDR) was conducted on all statistical tests at the 5% level. The significance of all p-values reported in this study remain unchanged after the correction **(Supplementary Material 4)**.

The strength of the correlation coefficients was assessed as follows[26]:

Correlation coefficient	Relationship
0 – 0.3	No relationship
0.3 – 0.5	Weak relationship
0.5 – 0.7	Moderate relationship
0.7 – 0.9	Strong relationship
0.9 – 1.0	Very strong relationship

Table 9. Strength of the relationship between two parameters based on the absolute correlation coefficient

Measurement of body forces

The insect's centre of volume and orientation were smoothed using a quintic smoothing spline fitted with a tolerance calculated to remove the same amount of noise as a 3rd order Butterworth filter with a cut-off frequency of 150Hz. The splines were then twice differentiated analytically to estimate the acceleration of the insect's centre of mass with respect to the lab coordinate system. Newton's Second Law equation was used to estimate the total aerodynamic force acting on the insect and was resolved in the primary body-fixed axis system $\{x_B, y_B, z_B\}$.

Quasi-Steady Blade Element Model

A blade element model was applied to estimate the aerodynamic forces of the flies in flight. Dipterans operate at high angles of attack, which result in high lift and drag forces and flow separation over the wing, generating a leading edge vortex that allows a continuation of the lift slope into a higher angle of attack. The blade element model used in this study was developed by Walker & Taylor (in prep.), and models

the total aerodynamic force of a flapping wing to be the sum of the circulatory force (lift and drag) and the added mass force.

Circulatory force

Circulatory force is determined using the following lift and drag equations:

$$L = \frac{1}{2}\rho U^2 S C_L 1_{U_\perp}$$

$$D = \frac{1}{2}\rho U^2 S C_D 1_{U_\parallel}$$

where ρ is air density, U is the scalar velocity of the wing relative to the air, and S is the wing surface area. $1_{U_\perp}$ is a unit vector indicating that lift operates perpendicular to the air flow, and $1_{U_\parallel}$ indicates that drag operates parallel to the air flow. C_L is the lift coefficient, and C_D is the drag coefficient, which vary as a function of the angle of attack α, the angle between the wing chord and the oncoming air flow, and allow the lift and drag forces to be predicted for an unsteady, separated flow. The simplest model assumes that C_L and C_D are orthogonal components that vary as a sine function of α, with a slope C_{F_α} when α = 0:

$$C_F \equiv \sqrt{C_L^2 + C_D^2} = C_{F_\alpha} \sin\alpha$$

This equation can be rearranged in terms of the lift and drag coefficients:

$$C_L = C_{F_\alpha} \sin\alpha \cos\alpha$$

$$C_D = C_{F_\alpha} \sin^2\alpha$$

However, this model is simplistic, as wing camber may mean that no lift is generated at an angle of attack other than 0. Likewise, the drag coefficient inaccurately models the wing as an idealised flat-plate, when in reality there is profile drag even when α = 0. C_{F_α} denotes the maximum slope of the lift and drag coefficients, but these are not necessarily identical in C_L and C_D. We can therefore generate a new, more precise model by adding lift and drag offset terms to the lift and drag equations, and splitting C_{F_α} into $C_{L_\alpha}$and C_{D_α}:

$$C_L = C_{L_\alpha} \sin\alpha \cos\alpha + C_{L_0}$$

$$C_D = C_{D_\alpha} \sin^2\alpha + C_{D_0}$$

Added mass force

The added mass force is the inertia added to the wing as the wing flaps back and forth through the air, and can be modelled as:

$$A = -\frac{\pi}{4}\gamma\rho C^2 R a_{C_\perp} 1_{C_\perp}$$

where γ is the added mass coefficient, which accounts for the shape of the wing, ρ is the air density, C is the chord length, R is the wing length, $a_{C_\perp}$ is the wing's acceleration normal to the wing surface at mid-chord length and $1_{C_\perp}$ is the unit vector of the normal of the wing surface. See Walker et al. (in prep) for more information.

The quasi-steady blade element model approximates aerodynamic force by dividing the wing into 20 blade elements and integrating the force calculated from steady state equations over 100 consecutive time steps per wing beat. The quasi-

steady assumption assumes that the force generated by each blade element is independent from its time history and from the other blade elements.

The velocity and angle of attack of each blade element was calculated at the theoretical centre of circulation of the wing, which lies at the three quarter chord length from the leading edge, as it allows for the wing's translational and rotational velocity to be simultaneously optimised[27,28].

RESULTS

A total of 4054 wing beats from 265 individual fruit fly sequences, 2708 wing beats from 28 individual blow fly individuals and 26451 wing beats from 36 free-flying hoverflies were processed for kinematic analysis and for aerodynamic force estimation.

Morphometrics

Wing size in *Drosophila* does not correlate positively with body length within sexes **(Chapter 3)**, whereas in *Calliphora* **(Figure 8a)** and *Eristalis* wing length does scale with body size.

Advance ratio

The proportion of wing beats at different advance ratios were distributed differently in each species **(Figure 19)**. *Drosophila* is split between male and females to account for sexual dimorphism. The advance ratios were distributed differently in each species, with *Eristalis* peaking at close to hovering and slow forward flight speeds, *Calliphora* peaking at faster forward flight speeds and *Drosophila* lying in the middle, but with a noticeable difference between the two sexes **(See Chapter 2)**.

Very few wing beats were found in the backwards and hovering flight categories in both *Calliphora* and *Drosophila* **(Figure 20)**, so they were excluded from categorical analysis as there were too few wing beats in either category to be able to draw strong conclusions about the average wing beat of hovering and backwards flight. The kinematic morphospaces **(Figure 21)** and the correlation-standard deviation matrix **(Table 10)** display the relationship between each

kinematic parameter and advance ratio, and the relationship between all parameters, respectively, for all three species in a quantitative manner.

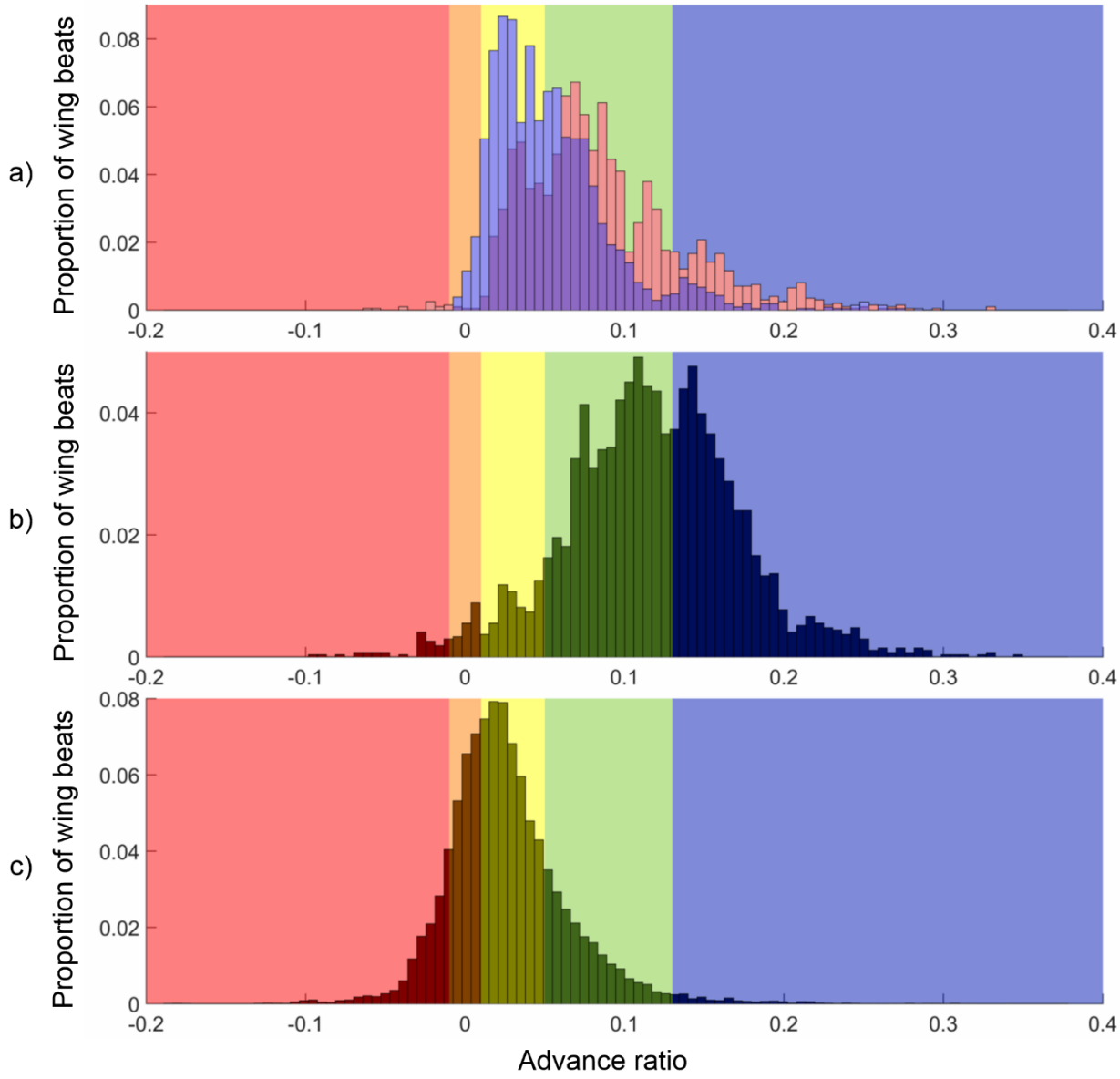

Figure 19. a) Distribution of advance ratio for male (blue) and female (red) *Drosophila melanogaster* b) Distribution of advance ratio for *Calliphora vicina* c) Distribution of advance ratio for *Eristalis tenax*

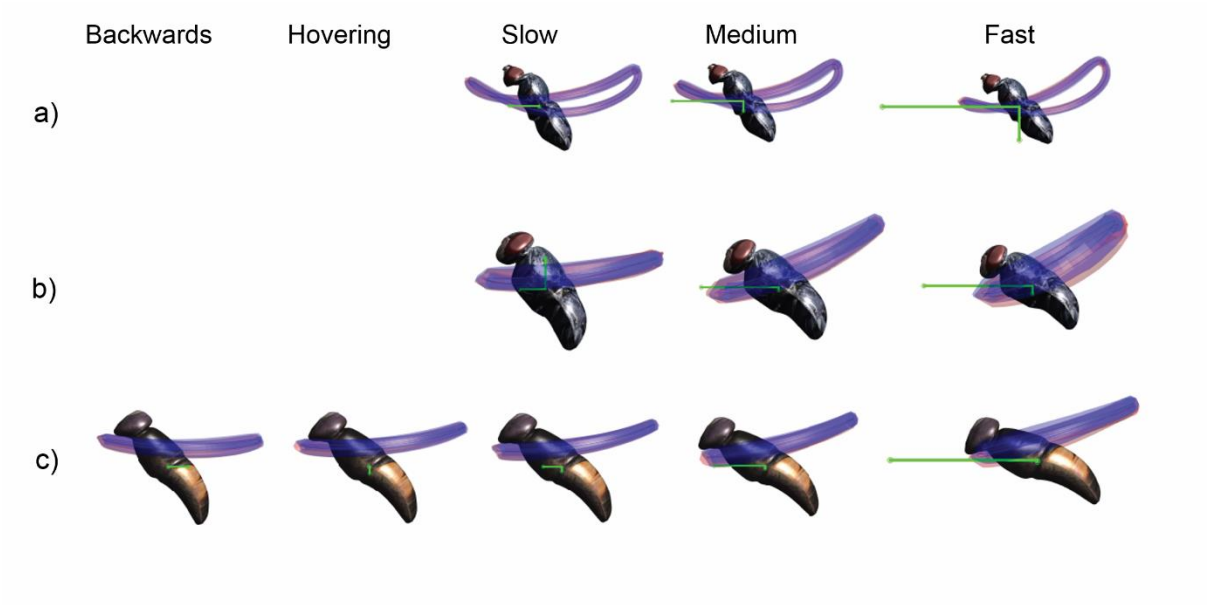

Figure 20. Mean wing tip trajectory with scaled mean heading and upward velocity (x_H and z_H) for backwards, hovering, slow, medium and fast forward flight for a) *Drosophila melanogaster;* b) *Calliphora vicina*; c) *Eristalis tenax*

Figure 21. (see series of horizontal plates overleaf) Kinematic morphospaces of *Drosophila melanogaster* (green), *Calliphora vicina* (yellow) and *Eristalis tenax* (blue) for advance ratio by a) wing beat frequency; b) stroke amplitude; c) stroke plane with regards to body; d) body tilt angle; e) relative timing of supination; f) relative timing of pronation.

(a)

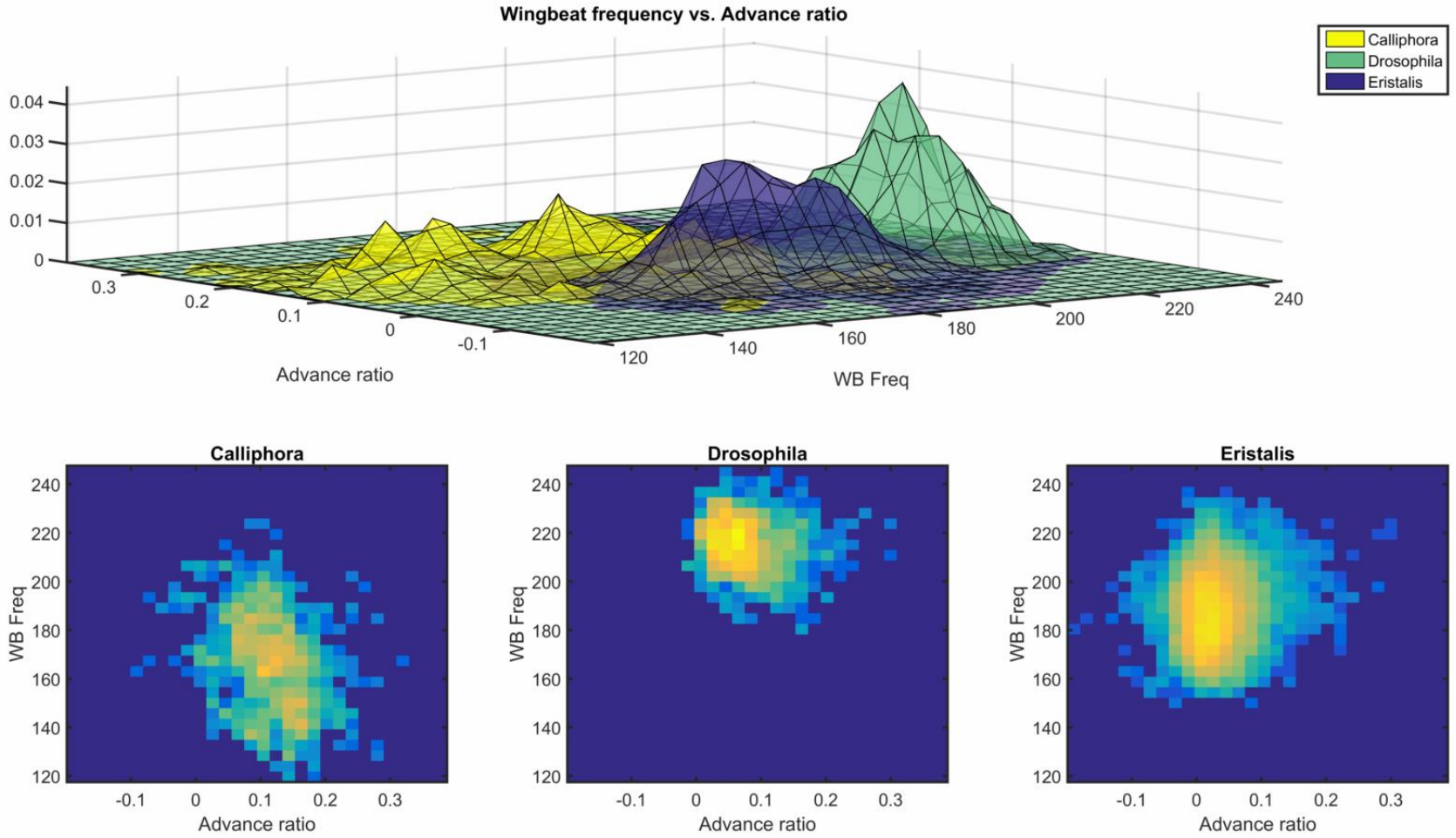
Wingbeat frequency vs. Advance ratio
Calliphora
Drosophila
Eristalis
0.04
0.03
0.02
0.01
0
0.3
0.2
0.1
0
-0.1
Advance ratio
120
140
160
180
200
220
240
WB Freq
Calliphora
Drosophila
Eristalis
WB Freq
Advance ratio
240
220
200
180
160
140
120
-0.1
0
0.1
0.2
0.3

(b)

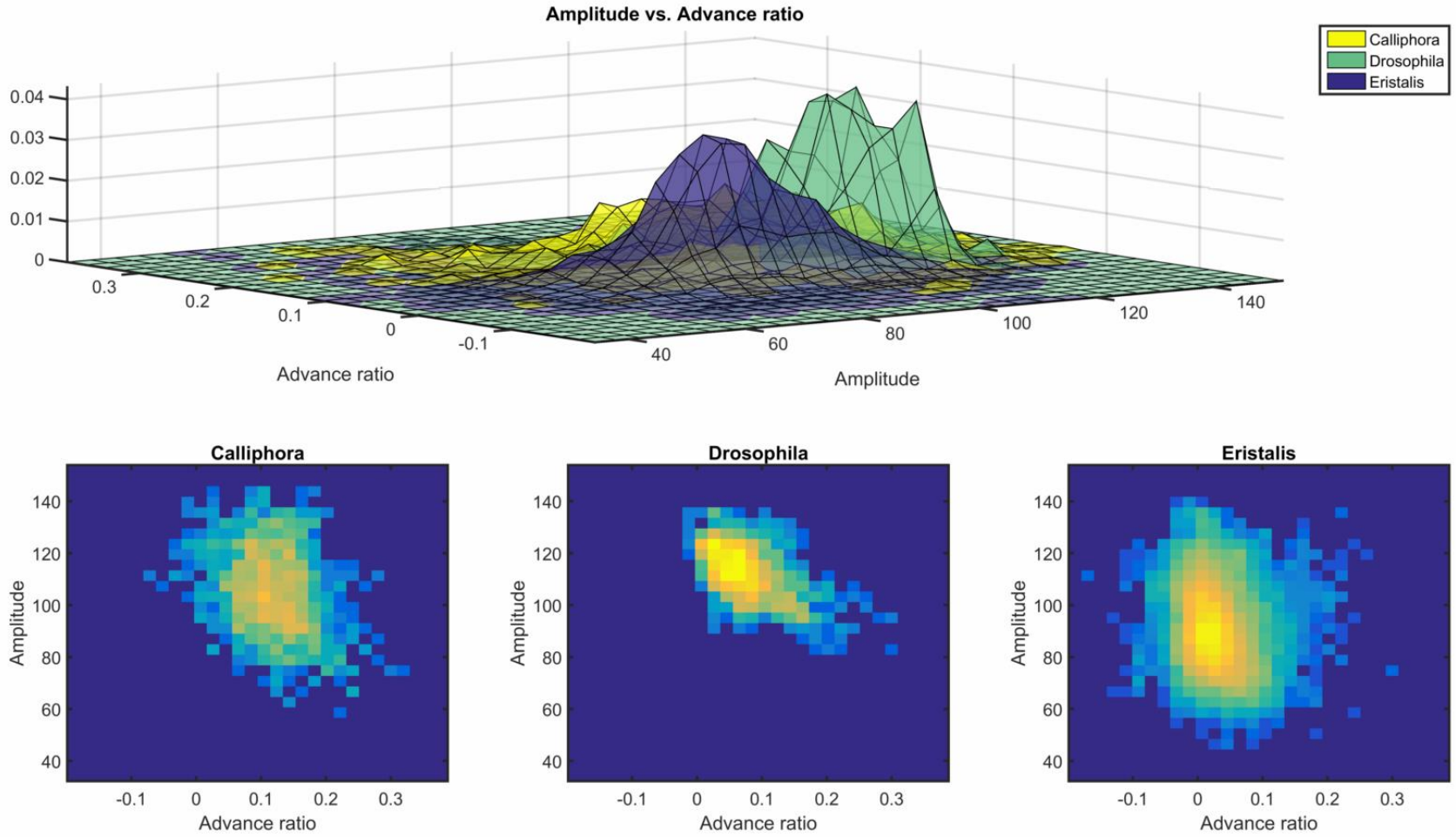
Amplitude vs. Advance ratio
Calliphora
Drosophila
Eristalis
0.04
0.03
0.02
0.01
0
0.3
0.2
0.1
0
-0.1
Advance ratio
40
60
80
100
120
140
Amplitude
Calliphora
Drosophila
Eristalis
Amplitude
Advance ratio
-0.1
0
0.1
0.2
0.3

(c)

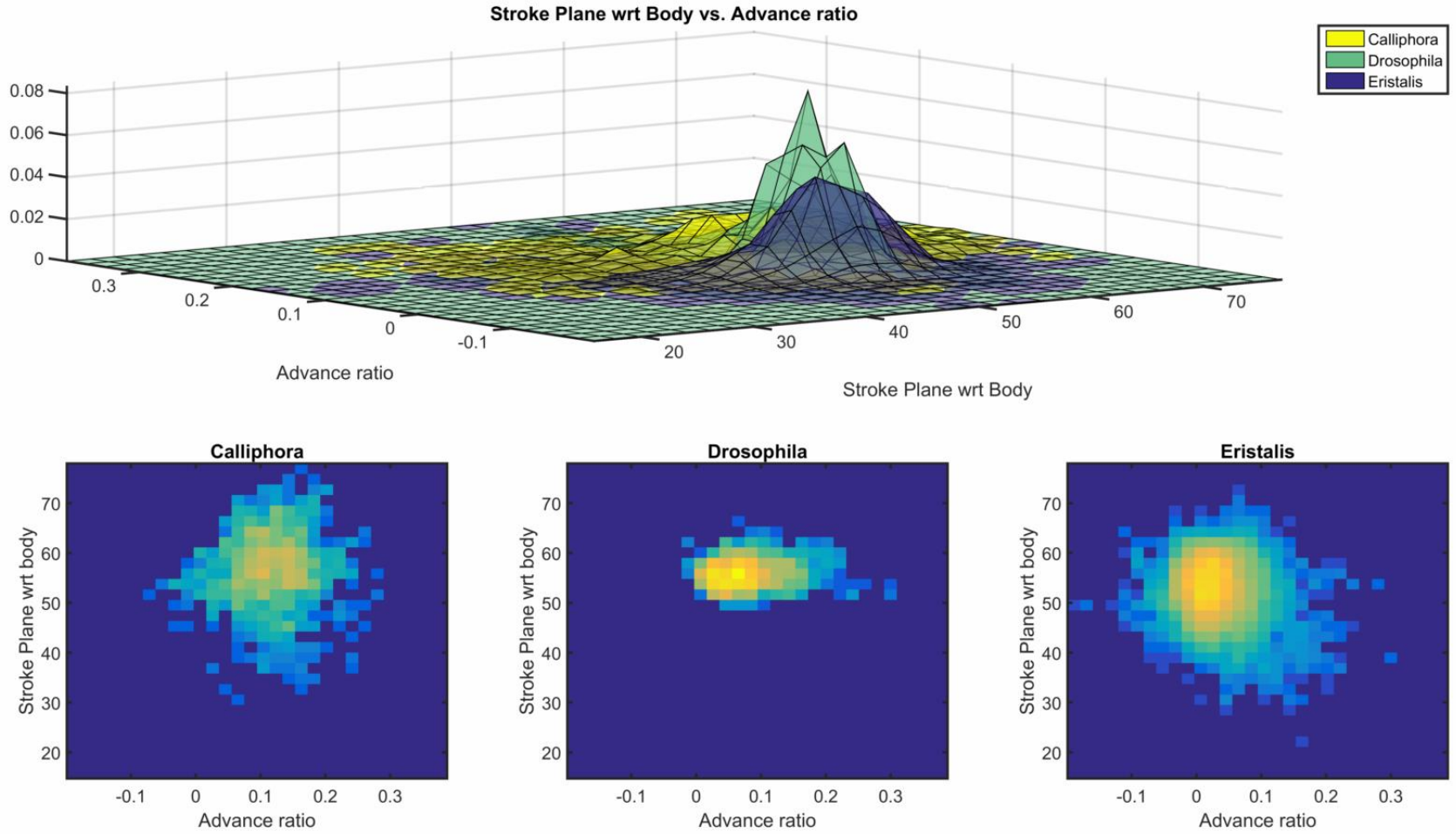
Stroke Plane wrt Body vs. Advance ratio
Calliphora
Drosophila
Eristalis
0.08
0.06
0.04
0.02
0
0.3
0.2
0.1
0
-0.1
Advance ratio
20
30
40
50
60
70
Stroke Plane wrt Body
Calliphora
Drosophila
Eristalis
Stroke Plane wrt body
70
60
50
40
30
20
-0.1
0
0.1
0.2
0.3
Advance ratio

(d)

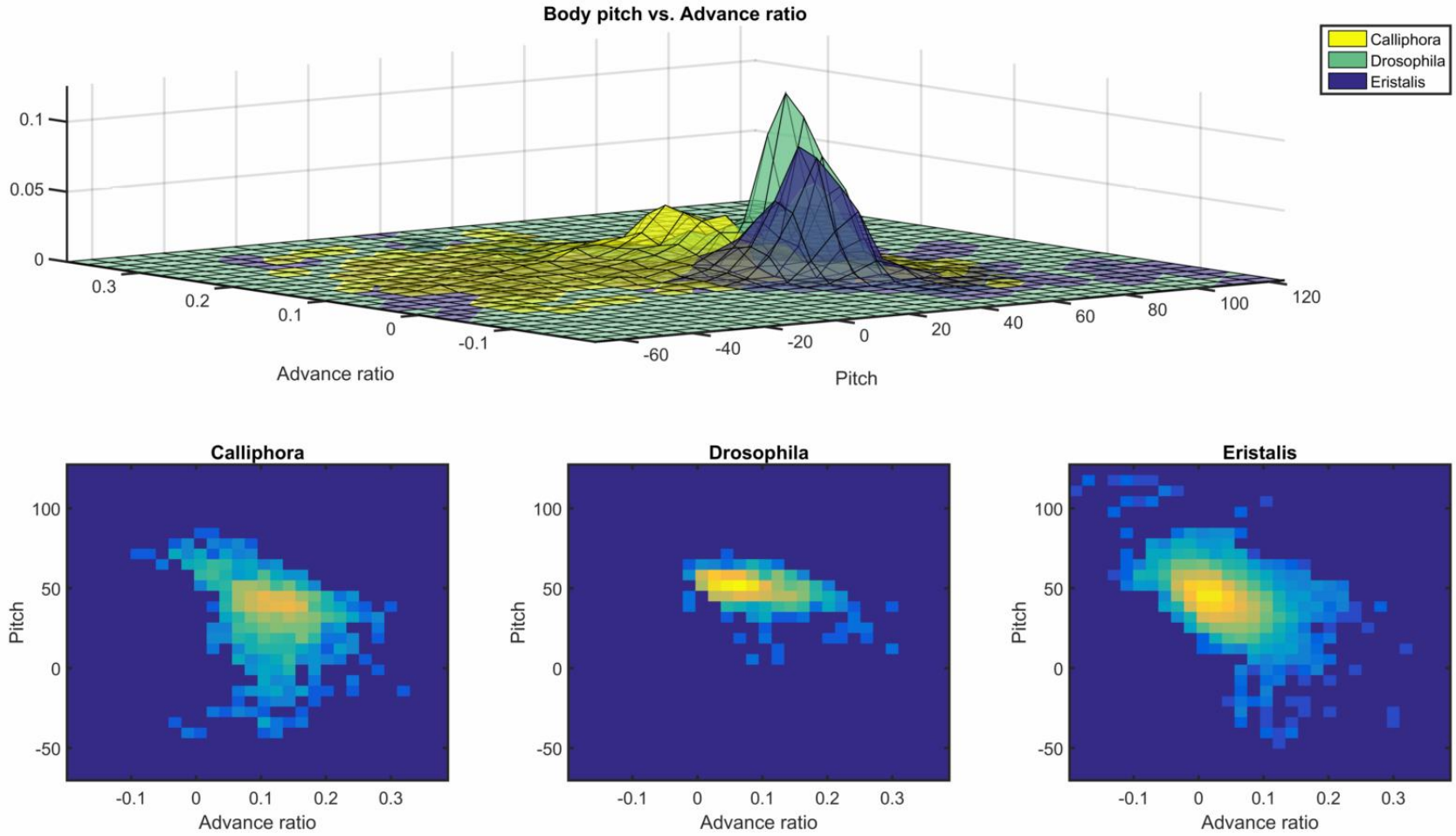
Body pitch vs. Advance ratio
Calliphora
Drosophila
Eristalis
0.1
0.05
0
0.3
0.2
0.1
0
-0.1
Advance ratio
-60
-40
-20
0
20
40
60
80
100
120
Pitch
Calliphora
Drosophila
Eristalis
100
50
0
-50
Pitch
-0.1
0
0.1
0.2
0.3
Advance ratio

(e)

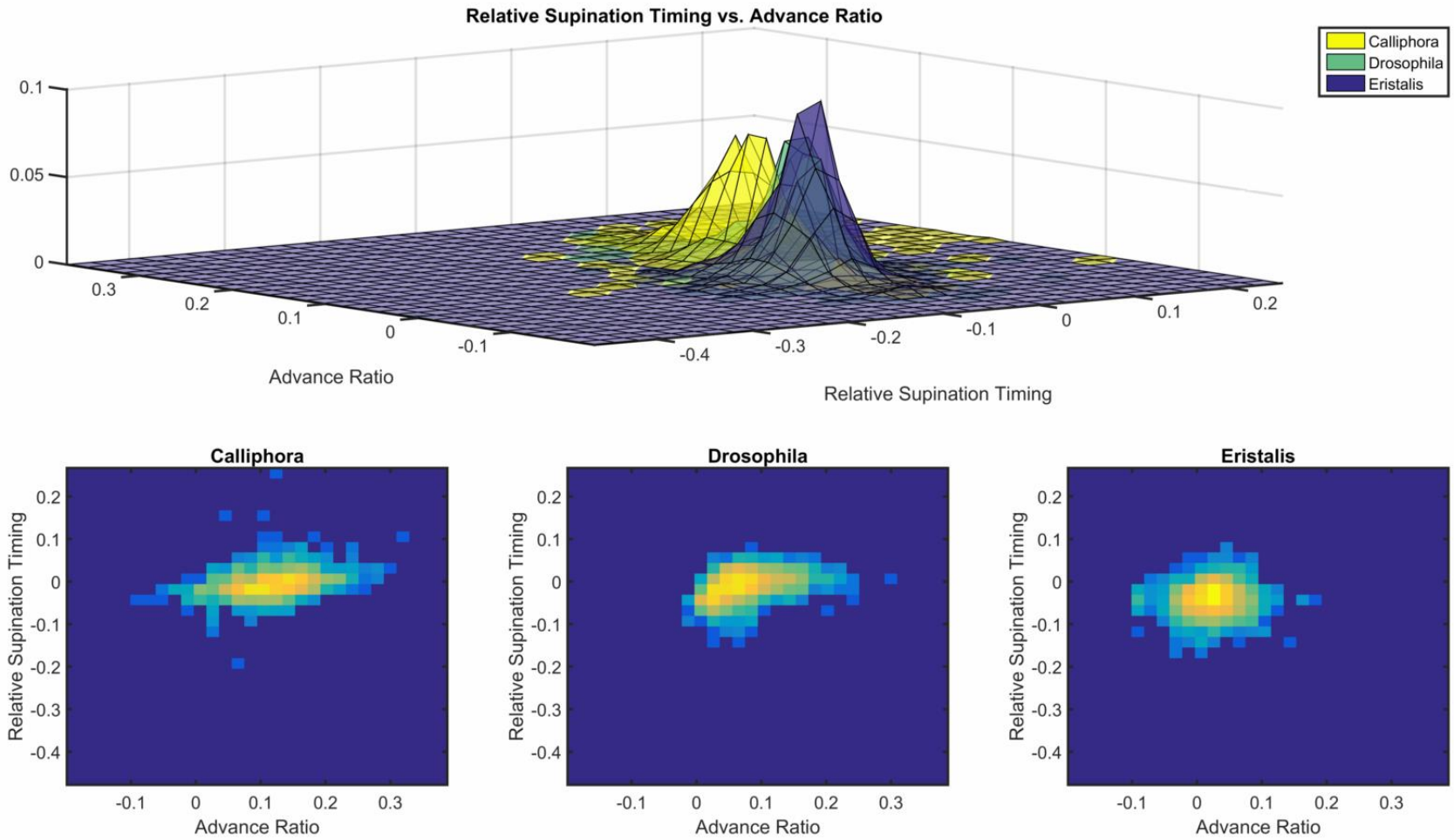
Relative Supination Timing vs. Advance Ratio
Calliphora
Drosophila
Eristalis
0.1
0.05
0
0.3
0.2
0.1
0
-0.1
Advance Ratio
-0.4
-0.3
-0.2
-0.1
0
0.1
0.2
Relative Supination Timing
Calliphora
Drosophila
Eristalis
Relative Supination Timing
Advance Ratio
0.2
0.1
0
-0.1
-0.2
-0.3
-0.4
-0.1
0
0.1
0.2
0.3

(f)

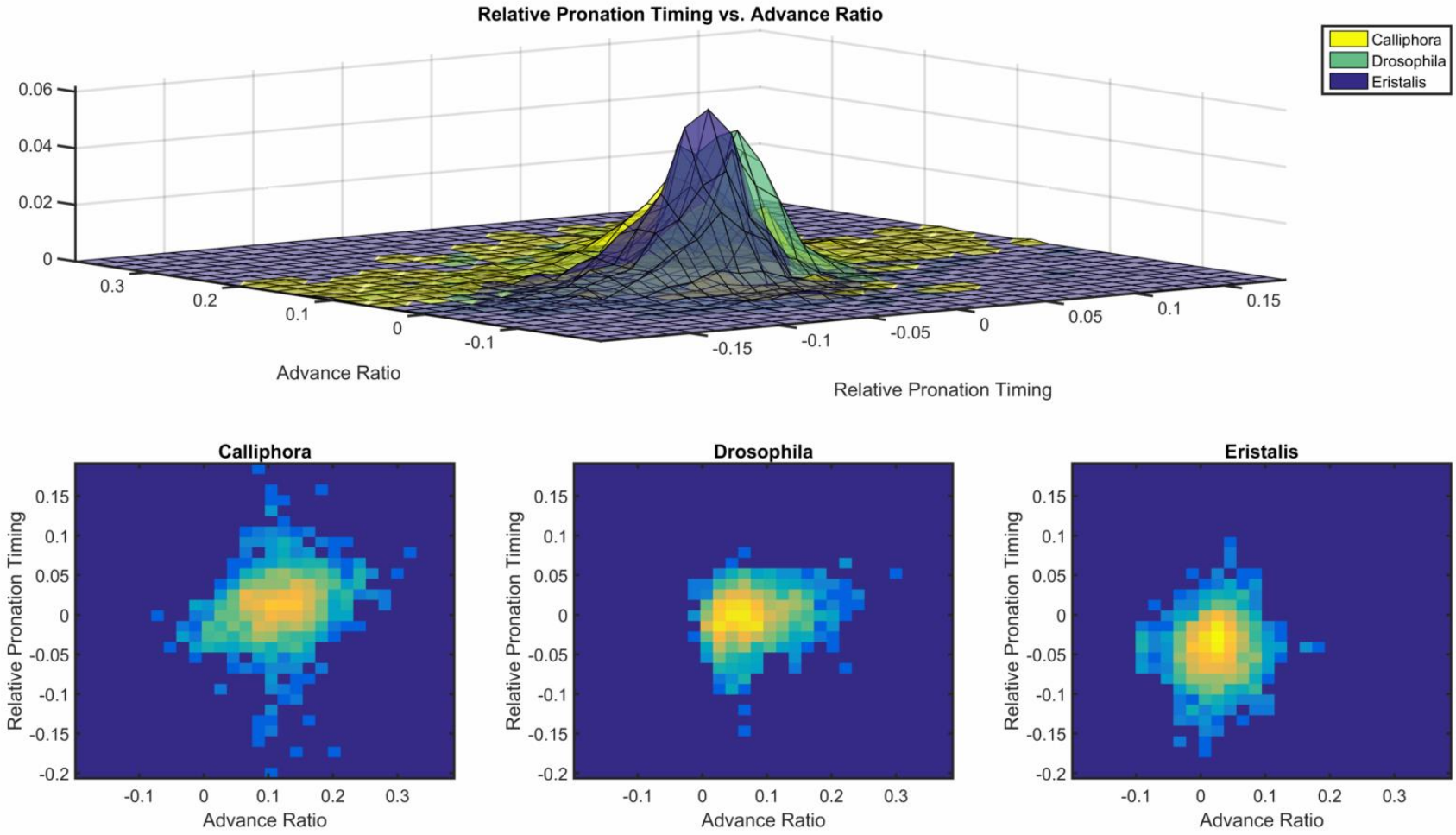
Relative Pronation Timing vs. Advance Ratio
Calliphora
Drosophila
Eristalis
0.06
0.04
0.02
0
0.3
0.2
0.1
0
-0.1
Advance Ratio
-0.15
-0.1
-0.05
0
0.05
0.1
0.15
Relative Pronation Timing
Calliphora
Drosophila
Eristalis
Relative Pronation Timing
Advance Ratio
0.15
0.1
0.05
0
-0.05
-0.1
-0.15
-0.2
-0.1
0
0.1
0.2
0.3

(a) *Drosophila melanogaster* correlation-standard deviation matrix

	WB	SA	SPB	SPW	Sup	Pron	Pitch	Roll	TSR	J
WB	0.55	0.01	-0.19	-0.10	-0.10	0.13	0.01	0.05	-0.48	-0.21
SA	0.01	0.59	0.04	-0.28	-0.48	-0.37	0.31	-0.07	-0.33	-0.52
SPB	-0.19	0.04	0.52	0.37	0.06	-0.13	0.09	0.07	0.27	0.25
SPW	-0.10	-0.28	0.37	0.50	0.20	0.08	-0.78	0.25	0.22	0.58
Sup	-0.10	-0.48	0.06	0.20	1.08	0.27	-0.19	-0.09	0.32	0.36
Pron	0.13	-0.37	-0.13	0.08	0.27	0.91	-0.14	-0.03	0.02	0.19
Pitch	0.01	0.31	0.09	-0.78	-0.19	-0.14	0.49	-0.29	-0.10	-0.42
Roll	0.05	-0.07	0.07	0.25	-0.09	-0.03	-0.29	0.61	0.09	0.23
TSR	-0.48	-0.33	0.27	0.22	0.32	0.02	-0.10	0.09	0.56	0.49
J	-0.21	-0.52	0.25	0.58	0.36	0.19	-0.42	0.23	0.49	0.96

(b) *Calliphora vicina* correlation-standard deviation matrix

	WB	SA	SPB	SPW	Sup	Pron	Pitch	Roll	TSR	J
WB	1.08	0.02	0.14	-0.02	-0.07	-0.08	0.10	0.16	0.17	-0.30
SA	0.02	1.04	0.06	-0.21	-0.29	-0.21	0.21	0.10	0.70	-0.30
SPB	0.14	0.06	1.41	-0.12	0.01	-0.03	0.54	-0.47	0.23	0.03
SPW	-0.02	-0.21	-0.12	1.35	0.12	0.20	-0.80	0.03	-0.03	0.45
Sup	-0.07	-0.29	0.01	0.12	0.92	0.14	-0.08	-0.14	-0.16	0.29
Pron	-0.08	-0.21	-0.03	0.20	0.14	1.22	-0.14	-0.11	-0.06	0.24
Pitch	0.10	0.21	0.54	-0.80	-0.08	-0.14	1.63	-0.34	0.18	-0.31
Roll	0.16	0.10	-0.47	0.03	-0.14	-0.11	-0.34	1.34	0.08	-0.19
TSR	0.17	0.70	0.23	-0.03	-0.16	-0.06	0.18	0.08	1.00	-0.12
J	-0.30	-0.30	0.03	0.45	0.29	0.24	-0.31	-0.19	-0.12	1.11

(c) *Eristalis tenax* correlation-standard deviation matrix

	WB	SA	SPB	SPW	Sup	Pron	Pitch	Roll	TSR	J
WB	0.77	-0.14	0.16	0.19	-0.14	0.16	-0.10	0.11	0.22	0.10
SA	-0.14	0.88	-0.37	-0.47	0.15	-0.48	0.39	0.16	0.48	-0.17
SPB	0.16	-0.37	0.97	0.36	0.11	0.01	-0.03	-0.30	-0.14	-0.13
SPW	0.19	-0.47	0.36	0.96	-0.17	0.37	-0.85	-0.22	0.00	0.39
Sup	-0.14	0.15	0.11	-0.17	0.95	-0.51	0.17	-0.03	-0.08	0.04
Pron	0.16	-0.48	0.01	0.37	-0.51	0.96	-0.34	-0.09	0.03	0.15
Pitch	-0.10	0.39	-0.03	-0.85	0.17	-0.34	0.92	0.07	0.01	-0.48
Roll	0.11	0.16	-0.30	-0.22	-0.03	-0.09	0.07	0.96	0.07	0.09
TSR	0.22	0.48	-0.14	0.00	-0.08	0.03	0.01	0.07	0.72	0.21
J	0.10	-0.17	-0.13	0.39	0.04	0.15	-0.48	0.09	0.21	0.78

Table 10. Correlation-standard deviation matrix with correlation coefficients and standard deviations (diagonal) for (a) *Drosophila melanogaster* (b) *Calliphora vicina* and (c) *Eristalis tenax*. WB = wing beat frequency; SA = stroke amplitude; SPB = stroke plane body; SPW = stroke plane world; Sup = supination; Pron = pronation; Pitch = pitch; Roll = roll; TSR = timing of stroke reversal; J = advance ratio.

Wing beat frequency and advance ratio are weakly inversely correlated in *Calliphora vicina* (r_{2708} = -0.30, p < .0001) **(Table 10b, see Table 9 for reference)**. The relationship is not strong enough to be meaningful in either *Drosophila melanogaster* (r_{4054} = -0.21, p < .0001) **(Table 10a)** or *Eristalis tenax* (r_{26541} = 0.10, p < .0001) **(Table 10c)**, but it is negative in the former and positive in the latter. Wing beat frequency and timing of stroke reversal are weakly negatively correlated in *Drosophila melanogaster* (r_{4054} = -0.48, p < .0001). The relationship is not strong enough to be meaningful in either of the other two flies (*Calliphora:* r_{2708} = -0.17, p < .0001; *Eristalis*: r_{26541} = 0.22, p < .0001), but it is positive in both.

The relationship between stroke amplitude and advance ratio is moderately negative in *Drosophila melanogaster* (r_{4054} = -0.52, p < .0001), and weakly negative in *Calliphora* (r_{2708} = -0.30, p < .0001). It is also negative in *Eristalis* (r_{26541} = -0.17, p < .0001), but it is not strong enough to be meaningful. Stroke amplitude moderately and weakly inversely correlated with timing of supination in *Drosophila* (r_{4054} = -0.48, p < .0001) and *Calliphora* respectively (r_{2708} = -0.29, p < .0001), not in *Eristalis* though, where it is positive but not meaningful (r_{26541} = 0.15, p < .0001). Stroke amplitude is weakly and moderately inversely correlated with timing of pronation in *Drosophila* (r_{4054} = -0.37, p < .0001) and *Eristalis* respectively (r_{26541} = -0.48, p < .0001), and is also negative in *Calliphora* (r_{2708} = -0.21, p < .0001), but not strongly enough to be meaningful. Stroke amplitude is weakly positively correlated with pitch in *Drosophila* (r_{4054} = 0.31, p < .0001) and *Eristalis* (r_{26541} = 0.39, p < .0001). The relationship is positive in *Calliphora* (r_{2708} = 0.21, p < .0001), but not strong enough to be meaningful.

Stroke amplitude is weakly inversely correlated with the timing of stroke reversal in *Drosophila* (r_{4054} = -0.33, p < .0001) but moderately positively correlated in *Eristalis* (r_{26541} = 0.48, p < .0001). Stroke amplitude is also weakly inversely correlated with stroke plane body (r_{26541} = -0.37, p < .0001) and moderately inversely correlated with stroke plane world (r_{26541} = -0.47, p < .0001) in *Eristalis*. In *Drosophila* (r_{4054} = 0.04, p = 0.0009) and *Calliphora* (r_{2708} = 0.06, p = 0.0001) there is no relationship between stroke plane body and stroke plane amplitude.

Stroke plane body and stroke plane world are weakly positively correlated in *Drosophila* (r_{4054} = 0.37, p < .0001) and *Eristalis* (r_{26541} = 0.36, p < .0001). The relationship is inverse in *Calliphora* (r_{2708} = -0.12, p < .0001), but not strong enough to be meaningful. For all three species, there is a strong inverse relationship between stroke plane angle with respect to world and pitch angle (*Drosophila*: r_{4054} = -0.78, p < .0001; *Calliphora*: r_{2708} = -0.80, p < .0001; *Eristalis*: r_{26541} = -0.85, p < .0001), meaning that the stroke plane angle decreases as pitch increases. Only in *Calliphora* is stroke plane body also moderately positively correlated with body pitch (r_{2708} = 0.54, p < .0001). Stroke plane world is weakly positively correlated with advance ratio in *Calliphora* (r_{2708} = 0.45, p < .0001) and *Eristalis* (r_{26541} = 0.39, p < .0001), and moderately so in *Drosophila* (r_{4054} = 0.58, p < .0001). Stroke plane world is also weakly correlated with timing of pronation in *Eristalis* (r_{26541} = 0.37, p < .0001). Stroke plane body is moderately negatively correlated with roll in *Calliphora* (r_{2708} = -0.47, p < .0001) and weakly so *Eristalis* (r_{26541} = -0.30, p < .0001).

Pitch and advance ratio are weakly inversely correlated in *Drosophila melanogaster* (r_{4054} = -0.42, p < .0001), *Calliphora* (r_{2708} = -0.31, p < .0001) and *Eristalis* (r_{26541} = -0.48, p < .0001). Pitch is also weakly inversely correlated with

pronation in *Eristalis* (r_{26541} = -0.34, p < .0001). Pitch and roll are weakly inversely correlated in *Calliphora* (r_{2708} = -0.34, p < .0001) and *Drosophila* (r_{4054} = -0.29, p < .0001).

In *Eristalis*, there is a moderate negative correlation between pronation and supination (r_{26541} = -0.51, p < .0001). Supination and advance ratio are weakly positively correlated in *Calliphora* (r_{2708} = 0.29, p < .0001) and *Drosophila* (r_{4054} = 0.36, p < .0001). Supination and the timing of stroke reversal (r_{4054} = 0.32, p < .0001), and the timing of stroke reversal and advance ratio (r_{4054} = 0.49, p < .0001) are also weakly and moderately positively correlated in *Drosophila* respectively.

Blade Element Model

The blade element model was run on all wing beats for the left and right wings of *Drosophila melanogaster* and *Calliphora vicina*. The error term was minimised using linear least squares and the Akaike Information Criterion (AIC) was used to rank the performance of each model.

The distribution of forces experienced along the *x*-, *y*- and *z*- axes of the body are 6.1±1.6μN, -0.034±0.42μN and -5.1±1.4μN respectively for *Drosophila melanogaster* and 0.54±0.39mN, 0.0058±0.13mN and -0.61±0.34mN for *Calliphora vicina*.

For *Drosophila melanogaster*, the model with two separate slope coefficients and no drag offset was selected **(Figure 21a)**, based on AIC ranking **(Table 11a)**, with the equations for C_L and C_D being:

$$C_L = 1.40\pi \sin\alpha \cos\alpha$$

$$C_D = 0.826\pi \sin^2\alpha$$

For *Calliphora vicina*, the model with two identical slope coefficients and a drag offset was selected **(Figure 21b)** based on AIC ranking **(Table 11b)**, with the equations for C_L and C_D being:

$$C_L = 0.977\pi \sin\alpha \cos\alpha$$

$$C_D = 0.977\pi \sin^2\alpha + 0.165$$

AIC	Model *Drosophila*
378.6	$C_L = C_{L_\alpha} \sin\alpha \cos\alpha$ $C_D = C_{D_\alpha} \sin^2\alpha$
1344.4	$C_L = C_{F_\alpha} \sin\alpha \cos\alpha$ $C_D = C_{F_\alpha} \sin^2\alpha + C_{D_0}$

Table 11a. AIC ranking for *Drosophila* slope coefficients.

AIC	Model *Calliphora*
481.8	$C_L = C_{F_\alpha} \sin\alpha \cos\alpha$ $C_D = C_{F_\alpha} \sin^2\alpha + C_{D_0}$
494.8	$C_L = C_{L_\alpha} \sin\alpha \cos\alpha$ $C_D = C_{D_\alpha} \sin^2\alpha$

Table 11a. AIC ranking for *Drosophila* slope coefficients.

For reference, **(Figure 21c)** displays the slope coefficients for *Eristalis tenax* from Walker & Taylor (in prep.).

We also measured the contribution to aerodynamic force production for each angle of attack across all wing beats for *Drosophila*, *Calliphora* and *Eristalis* **(Figure 22)**.

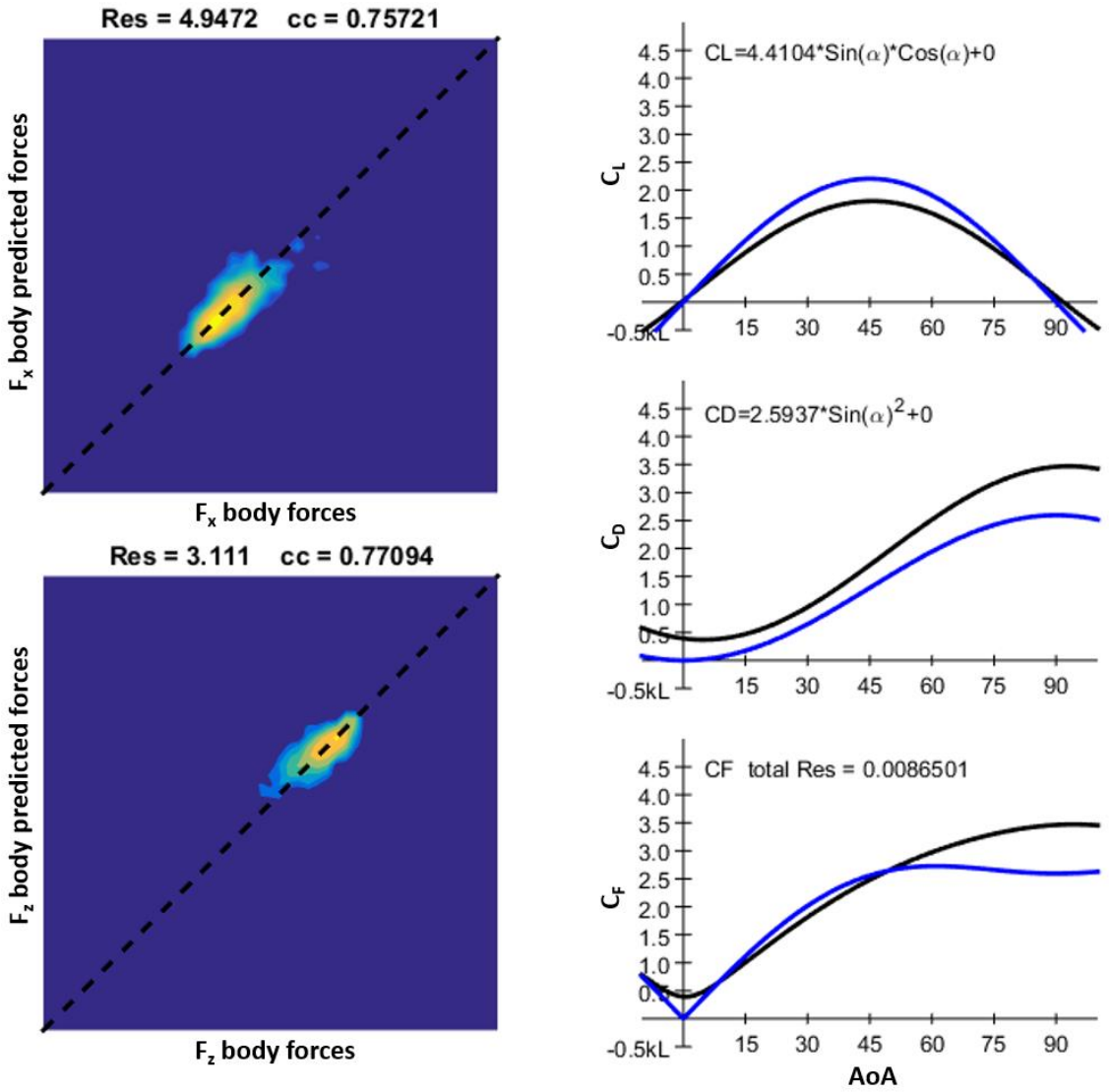

Figure 21a. Force estimation and slope coefficients for *Drosophila melanogaster*. Top left: F_x (anterior-posterior) body forces against predicted F_x body forces; bottom left: F_z (dorso-ventral) body forces against predicted F_z body forces; Top right: Lift coefficient by angle of attack; Middle right: Drag coefficient by angle of attack; Bottom right: Total circulatory force coefficient by angle of attack.

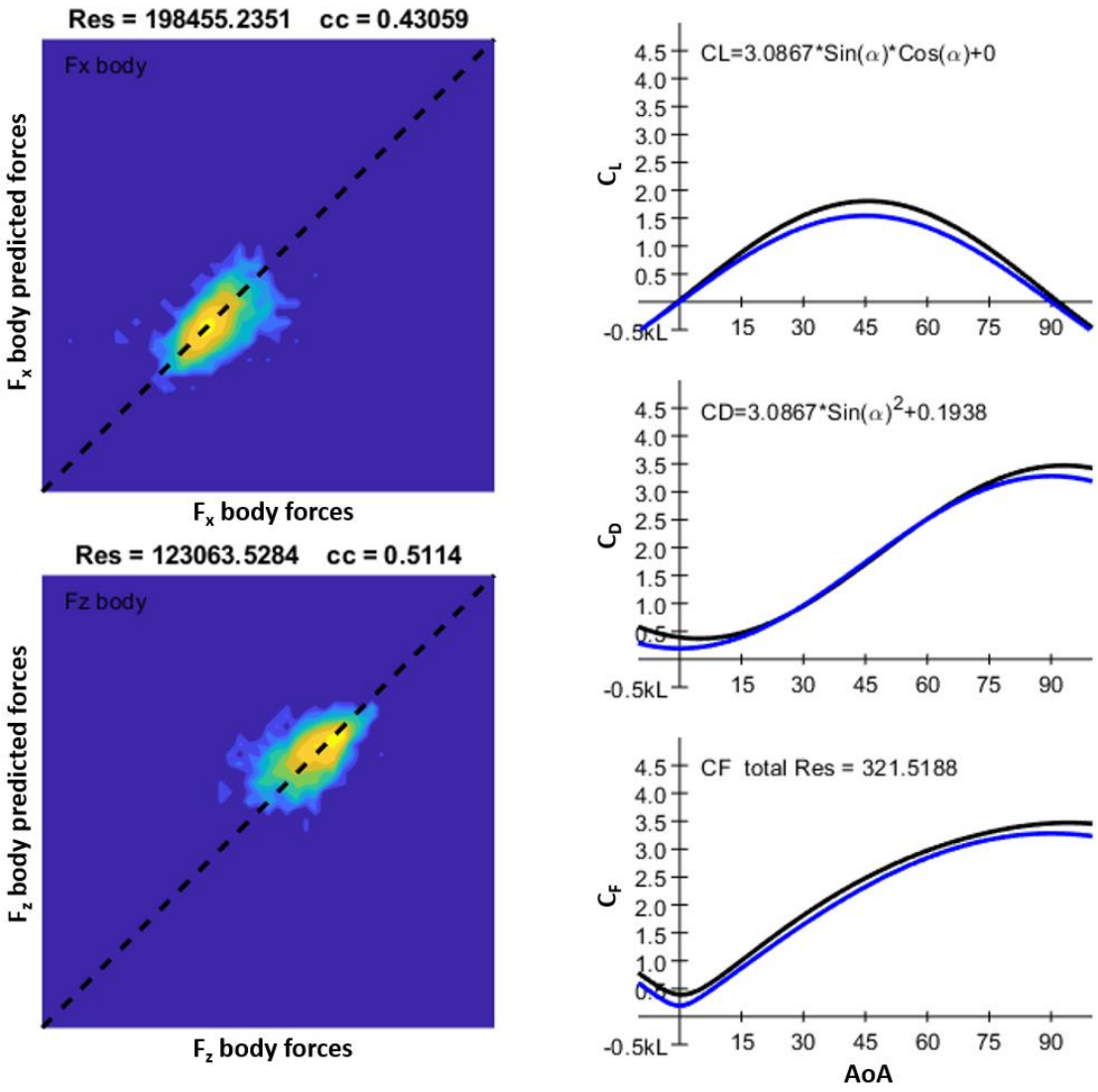

Figure 21b. Force estimation and slope coefficients for *Calliphora vicina*. Top left: F_x (anterior-posterior) body forces against predicted F_x body forces; bottom left: F_z (dorso-ventral) body forces against predicted F_z body forces; Top right: Lift coefficient by angle of attack; Middle right: Drag coefficient by angle of attack; Bottom right: Total circulatory force coefficient by angle of attack.

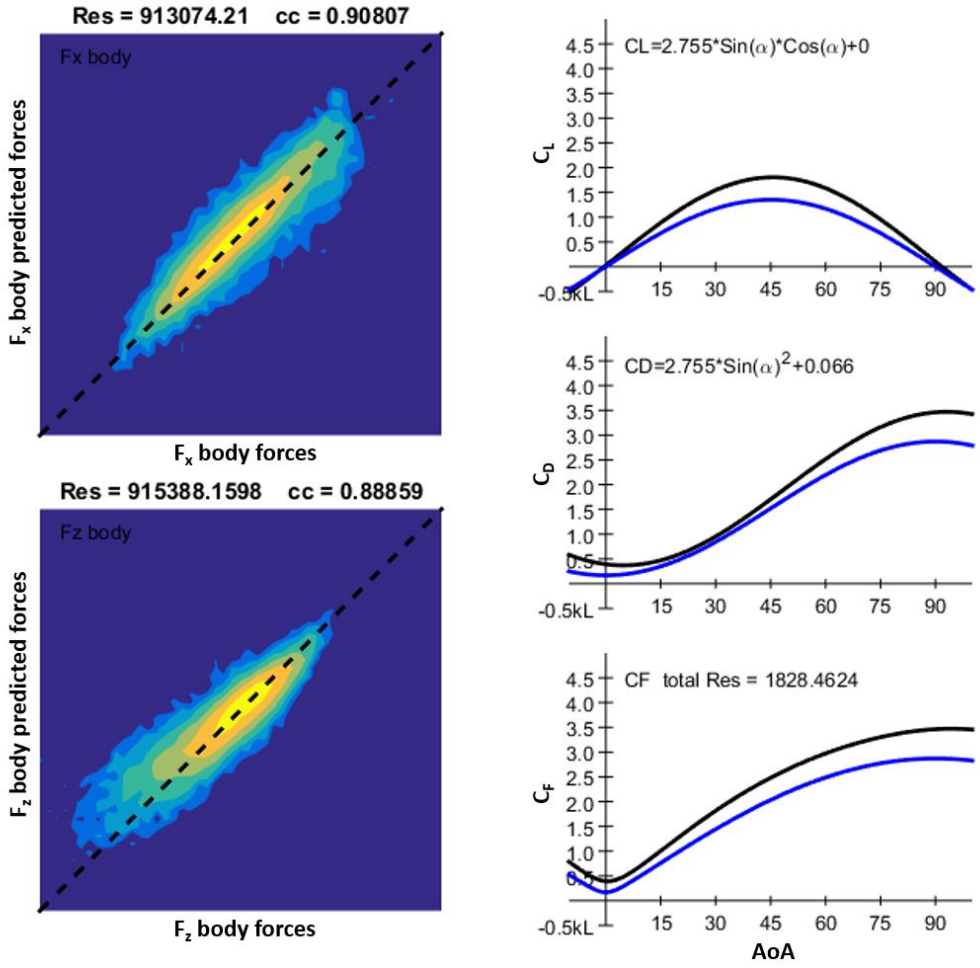

Figure 21c. From Walker & Taylor (in prep.) Force estimation and slope coefficients for *Eristalis tenax*. Top left: F_x (anterior-posterior) body forces against predicted F_x body forces; bottom left: F_z (dorso-ventral) body forces against predicted F_z body forces; Top right: Lift coefficient by angle of attack; Middle right: Drag coefficient by angle of attack; Bottom right: Force coefficient by angle of attack.

a)

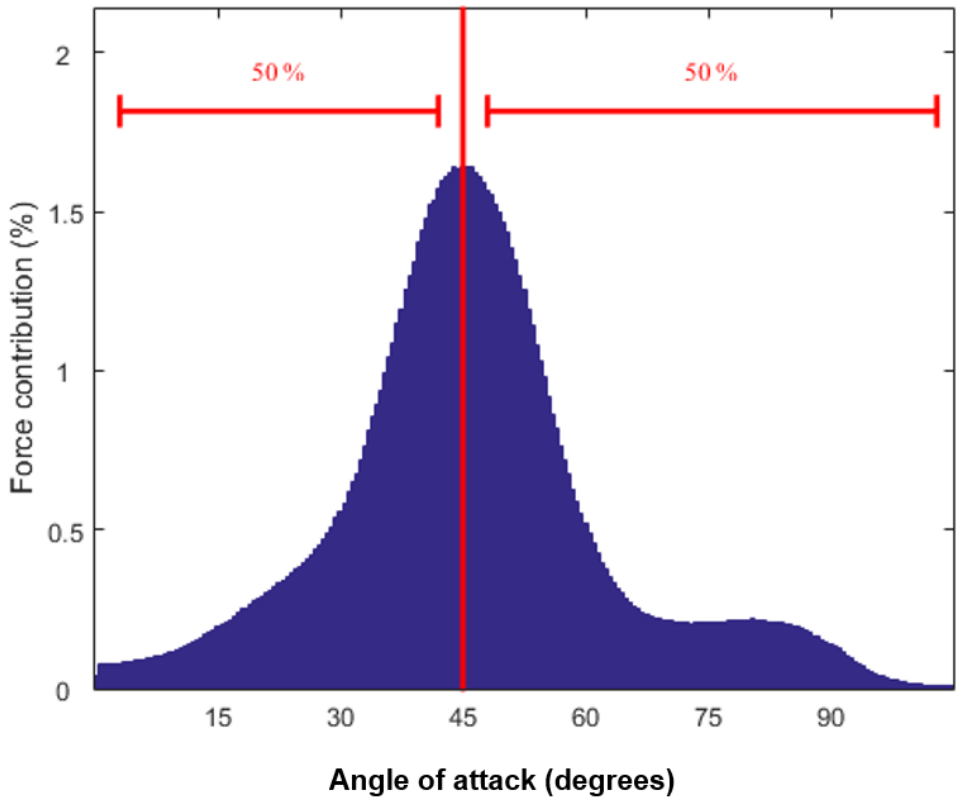
50 %
50 %
Force contribution (%)
2
1.5
1
0.5
0
15
30
45
60
75
90
Angle of attack (degrees)

b)

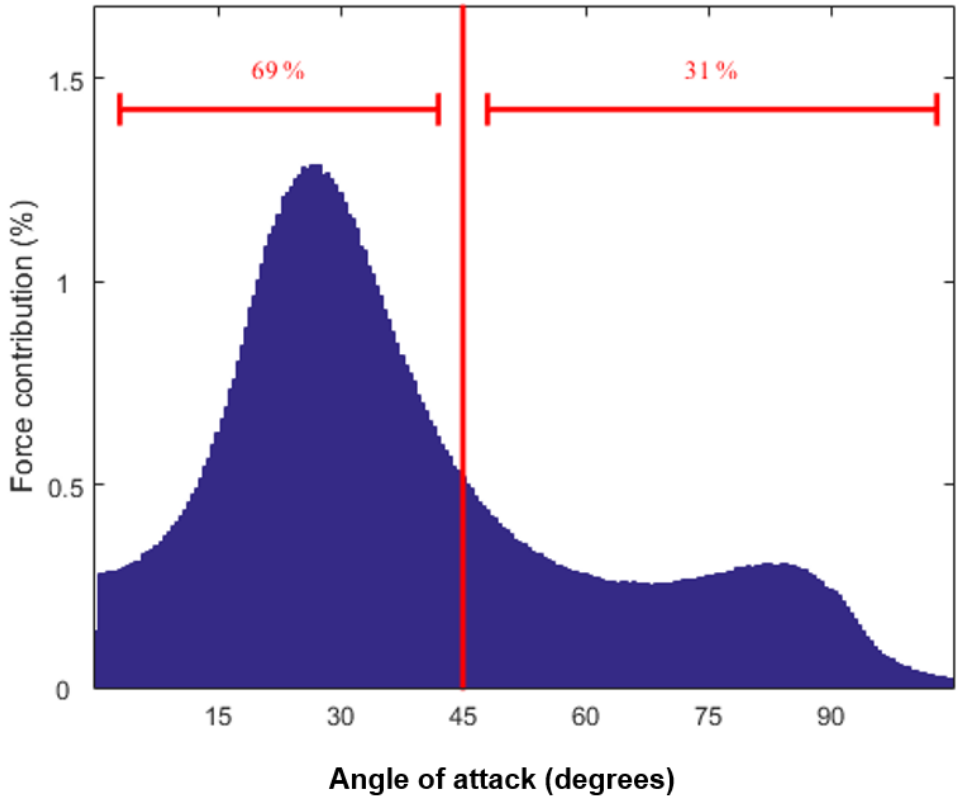
69 %
31 %
Force contribution (%)
1.5
1
0.5
0
15
30
45
60
75
90
Angle of attack (degrees)

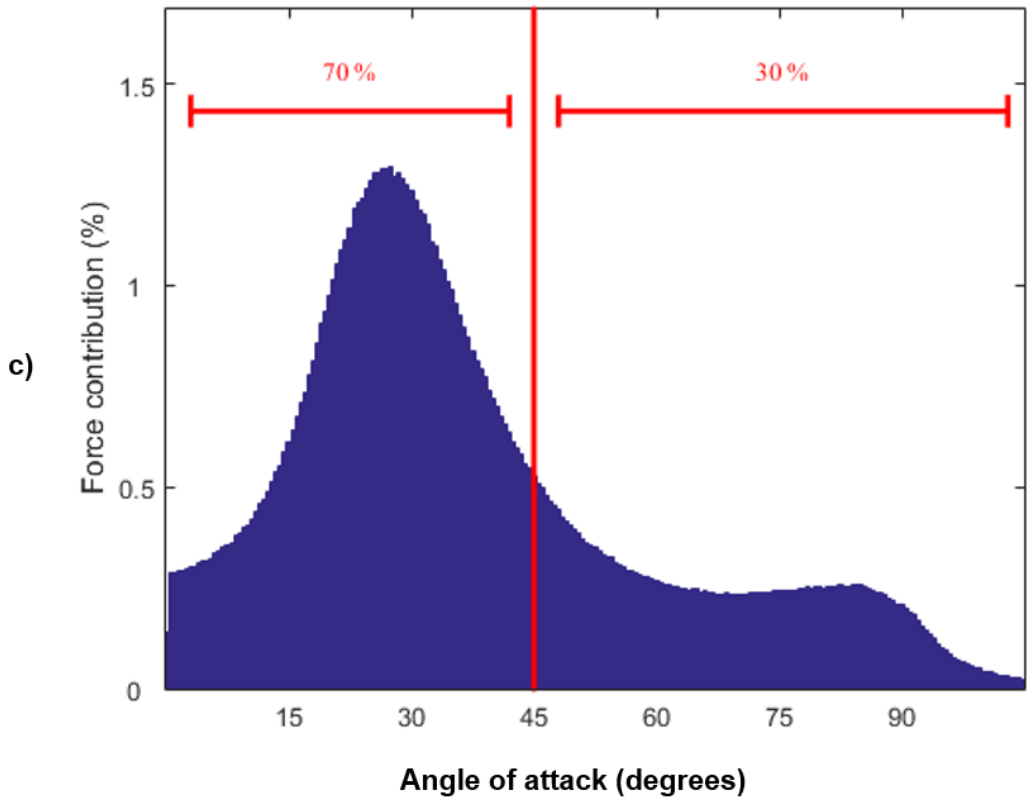

Figure 22. Aerodynamic force contribution profile across all analysed wing beats by angle of attack for a) *Drosophila melanogaster*; b) *Calliphora vicina*; c) *Eristalis tenax*. The red vertical guides displays the 45 degree mark, and indicates the percentage of aerodynamic forces generated above and below 45 degrees.

Both *Eristalis* and *Calliphora* have a very similar profile of aerodynamic force production, peaking at around 25-27 degrees of angle of attack, whereas *Drosophila* has the most peak forces at an angle of attack of 45 degrees.

DISCUSSION

True hovering flight was only found in *Eristalis tenax*, whereas the few wing beats in *Drosophila melanogaster* and *Calliphora vicina* at low advance ratio were always accompanied by a significant vertical component. This suggests that low heading velocity is indicative of vertical flight, such as gaining height rapidly or flying

over a looming object. This is consistent with their respective flight behaviour and ecology, as neither *Drosophila* nor *Calliphora* engage in hovering behaviour to communicate with individuals or to find food. There were also insufficient wing beats within the range of our definition of hovering flight, and these were excluded from discrete analysis as it was not possible to draw strong conclusions about low advance ratio from them. It is worth noting that due to the nature of the experimental set up, lower advance ratio wing beats are most likely overrepresented with respect to higher advance ratio wing beats as the fly spends less time in the recording volume. Hence, the almost complete absence of wing beats at low advance ratio for *Drosophila* and *Calliphora* further validates the fact that $J<|\pm 0.1|$ is not representative of empirically observable hovering behaviour.

The covariance matrices also reveal some clear differences between the different fly species.

Wing beat frequency decreases in *Calliphora* at increasing advance ratio, which would suggest that more power is required to fly at slower speeds. Maintaining a hovering position may be energy intensive for *Calliphora*, and particularly when slow advance ratios are accompanied by a vertical climb, which may explain the need for an increased wingbeat frequency. Interestingly, Sotavalta noted that the wing beat frequency of *Calliphora* increased from 120Hz to 210Hz between 0.5 to 5m/s, and whilst this contradicts our results, it would suggest that wing beat frequency increases with increased force production[29]. In a tethered experiment, Nachtigall and Roth showed that higher wing beat frequencies in *Calliphora* are used to increase lift production and that upwards velocity and acceleration were often high when paired with low advance ratios, such as when attempting to fly over an

oncoming object, both of which are consistent with our data suggesting that *Calliphora* does not engage in true hovering flight[30]. It is also worth noting that wing beat frequency is also partially controlled by their gear change mechanism system[31–33]. The same may also be true for *Drosophila*, as their lower advance ratio wingbeats also contain a significant vertical component, although the trend between wing beat frequency and advance ratio was not strong enough to be significant.

In *Drosophila*, a higher wingbeat frequency was correlated with an earlier timing of stroke reversal, and an earlier timing of stroke reversal was correlated with a lower advance ratio. This suggests that a longer downstroke period increases forward speed, and may play a role in determining wing beat frequency. The same pattern was not observed in either *Calliphora* or *Eristalis*, suggesting that wing beat frequency may be controlled differently.

Stroke amplitude decreased with increasing advance ratio in *Calliphora* and *Drosophila*, a trend Magnan noticed back in 1934[34]. This may suggest either that more power is required for hovering flight, or that a larger stroke amplitude aids hovering flight since it provides a greater arc through which the fly is able to adjust the net force production and displacement from the wing stroke so that it is closer to 0. Our data did not show a strong enough relationship between stroke amplitude and advance ratio in *Eristalis*. Meng & Sun noted that stroke amplitude first decreased somewhat when accelerating from hovering, before increasing again with flight speed[35]. Whilst their observation was purely descriptive, it is possible that there may be a non-linear relationship that affects and reduces the strength of the correlation. *Calliphora* displayed the greatest variation in stroke amplitude, which

may be related to the additional manoeuvrability conferred by their gear change mechanism.

The relationship between pitch and stroke amplitude in *Drosophila* and *Eristalis* is probably due to the relationship between pitch and advance ratio, and suggests that changing body pitch also enables them to adjust their stroke amplitude too. The absence of a relationship between pitch and stroke plane body in *Drosophila* and *Eristalis*, together with the significant relationship between pitch and stroke plane world, supports the helicopter model in both species. This is not the case for *Calliphora*, as the stroke plane body angle is also inversely correlated with pitch, a phenomenon previously observed by Ennos and Wagner[5,36]. This means that pitch is not used exclusively to change the direction of their flight force vector, and so can also adjust its stroke angle by other means, perhaps by activating different flight muscles or by adjusting its gear change mechanism stops.

Timing of wing rotation is correlated with advance ratio in all three species. A later timing of supination is associated with an increased advance ratio in *Drosophila* and *Calliphora*, which is consistent with Ennos' observations of *Calliphora vicina*, who noticed that supination was often delayed during fast forward flight and was faster than pronation. He hypothesised that the delay in supination leads to greater transverse flexion of the wing, during which the wing bends downwards without rotating. This shifts the torsional axis of the wing backwards leading to rapid supination. This motion makes the wing tip rise and generates stronger lift[4,5]. It is likely that the same mechanism applies to *Drosophila* as they engage in faster forward flight. *Eristalis* does not display any strong relationship between advance

ratio and timing of stroke reversal, suggesting that their forward speed control depends almost exclusively on their body pitch.

Overall the kinematic variables in *Drosophila* displayed less variation than in *Eristalis* and *Calliphora*. There are various potential reasons for this. One may be due to the comparatively lower Reynolds number of *Drosophila* and its smaller body size. Whilst *Eristalis* and *Calliphora* operate in the range of Re=1600 and Re=1200 respectively, *Drosophila* operates at Re=∼130. Since *Drosophila* operates at a lower Reynolds number, it is much more limited in how much force it can produce due to the high drag forces it faces as it increases forward flight speed. This may leave *Drosophila* with less scope for kinematic variation whilst maximising force production. *Eristalis* and *Calliphora* fly in transition flow, which is much less laminar than that of *Drosophila*, and therefore relies comparatively more on inertial forces. This may provide *Eristalis* and *Calliphora* with greater scope for further variation in their wing beat kinematics. Another possibility may be that since *Eristalis* and *Calliphora* are larger in size, they may have more space in their thorax for muscles and mechanisms such as the gear stop mechanism, allowing for greater kinematic variation.

In terms of aerodynamic force production, different models were selected for *Drosophila* and *Calliphora*. The lift and drag coefficients for *Eristalis* were estimated by Walker et al. (in prep) to be:

$$C_L = 0.877\pi \sin\alpha \cos\alpha$$

$$C_D = 0.877\pi \sin^2\alpha + 0.066$$

Compared to *Eristalis*, the slope coefficient for lift and drag are somewhat higher in *Calliphora* and *Drosophila.* The lift coefficient for *Drosophila* closely matches the estimate made for fruit flies by Dickson et. al.[37] where:

$$C_L \approx 1.1\pi \sin\alpha \cos\alpha + 0.058$$

The higher lift coefficient for *Drosophila* could be due to them operating at a lower Reynolds number, as fruit flies may be subject to relatively more unsteady effects compared to *Calliphora* and *Eristalis* who operate at a Reynolds number an order of magnitude higher. We expected the flies to display lower side-slip forces, and all had low variability in side-slip forces compared to forward and upward components[38]. This variability was more marked in *Drosophila* as the side-slip variation was two orders of magnitude lower compared to *Calliphora*.

With regards to the accuracy of the models, the lift and drag coefficients may be oversimplified due to the fixing of parameters to two degrees of freedom. In the case of *Drosophila*, a drag offset of 0 may not be entirely realistic, as even at an angle of attack of 0, a non-zero amount of drag is to be expected, as wings are three-dimensional objects.

The aerodynamic force contribution profile for *Calliphora* and *Eristalis* are very similar to each other, and both peak just shy of an angle of attack of 30˚. *Drosophila* peaks at 45˚, and is comparatively more symmetrical. This is likely to do with their body size, as *Drosophila* faces higher drag forces than *Eristalis* and *Calliphora*. *Eristalis* and *Calliphora* may produce peak aerodynamic forces at a lower angle of attack so as to optimise both lift and drag forces, whereas *Drosophila* faces high drag at higher forward speeds, so they may be primarily maximising lift production as an alternative strategy.

A recent modelling study showed that for flapping hovering kinematics at a Reynolds number of 300 and above, time dependent effects were influential and resulted in asymmetric phenomena occurring between the upstroke and downstroke. Under a low Reynolds regime of ~100, which is slightly below *Drosophila*, the aerodynamic force produced between the upstroke and the downstroke was more symmetric as the viscosity of the air dissipates the vortex structure faster[39]. Whilst this study focused on hovering kinematics, the marked difference in force production between the upstroke and downstroke across different Reynolds numbers may explain the differences in the aerodynamic force profile between *Drosophila* and *Calliphora* and *Eristalis*.

Whilst the differences in aerodynamic force production and lift and drag equations between the larger flies, *Eristalis* and *Calliphora*, and the smaller flies, *Drosophila*, are likely to do with their size difference and tackling distinct challenges with flow that they face on a physical level, in terms of kinematics *Drosophila* and *Calliphora* share more similarities compared to *Eristalis.* This could be due to shared behaviour and ecology, as neither of them displayed hovering behaviour, or it could be a by-product of phylogeny, as *Drosophila* and *Calliphora* are phylogenetically closer to each other than the Syrphids. Further research into other related Dipterans would be necessary to establish the role of phylogeny.

Our study shows that *Calliphora* and *Eristalis*, in spite of being similar in size, adjust their wing beat kinematics differently, reflecting their directed forward flight and saccadic hovering flight behaviours respectively. The findings from this study have implications in both further understanding the ecology and behaviour of these species as well as in technological innovation. By showing alternative ways in which

equivalent flight manoeuvres can be performed, it opens up further opportunities for the development of Nano-Air Vehicles with different flight strategies.

BIBLIOGRAPHY

1. Vogel, S. Flight in Drosophila I. Flight performance of tethered flies. *J. Exp. Biol.* **44,** 567–578 (1966).

2. Bender, J. & Dickinson, M. Visual stimulation of saccades in magnetically tethered Drosophila. *J. Exp. Biol.* **209,** 3170–3182 (2006).

3. Balint, C. N. & Dickinson, M. H. The correlation between wing kinematics and steering muscle activity in the blowfly Calliphora vicina. *J. Exp. Biol.* **204,** 4213–4226 (2001).

4. Ennos, R. A. A Comparative Study of the Flight Mechanism of Diptera. *Wild* **372,** 355–372 (1987).

5. Ennos, R. A. The kinematics and aerodynamics of the Free Flight of some Diptera. *J. Exp. Biol.* **142,** 49–85 (1989).

6. Ellington, C. P. The Aerodynamics of Hovering Insect Flight. III. Kinematics. *Philos. Trans. R. Soc. London* **B,** 41–78 (1984).

7. Dudley, R. & Ellington, C. P. Mechanics of forward flight in bumblebees. II. Quasi-steady lift and power requirements. *J. Exp. Biol.* **148,** 53–88 (1990).

8. Kutsch, W., Van Der Wall, M. & Fischer, H. Analysis of free forward flight of Schistocerca gregaria employing telemetric transmission of muscle potentials. *J. Exp. Zool.* **284,** 119–129 (1999).

9. Heinrich, B. Temperature regulation of the sphinx moth, Manduca sexta. II. Regulation of heat loss by control of blood circulation. *J. Exp. Biol.* **54,** 153–66 (1971).

10. Tammero, L. F. & Dickinson, M. H. The influence of visual landscape on the free flight behavior of the fruit fly Drosophila melanogaster. *J. Exp. Biol.* **205,** 327–343 (2002).

11. Schilstra, C. & Hateren, J. H. Blowfly flight and optic flow. I. Thorax kinematics and flight dynamics. *J. Exp. Biol.* **202,** 1481–1490 (1999).

12. van Hateren, J. H. & Schilstra, C. Blowfly flight and optic flow. II. Head movements during flight. *J. Exp. Biol.* **202,** 1481–1490 (1999).

13. Taylor, G. K. Dynamic flight stability in the desert locust Schistocerca gregaria. *J. Exp. Biol.* **206,** 2803–2829 (2003).

14. Wang, Z. J. Dissecting Insect Flight. *Annu. Rev. Fluid Mech.* **37,** 183–210 (2005).

15. Bomphrey, R. J., Lawson, N. J., Taylor, G. K. & Thomas, A. L. R. Application of digital particle image velocimetry to insect aerodynamics: Measurement of the leading-edge vortex and near wake of a Hawkmoth. *Exp. Fluids* **40,** 546–554 (2006).

16. Bomphrey, R. J., Henningsson, P., Michaelis, D. & Hollis, D. Tomographic particle image velocimetry of desert locust wakes: instantaneous volumes combine to reveal hidden vortex elements and rapid wake deformation. **77,** 3378–3386 (2012).

17. Ding, S., Li, X., Wang, N., Cameron, S. L. & Mao, M. The Phylogeny and

Evolutionary Timescale of Muscoidea (Diptera : Brachycera : Calyptratae) Inferred from Mitochondrial Genomes. 1–17 (2015). doi:10.1371/journal.pone.0134170

18. Colyer, C. N. & Hammond, C. O. *Flies of the British Isles*. (Frederick Warne & Co. Ltd., 1968).

19. Wiegmann, B. M. *et al.* Episodic radiations in the fly tree of life. doi:10.1073/pnas.1012675108/-/DCSupplemental.www.pnas.org/cgi/doi/10.1073/pnas.1012675108

20. Yeates, D. K., Wiegmann, B. M., Courtney, G. W. & Meier, R. Phylogeny and systematics of Diptera : Two decades of progress and prospects *. **590,** 565–590 (2007).

21. David, J. R. *et al.* Genetic variability of sexual size dimorphism in a natural population of Drosophila melanogaster: an isofemale-line approach. *J. Genet.* **82,** 79–88 (2003).

22. Marshall, S. A. *Flies: The Natural History & Diversity of Diptera*. (Firefly Books, 2012).

23. Bharti, M. Studies on life cycles of forensically important flies , Calliphora vicina and Musca domestica nebulo at different temperatures. *J. Entomol. Res.* **33,** 273–275 (2009).

24. Aak, A., Knudsen, G. K. & Soleng, A. Wind tunnel behavioural response and field trapping of the blowfly Calliphora vicina. *Med. Vet. Entomol.* **24,** 250–257 (2010).

25. Walker, S. M., Thomas, A. L. R. & Taylor, G. K. Operation of the alula as an

indicator of gear change in hoverflies. *J. R. Soc. Interface* **9,** 1194–1207 (2012).

26. Hinkle, D., Wiersma, W. & Jurs, S. *Applied Statistics for the Behavioral Sciences*. (Houghton Mifflin, 2003).

27. Sane, S. P. & Dickinson, M. H. The aerodynamic effects of wing rotation and a revised quasi-steady model of flapping flight. *J. Exp. Biol.* **205,** 1087–1096 (2002).

28. Walker, J. A. Rotational lift: something different or more of the same? *J. Exp. Biol.* **205,** 3783–3792 (2002).

29. Sotavalta, O. The flight-tone (wing stroke frequency) of insects. *Acta Entomol. Fenn.* **4,** 1–117 (1947).

30. Nachtigall, W. & Roth, W. Correlations Between Stationary Measurable Parameters of Wing Movement and Aerodynamic Force Production in the Blowfly (Calliphora vicina R . -D .). *J. Comp. Physiol. A* **150,** 251–260 (1983).

31. Nalbach, G. The gear change mechanism of the blowfly (Calliphora erythrocephala) in tethered flight. *J. Comp. Physiol. A* **165,** 321–331 (1989).

32. Page, J. W. The Gear Change Mechanism of Dipteran Flight. in *Society of Experimental Biology: Mechanics and Biological Function of the Arthropod Exoskeleton* (2015).

33. Page, J. W., Taylor, G. K. & Walker, S. M. The Gear Change Mechanism in Calliphora vicina. 1–26 (2018).

34. Magnan, A. *Le vol des insectes*. (Hermann, 1934).

35. Meng, X. G. & Sun, M. Wing and body kinematics of forward flight in drone-flies. *Bioinspir. Biomim.* **11,** 056002 (2016).

36. Wagner, H. Flight Performance and Visual Control of Flight of the Free-Flying Houseflu (Musca Domestica L.) I. Organization of the Flight Motor. *Philos. Trans. R. Soc. London* **B,** 527–551 (1986).

37. Dickson, W. B., Straw, A. D. & Dickinson, M. H. Integrative Model of Drosophila Flight. *AIAA J.* **46,** 2150–2164 (2008).

38. Blondeau, J. Aerodynamic Capabilities of Flies, as Revealed by a New Technique. *J. Exp. Biol.* **92,** 155–163 (1981).

39. Tang, J., Viieru, D. & Shyy, W. Effects of Reynolds Number and Flapping Kinematics on Hovering Aerodynamics. *AIAA J.* **46,** 967–976 (2008).

Chapter 6

General Discussion

General Discussion

This thesis provides new insights into the ways that three species of Dipteran flies, *Drosophila melanogaster*, *Calliphora vicina* and *Eristalis tenax,* alter their kinematics in free-flight. I have also contributed two high-resolution datasets of wing beat kinematics belonging to *Drosophila melanogaster* and *Calliphora vicina*, and a critical appraisal of different clustering algorithms as methods of reducing data dimensionality and processing detailed flight kinematic data.

Chapter 2 provided a critical assessment of the *k*-means clustering algorithm, originally laid out by Geurten et al.[1,2], as a way of partitioning dipteran body kinematics. Modelling complex behaviour and phenomena, as well as reducing the dimensionality of large datasets, has always been a challenge in the field of biomechanics. My results showed that the shift in body kinematics of *Eristalis* and *Drosophila* was continuous, and therefore, an unsuitable target for meaningful partitioning under the assumptions of the *k*-means clustering algorithm.

In Chapter 3, I showed that sexual dimorphism affects wing beat kinematics in *Drosophila* beyond simple differences in wing length, although there is a high degree of overlap across all kinematic parameters. Sex may therefore be a parameter worth controlling for in studies employing both male and female fruit flies. Since the female flies faster than the male on average, studies that only use flies of one sex should consider testing the same hypotheses on the other sex, in order to control for potential differences that are the result of sexual selection and sexually dimorphic behaviour.

In Chapter 4, I highlighted the difference between tethered and free-flight in *Calliphora vicina* and, using a classified tethered dataset, developed a methodology that incorporated the *k*-NN clustering algorithm as a means of predicting the gear stop position of free-flying *Calliphora* based on its wing beat kinematics. The estimated accuracy of the technique was ~81%, although suggestions for improving the algorithm were made. Overall, the *k*-NN algorithm could be a promising tool for categorising complex behaviours and phenomena that cannot be directly measured.

In Chapter 5, I contrasted the differences and similarities in kinematics between all three Dipteran species considered in the thesis, and applied a blade element model to estimate their lift and drag coefficients. When it came to kinematics, *Calliphora* and *Drosophila* were found to be more similar to each other than to *Eristalis*, whereas in terms of aerodynamic profile, *Eristalis* and *Calliphora* were more similar to each other than to *Drosophila*.

Limitations

Some of the main limitations of the thesis should be noted. Firstly, the way the flight recordings were collected presents a problem of pseudoreplication. In the *Drosophila* dataset, because multiple flies were present in the recording arena, we did not know which individual fruit fly was flying in each sequence. For this reason, each sequence is treated independently, even though it is likely that multiple sequences featured the same individual. In both my own *Calliphora* dataset and the *Eristalis* dataset from Walker et al.[3], the individual fly in the recording arena was known. However, in all three datasets there remains the limitation of greater similarity and a higher degree of autocorrelation between adjacent wing beats belonging to the same individual in a sequence, than between non-adjacent wing

beats in the same sequence, wing beats in separate sequences; and wing beats belonging to different individuals. Nonetheless, we used statistical approaches that should be robust to the biases presented and took account, whenever possible, of the hierarchy within the dataset, such as listing sequence and individual as nested random effects in linear mixed effect models.

The second limitation, which applies generally to most biological datasets, is that the two datasets collected for *Calliphora* and *Drosophila* could have been larger to cover a wider envelope of flight behaviour, especially in comparison with the number of wing beats recorded for *Eristalis*. This is connected to the third limitation, which is the bias of the experimental set-up towards collecting a greater number of wing beats with lower flight speeds. I have already addressed the trade-off between collecting detailed wing beat cycles at the expense of longer trajectories in individual flies in the discussion section of the preceding chapters. The functional recording volume for our data collection was relatively small because of the need to obtain four perspectives of the fly for the shape-carving tracker and to accurately calculate wing torsion throughout the wing beat cycle. As a result, we were only able to collect short snapshots of the fly's passage through the recording volume. This means that wing beats associated with flights performed at lower speeds are more likely to be overrepresented in our data, regardless of whether this was their preferred natural flight speed. On the one hand, this starkly highlighted the lack of true hovering and slow forward flight in *Drosophila* and *Calliphora*, but it also means that they may be less than ideal candidates for this style of data collection in comparison with *Eristalis*, which readily hovered in the recording volume. Nonetheless, most insects engage in behaviours that do not involve hovering, so that collecting detailed datasets of diverse free-flight behaviour continues to be of scientific interest.

With respect to the *k*-means clustering algorithm, although a substantial number of iterations were employed to test the robustness and stability of the different number of clusters *k*, the larger distance values for higher numbers of clusters in *Drosophila* and *Eristalis* suggests that more iterations are required to obtain accurate estimates of the quality of the clusters. Running the *k*-means clustering algorithm on such a large dataset was computationally expensive, and access to a cloud computer cluster would be necessary in order to reach the number of iterations required to draw solid conclusions for a higher *k* number of clusters.

Finally, there was no real way of verifying whether the classifications made by the *k*-NN algorithm on our free-flight dataset were accurate or not. Additionally, the degree of overlap across kinematic parameters between gears in the tethered dataset showed that the shift between wing beat kinematics is still reasonably continuous. This highlights the fact that there may be more factors at play that have been overlooked.

Future directions

These findings open up various paths for future research. Data reduction is a valid and useful tool in kinematic analysis, but from a methodological and technical point of view, this research has shown that attempts to oversimplify when analysing detailed kinematic data are often futile. The kinematic parameters we have studied were shown to be continuous and to display considerable overlap between different partitions of interest, which means that we should be wary of the assumptions and limitations of the clustering techniques employed, and the extent to which we can draw conclusions from them.

My thesis has also furthered our understanding of insect flight, particularly with regard to the free-flight kinematics of *Drosophila melanogaster* and *Calliphora vicina*. The various similarities and differences in kinematics observed across the three species opens up further research questions. How much of shared kinematics is a by-product of shared morphology and phylogeny, and how much is a result of sharing similar ecologies, such that their flight kinematics have adapted and converged in order to adjust to their ecological niches?

My thesis also begins to explore the complex relationship between natural and sexual selection in *Drosophila melanogaster*. Whether fruit fly flight is optimised for certain aspects of flight performance, or whether some aspects of it are suboptimal as a result of the trade-off with sexual selection, is a question that lies beyond the scope of this thesis. Nevertheless, it would be interesting to explore it further by comparing their flight kinematics to that of another *Drosophila* species or Brachyceran fly that operates at a similar Reynolds number, but does not engage in courtship song.

All of these are questions to do with evolutionary biology that are beyond the scope of this thesis. Nevertheless, the answers would be invaluable for influencing and designing future bio-inspired nano-UAV technology. Given the specific differences in aerodynamic performance and kinematics that have been noted in these three species, UAV designers should consider basing designs on species that have similar flight needs and properties that match their own specific purposes. For instance, a surveillance nano-UAV that needs to be able to remain stationary in the air would preferably be modelled on the kinematics of an organism with a similar biological behaviour, such as a hoverfly. On the other hand, a nano-UAV used for

search and tracking would be better modelled on the blowfly or fruit fly, depending on its overall size.

Conclusions

In the preceding chapters, I have used and developed a suite of tools to research a large, detailed volume of free-flight kinematic data from three dipteran species, and explored different ways in which the data could be partitioned and reduced in dimensionality.

My findings show that while *Drosophila*, *Calliphora* and *Eristalis* display distinct relationships between different flight kinematic parameters, with each occupying a separate kinematic morphospace, there is also a considerable amount of overlap. Furthermore, there is no evidence of obvious clusters or switch-like behaviours in their kinematics, indicating that they shift continuously through their wing and body kinematics.

The difficulty in partitioning the data using clustering algorithms, and the degree of overlap across sex in *Drosophila*, the wing kinematics associated with the predicted gear stop in *Calliphora* and the body kinematics of *Drosophila* and *Eristalis*, all indicate that flight kinematics are continuous and complex. As such, attempts to depart from detail and oversimplify the relationships between them will not yield suitable results.

BIBLIOGRAPHY

1. Geurten, B. R. H., Kern, R., Braun, E. & Egelhaaf, M. A syntax of hoverfly flight prototypes. *J. Exp. Biol.* **213,** 2461–2475 (2010).

2. Braun, E., Geurten, B. & Egelhaaf, M. Identifying prototypical components in behaviour using clustering algorithms. *PLoS One* **5,** (2010).

3. Walker, S. M., Thomas, A. L. R. & Taylor, G. K. Operation of the alula as an indicator of gear change in hoverflies. *J. R. Soc. Interface* **9,** 1194–1207 (2012).

Appendices

Supplementary Material

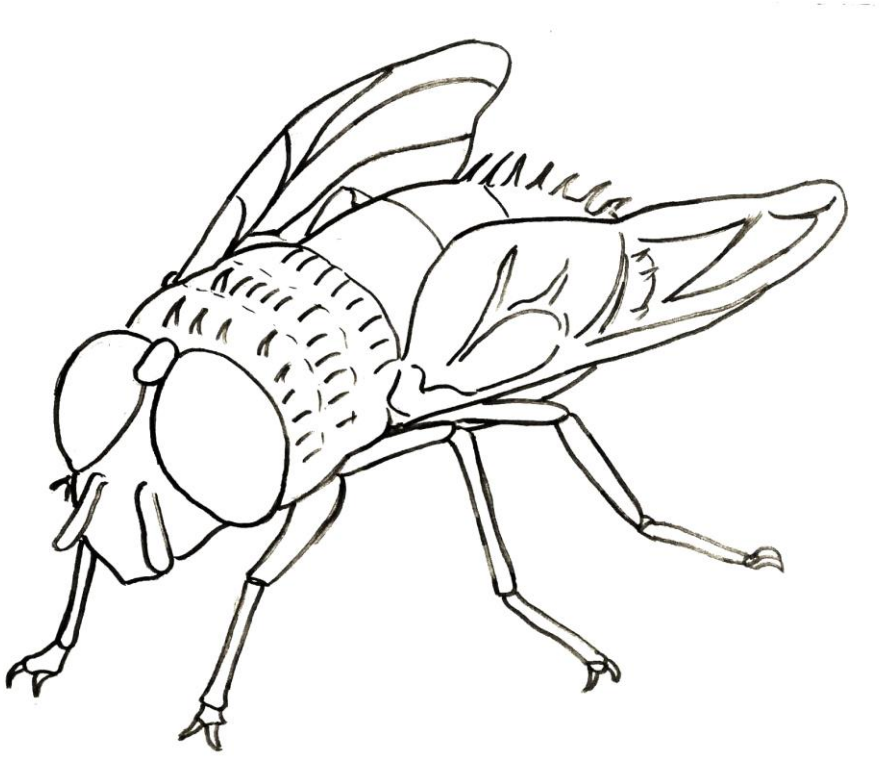

SUPPLEMENTARY MATERIAL 1

Drosophila melanogaster False Discovery Rate

Test name	raw p-value	Adjusted p-value	Significant?
Minimum stroke angle vs. stroke amplitude	0.000E+00	8.77E-04	1
Peak deviation angle vs. stroke amplitude	0.000E+00	1.75E-03	1
Stroke reversal vs. WB_freq	3.132E-232	2.63E-03	1
Test of correlation between two previous	2.400E-207	3.51E-03	1
Stroke reversal vs. Heading velocity	8.992E-189	4.39E-03	1
Wing beat frequency males vs. females	4.116E-178	5.26E-03	1
Heading velocity female vs. males	1.747E-144	6.14E-03	1
Supination stroke amplitude Pearson females	1.391E-133	7.02E-03	1
Peak deviation angle males vs. females	7.095E-128	7.89E-03	1
Supination stroke amplitude Pearson males	7.883E-104	8.77E-03	1
Minimum stroke angle males vs. females	1.985E-73	9.65E-03	1
Wing length male vs. females	3.899E-73	1.05E-02	1
Stroke plane angle females vs. males	6.441E-64	1.14E-02	1
Supination stroke reversal Pearson females	2.306E-54	1.23E-02	1
Supination stroke reversal Pearson males	6.706E-44	1.32E-02	1
Pronation and Supination females	1.400E-43	1.40E-02	1
Timing of pronation males vs females	1.116E-40	1.49E-02	1
Test of correlation between two previous supination	1.765E-38	1.58E-02	1
Body volume male vs. females	1.201E-33	1.67E-02	1
Stroke plane amplitude male vs. females	5.077E-33	1.75E-02	1
Wing beat correlation with heading velocity	1.645E-32	1.84E-02	1
Pronation and Supination males	6.826E-31	1.93E-02	1
Stroke reversal females vs. males	6.313E-30	2.02E-02	1
Body length male vs. females	1.065E-27	2.11E-02	1
Stroke amplitude and upwards acceleration regression	2.865E-17	2.19E-02	1
Body length vs wing length variance males	4.537E-08	2.28E-02	1
Wing beats in male vs. female sequences	7.046E-08	2.37E-02	1
Minimum stroke angle vs upwards velocity females	4.992E-07	2.46E-02	1
Stroke plane amplitude vs wing length females	2.290E-06	2.54E-02	1
Temperature vs. stroke amplitude males	2.810E-06	2.63E-02	1
Minimum stroke angle vs heading velocity females	4.476E-06	2.72E-02	1
Minimum stroke angle vs upwards velocity males	5.540E-06	2.81E-02	1
Minimum stroke angle vs heading velocity males	3.556E-05	2.89E-02	1
Air temperature correlation with flight speed males	3.575E-05	2.98E-02	1
Body length vs wing length variance females	2.000E-04	3.07E-02	1
Timing of supination males vs females	9.000E-04	3.16E-02	1
Body length vs. wing length correlation females	1.130E-02	3.25E-02	1
Stroke plane angle upstroke vs downstroke females	3.160E-02	3.33E-02	1
Stroke plane amplitude vs wing length males	3.390E-02	3.42E-02	1

Wing chord male vs. females	8.460E-02	3.51E-02	0
Wing length variance between sex	1.238E-01	3.60E-02	0
Stroke amplitude and heading acceleration regression	1.272E-01	3.68E-02	0
Air temperature correlation with flight speed females	1.300E-01	3.77E-02	0
Body length variance between sex	1.450E-01	3.86E-02	0
Temperature vs. stroke amplitude females	1.926E-01	3.95E-02	0
Rearing density wing length males	2.407E-01	4.04E-02	0
Stroke plane amplitude upstroke vs downstroke females	2.596E-01	4.12E-02	0
Pronation and stroke reversal	2.596E-01	4.21E-02	0
Body length vs. wing length correlation males	2.957E-01	4.30E-02	0
Rearing density wing length females	3.897E-01	4.39E-02	0
Stroke plane amplitude upstroke vs downstroke males	4.095E-01	4.47E-02	0
Rearing density body length females	5.687E-01	4.56E-02	0
Stroke plane angle upstroke vs downstroke males	5.853E-01	4.65E-02	0
Ratio wing length and body length	6.019E-01	4.74E-02	0
Wing beat frequency vs temperature females	6.079E-01	4.82E-02	0
Wing beat frequency vs temperature males	7.268E-01	4.91E-02	0
Rearing density body length males	9.046E-01	5.00E-02	0

SUPPLEMENTARY MATERIAL 2

Calliphora vicina optimal *k* neighbours and predicted success rate of test-validation and cross-validation for all combination of input parameters

	Only Gears 0 -3					
	Test-validation			Cross-validation		
Parameters	%	*k*	rank	%	*k*	rank
WBF	77.10	25	2	71.28	183	13
SPA	76.55	42	3	73.26	111	12
TSR	69.28	1	11	65.70	171	15
PSA	70.09	28	8	68.31	139	14
WBF, SPA	80.39	6	1	81.56	86	6
WBF, TSR	69.53	9	10	77.10	195	10
WBF, PSA	73.78	5	5	80.36	106	8
SPA, TSR	69.27	5	13	77.79	75	9
SPA, PSA	70.24	4	6	80.72	177	7
TSR, PSA	69.27	5	13	73.76	146	11
WBF, SPA, TSR	69.27	5	13	84.55	33	3
WBF, SPA, PSA	75.31	9	4	87.19	26	2
WBF, TSR, PSA	70.11	31	7	82.33	22	5
SPA, TSR, PSA	69.28	3	11	82.74	86	4
WBF, SPA, TSR, PSA	69.74	3	9	89.03	24	1

WBF = wing beat frequency, SPA = stroke plane amplitude, TSR = timing of stroke reversal, PSA = peak stroke angle, % = percentage of correct predictions from training dataset, *k* = optimal number of neighbours, rank = rank from highest % (1) to lowest (15).

SUPPLEMENTARY MATERIAL 3

Calliphora vicina summary heading and upwards velocity components

Component	Mean	Maximum	Minimum	(+) rate	(-) rate
Upwards (m/s)	-0.022±0.35	1.29	-1.68	0.24±0.21	-0.28±0.25
Heading (m/s)	0.70±0.30	1.50	-0.61	0.72±0.28	-0.18±0.16

For the upward component, mean, maximum and minimum upwards velocity, mean ascent rate and mean descent rate in m/s. For the forwards component, mean, maximum and minimum heading velocity, and mean forwards and backwards velocity in m/s.

SUPPLEMENTARY MATERIAL 4

Correlation-standard deviation matrix False Discovery Rate

Test name	Species	raw p-value	rank	Adjusted p-value	Significant?
SPW-Pitch	(*Drosophila*)	0.000E+00	1	3.73E-04	1
SPW-J	(*Drosophila*)	0.000E+00	2	7.41E-04	1
SA-TSR	(*Calliphora*)	0.000E+00	3	1.11E-03	1
SPW-Pitch	(*Calliphora*)	0.000E+00	4	1.48E-03	1
SA-SPB	(*Eristalis*)	0.000E+00	5	1.85E-03	1
SA-SPW	(*Eristalis*)	0.000E+00	6	2.22E-03	1
SA-Pron	(*Eristalis*)	0.000E+00	7	2.59E-03	1
SA-Pitch	(*Eristalis*)	0.000E+00	8	2.96E-03	1
SA-TSR	(*Eristalis*)	0.000E+00	9	3.33E-03	1
SPB-SPW	(*Eristalis*)	0.000E+00	10	3.70E-03	1
SPB-Roll	(*Eristalis*)	0.000E+00	11	4.07E-03	1
SPW-Pron	(*Eristalis*)	0.000E+00	12	4.44E-03	1
SPW-Pitch	(*Eristalis*)	0.000E+00	13	4.81E-03	1
SPW-J	(*Eristalis*)	0.000E+00	14	5.19E-03	1
Sup-Pron	(*Eristalis*)	0.000E+00	15	5.56E-03	1
Pron-Pitch	(*Eristalis*)	0.000E+00	16	5.93E-03	1
Pitch-J	(*Eristalis*)	0.000E+00	17	6.30E-03	1
SPW-Roll	(*Eristalis*)	1.552E-298	18	6.67E-03	1
SA-J	(*Drosophila*)	1.922E-285	19	7.04E-03	1
WB-TSR	(*Eristalis*)	7.317E-277	20	7.41E-03	1
TSR-J	(*Eristalis*)	9.027E-270	21	7.78E-03	1
TSR-J	(*Drosophila*)	1.921E-247	22	8.15E-03	1
SA-Sup	(*Drosophila*)	7.970E-236	23	8.52E-03	1
WB-TSR	(*Drosophila*)	3.132E-232	24	8.89E-03	1
WB-SPW	(*Eristalis*)	4.179E-225	25	9.26E-03	1
SPB-Pitch	(*Calliphora*)	2.399E-208	26	9.63E-03	1
Pitch-J	(*Drosophila*)	7.469E-176	27	1.00E-02	1
SPW-Sup	(*Eristalis*)	4.387E-173	28	1.04E-02	1
Sup-Pitch	(*Eristalis*)	5.486E-171	29	1.07E-02	1
SA-J	(*Eristalis*)	2.077E-170	30	1.11E-02	1
SA-Roll	(*Eristalis*)	1.790E-150	31	1.15E-02	1
SPB-Roll	(*Calliphora*)	9.861E-147	32	1.19E-02	1
WB-SPB	(*Eristalis*)	1.540E-145	33	1.22E-02	1
SPW-J	(*Calliphora*)	1.685E-138	34	1.26E-02	1
WB-Pron	(*Eristalis*)	3.878E-138	35	1.30E-02	1
Pron-J	(*Eristalis*)	2.374E-133	36	1.33E-02	1
SA-Sup	(*Eristalis*)	1.674E-131	37	1.37E-02	1
SPB-SPW	(*Drosophila*)	7.056E-130	38	1.41E-02	1
Sup-J	(*Drosophila*)	3.773E-127	39	1.44E-02	1

SA-Pron	(*Drosophila*)	1.030E-124	40	1.48E-02	1
WB-Sup	(*Eristalis*)	1.336E-112	41	1.52E-02	1
WB-SA (*Eristalis*)	(*Eristalis*)	8.991E-112	42	1.56E-02	1
SPB-TSR	(*Eristalis*)	6.648E-110	43	1.59E-02	1
SPB-J	(*Eristalis*)	2.418E-105	44	1.63E-02	1
SA-TSR	(*Drosophila*)	2.181E-103	45	1.67E-02	1
Sup-TSR	(*Drosophila*)	1.665E-98	46	1.70E-02	1
SA-Pitch	(*Drosophila*)	6.019E-89	47	1.74E-02	1
Pitch-Roll	(*Drosophila*)	1.402E-78	48	1.78E-02	1
SA-SPW	(*Drosophila*)	5.913E-73	49	1.81E-02	1
Pitch-Roll	(*Calliphora*)	9.448E-73	50	1.85E-02	1
WB-Roll	(*Eristalis*)	1.034E-66	51	1.89E-02	1
SPB-TSR	(*Drosophila*)	1.185E-66	52	1.93E-02	1
SPB-Sup	(*Eristalis*)	4.006E-65	53	1.96E-02	1
Sup-Pron	(*Drosophila*)	7.979E-64	54	2.00E-02	1
Pitch-J	(*Calliphora*)	2.408E-62	55	2.04E-02	1
SPW-Roll	(*Drosophila*)	2.651E-60	56	2.07E-02	1
SA-J	(*Calliphora*)	4.384E-59	57	2.11E-02	1
WB-J	(*Calliphora*)	1.608E-58	58	2.15E-02	1
WB-J	(*Eristalis*)	4.486E-58	59	2.19E-02	1
SPB-J	(*Drosophila*)	1.045E-56	60	2.22E-02	1
WB-Pitch	(*Eristalis*)	1.035E-54	61	2.26E-02	1
SA-Sup	(*Calliphora*)	1.614E-52	62	2.30E-02	1
Roll-J	(*Drosophila*)	8.692E-51	63	2.33E-02	1
Sup-J	(*Calliphora*)	1.405E-50	64	2.37E-02	1
Roll-J	(*Eristalis*)	2.817E-50	65	2.41E-02	1
Pron-Roll	(*Eristalis*)	1.680E-48	66	2.44E-02	1
SPW-TSR	(*Drosophila*)	4.514E-44	67	2.48E-02	1
WB-J	(*Drosophila*)	5.388E-42	68	2.52E-02	1
Sup-TSR	(*Eristalis*)	1.911E-39	69	2.56E-02	1
SPW-Sup	(*Drosophila*)	6.080E-37	70	2.59E-02	1
Pron-J	(*Calliphora*)	2.293E-34	71	2.63E-02	1
SPB-TSR	(*Calliphora*)	5.075E-34	72	2.67E-02	1
WB-SPB	(*Drosophila*)	2.459E-33	73	2.70E-02	1
Sup-Pitch	(*Drosophila*)	5.805E-33	74	2.74E-02	1
Pron-J	(*Drosophila*)	4.316E-32	75	2.78E-02	1
Pitch-Roll	(*Eristalis*)	1.319E-31	76	2.81E-02	1
SA-Pitch	(*Calliphora*)	1.167E-29	77	2.85E-02	1
Roll-TSR	(*Eristalis*)	2.362E-29	78	2.89E-02	1
SA-SPW	(*Calliphora*)	5.008E-29	79	2.93E-02	1
SA-Pron	(*Calliphora*)	9.591E-25	80	2.96E-02	1
Roll-J	(*Calliphora*)	1.452E-24	81	3.00E-02	1
SPW-Pron	(*Calliphora*)	6.533E-24	82	3.04E-02	1
Pitch-TSR	(*Calliphora*)	2.383E-20	83	3.07E-02	1

WB-TSR	(*Calliphora*)	2.223E-18	84	3.11E-02	1
WB-Roll	(*Calliphora*)	1.009E-17	85	3.15E-02	1
Pron-Pitch	(*Drosophila*)	1.026E-17	86	3.19E-02	1
Sup-TSR	(*Calliphora*)	3.520E-16	87	3.22E-02	1
SPB-Pron	(*Drosophila*)	4.854E-16	88	3.26E-02	1
WB-Pron	(*Drosophila*)	2.454E-15	89	3.30E-02	1
WB-SPB	(*Calliphora*)	1.814E-13	90	3.33E-02	1
Sup-Roll	(*Calliphora*)	3.413E-13	91	3.37E-02	1
Pron-Pitch	(*Calliphora*)	9.809E-13	92	3.41E-02	1
Sup-Pron	(*Calliphora*)	1.537E-12	93	3.44E-02	1
Pitch-TSR	(*Drosophila*)	5.361E-11	94	3.48E-02	1
TSR-J	(*Calliphora*)	7.377E-11	95	3.52E-02	1
WB-Sup	(*Drosophila*)	1.128E-10	96	3.56E-02	1
Sup-J	(*Eristalis*)	1.507E-10	97	3.59E-02	1
SPW-Sup	(*Calliphora*)	3.858E-10	98	3.63E-02	1
WB-SPW	(*Drosophila*)	8.894E-10	99	3.67E-02	1
SPB-SPW	(*Calliphora*)	1.365E-09	100	3.70E-02	1
Sup-Roll	(*Drosophila*)	2.086E-09	101	3.74E-02	1
Roll-TSR	(*Drosophila*)	1.974E-08	102	3.78E-02	1
WB-Pitch	(*Calliphora*)	4.696E-08	103	3.81E-02	1
SPB-Pitch	(*Drosophila*)	5.019E-08	104	3.85E-02	1
Pron-Roll	(*Calliphora*)	1.611E-07	105	3.89E-02	1
SPW-Pron	(*Drosophila*)	5.001E-07	106	3.93E-02	1
SA-Roll	(*Calliphora*)	5.265E-07	107	3.96E-02	1
Pron-TSR	(*Eristalis*)	8.879E-07	108	4.00E-02	1
Sup-Roll	(*Eristalis*)	9.100E-07	109	4.04E-02	1
SPB-Pitch	(*Eristalis*)	1.959E-06	110	4.07E-02	1
SPB-Roll	(*Drosophila*)	3.146E-06	111	4.11E-02	1
SA-Roll	(*Drosophila*)	6.261E-06	112	4.15E-02	1
Roll-TSR	(*Calliphora*)	1.189E-05	113	4.19E-02	1
Sup-Pitch	(*Calliphora*)	2.495E-05	114	4.22E-02	1
SPB-Sup	(*Drosophila*)	4.011E-05	115	4.26E-02	1
WB-Pron	(*Calliphora*)	1.470E-04	116	4.30E-02	1
WB-Sup	(*Calliphora*)	4.642E-04	117	4.33E-02	1
SA-SPB	(*Calliphora*)	1.041E-03	118	4.37E-02	1
WB-Roll	(*Drosophila*)	2.170E-03	119	4.41E-02	1
Pron-TSR	(*Calliphora*)	6.108E-03	120	4.44E-02	1
SA-SPB	(*Drosophila*)	9.146E-03	121	4.48E-02	1
SPB-Pron	(*Eristalis*)	1.679E-02	122	4.52E-02	1
Pron-Roll	(*Drosophila*)	4.652E-02	123	4.56E-02	0
SPW-TSR	(*Calliphora*)	1.072E-01	124	4.59E-02	0
Pitch-TSR	(*Eristalis*)	1.132E-01	125	4.63E-02	0
SPB-J	(*Calliphora*)	1.244E-01	126	4.67E-02	0
SPW-Roll	(*Calliphora*)	1.252E-01	127	4.70E-02	0

SPB-Pron	(*Calliphora*)	1.470E-01	128	4.74E-02	0
WB-SPW	(*Calliphora*)	2.435E-01	129	4.78E-02	0
WB-SA (*Calliphora*)	(*Calliphora*)	2.495E-01	130	4.81E-02	0
Pron-TSR	(*Drosophila*)	2.596E-01	131	4.85E-02	0
WB-SA	(*Drosophila*)	4.783E-01	132	4.89E-02	0
SPB-Sup	(*Calliphora*)	4.934E-01	133	4.93E-02	0
WB-Pitch	(*Drosophila*)	7.235E-01	134	4.96E-02	0
SPW-TSR	(*Eristalis*)	8.947E-01	135	5.00E-02	0